The role of abiotic and biotic factors in glucosinolate changes in Brassicales

---

Von der Naturwissenschaftlichen Fakultät

der Gottfried Wilhelm Leibniz Universität Hannover

zur Erlangung des Grades

Doktor der Naturwissenschaften (Dr. rer. nat.)

genehmigte Dissertation

von

Johann Hornbacher, M. Sc.

2022

Referentin: Prof. Dr. rer. nat. Jutta Papenbrock

Korreferent: Prof. Dr. rer. nat. Jonathan Gershenzon

Korreferent: Dr. rer. nat. Sascha Offermann

Tag der Promotion: 21.12.2021

Erklärung kumulative Dissertation

aus:

Gemeinsame Ordnung für die Promotion zur Doktorin der Naturwissenschaften oder zum Doktor der Naturwissenschaften (Dr. rer. nat.) an der Gottfried Wilhelm Leibniz Universität Hannover (25.03.2013),

§ 8 Dissertation A: (3)

„[...] 2Es ist eine ausführliche Darstellung voranzustellen, die eine kritische Einordnung der Forschungsthemen und wichtigsten Erkenntnisse aus den Publikationen in den Kontext der wissenschaftlichen Literatur zum Thema vornimmt [...]“

Die voranzustellende ausführliche Darstellung ist in dieser Arbeit aufgeteilt in die Kapitel 2.1 und 4.3.

B: (3)

„[...] sowie die individuellen eigenen Beiträge und ggf. die Beiträge weiterer Autoren an den jeweiligen Publikationen darlegt.“

Publikation (Kapitel 2.1)

Schuchardt, J. P., Hahn, A., Greupner, T., Wasserfurth, P., Del Mar Rosales, M., Hornbacher, J., **Papenbrock, J.** (2019) Watercress – cultivation methods and health effects. *Journal of Applied Botany and Food Quality*, **92:** 232-239. DOI: 10.5073/JABFQ.2019.092.032.

Die Idee für die Experimente wurde von J. P. Schuchardt, A. Hahn und J. Papenbrock entwickelt. Die Pflanzenanzucht wurde von M. Del Mar Rosales durchgeführt. Die Glucosinolatanalyse, Auswertung der Daten, Erstellung der Grafiken und die dazugehörige Diskussion wurden von J. Hornbacher angefertigt. Die Beteiligung von J. Hornbacher an dieser Publikation lag bei 10%.

Publikation (Kapitel 2.2)

Chapter 3: Schulze H., Hornbacher J., Wasserfurth P., Reichel T., Günther T., Krings U., Krüger K., Hahn A., **Papenbrock J.**, Schuchardt JP. (2021). Immunomodulating effect of the

consumption of watercress (*Nasturtium officinale*) on exercise-induced inflammation in humans. *Foods*, **10**: 1774. DOI: 10.3390/foods10081774.

Die Idee für die Experimente wurde von H. Schulze, J. P. Schuchardt, K. Krüger, und A. Hahn entwickelt. Die Studie wurde von H. Schulze und P. Wasserfurth durchgeführt. Das Manuskript wurde von H. Schulze und J. P. Schuchardt angefertigt. Die Anzucht des Pflanzenmaterials, Analyse der Glucosinolate, Phenole, Flavonoide, Carotinoide und des ORAC-Tests sowie das Schreiben der glucosinolatbezogenen Teile der Publikation wurden von J. Hornbacher durchgeführt. Die Cytokin-Analyse wurde von T. Reichel bearbeitet. T. Günther hat die Analyse der Tocopherole durchgeführt. Entzündungsmarker wurden von K. Krüger gemessen. Das Manuskript wurde von J. Hornbacher, K. Krüger, J. Papenbrock und J. P. Schuchardt überarbeitet. Die Beteiligung von J. Hornbacher an dieser Publikation lag bei 25%.

Publikation (Kapitel 2.3)

Lewerenz, L., Heinrichs, H., Hornbacher, J., Papenbrock, J., Nguyen-Thanh, B., Selmar, D. (2020) Protein content and glucosinolates from *Moringa oleifera* Lam. – New insights into an auspicious commodity. *Journal of Applied Botany and Food Quality*, **93**: 257-265. DOI: 10.5073/JABFQ.2020.093.032.

Die Idee für die Experimente wurde von D. Selmar und L. Lewerenz entwickelt. Die Messung von Hydroxybenzylalkohol wurde von L. Lewerenz durchgeführt. Der Abbau von Glucosinolaten über die Zeit wurde von J. Hornbacher gemessen. Große Anteile des Manuskripts wurden von L. Lewerenz geschrieben und von J. Papenbrock sowie J. Hornbacher überarbeitet. Die Beteiligung von J. Hornbacher an dieser Publikation lag bei 15%.

Publikation (Kapitel 3.1)

Rupp, I. S., Hornbacher, J., Horst-Nießen, I., Schaarschmidt, F., Riemenschneider, A., **Papenbrock, J.** (2020) The diurnal rhythm of *Brassica napus* L. influences contents of sulfur-containing defense compounds and occurrence of vascular occlusions during an infection with *Verticillium longisporum. Agronomy,* **10**: 1227. DOI: 10.3390/agronomy10091227.

Die Idee für die Experimente wurde von J. Papenbrock und I. S. Rupp entwickelt. Die Pflanzenanzucht von *Brassica napus* wurde von I. S. Rupp durchgeführt. Die Infektionsversuche wurden von I. S. Rupp unter Mithilfe von J. Hornbacher durchgeführt. Die

Analyse der schwefelhaltigen Metabolite Glutathion, Cystein und Glucosinolate wurde von I. S. Rupp durchgeführt. Die Messung der Glucosinolate in *B. napus* wurde von J. Hornbacher durchgeführt. Die Expressionsanalyse wurde von I. Horst-Nießen durchgeführt. Die statistische Auswertung erfolgte durch F. Schaarschmidt. Große Anteile des Manuskripts wurden von I. S. Rupp und J. Hornbacher geschrieben und von J. Papenbrock sowie J. Hornbacher überarbeitet. Die Beteiligung von J. Hornbacher an dieser Publikation lag bei 25%.

Publikation (Kapitel 3.2)

Zamani-Noor, N., Hornbacher, J., Comel, C. J., Papenbrock, J. (2021) Variation of glucosinolate contents in clubroot-resistant and -susceptible *Brassica napus* cultivars in response to virulence of *Plasmodiophora brassicae. Pathogens,* **10**: 563. DOI: 10.3390/pathogens10050563.

Die Idee für die Experimente wurde von J. Papenbrock, N. Zamani-Noor und C. J. Comel entwickelt. Die Pflanzenanzucht von *Brassica napus* wurde von C. J. Comel durchgeführt. Die Infektionsversuche wurden von C. J. Comel durchgeführt. Die Messung der Glucosinolate in *B. napus* wurde von C. J. Comel sowie J. Hornbacher durchgeführt. Große Anteile des Manuskripts wurden von N. Zamani-Noor und J. Hornbacher geschrieben und von J. Papenbrock sowie J. Hornbacher überarbeitet. Die Beteiligung von J. Hornbacher an dieser Publikation lag bei 35%.

Publikation (Kapitel 4.1)

Hornbacher J., Rumlow A., Pallmann P., Turcios, A. E. Riemenschneider A., **Papenbrock J.** (2019) The levels of sulfur-containing metabolites in *Brassica napus* are not influenced by the circadian clock but diurnally. *Journal of Plant Biology*, **62**: 359-373. DOI: 10.1007/s12374-019-0143-x.

Die Idee für die Experimente wurde von J. Papenbrock, A. Riemenschneider und A. Rumlow geb. Weese entwickelt. Die Pflanzenanzucht von *Brassica napus* für die Untersuchungen im Tagesverlauf wurde von A. Riemenschneider und A. Rumlow geb. Weese durchgeführt. Die Infektionsversuche wurden allein von A. Rumlow geb. Weese durchgeführt. Die Analyse der schwefelhaltigen Metabolite Glutathion, Cystein und der Glucosinolate sowie die Analyse des Gesamtschwefels wurden von A. Rumlow geb. Weese durchgeführt. Die Messung des Sulfats wurde von E. Bloem durchgeführt. Die Identifizierung der Glucosinolate in *B. napus* sowie die

Optimierung der Methode zur Quantifizierung wurden von J. Hornbacher durchgeführt. Die Expressionsanalyse wurde ebenfalls von A. Rumlow geb. Weese durchgeführt. Die statistische Auswertung zur 24-h-Rhythmik erfolgte durch P. Pallmann. Die statistische Analyse der restlichen Daten erfolgte durch A. Rumlow geb. Weese. Große Anteile des Manuskripts wurden von A. Rumlow geb. Weese geschrieben und von J. Papenbrock sowie J. Hornbacher überarbeitet. Die Beteiligung von J. Hornbacher an dieser Publikation lag bei 30%.

Publikation (Kapitel 4.2)

Boestfleisch, C., Hornbacher, J., Rumlow, A., **Papenbrock, J.** (2017) Salinity influences single glucosinolate content in the halophyte *Lepidium latifolium*. In: Sulfur metabolism in higher plants – Fundamental, environmental and agricultural aspects, De Kok, L., Hawkesford, M., Haneklaus, S. & Schnug, E. (eds.), Springer, Cham. DOI: 10.1007/978-3-319-56526-2_10, pp. 103-114.

Die Idee für die Experimente wurde von J. Papenbrock und C. Boestfleisch entwickelt. Die Pflanzenanzucht und die Analyse von Flavonoiden, Phenolen, Ascorbat und ORAC wurden von C. Boestfleisch durchgeführt. Die Glucosinolate wurden von J. Hornbacher mit der Methode von A. Rumlow bestimmt. Die Auswertung der Daten sowie die Erstellung von Graphen und Tabellen wurden von C. Boestfleisch durchgeführt. Das Manuskript wurde in großen Anteilen (Ausnahme: die Glucosinolatmethode im Material- und Methodenteil sowie die dazugehörige Diskussion) von C. Boestfleisch geschrieben und von J. Papenbrock sowie J. Hornbacher teilweise überarbeitet. Die Beteiligung von J. Hornbacher an dieser Publikation lag bei 20%.

Publikation (Kapitel 4.3)

Hornbacher, J., Horst-Nießen, I., Herrfurth, C., Feussner, I., Papenbrock, J. (2022) First experimental evidence suggests use of glucobrassicin as source of auxin in drought-stressed *Arabidopsis thaliana.* Frontiers in Plant Science, **13:** 1025969. doi: 10.3389/fpls.2022.1025969

Die Idee für die Experimente wurde von J. Papenbrock, I. Horst-Nießen und J. Hornbacher entwickelt. Die Pflanzenanzucht sowie die Analyse von Glucosinolaten, Stressparametern und die Inkorporation von Deuterium wurden von J. Hornbacher durchgeführt. Die Erstellung von Tabellen und Grafiken wurde von J. Hornbacher durchgeführt. Transkriptionsmessungen wurden von I. Horst-Nießen durchgeführt. Messungen von Indol-3-acetonitril sowie

Raphanusamsäure und Indol-3-essigsäure wurden von C. Herrfurth vorgenommen und gemeinsam mit J. Hornbacher ausgewertet. Das Manuskript wurde von J. Hornbacher angefertigt und von J. Papenbrock teilweise überarbeitet. Die Beteiligung von J. Hornbacher an dieser Publikation lag bei ca. 60%.

Die prozentuale Beteiligung von J. Hornbacher an den jeweiligen Publikationen wurde basierend auf der Methode von Boyer et al. (2017) abgeschätzt.

Summary

In this work the glucosinolate (GSL) contents in edible plants and the response of GSL contents to biotic and abiotic stress were analyzed.

Fluctuations in GSL contents in *Nasturtium officinale* were determined in the course of a growing season and in administered *N. officinale* during a human trial. Results showed only minor changes in GSL contents, which are similar during the development of *N. officinale* and cultivation of different batches. Hydrolysis of GSLs was analyzed in *Moringa oleifera* and potential breakdown products were discussed on the basis of structurally related GSLs.

Glucosinolate changes were also investigated as a result of biotic stress. Higher contents of gluconasturtiin were observed in *Brassica napus* infected with *Verticillium longisporum*. Direct growth inhibitory aspects of gluconasturtiin-derived breakdown products were discussed. Infection of *B. napus* with *Plasmodiophora brassicae* on the other hand resulted in lower contents of GSLs. Regulation of gluconasturtiin biosynthesis by more virulent pathotypes might be the cause for differing contents between plants infected with pathotypes differing in their virulence.

Furthermore, the influence of abiotic stress on GSL contents in plants was analyzed in this study. Rhythmic GSL fluctuations were observed in *B. napus* grown in light/dark and continuous light conditions and the influence of the expression of genes involved in biosynthesis and breakdown of GSLs were discussed. The influence of salt stress on *Lepidium latifolium* revealed significantly higher contents of the aliphatic GSL sinigrin, which might be involved in water homeostasis in the plant.

Lastly, it was observed that drought stress resulted in higher contents of the indolic GSL glucobrassicin (GB) in *Arabidopsis thaliana*. The investigation of deuterium incorporation into GB revealed higher biosynthesis of GB during drought stress. The expression analysis of genes responsible for breakdown of GSLs and synthesis of indole-3-acetic acid (IAA) strongly suggests glucobrassicin as a source of IAA in drought-stressed plants.

Keywords: human nutrition, biotic stress, abiotic stress, salt stress, drought stress, glucosinolates, auxin, *Nasturtium officinale*, *Moringa oleifera*, *Lepidium latifolium*, *Brassica napus*, *Arabidopsis thaliana*

Zusammenfassung

Diese Arbeit untersuchte den Glucosinolatgehalt in essbaren Pflanzen sowie den Einfluss von biotischen und abiotischen Faktoren auf die Konzentration einzelner Glucosinolate (GSL).

Untersuchungen der Glucosinolatkonzentrationen in *Nasturtium officinale* innerhalb einer Saison sowie während einer Humanstudie zeigten jeweils nur geringe Unterschiede. Außerdem wurde der Abbau von GSLs in *Moringa oleifera* untersucht und die Entstehung potentieller Abbauprodukte mit Hilfe strukturell verwandter GSLs diskutiert.

Unterschiedliche GSLs-Konzentrationen wurden auch als Folge von biotischem Stress beobachtet. So wurden höhere Gehalte von Gluconasturtiin in *Brassica napus* infolge einer Infektion mit *Verticillium longisporum* beobachtet. Der direkte wachstumshemmende Effekt von Produkten, die durch den Abbau von Gluconasturtiin entstehen, wurde diskutiert. Anders als bei einer Infektion mit *V. longisporum* führte eine Infektion mit *Plasmodiophora brassicae* in *B. napus* zu geringeren Konzentrationen aller GSLs im Vergleich zur Kontrolle. Unterschiedliche Glucosinolatkonzentrationen in infizierten Pflanzen könnten auf die unterschiedlichen Effekte der Pathogene auf die Morphoplogie der Wirtspflanze zurückgeführt werden.

Weiterhin wurde der Einfluss von abiotischem Stress auf den Gehalt von GSLs untersucht. So wurden zum einen rhythmische Schwankungen in der GSLs-Konzentration in *B. napus* in hell/dunkel, sowie kontinuierlichem Dauerlicht beobachtet. Dabei wurde der potentielle Einfluss der Expression von Genen, die in der Biosynthese und dem Abbau von GSLs involviert sind, diskutiert. Zum anderen wurden bei der Beobachtung des Einflusses von Salzstress signifikant höhere Konzentrationen von Sinigrin in *Lepidium latifolium* festgestellt. Sinigrin bzw. seine Abbauprodukte könnten auch in *L. latifolium* für die Aufrechterhaltung des Wasserhaushaltes verantwortlich sein.

Zuletzt konnte gezeigt werden, dass Trockenstress zu signifikant höheren Gehalten von Glucobrassicin (GB) in *Arabidopsis thaliana* führt. Die Untersuchung des Einbaus von Deuterium in GB offenbarte deutlich eine erhöhte Biosynthese von GB in trockengestressten Pflanzen. Die Expressionsanalyse von Genen, die in den Abbau von GSLs sowie in die Synthese von Indol-3-essigsäure involviert sind, legen GB dabei als eine Quelle für die Synthese von Indol-3-essigsäure in trockengestressten Pflanzen nahe.

Schlüsselwörter: Humanernährung biotischer Stress, Abiotischer stress, Salzstress, Trockenstress, Glucosinolate, Auxin, *Nasturtium officinale*, *Moringa oleifera*, *Lepidium latifolium*, *Brassica napus*, *Arabidopsis thaliana*

Inhaltsverzeichnis

List of abbreviations

Acronyms

ABA	Abscisic acid
aGSL	Aliphatic glucosinolate
AITC	Allyl isothiocyanate
BCAT	Branched chain amino acid transferase
BGLU	Beta-thioglucosidase
Col-0	*Arabidopsis thaliana* Columbia-0 ecotype
DTC	Dithiocarbamate
ESP	Epithionitrile specifier protein
GB	Glucobrassicin
Gln	Glutamine
Glu	Glutamic acid
GSH	Glutathione
GSL	Glucosinolate
GSLs	Glucosinolates
GSTU	Glutathione-S-transferase
GTR	Glucosinolate transporter
I3C	Indole-3-carbinol
IAA	Indole-3-acetic acid
IAN	Indole-3-acetonitril
IAOX	Indole-3-acetaldoxime
ICHO	Indole-3-carbaldehyde
ICOOH	Indole-3-carboxylic acid
iGSL	Indolic glucosinolate
ITC	Isothiocyanate
Met	Methionine
MYR	Myrosinase
NaCl	Sodium chloride
NSP	Nitrile specifier protein
PEITC	Phenylethyl isothiocyanate
Phe	Phenylalanine
SA	Salicylic acid
TGG	Thioglucosidase

Chapter 1
General Introduction

1.1 Introduction into Glucosinolates

Glucosinolates (GSLs) are specialized metabolites mainly synthesized by plants belonging to the Brassicales order. Nevertheless, members of the Euphorbiaceae (Malpighiales), Phytolaccaceae (Caryophyllales) and Pittosporaceae (Apiales) were also found to be able to synthesize GSLs (Fahey et al., 2001). Some members of the Brassicales order represent important crop plants including canola (*Brassica napus*) and several varieties of *Brassica oleracea* like cabbage and broccoli (Mitreiter & Gigolashvili, 2021).

Structurally, a pyranose form of D-glucose in beta-linkage attached to an aglucone consisting of a thiohydroximate with a sulfate ester group at the oxygen and a variable side chain is common to all GSLs (Blažević et al., 2020).

Depending on the amino acids they are derived from, GSLs are divided into three groups. Aliphatic glucosinolates (aGSLs) are synthesized from alanine, valine, leucine, isoleucine or methionine, whereas phenylalanine or tyrosine are used for the synthesis of aromatic GSLs and tryptophan for the synthesis of indolic ones (Mitreiter & Gigolashvili, 2021).

1.1.2 Glucosinolate biosynthesis

Biosynthesis of GSLs can be divided into three main steps. In the first step, the chain of methionine and phenylalanine can be elongated. The core GSL structure is established in the second step, which is followed by the modification of the variable side chain in the third (Sønderby et al., 2010).

The branched-chain amino acid transferase (BCAT) deaminates methionine (Met) to yield a 2-oxo acid, which condensates with acetyl-CoA with the help of a methylthioalkylmalate synthase (MAM). Next, an isopropylmalate isomerase is responsible for isomerization followed by oxidative decarboxylation by isopropylmalate dehydrogenase. The resulting 2-oxo acid, which is elongated by a single methylene group (-CH_2), can reenter the chain elongation pathway or enter the core GSL synthesis pathway after being transaminated by BCAT to homoMet (Sønderby et al., 2010).

Cytochromes P450 of the CYP79 family convert precursor amino acids into aldoximes (Fig. 1). CYP79B2 and CYP79B3 are both responsible for the conversion of tryptophan (Trp), CYP79A2 converts phenylalanine (Phe) and CYPF1 accepts all chain-elongated Met derivatives, whereas CYP79F2 only accepts Met derivatives with longer side chains. With the action of cytochromes P450 of the CYP83 family, aldoximes are further oxidized to either nitrile oxides or aci-nitro compounds. Tryptophan and Phe derived acetaldoximes are converted by CYP83B1, whereas CYP83A1 is responsible for the conversion of Met derived aldoximes.

After the conjugation of aldoximes to a sulfur donor, which happens without the involvement of enzymes, the C-S lyase SUR1 converts the S-alkylthiohydroximates to thiohydroximates. Desulfoglucosinolates (dsGSLs) are then synthesized by transfer of S-glucose with the help of the glucosyltransferase of the UGT74 family. In the last step, dsGSLs are sulfated into GSLs by the three sulfurtransferases SOT16, SOT17 and SOT18, using GSH as sulfur donor (Sønderby et al., 2010).

Side chain modification of aGSLs is performed by flavin monooxygenases $FMO_{GS\text{-}OX1}$, resulting in S-oxygenation of GSLs. Subsequently, the 2-oxoglutarate-dependant dioxygenase AOP2 converts S-oxygenated GSLs to alkenyl GSLs whereas AOP3 is responsible for the conversion to hydroxyalkyl GSL (Sønderby et al., 2010). The indolic side chain of the parent GSL glucobrassicin (GB) is hydroxylated by CYP81F4 and CYP81F2, CYP81F3 to yield neoglucobrassicin and 4-methoxyglucobrassicin respectively after methylation of indole glucosinolate methyltransferases (IGMT) 1 and IGMT2 (Pfalz et al., 2011).

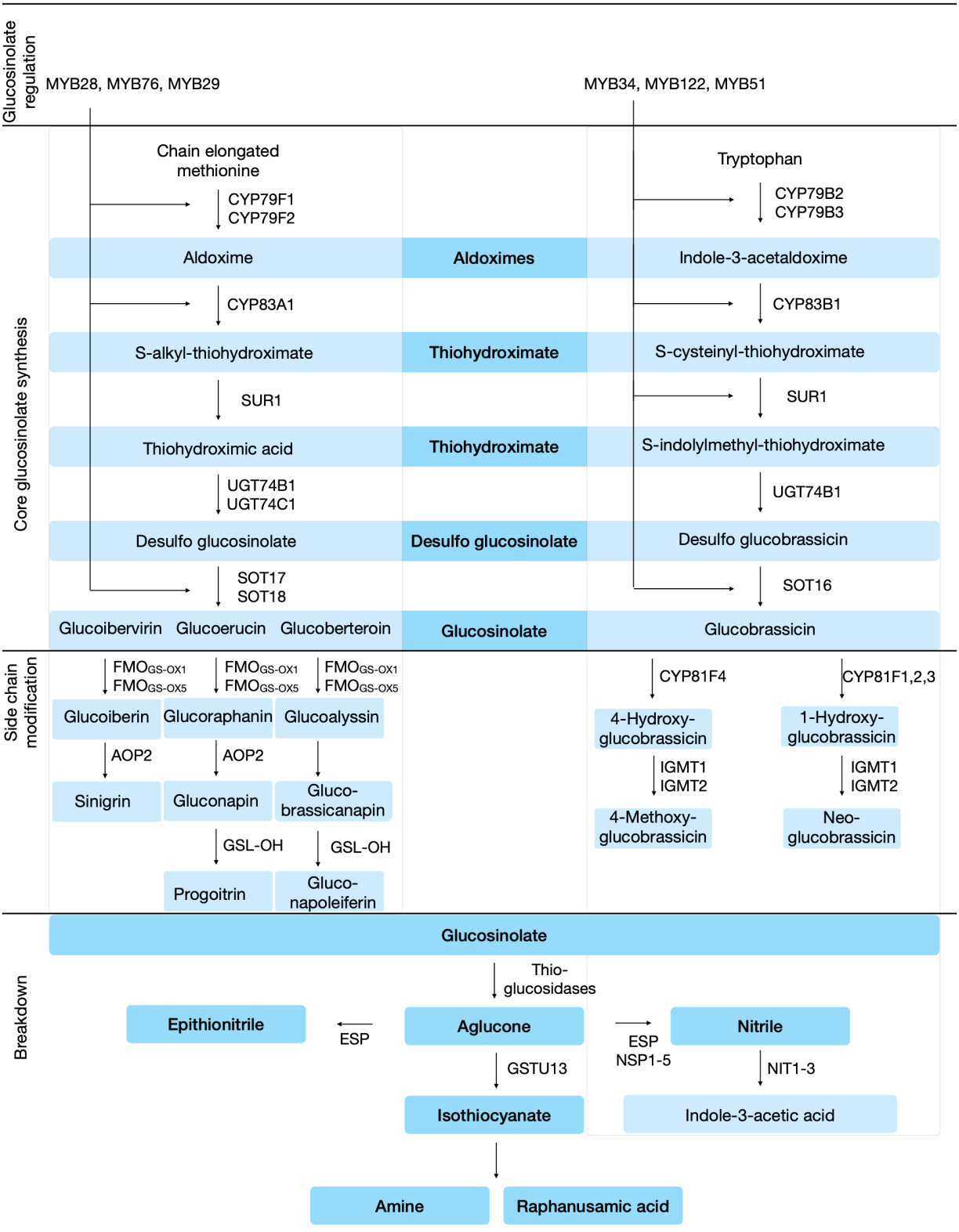

Figure 1: Regulation, synthesis of core structure, side chain modification and breakdown of glucosinolates. Modified and combined after Wittstock et al. (2010), Frerigmann & Gigolashvili (2014), Seo & Kim (2017) and Chhajed et al. (2020).

1.1.2 Regulation of glucosinolate biosynthesis

Six myeloblastosis (MYB) transcription factors (TFs) were identified to positively regulate GSL biosynthesis. Among them, MYB28, MYB29 and MYB76 (Hirai et al., 2007; Sønderby et al., 2007) are responsible for the regulation of aGSLs, whereas MYB34, MYB51 and MYB122 regulate iGSLs (Celenza et al., 2005; Gigolashvili et al., 2007).

Analysis of corresponding mutants revealed partial redundancy but also distinct functions of some of these TFs. While MYB28 is responsible for the synthesis of long-chained aGSLs (three to six cycles of chain elongation), the loss of either MYB28 or MYB29 leads to a reduction of short-chained aGSLs (up to two cycles of chain elongation). Missing of both TFs in the double mutant *myb28myb29* leads to barely detectable contents of aGSLs. The presence of functional MYB76 is held responsible for the minute contents of aGSLs left in the *myb28myb29* double mutant, but it is not enough to compensate for the loss of its related TFs (Beekwilder et al., 2008).

Investigation of MYB TFs responsible for iGSL regulation revealed regulation of GB and neoglucobrassicin synthesis by MYB34, while MYB51 is involved in the regulation of all three iGSLs GB, 4-methoxyglucobrassicin and neoglucobrassicin in *A. thaliana* leaves. Loss of both MYB34 and MYB54 in the double mutant leads to only small amounts of iGSLs which are comparable to the contents in the *myb34myb54myb122* triple mutant highlighting the insignificant contribution of MYB122 to the regulation of iGSLs at least in standard growing conditions (Frerigmann & Gigolashvili, 2014).

1.1.4 Glucosinolate hydrolysis

1.1.4.1 Classicalal myrosinases

Thioglucosidases [EC 3.2.1.147] are enzymes present in plants, microorganisms and insects. Among them are myrosinases which are specialized to the cleavage of the thioglucosidic bonds of GSLs. The group of myrosinases consist of the two subclasses Myr I and Myr II. Through in situ hybridization, promoter-reporter gene experiments and immunolocalization in plants, members of the Myr I subclass TGG1 and TGG2 were found to be localized mainly in myrosin cells (Bhat & Vyas, 2019). Their main function is believed to be the involvement in pathogen defense because of their spatial separation from GSL-containing S-cells (Sugiyama & Hirai, 2019). Root located TGG4 and TGG5 belonging to the Myr II subclass were found to perform their hydrolytic activity even at temperatures above

60°C and above concentrations of 500 mM NaCl indicating their contribution in abiotic stress situations (Andersson et al., 2009).

Myrosinases differ in their acceptance and conversion rates of different GSLs which explains the expression of multiple myrosinases in plants or specialized expression patterns in different organs (Wittstock et al., 2016).

Myrosinases hydrolyze GSLs through the formation of a glucosyl enzyme complex (Fig.1). A nucleophilic attack of an anomeric carbon of GSLs is performed by the Glu (Glu409) residue of the catalytic site of myrosinases. The aglucone part is released from the complex further disintegrating to ITCs and sulfate. Hydrolysis of the glucosyl enzyme complex is achieved by H_2O positioning with a Gln residue and ascorbic acid as coenzyme acting as catalytic base. By deprotonation of the water residue of the complex, the glucose is finally released (Bhat & Vyas, 2019).

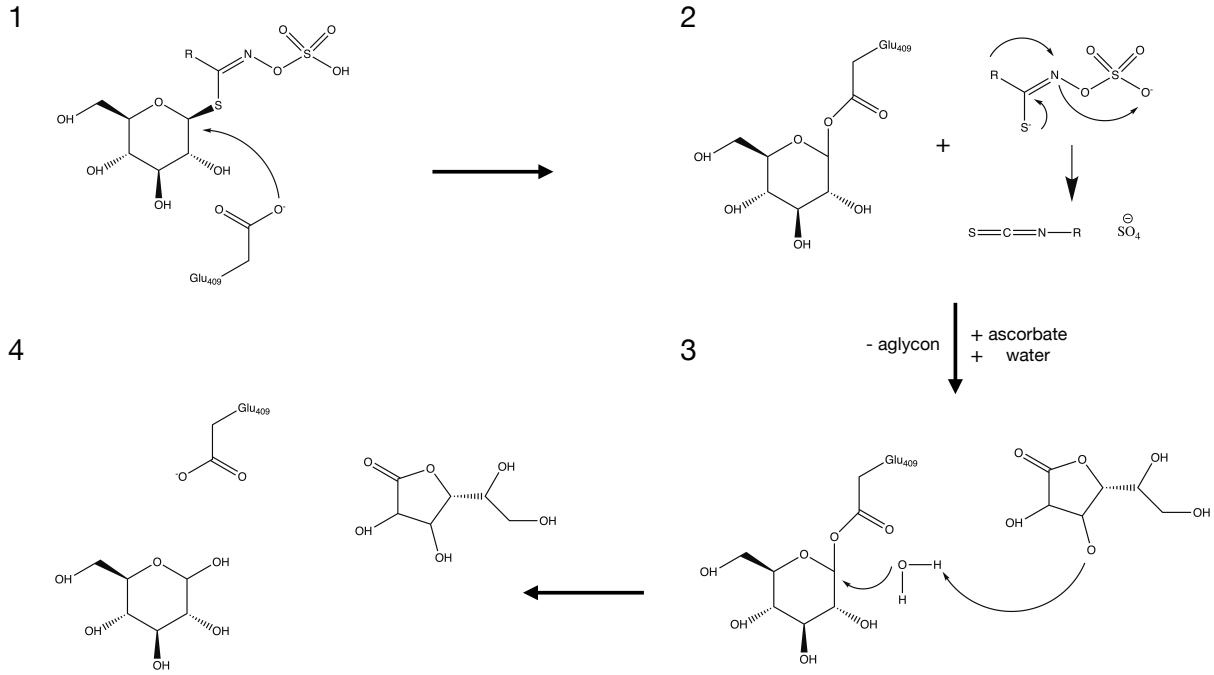

Figure 2: Hydrolysis of glucosinolates by myrosinases in the presence of ascorbic acid. 1. Nucleophilic attack of Glu409 on anomeric carbon of glucosinolates and formation of glucosyl enzyme complex. 2. Release of sulfate aglucone which undergoes Lossen-type rearrangement to isothiocyanates. 3. Deprotonation of water by ascorbic acid. 4. Release of glucose from glucosyl enzyme complex. Figure was prepared using ChemDraw (Professional, Version 20.0.0.38, PerkinElmer, Waltham, United States). Modified after Bhat & Vyas (2019).

1.1.4.2 Atypical myrosinases

Thioglucosidases lacking a Gln residue for H_2O positioning were termed atypical myrosinases. Instead, additional basic residues aid in the release of glucose in the final step,

making ascorbic acid as cofactor obsolete (Sugiyama & Hirai, 2019). Although beta glucosidases (BGLU) 18-33 have primarily other functions and higher affinities towards *O*-glucosides, they are able to perform GSL hydrolyses. Among them, PEN2 (BGLU16) was found to be involved in the resistance of *A. thaliana* towards powdery mildew by degradation of iGSLs (Bednarek, 2012). The primary function of the atypical myrosinase BGLU18 is the hydrolysis of an inactive abscisic acid (ABA) glucosyl ester, thereby releasing active ABA especially as a response to drought stress (Lee et al., 2006). The presence of BGLU18 in ER bodies, an organelle restricted to a few families of the order Brassicales, indicates the acceptance of substrates other than GSLs (Sugiyama & Hirai, 2019).

1.1.4.3 Regulation of glucosinolate hydrolysis outcome

Glucosinolate turnover in intact tissues would result in damage to cells due to the reactive nature of ITCs. Because of this reason, upon the hydrolysis of GSLs, formed ITCs are conjugated to glutathione (GSH) with the glutathione-S-transferase GSTU13. This conjugate is further metabolized to an amine and raphanusamic acid by an unknow protein (Blažević et al., 2020). However, direction of the hydrolysis outcome of GSLs can also be achieved with presence of specifier proteins. The epithiospecifier protein (ESP) shifts the outcome of the reaction towards epithionitriles and nitriles while action of nitrile specifier proteins leads to enhanced formation of nitriles (Burow & Wittstock, 2009; Kissen & Bones, 2009). Only one gene encoding for ESP is known in *A. thaliana*, however, the ecotype Col-0 was found to regulate ESP translation by alternative splicing leading to a transcript that is not translated into a protein (Kissen et al., 2012). Five NSP proteins (NSP1-NSP5) are described in *A. thaliana*. Expression of the gene encoding for the most abundant specifier protein NSP1 is found in all organs, while *NSP2* is expressed in seeds and inflorescences. *NSP3* and *NSP4* are higher expressed in seeds and roots, but expression is found in all organs. *NSP5* was found to be highly expressed in seeds, inflorescences, roots and senescent rosette leaves. All specifier proteins accept unstable aglucones as substrates making the determination of kinetic constants impossible (Wittstock, 2010).

1.2 Importance of glucosinolates in human nutrition

Among the most harvested vegetables in Germany, white cabbage ranks in the third place and together with other *Brassica* crops, 950,000 tons of *Brassica* crops were harvested in Germany in 2020 alone (Statistisches Bundesamt 2021). But *Brassica* crops are not only widely produced but also popular among German consumers. In 2019 and 2020, with 388,000 tons,

white and red cabbage marked the fifth place in the ranking of most consumed vegetables in Germany (Statistisches Bundesamt 2021).

Because of the widespread consumption of *Brassica* vegetables, it is assumed, that considerable amounts of GSLs as well as breakdown products are ingested. Consumption of GSLs is estimated to be around 14 mg d^{-1} in Germany, 6.5 mg d^{-1} in Spain and 46 mg d^{-1} in the United Kingdom. However, estimations based on the dietary exposure of *Brassica* vegetables are prone to huge fluctuations due to form of preparation of consumed vegetables and variation of GSL contents in harvested crops (Wu & Pehrsson, 2021).

While consuming fresh vegetables, cells and cell compartments get destroyed by chewing, bringing GSLs and thioglucosidases together. Thereby, an array of breakdown products is released (Oliviero et al., 2018). Cooking on the other hand inactivates thioglucosidases and specifier proteins leaving GSLs intact. Nevertheless, intact GSLs can also be converted to breakdown products by the gut microbiome. However, estimation of GSL conversion to ITCs analyzed as urinary dithiocarbamates (DTCs) revealed huge differences among individuals ranging from conversion rates of 1% to 40% (Fahey et al., 2012). Composition of gut microbiome most likely is responsible for differences in gut ITC generation since not all bacteria express thioglucosidases (Tian et al., 2018). Furthermore, bacteria derived thioglucosidases differ in their substrate specificity or hydrolyze GSLs after desulfation to yield nitriles (Fahey, 2012).

1.2.1 Antimicrobial activity of glucosinolates

Thiocyanates, nitriles and especially ITCs were found to be particularly effective in their antifungal and antimycotic activity (Saladino et al., 2017). It is hypothesized that ITCs exert their antimicrobial properties through their chemical reactivity. The electrophilic carbon of ITCs readily reacts with thiols, alcohols and amines to yield thiourea or O-thiocarbamate derivates and DTCs respectively. Since highly abundant reaction partners present in cells would therefore be GSH and thiol side chains of proteins, ITCs are most likely involved in perturbation of redox homeostasis (Plaszkó et al., 2021). It was shown that high concentrations of allyl ITC lead to GSH depletion in the human pathogenic yeast *Candida albicans*. However, oxidative stress and reduction in growth was already observed at low concentrations without alterations of the GSH pool indicating additional modes of action (Bertóti et al., 2016). Application of aqueous *Moringa peregrina* seed extracts to *Salmonella enterica* cultures lead to disintegration of the cell membrane, formation of holes and subsequent disruption of the cell wall and cell death, highlighting the reactive nature of ITCs (Romeo et al., 2018).

1.2.2 Antioxidant and anti-inflammatory activity of glucosinolates

Additionally, ITCs demonstrated chemopreventive properties, reduction of complications in diabetes patients, reduction of cardiovascular disease risk and alleviation of respiratory conditions (Palliyaguru et al., 2018). Most effects observed after administration of ITCs can be traced back to the activation of the nuclear factor erythroid 2-related factor 2 (Nrf2) and the repression of the nuclear factor kappa-light-chain-enhancer of activated B cells family (NF-κB) (Burčul et al., 2018). Nrf2 is responsible for the control of cellular oxidant level by regulation of genes responsible for antioxidant enzymes, oxidant signaling proteins and drug metabolism and is therefore involved in the protection of cells against toxicity (Ma, 2013). The transcription factor NF-κB activates transcription of genes involved in cell survival, differentiation, proliferation and apoptosis. Nevertheless, deregulation of NF-κB can lead to inflammation and cancer (Khongthong et al., 2019).

1.2.3 Antinutritional glucosinolates

Although most GSLs and their breakdown products are believed to be beneficial to human health, some are known to exhibit detrimental properties. It was shown by Baasanjav-Gerber (2011), that neoglucobrassicin was able to induce genotoxicity through formation of DNA adducts in *Salmonella typhimurium*. Results obtained differed depending on the organism the genetic material was derived from, highlighting the need for further research in this area. Furthermore, progoitrin is known to be goitrogenic through the formation of goitrin upon hydrolysis (Choi et al., 2014). However, antinutritional effects of progoitrin can be counteracted with sufficient supply of iodine (Zukalová & Vašák, 2002).

If fresh or even cooked vegetables are consumed, the ingestion of GSLs and their breakdown products is almost inevitable because of their abundance in *Brassica* crops. Although beneficial effects were reported for most GSL structures, others need further investigation.

1.3 Plant response to abiotic stress

Abiotic stress like drought and salt stress leads to the closure of stomata in order to avoid further water loss (Godoy et al., 2021). Therefore, uptake of CO_2 is reduced which subsequently results in a higher activity of the photorespiratory pathway. Additionally, diminished electron flow through the photosynthetic electron transport chain leads to the formation of reactive

oxygen species (ROS) (Nadarajah, 2020) (Fig. 3). The accumulation of ROS and the shift to an oxidative environment lead to the degradation of enzymes, proteins and nucleic acids. In order to restore the redox balance, plants synthesize metabolites like ascorbic acid, tocopherols and glutathione (GSH) which are able to scavenge ROS. Furthermore, enzymes like catalase, peroxidases and glutathione reductase are used to neutralize ROS (Choudhury et al., 2013). Depending on the severity of the stress, diminished photosynthesis and the expense invested in the synthesis of ROS-scavenging metabolites result in growth retardation and crop losses (Nadarajah, 2020).

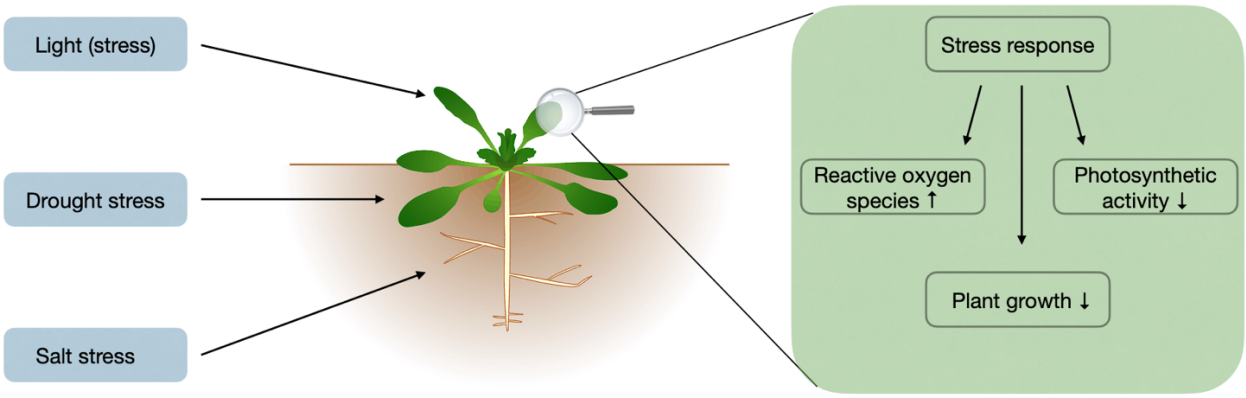

Figure 3: Response of Plants to abiotic stress. Environmental influences like light or stress factors like drought or salt stress can lead to the accumulation of reactive oxygen species, lower photosynthetic activity and reduced plant growth. Combined and modified after Sha Valli Khan et al. (2014) and Zhu (2016).

1.3.1 Climate change and its effect on agriculture

In the time of our existence on earth climate has changed considerably and drastically, leaving us hints on how this change might continue in the near future (Le Treut et al., 2007).

Analysis of drought events from 1951 to 2016 identified Amazonia, South America, the Mediterranean region, Africa and parts of China as drought hotspots. Furthermore, increased temperature overweighed increased precipitations in North America, Europe, central Asia and Australia resulting in more frequent droughts (Spinoni et al., 2019). Drought incidences, duration and severities are expected to rise even when optimistic parameters are used to predict future outcomes (Liu et al., 2018; Naumann et al., 2018; Spinoni et al., 2020). Drought accounts for major crop losses especially in globally important crops like maize, soybeans and wheat (Matiu et al., 2017) and yield loss risk is calculated to rise by about 20% if drought scenarios worsen in the future (Leng & Hall, 2019). Since a large proportion of vegetables consumed and crop plants used for biofuel production belong to the Brassicales order, investigation of their

response to abiotic stress is needed. The gained knowledge of biochemical processes in abiotically stressed plants could be used for future improvements of crop performance. Furthermore, light abiotic stresses could be applied to plants to enhance contents of specialized metabolites like GSLs in order to improve their nutritional value.

1.3.1 Influence of abiotic stress on glucosinolates

Changes in GSL contents were observed in abiotic stresses like salt and drought stress, light quality and nutrient deficiency (Martínez-Ballesta et al., 2013). Explanation of GSL changes is evident for some abiotic factors but still needs more research to elucidate the function in others. Extended darkness for example leads to carbohydrate starvation and degradation of GSLs which are probably used as carbon and sulfur storage (Brandt et al., 2018). The function as sulfur storage becomes even more obvious in sulfur deficient plants. Under sulfur starvation, BGLU28 and BGLU30 were found to catabolize GSLs and expression of Sulfate Transporters 1 and 2 were found to be upregulated in *bglu28bglu30* mutants (Zhang et al., 2020). The reason for differing GSL concentration in salt-stressed plants is not clarified to date. Since strong osmotic stress as a result of salt administration can lead to damage of cells, the differentiation between the effects of salt stress and tissue disruption can be challenging (Martínez-Ballesta, 2013). However, the presence of TGG1 in guard cells of stomata and GSL degradation was found to be involved in stomatal aperture and therefore in water homeostasis in plants (Zhao et al., 2008). Furthermore, it was shown that the degradation of aGSLs seems to alleviate drought stress through the regulation of stomatal aperture, thereby showing a clear role of GSLs in abiotic stress situations (Salehin et al., 2019).

1.4 Plant responses to biotic stress

Biotic stressors account for an estimated crop loss of 20-40% worldwide (Douglas, 2018). Due to selection of crop plants for high yield, taste and appearance, they are less tolerant to abiotic and biotic stress conditions compared to their non-selected relatives (Hussain, 2015). Additionally, when already subjected to abiotic stress, plants are more susceptible to biotic influences endangering crop performance in an additive manner (Dresselhaus & Hückehoven, 2018). Influence from biotic stressors results in a stress response of the plant resulting in redirection of resources from biomass production to plant defense. Subsequently, the crop loss depends on the physical damage the plants experience and the expense that was invested into the defense response (Peterson & Higley, 2000). Currently, the most effective way to cope with biotic stressors is the use of pesticides which, when used inaccurately and in excess, can lead

to development of resistant pathogens, perturbances of biodiversity and potentially toxic residues on final products (Kaur et al., 2019; El-Nahhal & El-Nahhal, 2021). An additional approach, however, could be to include crop resistance into breeding approaches. Since a huge percentage of crops grown and consumed belong to the Brassicales order (Fig. 1), investigation of their specialized metabolites could be helpful to cope with biotic stressors. Glucosinolates were found to be active against a range of biotic stressors like fungal and bacterial infections as well as against herbivores and aphids (Liu et al., 2021).

1.4.2 Effect of glucosinolates on biotic stressors

In insects, GSLs exhibit their repellant action mostly through the reactivity of their breakdown products, resulting in the inhibition of enzymes, depletion of amino acids and disruption of redox homeostasis (Jeschke et al., 2016; Agnihotri et al., 2018). However, herbivores are able to specialize to GSL containing plants in order to avoid competition. This phenomenon can be exemplarily observed by the emergence of certain GSL groups in families of the Brassicales order and the parallel emergence of certain lineages developing feeding preferences for plants synthesizing these compounds. Nevertheless, plants are still able to counteract feeding by regulation of GSL biosynthesis towards the increase of GSL contents or by changing its pattern (Chhajed, 2020).

The defense of GSL containing plants against fungi relies on accumulation of ROS, depolarization of the mitochondrial membrane and decreased oxygen consumption and the establishment of physical barriers through generation of breakdown products (Clay et al., 2009; Poveda et al., 2020). Many ITCs found in different plant species were observed to exhibit antifungal properties. However, some pathogenic fungi are also able to counteract the chemical defense e.g. through detoxification of ITCs.

In order to create more resilient crops that can withstand biotic stressors, counteractive measures initiated by plants as a response to pathogens have to be unveiled and understood first. Understanding the mechanisms of GSL mediated resistance will provide possibilities to improve crop resistance through introduction of beneficial traits possibly involved in GSL regulation, synthesis and breakdown.

Aims of this thesis

The overall goal of this thesis is to study changes in GSL contents in plants used for human nutrition and in plants exposed to biotic and abiotic stress and to discuss their potential roles.

Specific objectives

To monitor GSL contents in *Nasturtium officinale* in the course of a growing season and during a human trial.

To compare GSL hydrolysis in *Moringa oleifera* in comparison to other species and to discuss potential breakdown products.

To analyze the effect of an infection with *Verticillium longisporum* and *Plasmodiophora brassicae* on the GSL contents in *Brassica napus* and to discuss their potential role in the plant.

To analyze changes in GSL contents in the course of the day in *Brassica napus* and to discuss underlying mechanisms behind rhythmic changes.

To analyze the effect of salt stress on the content of GSLs in *Lepidium latifolium* and to discuss the potential involvement of sinigrin in water homeostasis.

To analyze the effect of drought stress on the GSL changes in *Arabidopsis thaliana* and to investigate the involvement of iGSL breakdown to the contribution of IAA synthesis in drought-stressed plants.

References

Agnihotri AR, Hulagabali CV, Adhav AS and Joshi RS (2018) Mechanistic insight in potential dual role of sinigrin against *Helicoverpa armigera*. Phytochemistry **145**: 121-127. doi: 10.1016/j.phytochem.2017.10.014.

Andersson D, Chakrabarty R, Bejai S, Zhang J, Rask L and Meijer J (2009) Myrosinases from root and leaves of *Arabidopsis thaliana* have different catalytic properties. Phytochemistry **70**: 1345–1354. doi: 10.1016/j.phytochem.2009.07.036.

Baasanjav-Gerber C, Monien BH, Mewis I, Schreiner M, Barillari J, Iori R and Glatt H (2011) Identification of glucosinolate congeners able to form DNA adducts and to induce mutations upon activation by myrosinase. Mol Nutr Food Res **55**: 783–792. doi: 10.1002/mnfr.201000352.

Bednarek P (2012) Sulfur-containing secondary metabolites from *Arabidopsis thaliana* and other Brassicaceae with function in plant immunity. ChemBioChem **13**: 1846–1859. doi: 10.1002/cbic.201200086.

Beekwilder J, van Leeuwen W, van Dam NM, Bertossi M, Grandi V, Mizzi L, Soloviev M, Szabados L, Molthoff JW, Schipper B, Verbocht H, de Vos RCH, Morandini P, Aarts MGM and Bovy A (2008) The impact of the absence of aliphatic glucosinolates on insect herbivory in *Arabidopsis*. PLoS One **3**: e2068 doi: 10.1371/journal.pone.0002068.

Bertóti R, Vasas G, Gonda S, Nguyen NM, Szőke É, Jakab Á, Pócsi I and Emri T (2016) Glutathione protects *Candida albicans* against horseradish volatile oil. J Basic Microbiol **10**: 1071–1079. doi: 10.1002/jobm.201600082.

Bhat R and Vyas D (2019) Myrosinase: insights on structural, catalytic, regulatory, and environmental interactions. Crit Rev Biotechnol **39**: 508–523. doi: 10.1080/07388551.2019.1576024.

Blažević I, Montaut S, Burčul F, Olsen CE, Burow M, Rollin P and Agerbirk N (2020) Glucosinolate structural diversity, identification, chemical synthesis and metabolism in plants. Phytochemistry **169**: 112100. doi: 10.1016/j.phytochem.2019.112100.

Brandt S, Fachinger S, Tohge T, Fernie AR, Braun H-P and Hildebrandt TM (2018) Extended darkness induces internal turnover of glucosinolates in *Arabidopsis thaliana* leaves. PLoS One **13**: e0202153. doi: 10.1371/journal.pone.0202153.

Burčul F, Generalić Mekinić I, Radan M, Rollin P and Blažević I (2018) Isothiocyanates:

cholinesterase inhibiting, antioxidant, and anti-inflammatory activity. J Enzyme Inhib Med Chem **33**: 577–582. doi: 10.1080/14756366.2018.1442832.

Burow M and Wittstock U (2009) Regulation and function of specifier proteins in plants. Phytochem Rev **8**: 87–99. doi: 10.1007/s11101-008-9113-5.

Celenza JL, Quiel JA, Smolen GA, Merrikh H, Silvestro AR, Normanly J and Bender J (2005) The *Arabidopsis* ATR1 Myb transcription factor controls indolic glucosinolate homeostasis. Plant Physiol **137**: 253–262. doi: 10.1104/pp.104.054395.

Chhajed S, Mostafa I, He Y, Abou-Hashem M, El-Domiaty M and Chen S (2020) Glucosinolate biosynthesis and the glucosinolate–myrosinase system in plant defense. Agronomy **10**: 1786. doi: 10.3390/agronomy10111786.

Choi E-J, Zhang P and Kwon H (2014) Determination of goitrogenic metabolites in the serum of male Wistar rat fed structurally different glucosinolates. Toxicol Res **30**: 109–116. doi: 10.5487/TR.2014.30.2.109.

Choudhury S, Panda P, Sahoo L and Panda SK (2013) Reactive oxygen species signaling in plants under abiotic stress. Plant Signal Behav **8**: e23681. doi: 10.4161/psb.23681.

Clay NK, Adio AM, Denoux C, Jander G and Ausubel FM (2009) Glucosinolate metabolites required for an *Arabidopsis* innate immune response. Science **323**: 95-101. doi: 10.1126/science.1164627 .

Douglas AE (2018) Strategies for enhanced crop resistance to insect pests. Annu Rev Plant Biol **69**: 637–660. doi: 10.1146/annurev-arplant-042817-040248.

Dresselhaus T and Hückelhoven R (2018) Biotic and abiotic stress responses in crop plants. Agronomy **8**: 267. doi: 10.3390/agronomy8110267.

El-Nahhal Y and El-Nahhal I (2021) Cardiotoxicity of some pesticides and their amelioration. Environ Sci Pollut Res **28**: 44726–44754. doi: 10.1007/s11356-021-14999-9.

Fahey JW, Zalcmann AT and Talalay P (2001) The chemical diversity and distribution of glucosinolates and isothiocyanates among plants. Phytochemistry **56**: 5-51. doi: 10.1016/s0031-9422(00)00316-2.

Fahey JW, Wehage SL, Holtzclaw WD, Kensler TW, Egner PA, Shapiro TA and Talalay P (2012) Protection of humans by plant glucosinolates: Efficiency of conversion of glucosinolates to isothiocyanates by the gastrointestinal microflora. Cancer Prev Res **5**: 603–611. doi: 10.1158/1940-6207.CAPR-11-0538.

Frerigmann H and Gigolashvili T (2014) MYB34, MYB51, and MYB122 distinctly regulate indolic glucosinolate biosynthesis in *Arabidopsis thaliana*. Mol Plant **7**: 814–828. doi: 10.1093/mp/ssu004.

Gigolashvili T, Berger B, Mock H-P, Müller C, Weisshaar B and Flügge U-I (2007) The transcription factor HIG1/MYB51 regulates indolic glucosinolate biosynthesis in *Arabidopsis thaliana*. Plant J **50**: 886–901. doi: 10.1111/j.1365-313X.2007.03099.x.

Godoy F, Olivos-Hernández K, Stange C and Handford M (2021) Abiotic stress in crop species: Improving tolerance by applying plant metabolites. Plants **10**:186. doi: 10.3390/plants10020186.

Hirai MY, Sugiyama K, Sawada Y, Tohge T, Obayashi T, Suzuki A, Araki R, Sakurai N, Suzuki H, Aoki K, Goda H, Nishizawa OI, Shibata D and Saito K (2007) Omics-based identification of *Arabidopsis* Myb transcription factors regulating aliphatic glucosinolate biosynthesis. Proc Natl Acad Sci U S A **104**: 6478–6483. doi: 10.1073/pnas.0611629104.

Hussain B (2015) Modernization in plant breeding approaches for improving biotic stress resistance in crop plants. Turkish J Agric For **39**: 515–530. doi: 10.3906/tar-1406-176.

Jeschke V, Gershenzon J and Vassão DG (2016) A mode of action of glucosinolate-derived isothiocyanates: detoxification depletes glutathione and cysteine levels with ramifications on protein metabolism in *Spodoptera littoralis*. Insect Biochem Mol Biol **71**: 37–48. doi: 10.1016/j.ibmb.2016.02.002.

Kariñho-Betancourt E (2020) Coevolution: Plant-herbivore interactions and secondary metabolites of plants. In: Co-evolution of secondary metabolites, Mérillon J-M, Ramawat KG (eds.). Springer, Cham. 47–76. doi: 10.1007/978-3-319-96397-6_41.

Kaur R, Mavi GK, Raghav S and Khan I (2019) Pesticides classification and its impact on environment. Int J Curr Microbiol Appl Sci **8**: 1889–1897. doi: 10.20546/ijcmas.2019.803.224.

Khongthong P, Roseweir AK and Edwards J (2019) The NF-KB pathway and endocrine therapy resistance in breast cancer. Endocr Relat Cancer **26**: R369–R380. doi: 10.1530/ERC-19-0087.

Kissen R, Hyldbakk E, Wang C-WV, Sørmo CG, Rossiter JT and Bones AM (2012) Ecotype dependent expression and alternative splicing of epithiospecifier protein (ESP) in *Arabidopsis thaliana*. Plant Mol Biol **78**: 361–375. doi: 10.1007/s11103-011-9869-7.

Kissen R and Bones AM (2009) Nitrile-specifier proteins involved in glucosinolate hydrolysis

in *Arabidopsis thaliana*. J Biol Chem **284**: 12057–12070. doi: 10.1074/jbc.M807500200.

Lee KH, Piao HL, Kim H-Y, Choi SM, Jiang F, Hartung W, Hwang I, Kwak JM, Lee I-J and Hwang I (2006) Activation of glucosidase via stress-induced polymerization rapidly increases active pools of abscisic acid. Cell **126**: 1109–1120. doi: 10.1016/j.cell.2006.07.034.

Leng G and Hall J (2019) Crop yield sensitivity of global major agricultural countries to droughts and the projected changes in the future. Sci Total Environ **654**: 811–821. doi: 10.1016/j.scitotenv.2018.10.434.

Liu W, Sun F, Ho Lim W, Zhang J, Wang H, Shiogama H and Zhang Y (2018) Global drought and severe drought-affected populations in 1.5 and 2 °C warmer worlds. Earth Syst Dyn **9**: 267–283. doi: 10.5194/esd-9-267-2018.

Liu Z, Wang H, Xie J, Lv J, Zhang G, Hu L, Luo S, Li L and Yu J (2021) The roles of cruciferae glucosinolates in disease and pest resistance. Plants **10**: 1097. doi: 10.3390/plants10061097.

Ma Q (2013) Role of Nrf2 in oxidative stress and toxicity. Annu Rev Pharmacol Toxicol **53**: 401–426. doi: 10.1146/annurev-pharmtox-011112-140320.

Martínez-Ballesta M del C, Moreno DA and Carvajal M (2013) The physiological importance of glucosinolates on plant response to abiotic stress in *Brassica*. Int J Mol Sci **14**: 11607–11625. doi: 10.3390/ijms140611607.

Matiu M, Ankerst DP and Menzel A (2017) Interactions between temperature and drought in global and regional crop yield variability during 1961-2014. PLoS One **12**: e0178339. doi: 10.1371/journal.pone.0178339.

Mitreiter S and Gigolashvili T (2021) Regulation of glucosinolate biosynthesis. J Exp Bot **72**: 70–91. doi: 10.1093/jxb/eraa479.

Nadarajah, K.K. (2020) ROS homeostasis in abiotic stress tolerance in plants. Int Jol Mol Sci **21**: 5208.

Naumann G, Alfieri L, Wyser K, Mentaschi L, Betts RA, Carrao H, Spinoni J, Vogt J and Feyen L (2018) Global changes in drought conditions under different levels of warming. Geophys Res Lett **45**: 3285–3296. doi: 10.1002/2017GL076521.

Oliviero T, Verkerk R and Dekker M (2018) Isothiocyanates from *Brassica* vegetables—Effects of processing, cooking, mastication, and digestion. Mol Nutr Food Res **62**: 1701069. doi: 10.1002/mnfr.201701069.

Palliyaguru DL, Yuan JM, Kensler TW and Fahey JW (2018) Isothiocyanates: Translating the power of plants to people. Mol Nutr Food Res **62**: 1700965. doi: 10.1002/mnfr.201700965.

Peterson RKD and Higley LG (2000) Illuminating the black box: The relationship between injury and yield. In Biotic stress and yield loss.15-26. CRC Press.

Pfalz M, Mikkelsen MD, Bednarek P, Olsen CE, Halkier BA and Kroymann J (2011) Metabolic engineering in *Nicotiana benthamiana* reveals key enzyme functions in *Arabidopsis* indole glucosinolate modification. Plant Cell **23**: 716–729. doi: 10.1105/tpc.110.081711.

Plaszkó T, Szűcs Z, Vasas G and Gonda S (2021) Effects of glucosinolate-derived isothiocyanates on fungi: A comprehensive review on direct effects, mechanisms, structure-activity relationship data and possible agricultural applications. J Fungi **7**: 539. doi: 10.3390/jof7070539.

Poveda J, Eugui D and Velasco P (2020) Natural control of plant pathogens through glucosinolates : an effective strategy against fungi and oomycetes. Phytochem Rev **19**: 1045-1059. doi: 10.1007/s11101-020-09699-0.

Romeo L, Iori R, Rollin P, Bramanti P and Mazzon E (2018) Isothiocyanates: An overview of their antimicrobial activity against human infections. Molecules **23**: 624. doi: 10.3390/molecules23030624.

Saladino F, Bordin K, Luciano FB, Franzón MF, Mañes J and Meca G (2017) Antimicrobial activity of the glucosinolates. In: Glucosinolates, Mérillon J-M, Ramawat KG (eds.). Springer, Cham. 249-274, doi: 10.1007/978-3-319-25462-3.

Salehin M, Li B, Tang M, Katz E, Song L, Ecker JR, Kliebenstein DJ and Estelle M (2019) Auxin-sensitive Aux/IAA proteins mediate drought tolerance in *Arabidopsis* by regulating glucosinolate levels. Nat Commun **10**: 572305. doi: 10.1038/s41467-019-12002-1.

Seo MS and Kim JS (2017) Understanding of MYB transcription factors involved in glucosinolate biosynthesis in Brassicaceae. Molecules **22**: 1549. doi: 10.3390/molecules22091549.

Sha Valli Khan PS, Nagamallaiah GV, Dhanunjay Rao M, Sergeant K and Hausman JF (2014) Chapter 2—Abiotic Stress Tolerance in Plants: Insights from Proteomics. Emerging Technologies and Management of Crop Stress Tolerance; Academic Press: Cambridge, MA, USA, 23-68.

Sønderby IE, Hansen BG, Bjarnholt N, Ticconi C, Halkier BA and Kliebenstein DJ (2007)

A systems biology approach identifies a R2R3 MYB gene subfamily with distinct and overlapping functions in regulation of aliphatic glucosinolates. PLoS One **2**: e1322. doi: 10.1371/journal.pone.0001322.

Sønderby IE, Geu-Flores F and Halkier BA (2010) Biosynthesis of glucosinolates - gene discovery and beyond. Trends Plant Sci **15**: 283–290. doi: 10.1016/j.tplants.2010.02.005.

Spinoni J, Barbosa P, De Jager A, McCormick N, Naumann G, Vogt JV, Magni D, Masante D and Mazzeschi M (2019) A new global database of meteorological drought events from 1951 to 2016. J Hydrol Reg Stud **22**: 100593. doi: 10.1016/j.ejrh.2019.100593.

Spinoni J, Barbosa P, Bucchignani E, Cassano J, Cavazos T, Christensen JH, Christensen OB, Coppola E, Evans J, Geyer B, Giorgi F, Hadjinicolaou P, Jacob D, Katzfey J, Koenigk T, Laprise R, Lennard CJ, Kurnaz ML, Delei LI, Llopart M, McCormick N, Naumann G, Nikulin G, Ozturk T, Panitz HJ, da Rocha RP, Rockel B, Solman SA, Syktus J, Tangang F, Teichmann C, Vautard R, Vogt JV, Winger K, Zittis G and Dosio A (2020) Future global meteorological drought hot spots: A study based on CORDEX data. J Clim **33**: 3635–3661. doi: 10.1175/JCLI-D-19-0084.1.

Sugiyama R and Hirai MY (2019) Atypical Myrosinase as a mediator of glucosinolate functions in plants. Front Plant Sci **10**: 1008. doi: 10.3389/fpls.2019.01008.

Tian S, Liu X, Lei P, Zhang X and Shan Y (2018) Microbiota: a mediator to transform glucosinolate precursors in cruciferous vegetables to the active isothiocyanates. J Sci Food Agric **98**: 1255–1260. doi: 10.1002/jsfa.8654.

Le Treut H, Somerville R, Cubasch U, Ding Y, Mauritzen C, Mokssit A, Peterson T and Prather M (2007) Historical overview of climate change. In: Climate Change 2007: The Physical Science Basis. Cambridge University Press, Cambridge, United Kingdom and New York, NY, USA.

Wittstock U, Kurzbach E, Herfurth A-M and Stauber EJ (2016) Glucosinolate breakdown. Advances in botanical research. **80**: 125–169. doi: https://doi.org/10.1016/bs.abr.2016.06.006.

Wittstock U and Burow M (2010) Glucosinolate breakdown in *Arabidopsis*: Mechanism, regulation and biological significance. Arab B **8**: e0134. doi: 10.1199/tab.0134.

Wu X and Pehrsson PR (2021) Current knowledge and challenges on the development of a dietary glucosinolate database in the United States. Curr Dev Nutr 8: nzab102. doi: 10.1093/cdn/nzab102.

Zhang L, Kawaguchi R, Morikawa-Ichinose T, Allahham A, Kim SJ and Maruyama-Nakashita A (2020) Sulfur deficiency-induced glucosinolate catabolism attributed to two β-glucosidases, bglu28 and bglu30, is required for plant growth maintenance under sulfur deficiency. Plant Cell Physiol **61**: 803–813. doi: 10.1093/pcp/pcaa006.

Zhao Z, Zhang W, Stanley BA and Assmann SM (2008) Functional proteomics of *Arabidopsis thaliana* guard cells uncovers new stomatal signaling pathways. Plant Cell **20**: 3210–3226. doi: 10.1105/tpc.108.063263.

Zhu, J-K (2016) Abiotic stress signaling and responses in plants. Cell **167**: 313-324.

Zukalová H and Vašák J (2002) The role and effects of glucosinolates of *Brassica* species - A review. Rostl Vyroba **48**: 175–180. doi: 10.17221/4217-pse.

Chapter 2

Glucosinolates in human nutrition

Chapter 2.1 Watercress – cultivation methods and health effects

Journal of Applied Botany and Food Quality 92, 232 - 239 (2019), DOI:10.5073/JABFQ.2019.092.032

[1]Institute of Food Science and Human Nutrition, Leibniz University Hannover, Hannover, Germany
[2]Institute of Botany, Leibniz University Hannover, Hannover, Germany

Watercress – cultivation methods and health effects

Jan Philipp Schuchardt[1], Andreas Hahn[1], Theresa Greupner[1], Paulina Wasserfurth[1], María Rosales-López[2], Johann Hornbacher[2], Jutta Papenbrock[2*]

(Submitted: May 18, 2019; Accepted: July 20, 2019)

Summary

Watercress, *Nasturtium officinale* R. Br., is a native water or semi-aquatic plant that has a high nutrient density. Physiologically relevant are the various glucosinolates, which possess positive health effects in form of their thio- and isothiocyanates. In an interdisciplinary project, we aim to develop a hydroponic, and finally an aquaponic, circulatory cultivation system and to study the health effects of watercress. In humans, there is a lack of data-based knowledge on potential beneficial health effects of watercress. Growth of watercress was followed during one season in an open-door hydroponic system. Watercress was also cultivated in the greenhouse in different substrates with different concentrations of nutrients and salt. The biomass production is strongly dependent on the temperature. The glucosinolate contents differ significantly during the growing season, especially during flowering. Watercress naturally grows in nutrient-rich fresh waters, however, when cultivated at NaCl concentrations of up to 120 mM the gain in biomass is still high. In a human proof-of-concept study, indications for antioxidant and anti-inflammatory effects of fresh watercress were observed already after a single dose intake of fresh watercress (85 g). Further in vivo and in vitro studies are planned to study health beneficial effects of watercress and its metabolic activity.

Keywords: Anti-inflammatory, antioxidative, gluconasturtiin, glucosinolates, hydroponic cultivation, PEITC.

Introduction

Watercress (*Nasturtium officinale* R. Br.), a member of the Brassicaceae, is a perennial aquatic or semi-aquatic plant species native to Europe and Asia. Watercress grows in nutrient-rich, streaming freshwater (Kopsell et al., 2007). Watercress is traditionally used as winter salad as it grows in flowing water even at cool temperatures as long as the water is not frozen. Due to its special demands, the cultivation of watercress declined although nutritionally valuable metabolites have been identified. Usually, watercress is cultivated in sophisticated held back streaming waters, but also grows well in moist soil or hydroponic cultures. When commercially grown, watercress cuttings or seedlings are planted into beds with a mixture of soil and gravel, leveled out to ensure even water flow through the beds. Upper parts of the watercress are harvested several times per growing season, leaving enough stem to ensure new growth (Tab. 1). The species needs low amounts of nitrogen and phosphate in comparison to other plant species while producing large amounts of biomass (Kopsell et al., 2007). As it is quite low in energy, watercress has a high nutrient density for vitamins B1, B2, B3, B6, E, C, polyphenols (flavonoids, phenolic acids, proanthocyanidins) as well as terpenes (including carotenoids) (Klimek-Szczykutowicz et al., 2018).

Like all members of the Brassicaceae plant species watercress contains mustard oil glycosides or glucosinolates (GLs). These nitrogen and sulfur containing secondary metabolites are derived from amino acids and are synthesized by the plant to cope with biotic stressors. Glucosinolates and thioglucosidases (EC 3.2.1.147) are usually stored in different cells or cell compartments, but get together once the plant tissues are disrupted (Ahuja et al., 2016). Thioglucosidases then hydrolyze the GLs leaving an unstable aglucone behind, which further reacts to thiocyanates, isothiocyanates and nitriles depending on pH, metal ions and present specifier proteins (Chen et al., 2019). In the case of watercress, the eponymous GL gluconasturtiin predominates, a precursor of the breakdown product phenethyl isothiocyanate (PEITC). Isothiocyanates and thiocyanates are very reactive substances leading to numerous conjugates with thiol containing compounds like N-acetylcysteine, glutathione, cysteine and many more, forming stable dithiocarbamates (Müller et al., 2018).

Several health beneficial effects have been postulated for watercress. These include antioxidant, anti-inflammatory, immunomodulating, anti-diabetic, anti-allergic, antibacterial, hypolipemic, cardioprotective and anticancer effects as well as beneficial effects on the reproductive system (summarized in Tab. 2-4). Most of these effects have been observed in vitro (Tab. 2) and in animal studies (Tab. 3), while only a few human intervention studies have been carried out (Tab. 4). However, findings from in vitro studies do not necessarily apply in vivo, especially when looking at antioxidant effects of compounds (Berger et al., 2012). Although some studies analyzed the administration of isolated PEITC (Yuan et al., 2016), which is the main isothiocyanate of watercress, the investigation of single compounds does not necessarily allow drawing conclusions from the effects of whole watercress – an edible green with other known health-promoting ingredients.

Overall, the data on the nutritional effects of watercress is very limited. The few human studies that administered watercress focused on

Tab. 1: Cultivation methods of watercress.

Cultivation method	Place	Substrate used	Reference
Beds with flowing water	Germany (Erfurt)	Soil mixed with gravel	Pink, 1993
Beds with flowing water	Great Britain (Dorset, Hampshire)	Soil mixed with gravel	Casey & Smith, 1994; Crisp, 1970
Beds with flowing water	USA (California, Hawaii, Florida)	Soil or sand	Fennell, 2006
Hydroponics or overhead spray lines	Australia (Brisbane, Sydney, Melbourne)	Nutrient solution	Fennell, 2006

* Corresponding author

Tab. 2: Health effects of watercress – in vitro studies.

Effect	Dosage form	Cell line/ experimental model	Results/Mechanism(s)	Reference
Anticancer	Extract of watercress	Human MDA-MB-231 breast cancer cells	• Suppression of invasive potential • Inhibition of metallo-proteinase 9	Rose et al., 2005
Anticancer	Extract of watercress	Human HT115 colon cancer cells	• Suppression of invasive potential	Boyd et al., 2006
Anticancer	PEITC	Biliary tract cancer cells	• Reduction in cisplatin resistance • Increased rate of apoptosis of cancer cells • Inhibited xenograft tumor growth	Li et al., 2016
Anticancer	Extract of watercress	Human colon cancer cells (HT29 cells)	• Watercress extract proved to be effective against tumor initiation, proliferation and metastasis: ▫ Inhibition of DNA damage (initiation) ▫ Accumulation of cells in the S phase of the cell cycle (proliferation) ▫ Inhibition of invasion through matrigel (metastasis)	Boyd et al., 2006
Antioxidant, hypolipidemic and cardio-protective	Extracts of watercress	Rat liver homogenate	• Reduced serum alanine aminotransferase and aspartate aminotransferase levels compared to high-fat diet groups • Reducing power in a ferric reducing antioxidant power assay • Concentration-dependent scavenging ability on 2,2-azinobis 3-ethylbenzothiazoline-6-sulfonate, 1,1-diphenyl-2-picrylhydrazyl, nitric oxide radicals, and hydrogen peroxide • Chelating ability on ferrous ions • Prevention of thiobarbituric acid reactive substances formation in ferrous ion/ascorbate induced lipid peroxidation in a dose dependent manner	Bahramikia and Yazdanparast, 2010
Antioxidant and antidiabetic	Watercress juice	Digestive enzymes: α-glucosidase, α -amylase and lipase	• Inhibition of α-glucosidase, α-amylase and lipase	Spínola et al., 2017
Antioxidant	Extract of watercress (aqueous and ethanolic)	Direct measurement of antioxidant capacity of watercress extract	• Improved total antioxidant activity, reducing power, DPPH* radicals and superoxide anion radicals scavenging activities	Ozen, 2009
Antioxidant and anticancer	Extract of watercress & PEITC	Human PBMC	• Increased gene expression of detoxification enzymes (GP×1 and SOD2) • Increased SOD2 activity	Hofmann et al., 2009
Anti-inflammatory	PEITC	Murine raw 264.7 macrophages	• Inhibition of NO production → decreased production of TNFα and IL-10 by activated macrophages • Increased NO clearance	Tsai et al., 2010
Antiallergic	Extract of watercress (ethanol)	Rat peritoneal mast cells and rat basophilic leukemia cells (RBL-2H3)	• Inhibition of histamine release	Hoshino et al., 1998
Antibacterial	Extract of watercress (methanol)	Gramnegative bacteria (e.g. *Escherichia coli*, *Klebsiella pneumoniae*) and Grampositive bacteria (e.g. *Enterococcus faecalis* and *Bacillus cereus*)	• Antibacterial activity for all bacterial strains • Highest inhibitory activity against *Bacillus cereus* and *Escherichia coli*	Zafar et al., 2017
Antibacterial	Extract of watercress (chloroform)	*Mycobacterium tuberculosis* H37Rv bacteria	• Inhibitory activity against *Mycobacterium tuberculosis* H37Rv bacteria	Quezada-Lázaro et al., 2016

DPPH, 2,2-diphenyl-1-picrylhydrazyl; GP×1, glutathione peroxidase 1; IL-10, Interleukin 10; NO, nitric oxide; PEITC, phenethyl isothiocyanate; SOD, superoxide dismutase; TNFα, tumor necrosis factor α.

antioxidant (Fogarty et al., 2013; Gill et al., 2007) and anticancer effects (Hoffmann et al., 2009), while anti-inflammatory effects have not been investigated in humans so far.

In an interdisciplinary research project, we aim to optimize the cultivation of watercress in aquaponic circulatory systems. Another aim of the project is to study the health effects of freshly harvested watercress in vivo. A proof-of-concept study was conducted to prove the applicability of a specific study design to investigate antioxidative and anti-inflammatory effects of watercress in humans. The effect of a single watercress dose on markers of oxidative stress/lipid peroxidation (malondialdehyde, MDA) and inflammation (IL-6, TNFα and IL-10) was investigated in subjects who had to complete a high-intensity training to induce oxidative stress and a pro-inflammatory condition.

Tab. 3: Health effects of watercress – animal studies.

Effect	Dosage form	Species	Results/Mechanism(s)	Reference
Anticancer	Aqueous solution of watercress	Swiss mice	• Suppression of Ehrlich tumor growth	DE SOUZA et al., 2016
Anti-inflammatory	Extract of watercress	Rats	• Inhibition of carrageenan-induced paw edema • Activity against formalin-evoked paw edema • Decreased swelling and tissue damage induced by carrageenan or TPA	SADEGHI et al., 2014
Antioxidative, hypolipemic and cardioprotective	Extract of watercress	(Hypercholesterolaemic) rats	• Decrease of hepatic MDA, GR and GPx activities • Reduced total cholesterol, triglycerides and low-density lipoprotein • Increased levels of blood high-density lipoprotein cholesterol	YAZDANPARAST et al., 2008
Antioxidant and anti-inflammatory	Extract of watercress	Rats	• Protection against increase in ROS, GSH, LPO and PCO in gentamicin-induced nephrotoxicity • Protection against increase in NO and TNFα in gentamicin-induced nephrotoxicity	SHAHANI et al., 2017
Antioxidant and antidiabetic	Extract of watercress	(Diabetic) rats	• Improvement of antioxidant status: SOD, GR, GPx, MDA in plasma and different tissues, total antioxidant status • Hypoglycemic effect of aqueous watercress extract was 76.6 % higher than that of insulin; glucose levels were normalized on the third week up to the eighth week	FENTON-NAVARRO et al., 2018
Antidiabetic	Different extracts of watercress (ethyl acetate, methanol and aqueous)	(Diabetic) rats	• Decrease of blood glucose after 1 week and 2 months	HOSEINI et al., 2009
Antidiabetic and hypolipidemic	Extract of watercress (hydro-alcoholic)	(Diabetic) rats	• Decrease of serum glucose, total cholesterol and LDL-cholesterol	HADJZADEH et al., 2015
Antioxidant	Extract of watercress (hydro-alcoholic)	Rats	• Attenuation of Vancomycin-induced nephrotoxicity • MDA levels decreased compared to control	KARAMI et al., 2018
Antioxidant	Watercress juice	Mice	• Enhancement of superoxide dismutase activity in erythrocytes • Improved glutathione balance • Diminished lipid oxidation in all matrices	CASANOVA et al., 2017
Antioxidant	Extract of watercress (ethanolic)	Rats	• Decreased lipid peroxidation in liver, brain and kidney	OZEN, 2009
Antioxidant	Watercress oil	Rabbits	• Improved SOD activity and GSH concentrations	ALAGAWANY et al., 2018
Immuno-modulating	Extract of watercress	Rainbow trout	• Enhancement of hematological and immunological parameters (including Hb and MCHC, lysozyme and complement activities, total protein and globulin levels)	ASADI et al., 2012
Reproductive system	Extract of watercress (hydro-alcoholic)	(Diabetic) rats	• Increased levels of testosterone, LH, FSH, and fast-motility sperm	MOHAMMADI et al., 2017

FSH, follicle stimulating hormone; GPx, glutathione peroxidase; GR, glutathione reductase; GSH, glutathione; Hb, hemoglobin; LDL, low density lipoprotein; LH, lh luteinizing hormone; LPO, lipid peroxidation; MCHC, mean corpuscular hemoglobin concentration; MDA, malondialdehyde; NO, nitric oxide; PCO, protein carbonyl; PEITC, phenethyl isothiocyanate; ROS, reactive oxygen species; SOD, superoxide dismutase; TNFα, tumor necrosis factor α, TPA, 12-O-tetradecanoylphorbol-13-acetate.

Materials and methods

Plant material

The watercress cultivar was originally obtained from the nursery Fischer, Erfurt (http://erfurt-hochheim.de/gewerbe_und_handel/handel/?id=75). It was further propagated on the trout farm of the family Göckemeyer in Poggenhagen (http://www.edelkrebs-niedersachsen.de/forellen/). There, cuttings have been taken for propagation in the greenhouse at the Institute of Botany, Leibniz University Hannover.

Sampling and cultivation experiments

Growth of watercress was followed during one growth season in an outdoor hydroponic system and samples were collected every two

Tab. 4: Health effects of watercress – human studies.

Effect	Dosage form	Results/Mechanism(s)	Reference
Anticancer and antioxidant	Fresh watercress	• Reduced lymphocyte DNA damage • Altered blood antioxidant status	GILL et al., 2007
Anticancer	Fresh watercress	• Genotype dependent increase in GPx and SOD enzyme activity in red blood cells in GSTM1*0, but not in GSTM1*1	HOFMANN et al., 2009
Anticancer and antioxidant	Fresh watercress	• Decrease of exercise induced DNA damage and lipid peroxidation	FOGARTY et al., 2013
Anticancer	PEITC	• Inhibition of metabolic activation and lung carcinogenicity of tobacco	YUAN et al., 2016b

GPx, glutathione peroxidase; GSTM1, Glutathion S-Transferase M1; PEITC, phenethyl isothiocyanate.

weeks from April 2017 till November 2017. Cultivation of watercress was established by testing different substrates (soil, soil/sand mixtures, water) and with different concentrations of nutrients (nitrogen and phosphate) and NaCl.

Glucosinolate measurements by HPLC / LC-MS

GLs were analyzed by HPLC according to BOESTFLEISCH et al. (2017) with modifications. All standard substances were checked for identity by LC-MS. The GL contents in the watercress samples were measured in triplicates.

Human study design and subjects

In a cross-over study, 4 subjects consumed a single dose of 85 g of fresh watercress (along with 50 ml salad dressing, 50 g iceberg lettuce and 50 g cucumber) at breakfast. This amount has been selected since initial human studies also administered 85 g of raw watercress daily (GILL et al., 2007; FOGARTY et al., 2013). The diet was compared to a control breakfast (two buns with butter, cheese and 50 g iceberg lettuce). The study was conducted with healthy, untrained human subjects (1 male, 3 females, mean age: 28±6; mean BMI: 22.7±3.5 kg/m^2; mean weight: 66±18 kg) who had to complete a high-intensity training session to induce oxidative stress and a pro-inflammatory condition. The subjects were asked to refrain from consuming foods rich in polyphenols, vitamin E and vitamin C (especially berries, grapes, nuts), 7 days before the start of the study. On each of the 2 study days, fasting blood was taken from the subjects in the morning (baseline), followed by the consumption of the test breakfast (watercress or control). 120 minutes after breakfast, the subjects completed a 30-minute continuous running based endurance workout combined with bodyweight strength-endurance exercises (burpees, push-ups, squats and sit-ups) at 80% of their maximal heart rate (HRmax). Participants were instructed to perform 10 reps of each exercise in between replicated 400 m track runs. Throughout the workout, the HR was continuously recorded using a Polar A300 Fitness and Activity Tracker with a H7 Bluetooth heart rate sensor (Polar Electro Oy, Kempele, Finland). Five minutes after the training session, the second blood draw was taken (5 min post-exercise). The subjects were allowed to drink water ad libitum.

Concentrations of inflammatory cytokines and MDA were determined at baseline and 5 min post-exercise. Blood samples were obtained by venipuncture of an arm vein using Multifly needles (Sarstedt, Nümbrecht, Germany) into heparin plasma monovettes (Sarstedt, Nümbrecht, Germany). MDA was analyzed in heparin plasma using the TBARS Assay Kit from Cayman chemical (Biomol, Hamburg, Germany) according to the manufactures instructions. IL-10, IL-6 and TNFα were analyzed in whole blood cultures after *ex vivo* immune cell stimulation via lipopolysaccharide (LPS). Briefly, heparinized blood samples were diluted 1:4 with RPMI 1640 including HEPES and L-glutamine (Sigma-Aldrich, Hamburg, Germany) and added antibiotics (100 U/ml penicillin and 100 µg/ml streptomycin, Sigma-Aldrich, Hamburg, Germany). The blood was seeded into 12-well microtiter plates and stimulated with 10 ng/ml (final concentration) of LPS (Sigma-Aldrich, Hamburg, Germany) or medium alone in duplicates. Blood was incubated at 37 °C for 24 h. After incubation, IL-10, IL-6 and TNFα were simultaneously quantified in whole blood culture supernatant using a Bio-Plex Multiplex Immunoassay including a Bio-Plex MAGPIX™ multiplex reader.

Results

Growth of plants

In 2017, water and plant samples were taken from the outdoor culture system in Poggenhagen (Fig. 1A) every one to two weeks to analyze the nutrient requirements and plant constituents of watercress (data not shown). The biomass production is strongly dependent on the temperature and plants accumulate significantly higher contents of calcium and potassium as the season progresses with peaks reached in mid-summer. To be able to work under controlled conditions, cuttings have been prepared and rooted for propagation in the greenhouse. In the greenhouse, the watercress can be cultivated all year-round with constant biomass growth in 1/2-Hoagland nutrient solution (Fig. 1B). It can also be cultivated on different substrates (mixture of soil and sand or sand), but then the cultivation requires more care. The watercress is relatively salt-tolerant, even at about 120 mM NaCl in the nutrient solution, the plants are vital and show biomass growth (data not shown).

Glucosinolate levels

GLs were analyzed by LC-MS to identify all GLs. Afterwards an HPLC method was applied using detection at 229 nm to be able to analyze many samples in a cost-efficient way. A typical chromatogram is shown in Fig. 2A. The main GL found in watercress is gluconasturtiin (Fig. 2B). The GL contents differ significantly during the growing season, especially during flowering. Plants grown outside show similar contents of gluconasturtiin throughout the growing season with elevated levels in flowering plants and plants with developed pods when compared to plants early in the season which are not flowering. Contents of glucobrassicin, neoglucobrassicin and glucoarabishirsutain are lower in plants with developed pods later in the season compared to non-flowering plants early in the season. The contents of the GL 4-methoxyglucobrassicin on the other hand, show an increase in flowering plants with pods compared to plants with flower buds. Overall, the total content of indolic and aliphatic GLs drops in the course of the season, whereas the content of the aromatic GLs elevates slightly (Tab. 5). Flowering had even smaller effects on the GL levels and composition when plants cultivated in the greenhouse (data not shown).

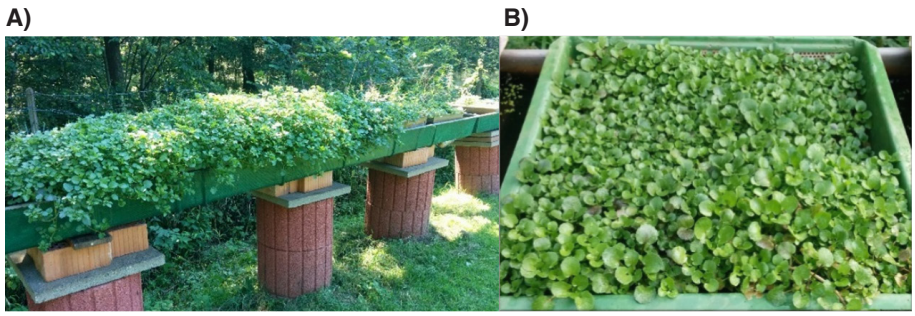

Fig. 1: Cultivation of watercress in A) Poggenhagen in the field and in the B) greenhouse.

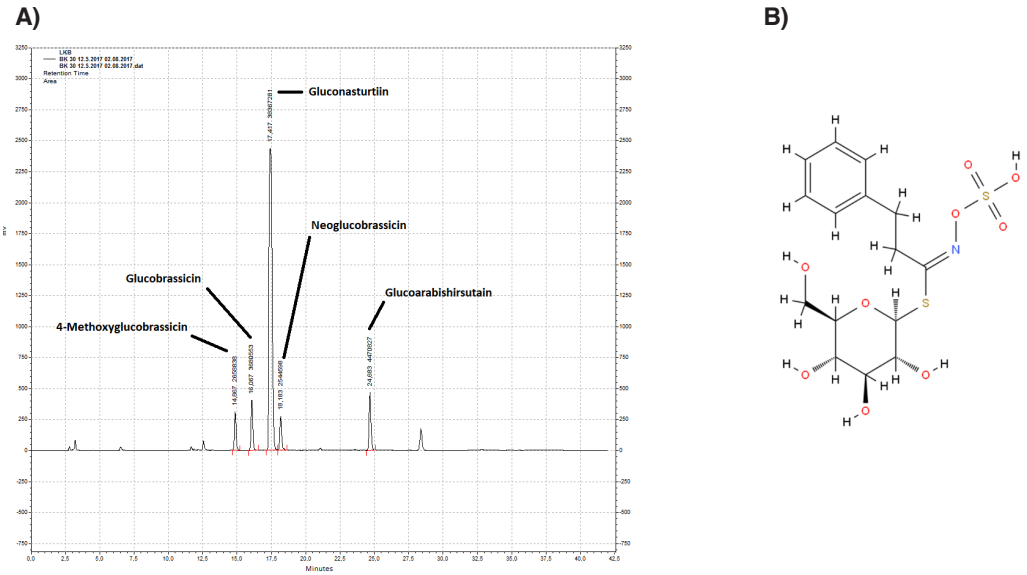

Fig. 2: A) HPLC chromatogram of a watercress extract. B) Gluconasturtiin (phenethyl glucosinolate, Chem Spider ID 7827641) is the most abundant glucosinolate in the eponymous watercress *Nasturtium officinale*.

To analyze the degradation of GLs after cutting the plants, freshly harvested watercress material was stored at 4 °C in the refrigerator in an inflated plastic bag for 1, 2, 3 and 5 d. No significant changes in the gluconasturtiin content occurred (data not shown).

Anti-inflammatory effects of watercress in humans

A trend for increasing concentrations of IL-10, IL-6, and TNFα in LPS-treated whole blood and MDA in plasma was observed 5 min post exercise after the control breakfast suggesting that the exercise protocol was effective in inducing a pro-inflammatory condition and oxidative stress, respectively (Fig. 3). Compared to the control breakfast, the increase of inflammatory cytokines and MDA concentrations 5 min post exercise after the watercress breakfast was lower.

Discussion

Successful cultivation of watercress in the greenhouse

It was demonstrated that watercress can be cultivated all year round in a greenhouse on either sandy substrate or in hydroponic nutrient solution. Therefore, it is not necessary to invent a system with running water. Even without constant aeration watercress produces large amounts of biomass, even at high nutrient or salt concentrations, which is in agreement with the literature (Kaddour et al., 2013; Fernàndez et al., 2016). The gain in biomass was strictly temperature-dependent. Therefore, for an all-year-round cultivation a greenhouse would be a prerequisite for controlled hydroponic and aquaponic cultivation.

The content of secondary metabolites changes during the season. Especially flowering has strong effects on the contents of GL. Therefore, the development of a watercress cultivation system avoid-

Tab. 5: Mean concentration of different glucosinolates (GLs) (µmol g DW^{-1}) in watercress in above ground plant material collected at different time points. Plants were growing in an outdoor aquaponic system and harvested to analyze changes in GL contents in the course of the season and developmental stage of the plants. The standard deviation represents the values for three biological replicates.

Sampling date	4-Methoxy-glucobrassicin	Glucobrassicin	Neo-glucobrassicin	Gluco-arabishirsutain	Gluconasturtiin
12.5.2017	0.144 ± 0.060	0.123 ± 0.012	0.063 ± 0.011	0.659 ± 0.117	5.028 ± 0.606
19.5.2017	0.128 ± 0.007	0.075 ± 0.009	0.04 ± 0.003	0.457 ± 0.111	5.427 ± 0.232
26.5.2017*	0.122 ± 0.018	0.109 ± 0.026	0.041 ± 0.110	0.390 ± 0.127	4.882 ± 0.782
09.6.2017**	0.176 ± 0.022	0.09 ± 0.016	0.041 ± 0.017	0.369 ± 0.106	6.017 ± 0.310
16.6.2017	0.187 ± 0.035	0.072 ± 0.010	0.043 ± 0.027	0.298 ± 0.146	6.418 ± 0.229
23.6.2017***	0.167 ± 0.079	0.038 ± 0.028	0.031 ± 0.011	0.219 ± 0.075	5.101 ± 1.691

*first flowers, **many flowers, ***no flowers anymore.

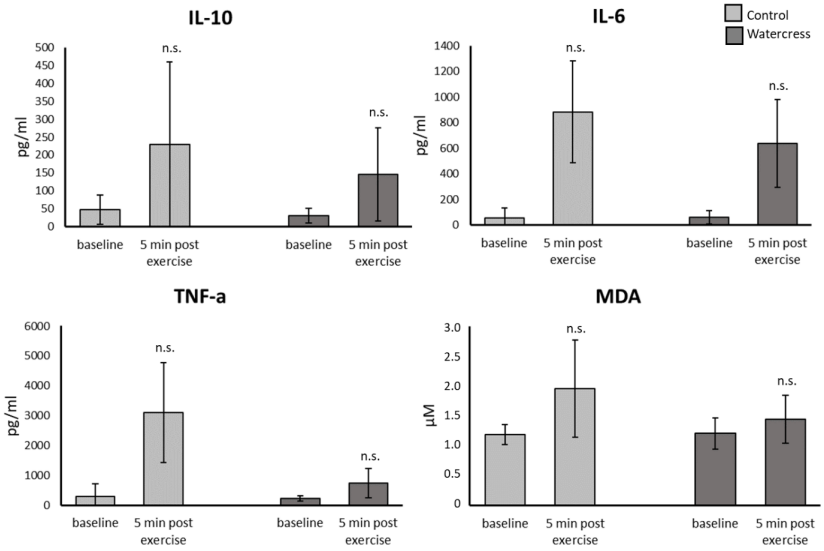

Fig. 3: Effect of acute watercress consumption on blood markers of inflammation (IL-10, IL-6, TNFα) and oxidative stress/lipid peroxidation (MDA) after high-intensity training in untrained subjects (n=4). MDA levels were measured in heparin plasma. Inflammatory cytokines were measured in *ex vivo* LPS-stimulated whole blood cultures.

ing flowering at all would be preferable. Temperature probably also contributes to changes in GL content and pattern, since contents seem to be influenced not only by daytime temperature, but also by the difference between daytime and nighttime temperature (Engelen-Eigels et al., 2006).

Anti-inflammatory effects of watercress in humans – a new approach

Anti-inflammatory effects of watercress have not yet been investigated in humans. Isothiocyanates in general have been shown to possess anti-inflammatory properties through the regulation of cytokines of the TNF family primarily via activation of the NF-κB pathway (Heiss et al., 2001; Wierinckx et al., 2005; Dey et al., 2006; Karmakar et al., 2006). Also, studies with knockout mice showed that the nuclear factor erythroid 2-related factor 2 (Nrf2) plays an important role in the anti-inflammatory and antioxidative effects of PEITC (Boyanapalli et al., 2014).

Although, the differences of IL-10, IL-6, TNFα and MDA concentrations between control and watercress were not statistically significant due to high interindividual differences and a low case-number, the results of the present pilot study can be interpreted as a trend towards an anti-inflammatory and antioxidant effect of fresh watercress even at a single dose. Measurable effects after a single dose of watercress were also shown by Fogarty et al. (2013). In particular, the applied model for the induction of oxidative stress and inflammation in combination with cytokine analysis in whole blood cultures after *ex vivo* immune cell stimulation appears applicable to the relevant question. To consolidate these preliminary results, we plan to apply the outlined study protocol with a larger sample size over a longer intervention time in future studies. In addition, studies with patients suffering from diseases associated/accompanied with increased oxidative stress and inflammation (e.g. asthma) are planned. In these studies, additional biomarkers are necessary to examine the beneficial effects of watercress on human health. However, long-term studies with fresh watercress are difficult to realize due to its sharp taste,

gastric discomfort causing effects (two subjects complained about slight gastric discomfort after the watercress consumption), limited shelf life, and elaborate logistics in the daily distribution.

Conclusion/Outlook

As demonstrated, watercress can be successfully cultivated all year round in the greenhouse without a reduction in its valuable contents. To optimize the utilization of nutrients, the hydroponic culture will be combined with the cultivation of fish in one greenhouse in the near future. To circumvent the problem of limited shelf life other methods will be developed to provide humans with the valuable metabolites of watercress.

The human pilot study indicates that fresh watercress has positive effects on oxidative stress and inflammatory markers under induced pro-oxidative and pro-inflammatory conditions. Future long-term intervention studies with larger collectives must be carried out to confirm these results. In the ongoing project we aim to develop watercress dosage forms to overcome these obstacles. Processing technologies like gentle freeze-drying, grinding, subsequent encapsulation and gastric juice resistant coatings appear proper to ensure high tolerability, preservation of valuable ingredients (primarily gluconasturtiin and myrosinase), high bioavailability and compliance in long-term intervention studies. In future clinical studies with watercress extracts, the dose and duration must be carefully considered. A recent study observed an effect of PEITC in high concentrations on accumulation of reactive oxygen species and cytoskeletal changes, resulting as a consequence of cytotoxicity (Dayalan Naidu et al., 2018).

Authors' contributions

JPS, AH and JP conceived and designed the experiments. JPS, PW, MRL and JH performed the experiments. JPS, AH, TG and JP analyzed the data and prepared the manuscript. All authors read and approved the manuscript.

Acknowledgments

We would like to thank Stefan Göckemeyer, Poggenhagen, who drew our attention on this traditional vegetable and supported us with plants and advices on the outdoor cultivation of watercress. The authors acknowledge the financial support by the Faculty of Natural Sciences, Leibniz University Hannover, within the research initiative Soil - Plant - Human Interactions.

References

Ahuja, I., De Vos, R.C., Rohloff, J., Stoopen, G.M., Halle, K.K., Ahmad, S.J.N., Hoang L., Hall, R.D., Bones, A.M., 2016: *Arabidopsis* myrosinases link the glucosinolate-myrosinase system and the cuticle. Sci. Rep. 6, 38990. DOI: 10.1038/srep38990

Alagawany, M., Abd El-Hack, M., Al-Sagheer, A., Naiel, M., Saadeldin, I., Swelum, A., 2018: Dietary cold pressed watercress and coconut oil mixture enhances growth performance, intestinal microbiota, antioxidant status, and immunity of growing rabbits. Animals 8, 212. DOI: 10.3390/ani8110212

Asadi, M.S., Mirvaghefei, A.R., Nematollahi, M.A., Banaee, M., Ahmadi, K., 2012: Effects of watercress (*Nasturtium nasturtium*) extract on selected immunological parameters of rainbow trout (*Oncorhynchus mykiss*). Open Vet. J. 2, 32-39.

Bahramikia, S., Yazdanparast, R., 2010: Antioxidant efficacy of *Nasturtium officinale* extracts using various in vitro assay systems. J. Acupunct. Meridian Stud. 3, 283-290. DOI: 10.1016/S2005-2901(10)60049-0

Berger, R.G., Lunkenbein, S., Ströhle, A., Hahn, A., 2012: Antioxidants in food – mere myth or magic medicine. Crit. Rev. Food. Sci. Nutr. 52, 162-171. DOI: 10.1080/10408398.2010.499481

Boestfleisch, C., Hornbacher, J., Rumlow, A., Papenbrock, J., 2017: Contents of single glucosinolates are influenced by salinity in the halophyte *Lepidium latifolium*. In: De Kok, L., Hawkesford, M., Schnug, E. (eds.), Plant Sulfur Workshop Proceedings, Vol. 3, 2016/17, 103-114. Springer, Dordrecht. DOI: 10.1007/978-3-319-56526-2_10

Boyd, L.A., Mccann, M.J., Hashim, Y., Bennet, R.G., Gill, C.I.R., Rowland, I.R., 2006: Assessment of the anti-genotoxic, anti-proliferative, and anti-metastatic potential of crude watercress extract in human colon cancer cells. Nutr. Cancer 55, 232-241. DOI: 10.1207/s15327914nc5502_15

Boyanapalli, S.S., Paredes-Gonzalez, X., Fuentes, F., Zhang, C., Guo, Y., Pung, D., Saw, C.L., Kong, A.N., 2014: Nrf2 knockout attenuates the anti-inflammatory effects of phenethyl isothiocyanate and curcumin. Chem. Res. Toxicol. 27, 2036-2043. DOI: 10.1021/tx500234h

Casanova, N.A., Simoniello, M.F., Nigro, M.M.L., Carballo, M.A., 2017: Modulator effect of watercress against cyclophosphamide-induced oxidative stress in mice. Medicina (B Aires) 77, 201-206.

Casey, H., Smith, S.M., 1994: The effects of watercress growing on chalk headwater streams in Dorset and Hampshire. Environ. Pollut. 85(2), 217-228.

Chhajed, S., Misra, B.B., Tello, N., Chen, S., 2019: Chemodiversity of the glucosinolate-myrosinase system at the single cell-type resolution. Front. Plant Sci. 10, 618. DOI: 10.3389/fpls.2019.00618

Crisp, D.T., 1970: Input and output of minerals for a small watercress bed fed by chalk water. J. Appl. Ecol. 7, 117-140.

De Souza, D.A.D., Costa, P.M., Ribeiro, R.I., Vidigal, P.V., Pinto, F.C., 2016: Daily intake of watercress causes inhibition of experimental Ehrlich tumor growth. J. Bras. Patol. Med. Lab. 52, 393-399. DOI: 10.5935/1676-2444.20160063

Dey, M., Ribnicky, D., Kurmukov, A.G., Raskin, I., 2006: In vitro and in vivo anti-inflammatory activity of a seed preparation containing phenethylisothiocyanate. J. Pharmacol. Exp. Ther. 317, 326-333. DOI: 10.1124/jpet.105.096511

Engelen-Eigles, G., Holden, G., Cohen, J.D., Gardner, G., 2006: The effect of temperature, photoperiod, and light quality on gluconasturtiin concentration in watercress (*Nasturtium officinale* R. Br.). J. Agric. Food Chem. 54(2), 328-334. DOI: 10.1021/jf051857o

Fennell, J.F.M., 2006: Potential for watercress production in Australia. Rural Industries Research and Development Corporation, Kingston ACT, Australia.

Fenton-Navarro, B., Martínez, M.U., Castro, B.F., Castillo, O.M., López-Rodríguez, M., Arellanes, S.P., Hernández, A.V., 2018: Antioxidant and hypoglycemic effects of watercress (*Nasturtium officinale*) extracts in diabetic rats. Afr. J. Tradit. Complement. Altern. Med. 15, 68-79. DOI: 10.21010/ajtcam.v15i2.9

Fernández, J.A., Niñirola, D., Ochoa, J., Orsini, F., Pennisi, G., Gianquinto, G., Egea-Gilabert, C., 2016: Root adaptation and ion selectivity affects the nutritional value of salt-stressed hydroponically grown baby-leaf *Nasturtium officinale* and *Lactuca sativa*. Agr. Food Sci. 25(4), 230-239. DOI: 10.23986/afsci.58960

Fogarty, M.C., Hughes, C.M., Burke, G., Brown, J.C., Davison, G.W., 2013: Acute and chronic watercress supplementation attenuates exercise-induced peripheral mononuclear cell DNA damage and lipid peroxidation. Br. J. Nutr. 109, 293-301. DOI: 10.1017/S0007114512000992

Gill, C.I., Haldar, S., Boyd, L.A., Bennett, R., Whiteford, J., Butler, M., Pearson, J.R., Bradbury, I., Rowland, I.R., 2007: Watercress supplementation in diet reduces lymphocyte DNA damage and alters blood antioxidant status in healthy adults. Am. J. Clin. Nutr. 85, 504-10. DOI: 10.1093/ajcn/85.2.504

Hadjzadeh, M.A.R., Rajaei, Z., Moradi, R., Ghorbani, A., 2015: Effects of Hydroalcoholic extract of watercress (*Nasturtium officinale*) leaves on serum glucose and lipid levels in diabetic rats. Indian J. Physiol.

Pharmacol. 59, 223-30.

Heiss, E., Herhaus, C., Klimo, K., Bartsch, H., Gerhäuser, C., 2001: Nuclear factor kappa B is a molecular target for sulforaphane-mediated anti-inflammatory mechanisms. J. Biol. Chem. 276, 32008-32015. DOI: 10.1074/jbc.M104794200

Hofmann, T., Kuhnert, A., Schubert, A., Gill, C., Rowland, I.R., Pool-Zobel, B.L., Glei, M., 2009: Modulation of detoxification enzymes by watercress: in vitro and in vivo investigations in human peripheral blood cells. Eur. J. Nutr. 48, 483-91. DOI: 10.1007/s00394-009-0039-5

Hoseini, H.F., Gohari, A.R., Saeidnia, S., Majd, S., Hadjiakhoondi, A., 2009: The effect of *Nasturtium officinale* on blood glucose level in diabetic rats. PharmacologyOnLine 3, 866-871.

Hoshino, K., Akiyama, H., Goda, Y., Tanimura, A., Toyoda, M., 1998: Evaluation of antiallergic effects of extracts from ten kinds of vegetables using three in vitro assay systems. J. Food Hyg. Soc. Jpn. 39, 72-77.

Kaddour, R., Draoui, E., Baâtour, O., Mahmoudi, H., Tarchoun, I., Nasri, N., Lachaâl, M., 2013: Assessment of salt tolerance of *Nasturtium officinale* R. Br. using physiological and biochemical parameters. Acta Physiol. Plant. 35(12), 3427-3436. DOI: 10.1007/s11738-013-1377-8

Karami, M., Mostafazadeh, M., Sadeghi, H., Sadeghi, H., Mehraban, F., Panahi Kokhdan, E., Sayahi, M., Abtahi, S., 2018: Nephroprotective effect of *Nasturtium officinale* (Watercress) ethanol extract and vitamin E on vancomycin-induced nephrotoxicity in rats. J. Nat. Pharm. Prod. 13, e67178. DOI: 10.5812/jjnpp.67178

Karmakar, S., Weinberg, M.S., Banik, N.L., Patel, S.J., Ray, S.K., 2006: Activation of multiple molecular mechanisms for apoptosis in human malignant glioblastoma T98G and U87MG cells treated with sulforaphane. Neuroscience 141, 1265-1280. DOI: 10.1016/j.neuroscience.2006.04.075

Klimek-Szczykutowicz, M., Szopa, A., Ekiert, H., 2018: Chemical composition, traditional and professional use in medicine, application in environmental protection, position in food and cosmetics industries, and biotechnological studies of *Nasturtium officinale* (watercress) - a review. Fitoterapia.129, 283-292. DOI: 10.1016/j.fitote.2018.05.031

Kopsell, D.A., Barickman, T.C., Sams, C.C., Mcelroy, J.S., 2007: Influence of nitrogen and sulfur on biomass production and carotenoid and glucosinolate concentrations in watercress (*Nasturtium officinale* R. Br.). J. Agric. Food Chem. 55, 10628-10634. DOI: 10.1021/jf072793f

Li, Q., Zhan, M., Chen, W., Zhao, B., Yang, K., Yi, J., Huang, Q., Mohan, M., Hou, Z., Wang, J., 2016: Phenylethyl isothiocyanate reverses cisplatin resistance in biliary tract cancer cells via glutathionylation-dependent degradation of Mcl-1. Oncotarget 7, 10271-10282. DOI: 10.18632/oncotarget.7171

Müller, C., Schulz, M., Pagnotta, E., Ugolini, L., Yang, T., Matthes, A., Lazzeri, L., Agerbirk, N., 2018: The role of the glucosinolate-myrosinase system in mediating greater resistance of *Barbarea verna* than *B. vulgaris* to *Mamestra brassicae* larvae. J. Chem. Ecol. 44 (12), 1190-1205. DOI: 10.1007/s10886-018-1016-3

Mohammadi, J., Motlagh, F.T., Mohammadi, N., 2017: The effect of hydroalcoholic extract of watercress on parameters of reproductive and sex hormones on the diabetic rats. J. Pharm. Sci. Res. 9, 1334-1338.

Ozen, T., 2009: Investigation of antioxidant properties of *Nasturtium officinale* (watercress) leaf extracts. Acta Pol. Pharm. 66, 187-193.

Pink, D., 1993: Watercress: *Rorippa* spp. In: Genetic Improvement of Vegetable Crops, 579-583. Pergamon.

Quezada-Lázaro, R., Fernández-Zuñiga, E.A., García, A., Garza-González, E., Alvarez, L., Camacho-Corona, M.D.R., 2016: Antimycobacterial compounds from *Nasturtium officinale*. Afr. J. Tradit. Complement. Altern. Med. 13, 31. DOI: 10.4314/ajtcam.v13i2.3

Rose, P., Huang, Q., Ong, C.N., Whiteman, M., 2005: Broccoli and watercress suppress matrix metalloproteinase-9 activity and invasiveness of human MDA-MB-231 breast cancer cells. Toxicol. Appl. Pharmacol. 209, 105-113. DOI: 10.1016/j.taap.2005.04.010

Sadeghi, H., Mostafazadeh, M., Sadeghi, H., Naderian, M., Barmak, M.J., Talebianpoor, M.S., Mehraban, F., 2014: In vivo anti-inflammatory properties of aerial parts of *Nasturtium officinale*. Pharm. Biol. 52, 169-174. DOI: 10.3109/13880209.2013.821138

Shahani, S., Behzadfar, F., Jahani, D., Ghasemi, M., Shaki, F., 2017: Antioxidant and anti-inflammatory effects of *Nasturtium officinale* involved in attenuation of gentamicin-induced nephrotoxicity. Toxicol. Mech. Methods 27, 107-114. DOI: 10.1080/15376516.2016.1258748

Spínola, V., Pinto, J., Castilho, P.C., 2017: In vitro studies on the effect of watercress juice on digestive enzymes relevant to type 2 diabetes and obesity and antioxidant activity. J. Food Biochem. 41, e12335. DOI: 10.1111/jfbc.12335

Tsai, J.-T., Liu, H.-C., Chen, Y.-H., 2010: Suppression of inflammatory mediators by cruciferous vegetable-derived indole-3-carbinol and phenylethyl isothiocyanate in lipopolysaccharide activated macrophages. Mediators Inflamm. 2010, 1-5. DOI: 10.1155/2010/293642

Wierinckx, A., Breve, J., Mercier, D., Schultzberg, M., Drukarch, B., Van Dam, A.M., 2005: Detoxication enzyme inducers modify cytokine production in rat mixed glial cells. J. Neuroimmunol. 166, 132-143. DOI: 10.1016/j.jneuroim.2005.05.013

Yazdanparast, R., Bahramikia, S., Ardestani, A., 2008: *Nasturtium officinale* reduces oxidative stress and enhances antioxidant capacity in hypercholesterolaemic rats. Chem. Biol. Interact. 172, 176-184. DOI: 10.1016/j.cbi.2008.01.006

Yuan, J.M., Murphy, S.E., Stepanov, I., Wang, R., Carmella, S.G., Nelson, H.H., Hatsukami, D., Hecht, S.S., 2016a: 2-Phenethyl isothiocyanate, glutathione S-transferase M1 and T1 polymorphisms, and detoxification of volatile organic carcinogens and toxicants in tobacco smoke. Cancer Prev. Res. (Phila) 9, 598-606. DOI: 10.1158/1940-6207.CAPR-16-0032

Yuan, J.-M., Stepanov, I., Murphy, S.E., Wang, R., Allen, S., Jensen, L., Strayer, L., Adams-Haduch, J., Upadhyaya, P., Le, C., Kurzer, M.S., Nelson, H.H., Yu, M.C., Hasukami, D., Hecht, S.S., 2016b: Clinical trial of 2-phenethyl isothiocyanate as an inhibitor of metabolic activation of a tobacco-specific lung carcinogen in cigarette smokers. Cancer Prev. Res. (Phila) 9, 396-405. DOI: 10.1158/1940-6207.CAPR-15-0380

Zafar, R., Zahoor, M., Shah, A.B., Majid, F., 2017: Determination of antioxidants and antibacterial activities, total phenolic, polyphenol and pigment contents in *Nasturtium officinale*. PharmacologyOnLine 1, 11-18.

ORCID
Theresa Greupner 0000-0001-7510-4654
Juttta Papenbrock 0000-0003-0942-4072

Address of the corresponding author:
Jutta Papenbrock, Institute of Botany, Leibniz University Hannover, Herrenhäuser Str. 2, 30419 Hannover, Germany
E-mail: papenbrock@botanik.uni-hannover.de

Chapter 2.2 Immunomodulating effect of the consumption of watercress (*Nasturtium officinale*) on exercise-induced inflammation in humans

foods

MDPI

Article

Immunomodulating Effect of the Consumption of Watercress (*Nasturtium officinale*) on Exercise-Induced Inflammation in Humans

Hendrik Schulze [1], Johann Hornbacher [2], Paulina Wasserfurth [1], Thomas Reichel [3], Thorben Günther [4], Ulrich Krings [4], Karsten Krüger [3], Andreas Hahn [1], Jutta Papenbrock [2] and Jan P. Schuchardt [1,*]

[1] Institute of Food Science and Human Nutrition, Leibniz University Hannover, D-30167 Hannover, Germany; schulze@nutrition.uni-hannover.de (H.S.); wasserfurth@nutrition.uni-hannover.de (P.W.); hahn@nutrition.uni-hannover.de (A.H.)
[2] Institute of Botany, Leibniz University Hannover, D-30419 Hannover, Germany; j.hornbacher@botanik.uni-hannover.de (J.H.); jutta.papenbrock@botanik.uni-hannover.de (J.P.)
[3] Department of Exercise Physiology and Sports Therapy, Institute of Sport Science, Justus Liebig University Giessen, D-35394 Giessen, Germany; thomas.reichel@sport.uni-giessen.de (T.R.); karsten.krueger@sport.uni-giessen.de (K.K.)
[4] Institute of Food Chemistry, Leibniz University Hannover, D-30167 Hannover, Germany; thorben.detering@lci.uni-hannover.de (T.G.); krings@lci.uni-hannover.de (U.K.)
* Correspondence: schuchardt@nutrition.uni-hannover.de; Tel.: +49-511-7622987

Citation: Schulze, H.; Hornbacher, J.; Wasserfurth, P.; Reichel, T.; Günther, T.; Krings, U.; Krüger, K.; Hahn, A.; Papenbrock, J.; Schuchardt, J.P. Immunomodulating Effect of the Consumption of Watercress *(Nasturtium officinale)* on Exercise-Induced Inflammation in Humans. *Foods* **2021**, *10*, 1774. https://doi.org/10.3390/foods10081774

Academic Editors: Franziska S. Hanschen, Sascha Rohn and Laura Jaime

Received: 21 May 2021
Accepted: 28 July 2021
Published: 30 July 2021

Publisher's Note: MDPI stays neutral with regard to jurisdictional claims in published maps and institutional affiliations.

Abstract: The vegetable watercress (*Nasturtium officinale* R.Br.) is, besides being a generally nutritious food, a rich source of glucosinolates. Gluconasturtiin, the predominant glucosinolate in watercress, has been shown to have several health beneficial properties through its bioactive breakdown product phenethyl isothiocyanate. Little is known about the immunoregulatory effects of watercress. Moreover, anti-inflammatory effects have mostly been shown in in vitro or in animal models. Hence, we conducted a proof-of-concept study to investigate the effects of watercress on the human immune system. In a cross-over intervention study, 19 healthy subjects (26.5 ± 4.3 years; 14 males, 5 females) were given a single dose (85 g) of fresh self-grown watercress or a control meal. Two hours later, a 30 min high-intensity workout was conducted to promote exercise-induced inflammation. Blood samples were drawn before, 5 min after, and 3 h after the exercise unit. Inflammatory blood markers (IL-1β, IL-6, IL-10, TNF-α, MCP-1, MMP-9) were analyzed in whole blood cultures after ex vivo immune cell stimulation via lipopolysaccharides. A mild pro-inflammatory reaction was observed after watercress consumption indicated by an increase in IL-1β, IL-6, and TNF-α, whereas the immune response was more pronounced for both pro-inflammatory and anti-inflammatory markers (IL-1β, IL-6, IL-10, TNF-α) after the exercise unit compared to the control meal. During the recovery phase, watercress consumption led to a stronger anti-inflammatory downregulation of the pro-inflammatory cytokines IL-6 and TNF-α. In conclusion, we propose that watercress causes a stronger pro-inflammatory response and anti-inflammatory counter-regulation during and after exercise. The clinical relevance of these changes should be verified in future studies.

Keywords: watercress; cruciferous vegetables; glucosinolates; gluconasturtiin; anti-inflammatory; pro-inflammatory

1. Introduction

With the revival of domestic greens watercress (*Nasturtium officinale* R.Br.), a member of the Brassicaceae family, gains a growing interest in science. The semi-aquatic plant species native to Europe and Asia is often consumed as a salad or garnish, or as part of a soup, especially in the Mediterranean kitchen. It is valued for its high nutrient density caused by a low energy content and high amounts of vitamins (B1, B2, B3, B6, C, E), minerals (calcium, iron), and phytochemicals (polyphenols, terpenes) [1–3]. Like all members of the

Brassicaceae family, watercress contains mustard oil glycosides or glucosinolates (GLS), of which gluconasturtiin is the predominant GLS in watercress. As a precursor, it is converted into the bioactive compound phenethyl isothiocyanate (PEITC) upon tissue disruption due to the action of the thioglucosidase myrosinase.

Several studies investigated the health beneficial effects of watercress and PEITC including antioxidative, anti-inflammatory, antidiabetic, anti-allergic, antibacterial, hypolipemic, cardioprotective, and anticancer effects (reviewed in [2]). While most of these effects have been observed in vitro or in animal studies, only a few human intervention studies with watercress have been carried out. Moreover, human intervention studies that administered watercress have mainly focused on antioxidative [4,5] and anticancer effects [6]. The influence of watercress on the immune system, in particular anti-inflammatory activity, has barely been investigated in human studies thus far. There has yet been no confirmation that watercress and its ingredients gluconasturtiin/PEITC act in a similar way in humans compared to effects observed in vitro, namely, by inhibiting the pro-inflammatory nuclear factor kappa B (NfκB) pathway [7]. Because the NfκB pathway can be stimulated directly by reactive oxygen species (ROS) [8] or indirectly by the ROS-dependent heat shock response [9,10], antioxidants might attenuate the exercise-induced inflammation [11]. As a consequence, it is necessary to determine the levels of antioxidants and their capacity in watercress. Moreover, it remains unknown as to whether other gluconasturtiin metabolites are formed in vivo and how they contribute to an antioxidative effect such as that indicated for benzenepropanenitrile [12].

We performed a pilot study with four subjects to examine the effect of a single dose of fresh watercress on various biomarkers of exercise-induced inflammation [13]. On the basis of the results of that previous study, where we observed indications for anti-inflammatory effects, we conducted this follow-up study with a greater number of subjects to further characterize the inflammatory response of watercress consumption. After consuming 85 g of fresh watercress, untrained subjects had to complete a high-intensity workout to induce a pro-inflammatory condition. Inflammatory blood markers (IL-1β, IL-6, IL-10, TNF-α, MCP-1, MMP-9) were analyzed in whole blood cultures after ex vivo immune cell stimulation via lipopolysaccharides (LPS).

2. Materials and Methods

2.1. Plant Material

The administered watercress *(Nasturtium officinale)* was obtained from the Institute of Botany, Leibniz University Hannover. Cuttings were taken for propagation and cultivated in a hydroponic greenhouse system using a Hoagland solution. After 8 weeks, the plant material was harvested freshly on a daily basis. Following a 45 min wet transport, it was cut as little as necessary for consumption.

2.2. Analysis of Glucosinolates by HPLC/LC–MS

GLS were analyzed by HPLC–UV according to Hornbacher et al. [14]. The GLS content of the watercress samples were measured in triplicate. All standard substances were checked for identity. For the identification of the GSL in *N. officinale*, samples were analyzed by liquid chromatography–mass spectrometry (LC–MS). A volume of 10 µL was injected into the HPLC system (Shimadzu, Darmstadt, Germany) and separated on a Knauer Vertex Plus column (250 × 4 mm, 5 µm particle size, packing material ProntoSIL 120-5 C18-H) equipped with a pre-column (Knauer, Berlin, Germany). A water (solvent A)–methanol (solvent B), both containing 2 mM ammonium acetate, gradient was used with a flow rate of 0.8 mL/min at 30 °C. For measuring the samples, the following gradient was used: 10–90% B for 35 min, 90% for 2 min, 90–10% B for 1 min, and 10% B for 2 min. Detection of the spectra in the range 190–800 nm was performed with a diode array detector (SPD-M20A, Shimadzu, Darmstadt, Germany). The HPLC system was coupled to an AB Sciex TripleTOF mass spectrometer (AB Sciex TripleTOF 4600, Canby, OR, USA). At a temperature of 600 °C and an ion spray voltage floating of −4500 V, the negative

electrospray ionization (ESI) was performed. For the ion source gas one and two 50 psi were used and for the curtain gas 35 psi. In the range of 100–1500 Da in the TOF range, the mass spectra as well as the MS/MS spectra from 150–1500 Da at a collision energy of −10 eV were recorded. Peaks were identified by analyzing the characteristic mass fragments of ds-4-methoxyglucobrassicin (195, 398, 433, 795) and ds-glucoarabishirsutain (195, 382, 417, 763). Due to lack of standards of the GSLs fractions of the measured samples were collected in a fraction collector (FRC-10A Shimadzu, Darmstadt, Germany), dried in a vacuum centrifuge, and dissolved in 300 µL ultrapure water. The retention time for every GSL was determined by measuring either the collected fraction or the authentic standard (Phytolab, Vestenbergsgreuth, Germany) with the HPLC system, as described above.

2.3. Measurement of Antioxidant Contents and Antioxidant Capacity

The measurements of carotenoid, total phenol and total flavonoid contents, as well as the measurement of the oxygen radical absorbance capacity (ORAC), were performed according to Boestfleisch et al. [15].

Tocopherol contents were analyzed according to Cruz et al. [16] with modifications. Small portions of finely ground fresh sample (1.0 g) were weighed accurately into amber glass vials containing ascorbic acid (50 mg), butylated hydroxytoluene (1 mg), and internal standard (1 µg δ-tocopherol). Samples were homogenized with methanol (2 mL) by vortex mixing for 1 min. Then, dichloromethane (4 mL) was added and vortex-mixed for 1 min. Subsequently, 0.9% (w/v) NaCl (1 mL) was added, the mixture was homogenized (1 min) and centrifuged (3 min, 14,000× g), and the clear lower layer was transferred to an amber flask. Extraction was repeated twice with dichloromethane. The extracts were combined and vacuum-dried in a vacuum centrifuge (Eppendorf, Hamburg, Germany) at 25 °C. The extract was recovered with 1 mL of n-hexane and anhydrous sodium sulfate was added (around 100 mg). After an additional centrifugation (5 min, 14,000× g), the supernatant was analyzed immediately. Analysis was performed with an HPLC system equipped with a Nucleodur C18 column (250 mm × 4.6 mm; Macherey-Nagel, Düren, Germany). Tocopherols were separated with an isocratic gradient consisting of 90% n-hexane and 10% diethyl ether at room temperature and a flow rate of 1 mL/min. Analytes were monitored with a fluorescence detector (Shimadzu, Duisburg, Germany). Excitation was performed at 289 nm and fluorescence of analytes was analyzed at 331 nm.

2.4. Human Study Design and Subjects

An overview of the timeline of the study and the interventions in particular is shown in Figure 1. The inclusion criteria of the cross-over study were age between 18 and 35 years, BMI between 18 and 30 kg/m^2, and less than two hours of moderate exercise per week, classifying these participants as untrained. For the questionnaire-based assessment of the training status, we factored in leisure time physical activities such as jogging or weight-lifting, as well as daily non-athletic exertions such as movement by foot or bike. The exclusion criteria were cardiovascular or metabolic disease, smoking, pregnancy, drug or alcohol dependency, concurrent participation in another clinical trial or in another study within the last 30 days, and intake of antioxidative or antiphlogistic medicine or dietary supplements.

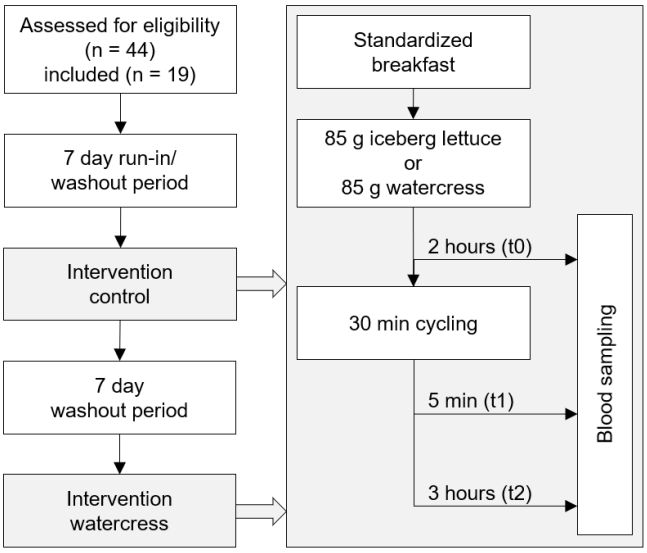

Figure 1. Flow diagram showing the timeline of the study.

As part of a run-in/washout phase, subjects refrained from consuming foods rich in polyphenols, vitamin C and E (mainly berries, nuts, and vegetables of the Brassicaceae family) seven days before each examination. To ensure compliance, participants received written instructions and a list of foods that should not be consumed. On the basis of the consumed amount in similar studies [4,5,13], subjects ate a single dose of 85 g of fresh watercress accompanied by a standard breakfast (two buns, cream cheese or oat spread, yoghurt or balsamic dressing). In the control group, 85 g of iceberg lettuce was administered instead. Two hours after consumption, the first blood sample (t0) was taken. Immediately after blood draw, the subjects completed a 30 min high-intensity endurance workout on echo bikes within a parameter range of 80–92% HR_{max}, 120–145 W, and a final rating of perceived exertion of 17.8. Throughout the workout, heart rates were recorded using a heart rate monitor watch with a Bluetooth heart rate sensor chest strap (RC 14.11, Sigma-Elektro, Neustadt, Germany). Additional blood samples were taken 5 min (t1) and 3 h (t2) after the end of the exercise. The subjects were served a lunch in the meantime consisting of a potato soup. All blood samples were obtained by venipuncture of an arm vein using Multifly needles (Sarstedt, Nürnbrecht, Germany) into heparin plasma monovettes (Sarstedt, Nürnbrecht, Germany). To assure that subjects did not enter the examination with elevated inflammatory markers due to an infection, we determined C-reactive protein in serum using serum monovettes (Sarstedt, Nürnbrecht, Germany). Both interventions (control and watercress) were conducted identically with an intermediary washout phase of 7 days.

The study was carried out following the rules of the Declaration of Helsinki and was approved by the Ethics Committee at the Medical Chamber of Lower Saxony (30/37/2020, Hannover, Germany, 10/2020).

2.5. Measurement of Inflammatory Markers by Bio-Plex Multiplex Immunoassay

The freshly drawn blood samples were stimulated ex vivo in whole blood cultures via lipopolysaccharides (LPS). Therefore, samples were immediately diluted 1:5 with the cell culture medium RPMI 1640 including 20 mmol HEPES and L-glutamine (Sigma-Aldrich, Hamburg, Germany) and added antibiotics (100 U/mL penicillin and 100 µg/mL streptomycin; Sigma-Aldrich, Hamburg, Germany). The samples were seeded into 12-well

microtiter plates and mixed with 10 ng/mL (final concentration) LPS from *Escherichia coli* (Sigma-Aldrich, Hamburg, Germany). The plates were incubated for 24 h at 37 °C without a CO_2 application. The used HEPES buffer is able to stabilize the pH over 24 h. The supernatants were frozen at −80 °C until analysis.

The levels of the inflammatory markers (IL-1β, IL-6, IL-10, TNF-α, MCP-1, MMP-9) in whole blood culture supernatant were simultaneously determined using a human Magnetic Luminex Assay (Bio-Techne, Abingdon, Oxon, UK) and a Magpix Luminex instrument (Luminex Corp, Austin, TX, USA).

2.6. Data Analysis and Statistical Methods

Data are presented as the means ± standard deviation. All variables were tested for normal distribution by Shapiro–Wilk test. In the case of not normally distributed data, a suitable transformation was applied, and parametric tests were used. Differences among inflammatory markers were analyzed using ANOVA with repeated measures. In addition, groups were compared using a *t*-test for dependent means. To calculate correlations, we utilized Pearson correlation (parametric data) and Spearman's rho correlation (non-parametric data). Statistical significance was regarded as values of $p \leq 0.05$. Analyses were conducted using Infostat (version 2012; University of Córdoba, Córdoba, Argentine) and SPSS (version 27; SPSS Inc., Chicago, IL, USA).

3. Results

Of the 21 recruited subjects, 19 completed the study (Table 1). Incomplete study data were excluded from statistical analyses. One subject failed to participate because of illness. Another subject showed increased serum levels of C-reactive protein (>0.5 mg/L), indicating an elevated systemic inflammation. No health- or workout-related incidents occurred during the study, with the exception of one subject taking a two-minute break from the exercise due to total exhaustion.

Table 1. Characterization of the study population.

Parameters	
Sex (*n*, females/males)	5/14
Age (years)	26.5 ± 4.3
Weight (kg)	72.9 ± 12.5
Height (m)	1.77 ± 0.09
BMI (kg/m^2)	23.3 ± 3.5
WHR (females/males)	0.74 ± 0.04/0.84 ± 0.05

BMI = body mass index, WHR = waist-to-hip ratio.

3.1. Plant Material

3.1.1. Levels of Glucosinolates

Gluconasturtiin was recognized as the predominant GLS in watercress with a fraction of 90.5 ± 1.1% of the total GLS content. In addition, minor amounts of glucoarabishirsutain (5.3 ± 0.8%), glucobrassicin (1.4 ± 0.4%), neoglucobrassicin (1.4 ± 0.3%), and 4-methoxyglucobrassicin (1.4 ± 0.4%) were found (Figure 2, Table A1). In the course of the study, GLS contents varied notably with the most impactful difference in gluconasturtiin of 36% at day 3 compared to the previous day. This resulted in a difference of 34% of the total GLS content while maintaining the partial composition of the GLS profile.

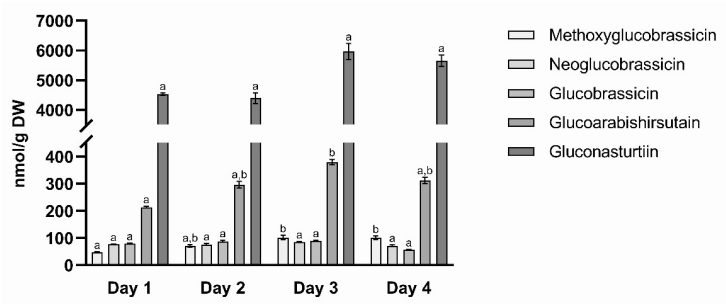

Figure 2. Mean concentration of different glucosinolates (GLS) (nmol/g DW) in watercress at different sampling times. The standard deviation represents the values for three technical replicates. Analysis of variance (ANOVA) was performed with Infostat. Means with a common letter are not significantly different.

3.1.2. Levels of Antioxidants and Antioxidant Capacity

Contents of flavonoids as well as ascorbic acid in analyzed watercress were similar at all sampling days (Table A2). Contents of total phenols were slightly higher in samples taken at day 3 and day 4, whereas carotenoid contents were slightly higher at day 2 and day 4. Tocopherol contents as well as ORAC were similar at all sampling days.

3.2. Levels of Inflammatory Blood Markers

Statistical analysis using the ANOVA with repeated measures showed significant differences between the sampling times for all analyzed parameters ($p \leq 0.001$). Hence, the acute exercise affected concentrations of all measured inflammatory markers. In addition, the same analysis pointed out that the consumption of watercress led to significant differences for the levels of IL-1β, IL-6, and IL-10 across all sampling times (IL-1β ($p = 0.006$), IL-6 ($p = 0.006$), IL-10 ($p \leq 0.001$)). The remaining parameters showed no significant differences (TNF-α ($p = 0.382$), MCP-1 ($p = 0.192$), MMP-9 ($p = 0.118$)). With regards of the varying GLS levels of the plant material, no correlations with the inflammatory markers were found.

Significantly higher concentrations of the pro-inflammatory cytokines IL-1β (16%), IL-6 (33%), and TNF-α (30%), as well as the enzyme MMP-9 (22%), were observed in the watercress group compared to the control group two hours after the watercress consumption (t0) (Figure 3, Table A3). Upon exercise-stimulation (t1), the control group showed a significant rise in all inflammatory markers, specifically IL-6 (33%), IL-10 (47%), MCP-1 (53%), and MMP-9 (53%) with IL-1β and TNF-α showing no reaction. Compared to the control breakfast, levels of IL-1β, IL-6, IL-10, and TNF-α were significantly higher after the watercress breakfast (31%, 32%, 51%, and 23%, respectively). To determine if the consumption of watercress resulted in a stronger increase of the cytokines regardless of the pre-exercise levels, we compared the differences (t1 − t0). Thereby, a significant stronger upregulation of the anti-inflammatory cytokine IL-10 was found. After the recovery phase (t2), all inflammatory markers except MMP-9 decreased. A comparison of the differences (t2 − t1) between the watercress and the control group revealed a significantly stronger downregulation of the pro-inflammatory cytokines IL-6 and TNF-α and a trend in IL-1β ($p = 0.062$). In the case of TNF-α, the level at t2 was even lower compared to the pre-exercise state of the control group. This post-exercise downregulation can also be observed in the ratio of the anti-inflammatory IL-10 and the pro-inflammatory IL-1β (Figure 4). The watercress consumption influenced the ratio 3 h after exercise towards the anti-inflammatory reaction.

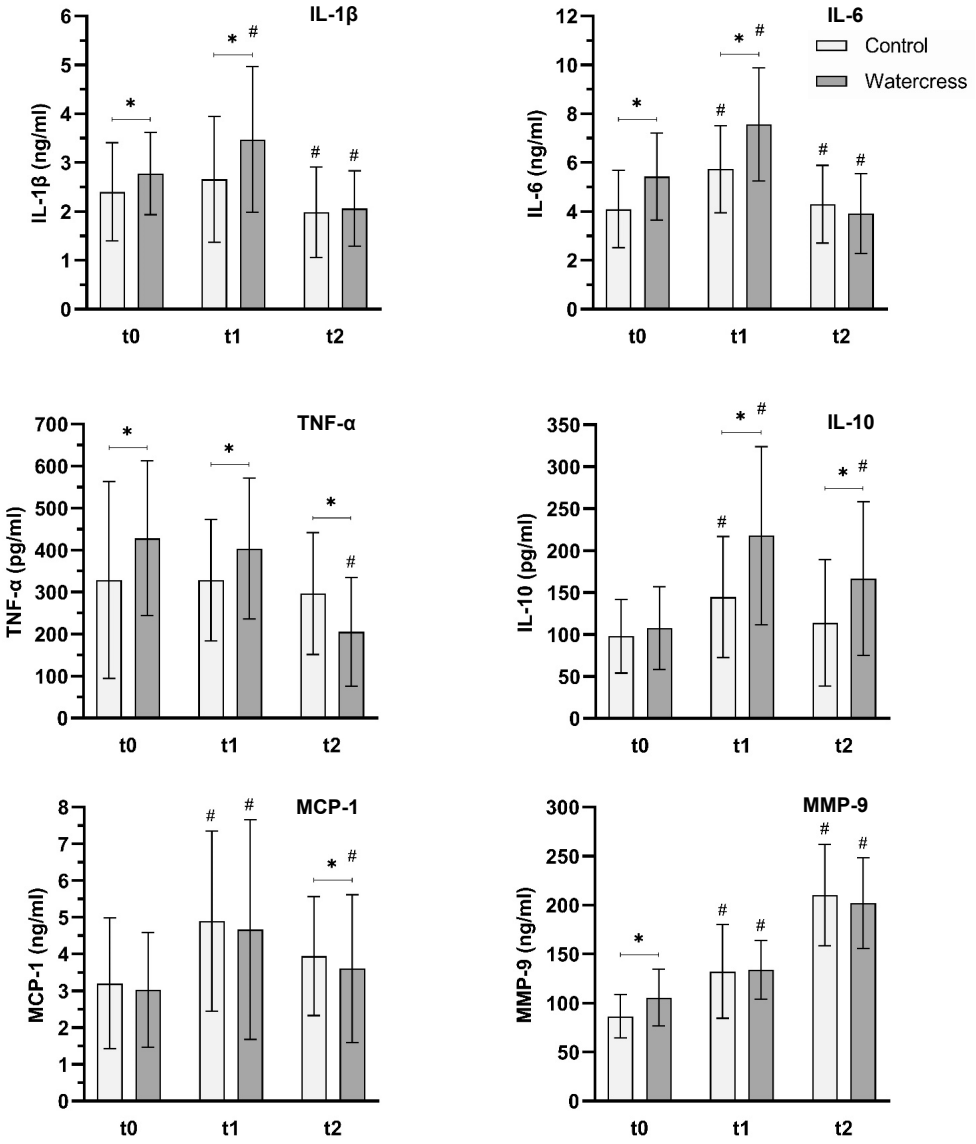

Figure 3. Effect of acute watercress consumption on blood markers of inflammation (IL-1β, IL-6, IL-10, TNF-α, MCP-1, MMP-9) in ex vivo LPS-stimulated whole blood cultures after high-intensity workout in untrained subjects. t0, pre-exercise; t1, 5 min post-exercise; t2, 3 h post-exercise. Analysis of variance (ANOVA) was performed with SPSS. * Significant difference between control and watercress. # Significant difference to previous sampling point.

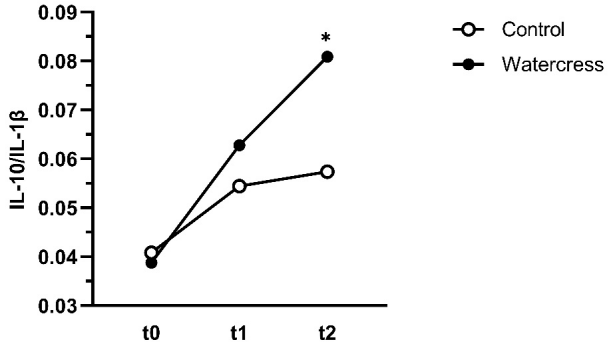

Figure 4. Effect of acute watercress consumption on the ratio of IL-10 (anti-inflammatory) and IL-1β (pro-inflammatory). t0, pre-exercise; t1, 5 min post-exercise; t1, 3 h post-exercise. Analysis of variance (ANOVA) was performed with SPSS. * Significant difference between control and watercress.

4. Discussion

Many food compounds are known to assure the maintenance of the immune system or improve its performance [17]. By interacting with ROS or affecting cytokine biology, their intake can modulate immune function. A wide variety of anti-inflammatory nutrients has been investigated thus far. While many act as antioxidants and, hence, indirectly modulate the ROS-dependent NfκB activation [18] such as ascorbic acid, glutathione, or carotenoids, others operate as pro-resolving mediators such as omega-3 fatty acids [19].

A common misconception is that pro-inflammatory processes at all times need to be annihilated to prevent the body from harm. Similar to oxidative stress, pro-inflammatory processes can have both detrimental and beneficial effects to the human body. When inflammatory processes become chronic, they often have negative impacts. Chronic low-grade inflammation is associated with a wide range of chronic conditions, such as the metabolic syndrome, cardiovascular disease, type 2 diabetes, and non-alcoholic fatty liver disease. However, if the body is able to resolve inflammatory processes, they can provide signals for adaptation in physiological contexts such as sport [20]. In its acute form, it is generally a beneficial procedure, which removes stimuli and initiates the repair system. As the first line of defense, pro-inflammatory cytokines such as IL-1β, IL-6, and TNF-α promote the activation and secretion of more cytokines and acute-phase proteins as well as the proliferation and differentiation of T- and B-cells. The time-delayed increase of the cytokine IL-10 has been widely recognized as a suppression of the inflammatory response by its downregulating effects on TNF-α and IL-1 [21–23]. The immune system acts through a fluctuation between a pro-inflammatory response and an anti-inflammatory or inflammation resolving counter-regulation. An increase in the magnitude of the fluctuation could be interpreted as positive for the capacity of the system. Thus, a mild activation of the immune system through dietary components might aid in resolving inflammation by a preceding mobilization. We assume that this immunomodulating effect also applies to watercress and its ingredients.

Upon exercise- and LPS-stimulation, a solid, non-excessive immune reaction was observed in IL-6 and IL-10, with a greater response after the watercress consumption. Interestingly, the subsequent inflammatory counter-regulation of IL-6, TNF-α, and IL-1β was more pronounced in the watercress group, which likely was a result of the higher exercise-induced levels of IL-10. This shift towards an anti-inflammatory response after the watercress consumption was supported by the increased ratio of IL-10 and IL-1β. Our results suggest that watercress intake stimulates the immune system, which might enhance its metabolic capacity. The finding that the consumption of watercress causes an initial pro-inflammatory reaction followed by a greater exercise-induced response in both pro- and

anti-inflammatory markers is remarkable and has not been observed thus far. We assume that gluconasturtiin, in particular PEITC, is responsible for the observed immunomodulating effect, where PEITC might operate as an activator in T-lymphocytes or macrophages or their receptors and thereby stimulates or sensitizes the cytokine production. It is also conceivable that PEITC activates the heat shock response, which leads to a stimulation of the pro-inflammatory NfκB pathway [24]. Another explanation is that specific components of watercress might interfere with the immunometabolism and thereby stimulate its function. Although the average contents of secondary metabolites besides gluconasturtiin and the ORAC are in the lower range of vegetables, it is likely that the observed effects are mainly caused by the GLS. The extraction procedure for the evaluation of the ORAC uses methanol as organic solvent, which inhibits the hydrolysis of gluconasturtiin to PEITC. However, PEITC would contribute only very little to the overall ORAC, since its capacity to scavenge ROS was reported to be 1.9 µg TE/mg PEITC [25]. The levels of gluconasturtiin in the obtained watercress resemble the results of the pilot study [13] and were in the same range of reported contents for raw watercress [26].

In contrast to our results, PEITC and watercress extracts have thus far been shown to possess only anti-inflammatory and no pro-inflammatory properties [27–31]. The pilot study, on which this investigation is based on, aligns with these observations [13]. In vitro studies presume the mechanism behind this effect of PEITC in the inhibition of the pro-inflammatory NfκB pathway in macrophages, possibly through the modulation of toll-like receptors [31–33]. Due to the redox-sensitivity of NfκB, the activation of the antioxidative nuclear factor erythroid 2-related factor 2 (Nrf2) pathway by PEITC plays a considerable role in its anti-inflammatory effect [34]. Previous human intervention studies have focused mainly on those antioxidative effects of watercress. They showed that a regular consumption as well as a single dose of watercress reduces the oxidative stress in various biomarkers [4,5]. On the basis of the antioxidative and thereby assumed anti-inflammatory effects, the outcome of this study does not align with the previous literature. Although PEITC is able to promote oxidative stress at very high concentrations, presumably acting as a scavenger for glutathione [35], it remains debatable as to whether a single dose of 85 g of watercress provides the body with the necessary range of concentration. In consequence of the redox-sensitivity of NfκB, an initial pro-oxidative effect after the consumption of watercress could explain the simultaneously increased cytokine levels of IL-1β, IL-6, and TNF-α. The pro-oxidative state would be further enhanced by the exercise, which subsequently results in an even more pronounced pro-inflammatory response in the watercress group and a stronger induction of the counter-regulatory Nrf2-mediated antioxidant response that is observed in the recovery phase.

5. Conclusions

The course of inflammatory markers after the watercress consumption with initially increasing pro-inflammatory markers and a higher release of an anti-inflammatory marker in the recovery phase has not yet been described in the literature. We interpret this observation with a mild activation of the immune system resulting in a stronger pro-inflammatory reaction, which is more effectively resolved by a powerful anti-inflammatory counter-regulation. This thesis and the clinical relevance have to be investigated in future studies. Moreover, cell culture studies are necessary to explore the underlying effects of watercress components on leukocytes. Likewise, it must not be ignored that the immune cells were stimulated ex vivo by LPS. The results and the possible effects on the immune system can therefore not be directly transferred to the situation in vivo. Because watercress is a complex food with considerable amounts of other potentially immunomodulating substances besides PEITC, a causal relationship between the observed effects and gluconasturtiin/PEITC cannot be stated. A clinical trial with isolated gluconasturtiin/PEITC should be conducted in order to confirm the effect and whether its magnitude is influenced by other components. The variable GLS levels of watercress show the need for developing standardized extracts or supplements. Thereby, future clinical trials are provided with a

standardized GLS dosage and can overcome logistic and sensory barriers of administering raw watercress.

Author Contributions: Conceptualization, K.K., A.H. and J.P.S.; methodology, J.H., K.K. and J.P.S.; formal analysis, H.S., J.H. and T.R.; investigation, H.S., J.H., P.W., T.R., U.K. and T.G.; resources, J.H., K.K., A.H. and J.P.S.; writing—original draft preparation, H.S. and J.P.S.; writing—review and editing, H.S., J.H., J.P., K.K. and J.P.S.; visualization, H.S.; supervision, J.P. and J.P.S.; project administration, J.P.S. All authors have read and agreed to the published version of the manuscript.

Funding: This research received no external funding.

Institutional Review Board Statement: The study was conducted according to the guidelines of the Declaration of Helsinki, and approved by the Ethics Committee at the Medical Chamber of Lower Saxony (30/37/2020, Hannover, Germany, 10/2020).

Informed Consent Statement: Informed consent was obtained from all subjects involved in the study.

Acknowledgments: We would like to thank Julia Volker for help in the laboratory. The publication of this article was funded by the Open Access Fund of Leibniz University Hannover.

Conflicts of Interest: The authors declare no conflict of interest.

Appendix A

Table A1. Mean concentration of different glucosinolates (GLS) (nmol/g DW) in watercress at different sampling times. The standard deviation represents the values for three technical replicates. Analysis of variance (ANOVA) was performed with Infostat. Means with a common letter are not significantly different.

GLS	Day 1	Day 2	Day 3	Day 4
4-Methoxyglucobrassicin	46.8 ± 2.1 ^{a}	70.6 ± 5.0 ^{a,b}	101.3 ± 8.3 ^{b}	101.5 ± 6.3 ^{b}
Glucobrassicin	79.3 ± 2.2 ^{a}	87.8 ± 3.2 ^{a}	90.5 ± 1.6 ^{a}	56.6 ± 1.3 ^{a}
Neoglucobrassicin	76.6 ± 1.4 ^{a}	76.4 ± 3.7 ^{a}	85.5 ± 1.7 ^{a}	71.3 ± 3.3 ^{a}
Glucoarabishirsutain	213.5 ± 2.6 ^{a}	296.4 ± 12.4 ^{a,b}	379.6 ± 10.1 ^{b}	311.8 ± 11.8 ^{a,b}
Gluconasturtiin	4525 ± 45 ^{a}	4393 ± 180 ^{a}	5966 ± 266 ^{a}	5655 ± 196 ^{a}
Total	4942 ± 46 ^{a}	4924 ± 201 ^{a}	6623 ± 285 ^{a}	6196 ± 215 ^{a}

Table A2. Mean contents of antioxidative substances (total flavonoids and phenols, ascorbic acid, α- and γ-tocopherol) and antioxidative capacity (ORAC) in watercress at different sampling times. The standard deviation represents the values for three technical replicates. Analysis of variance (ANOVA) was performed with Infostat. Means with a common letter are not significantly different.

Parameters	Day 1	Day 2	Day 3	Day 4
Total flavonoids (ng CE/g FW)	415 ± 20 ^{a}	470 ± 43 ^{a,b}	509 ± 49 ^{a,b}	529 ± 46 ^{b}
Total phenols (ng GAE/g FW)	832 ± 41 ^{a}	980 ± 90 ^{a,b}	1145 ± 42 ^{b}	1178 ± 128 ^{b}
Ascorbic acid (µg/g FW)	578 ± 31 ^{a}	638 ± 55 ^{a}	750 ± 85 ^{a}	687 ± 31 ^{a}
Carotenoids (µg/g FW)	84.9 ± 8.8 ^{a}	108.9 ± 7.7 ^{a}	90.3 ± 22.4 ^{a}	118.9 ± 16.3 ^{a}
α-Tocopherol (µg/g FW)	3.63 ± 0.02 ^{a}	5.11 ± 0.11 ^{b}	5.58 ± 0.17 ^{b}	5.27 ± 0.03 ^{b}
γ-Tocopherol (ng/g FW)	70.8 ± 5.5 ^{a}	86.9 ± 0.4 ^{a}	72.4 ± 3.6 ^{a}	60.6 ± 5.1 ^{a}
ORAC (µmol TE/g FW)	19.6 ± 2.7 ^{a}	20.3 ± 1.1 ^{a}	21.4 ± 1.5 ^{a}	20.7 ± 2.4 ^{a}

CE = catechin equivalents (standard curve was performed with catechin), GAE = gallic acid equivalents (standard curve was performed with gallic acid), ORAC = oxygen radical absorbance capacity, TE = trolox equivalents (standard curve was performed with trolox).

Table A3. Effect of acute watercress consumption on blood markers of inflammation (IL-1β, IL-6, IL-10, TNF-α, MCP-1, MMP-9) in ex vivo LPS-stimulated whole blood cultures after high-intensity workout in untrained subjects.

Parameter	Control			Watercress		
	t0	t1	t2	t0	t1	t2
IL-1β (ng/mL)	2.40 ± 0.98 *	2.66 ± 1.26 *	1.98 ± 0.90 #	2.77 ± 0.82 *	3.47 ± 1.45 *,#	2.06 ± 0.75 #
IL-6 (ng/mL)	4.09 ± 1.54 *	5.73 ± 1.73 *,#	4.29 ± 1.55 #	5.43 ± 1.73 *	7.56 ± 2.25 *,#	3.91 ± 1.59 #
IL-10 (pg/mL)	98.0 ± 42.6	144.5 ± 70.3 *,#	113.7 ± 73.2 *	107.6 ± 48.1	217.8 ± 103.3 *,#	166.6 ± 89.2 *,#
TNF-α (pg/mL)	328.3 ± 228.1 *	328.0 ± 140.5 *	296.6 ± 141.1 *	428.0 ± 179.3 *	403.4 ± 163.2 *	205.3 ± 126.1 *#
MCP-1 (ng/mL)	3.20 ± 1.73	4.89 ± 2.39 #	3.94 ± 1.57 *,#	3.02 ± 1.52	4.67 ± 2.91	3.60 ± 1.96 *,#
MMP-9 (ng mL)	86.6 ± 21.5 *	132.2 ± 46.5 #	210.2 ± 50.3 #	105.5 ± 28.3 *	133.9 ± 29.2 #	202.0 ± 45.2 #

t0, pre-exercise; t1, 5 min post-exercise; t2, 3 h post-exercise. * Significant difference between control and watercress. # Significant difference to previous sampling point.

References

1. Di Noia, J. Defining Powerhouse Fruits and Vegetables: A Nutrient Density Approach. *Prev. Chronic Dis.* **2014**, *11*, 130390. [CrossRef]
2. Klimek-Szczykutowicz, M.; Szopa, A.; Ekiert, H. Chemical Composition, Traditional and Professional Use in Medicine, Application in Environmental Protection, Position in Food and Cosmetics Industries, and Biotechnological Studies of Nasturtium Officinale (Watercress)—A Review. *Fitoterapia* **2018**, *129*, 283–292. [CrossRef] [PubMed]
3. de Souza, H.C.; dos Santos, A.M.P.; Fortunato, D.M.N.; Lima, D.C.; Fragoso, W.D.; Ferreira, S.L.C. Determination of the Mineral Composition of Watercress and Data Evaluation Using Multivariate Analysis. *Anal. Lett.* **2011**, *44*, 1758–1768. [CrossRef]
4. Fogarty, M.C.; Hughes, C.M.; Burke, G.; Brown, J.C.; Davison, G.W. Acute and Chronic Watercress Supplementation Attenuates Exercise-Induced Peripheral Mononuclear Cell DNA Damage and Lipid Peroxidation. *Br. J. Nutr.* **2013**, *109*, 293–301. [CrossRef]
5. Gill, C.I.; Haldar, S.; Boyd, L.A.; Bennett, R.; Whiteford, J.; Butler, M.; Pearson, J.R.; Bradbury, I.; Rowland, I.R. Watercress Supplementation in Diet Reduces Lymphocyte DNA Damage and Alters Blood Antioxidant Status in Healthy Adults. *Am. J. Clin. Nutr.* **2007**, *85*, 504–510. [CrossRef]
6. Hofmann, T.; Kuhnert, A.; Schubert, A.; Gill, C.; Rowland, I.R.; Pool-Zobel, B.L.; Glei, M. Modulation of Detoxification Enzymes by Watercress: In Vitro and in Vivo Investigations in Human Peripheral Blood Cells. *Eur. J. Nutr.* **2009**, *48*, 483–491. [CrossRef]
7. Cheung, K.L.; Kong, A.-N. Molecular Targets of Dietary Phenethyl Isothiocyanate and Sulforaphane for Cancer Chemoprevention. *AAPS J.* **2010**, *12*, 87–97. [CrossRef]
8. Schoonbroodt, S.; Ferreira, V.; Best-Belpomme, M.; Boelaert, J.R.; Legrand-Poels, S.; Korner, M.; Piette, J. Crucial Role of the Amino-Terminal Tyrosine Residue 42 and the Carboxyl-Terminal PEST Domain of I KBα in NF-KB Activation by an Oxidative Stress. *J. Immunol.* **2000**, *164*, 4292–4300. [CrossRef] [PubMed]
9. Fehrenbach, E.; Niess, A.M. Role of Heat Shock Proteins in the Exercise Response. *Exerc. Immunol. Rev.* **1999**, *5*, 57–77. [PubMed]
10. Asea, A.; Rehli, M.; Kabingu, E.; Boch, J.A.; Bare, O.; Auron, P.E.; Stevenson, M.A.; Calderwood, S.K. Novel Signal Transduction Pathway Utilized by Extracellular HSP70: Role of Toll-like Receptor (TLR) 2 and TLR4. *J. Biol. Chem.* **2002**, *277*, 15028–15034. [CrossRef] [PubMed]
11. Vassilakopoulos, T.; Karatza, M.-H.; Katsaounou, P.; Kollintza, A.; Zakynthinos, S.; Roussos, C. Antioxidants Attenuate the Plasma Cytokine Response to Exercise in Humans. *J. Appl. Physiol.* **2003**, *94*, 1025–1032. [CrossRef]
12. Azarmehr, N.; Afshar, P.; Moradi, M.; Sadeghi, H.; Sadeghi, H.; Alipoor, B.; Khalvati, B.; Barmoudeh, Z.; Abbaszadeh-Goudarzi, K.; Doustimotlagh, A.H. Hepatoprotective and Antioxidant Activity of Watercress Extract on Acetaminophen-Induced Hepatotoxicity in Rats. *Heliyon* **2019**, *5*, e02072. [CrossRef] [PubMed]
13. Schuchardt, J.P.; Hahn, A.; Greupner, T.; Wasserfurth, P.; Rosales-López, M.; Hornbacher, J.; Papenbrock, J. Watercress—Cultivation Methods and Health Effects. *J. Appl. Bot. Food Qual.* **2019**, *92*, 232–239. [CrossRef]
14. Hornbacher, J.; Rumlow, A.; Pallmann, P.; Turcios, A.E.; Riemenschneider, A.; Papenbrock, J. The Levels of Sulfur-Containing Metabolites in Brassica Napus Are Not Influenced by the Circadian Clock but Diurnally. *J. Plant Biol.* **2019**, *62*, 359–373. [CrossRef]
15. Boestfleisch, C.; Wagenseil, N.B.; Buhmann, A.K.; Seal, C.E.; Wade, E.M.; Muscolo, A.; Papenbrock, J. Manipulating the Antioxidant Capacity of Halophytes to Increase Their Cultural and Economic Value through Saline Cultivation. *AoB Plants* **2014**, *6*, plu046. [CrossRef] [PubMed]
16. Cruz, R.; Casal, S. Validation of a Fast and Accurate Chromatographic Method for Detailed Quantification of Vitamin E in Green Leafy Vegetables. *Food Chem.* **2013**, *141*, 1175–1180. [CrossRef] [PubMed]
17. Wu, D.; Lewis, E.D.; Pae, M.; Meydani, S.N. Nutritional Modulation of Immune Function: Analysis of Evidence, Mechanisms, and Clinical Relevance. *Front. Immunol.* **2019**, *9*, 1–19. [CrossRef]
18. Schreck, R.; Rieber, P.; Baeuerle, P.A. Reactive Oxygen Intermediates as Apparently Widely Used Messengers in the Activation of the NF-Kappa B Transcription Factor and HIV-1. *EMBO J.* **1991**, *10*, 2247–2258. [CrossRef]
19. Norling, L.V.; Ly, L.; Dalli, J. Resolving Inflammation by Using Nutrition Therapy: Roles for Specialized Pro-Resolving Mediators. *Curr. Opin. Clin. Nutr. Metab. Care* **2017**, *20*, 145–152. [CrossRef]

20. Gomez-Cabrera, M.C.; Viña, J.; Ji, L.L. Role of Redox Signaling and Inflammation in Skeletal Muscle Adaptations to Training. *Antioxidants* **2016**, *5*, 48. [CrossRef]
21. Cassatella, M.A.; Meda, L.; Bonora, S.; Ceska, M.; Constantin, G. Interleukin 10 (IL-10) Inhibits the Release of Proinflammatory Cytokines from Human Polymorphonuclear Leukocytes. Evidence for an Autocrine Role of Tumor Necrosis Factor and IL-1 Beta in Mediating the Production of IL-8 Triggered by Lipopolysaccharide. *J. Exp. Med.* **1993**, *178*, 2207–2211. [CrossRef]
22. Gérard, C.; Bruyns, C.; Marchant, A.; Abramowicz, D.; Vandenabeele, P.; Delvaux, A.; Fiers, W.; Goldman, M.; Velu, T. Interleukin 10 Reduces the Release of Tumor Necrosis Factor and Prevents Lethality in Experimental Endotoxemia. *J. Exp. Med.* **1993**, *177*, 547–550. [CrossRef]
23. O'Farrell, A.-M.; Liu, Y.; Moore, K.W.; Mui, A.L.-F. IL-10 Inhibits Macrophage Activation and Proliferation by Distinct Signaling Mechanisms: Evidence for Stat3-Dependent and -Independent Pathways. *EMBO J.* **1998**, *17*, 1006–1018. [CrossRef]
24. Naidu, S.D.; Suzuki, T.; Yamamoto, M.; Fahey, J.W.; Dinkova-Kostova, A.T. Phenethyl Isothiocyanate, a Dual Activator of Transcription Factors NRF2 and HSF1. *Mol. Nutr. Food Res.* **2018**, *62*, 1700908. [CrossRef] [PubMed]
25. Coscueta, E.R.; Reis, C.A.; Pintado, M. Phenylethyl Isothiocyanate Extracted from Watercress By-Products with Aqueous Micellar Systems: Development and Optimisation. *Antioxidants* **2020**, *9*, 698. [CrossRef]
26. Giallourou, N.; Oruna-Concha, M.J.; Harbourne, N. Effects of Domestic Processing Methods on the Phytochemical Content of Watercress (Nasturtium Officinale). *Food Chem.* **2016**, *212*, 411–419. [CrossRef] [PubMed]
27. Shahani, S.; Behzadfar, F.; Jahani, D.; Ghasemi, M.; Shaki, F. Antioxidant and Anti-Inflammatory Effects of Nasturtium Officinale Involved in Attenuation of Gentamicin-Induced Nephrotoxicity. *Toxicol. Mech. Methods* **2017**, *27*, 107–114. [CrossRef] [PubMed]
28. Tsai, J.-T.; Liu, H.-C.; Chen, Y.-H. Suppression of Inflammatory Mediators by Cruciferous Vegetable-Derived Indole-3-Carbinol and Phenylethyl Isothiocyanate in Lipopolysaccharide-Activated Macrophages. *Mediat. Inflamm.* **2010**, *2010*, 1–5. [CrossRef]
29. Sadeghi, H.; Mostafazadeh, M.; Sadeghi, H.; Naderian, M.; Barmak, M.J.; Talebianpoor, M.S.; Mehraban, F. In Vivo Anti-Inflammatory Properties of Aerial Parts of Nasturtium Officinale. *Pharm. Biol.* **2014**, *52*, 169–174. [CrossRef] [PubMed]
30. Rose, P.; Won, Y.K.; Ong, C.N.; Whiteman, M. β-Phenylethyl and 8-Methylsulphinyloctyl Isothiocyanates, Constituents of Watercress, Suppress LPS Induced Production of Nitric Oxide and Prostaglandin E2 in RAW 264.7 Macrophages. *Nitric Oxide* **2005**, *12*, 237–243. [CrossRef]
31. Park, H.-J.; Kim, S.-J.; Park, S.-J.; Eom, S.-H.; Gu, G.-J.; Kim, S.H.; Youn, H.-S. Phenethyl Isothiocyanate Regulates Inflammation through Suppression of the TRIF-Dependent Signaling Pathway of Toll-like Receptors. *Life Sci.* **2013**, *92*, 793–798. [CrossRef]
32. Xu, C.; Shen, G.; Chen, C.; Gélinas, C.; Kong, A.-N.T. Suppression of NF-KB and NF-KB-Regulated Gene Expression by Sulforaphane and PEITC through IκBα, IKK Pathway in Human Prostate Cancer PC-3 Cells. *Oncogene* **2005**, *24*, 4486–4495. [CrossRef] [PubMed]
33. Prawan, A.; Saw, C.L.L.; Khor, T.O.; Keum, Y.-S.; Yu, S.; Hu, L.; Kong, A.-N. Anti-NF-KB and Anti-Inflammatory Activities of Synthetic Isothiocyanates: Effect of Chemical Structures and Cellular Signaling. *Chem. Biol. Interact.* **2009**, *179*, 202–211. [CrossRef] [PubMed]
34. Boyanapalli, S.S.S.; Paredes-Gonzalez, X.; Fuentes, F.; Zhang, C.; Guo, Y.; Pung, D.; Saw, C.L.L.; Kong, A.-N.T. Nrf2 Knockout Attenuates the Anti-Inflammatory Effects of Phenethyl Isothiocyanate and Curcumin. *Chem. Res. Toxicol.* **2014**, *27*, 2036–2043. [CrossRef]
35. Kassie, F.; Knasmüller, S. Genotoxic Effects of Allyl Isothiocyanate (AITC) and Phenethyl Isothiocyanate (PEITC). *Chem. Biol. Interact.* **2000**, *127*, 163–180. [CrossRef]

Chapter 2.3 Protein content and glucosinolates from *Moringa oleifera* Lam. – New insights into an auspicious commodity

Journal of Applied Botany and Food Quality 93, 257 - 265 (2020), DOI:10.5073/JABFQ.2020.093.032

[1]Institute of Plant Biology, TU Braunschweig, Germany
[2]africrops! GmbH, Berlin, Germany
[3]Institute of Botany, Leibniz University Hannover, Germany
[4]Institute of Food Chemistry, TU Braunschweig, Germany

Protein content and glucosinolates from *Moringa oleifera* Lam. – New insights into an auspicious commodity

Laura Lewerenz[1], Heinrich Heinrichs[2], Johann Hornbacher[3], Jutta Papenbrock[3], Binh Nguyen-Thanh[4], Dirk Selmar[1]

(Submitted: July 24, 2020; Accepted: November 26, 2020)

Summary

Moringa oleifera is considered to be one of the most valuable and beneficial crop tree species. The great nutritiousness is assigned to its high leaf protein content, and its health-promoting effect to the anti-carcinogenic properties of its genuine glucosinolates and their degradation products.

From a plant physiological perception protein contents of 30% seem to be quite high. Accordingly, a reconsideration of these findings became necessary. The related inquiry unveils that also in the leaves of many other plant species such high protein contents are reported, provided that they are quantified by Kjeldahl nitrogen determinations. But, it is rather likely that the nitrogen accounting for the putative high protein contents is due to insoluble cell wall bound hydroxyproline-rich glycoproteins. Due to their extreme insolubility, these compounds cannot be digested easily, and thus, they do not contribute to the nutritiousness of *M. oleifera* leaves.

In contrast to classical glucosinolates, those occurring in *M. oleifera* are characterized by an attachment of a rhamnose to the aglycone. In consequence, the products generated during the myrosinase-catalysed hydrolysis correspond to non-volatile rhamnosides of isothiocyanates. Since over time, olfactorily active substances emerge, the rhamnose moiety has to be cleaved off, putatively by a corresponding rhamnosidase.

Key words: Glucosinolates; *Moringa oleifera*; protein contents.

Introduction

Moringa oleifera Lam. is considered as a valuable and beneficial crop plant, and especially the leaves of this tree species are consumed and employed all over the world for nutrition and health care (ANWAR et al., 2006; FALOWO et al., 2018). Whereas their high nutritional value is particularly attributed to the tremendously high protein content (MAKKAR and BECKER 1997; MOYO et al., 2011), the reports on the health beneficial effects (PATEL et al., 2010; JUNG, 2014) are primarily based on the exceptional glucosinolates (RAZIS et al., 2014), which are present in high concentrations in *M. oleifera* leaves as well as on various antioxidants (DA SILVA ALVES et al., 2017), vitamins and minerals (PATEL et al., 2010; MOYO et al., 2011; RAZIS et al., 2014). This case study focuses on the high protein content and on the unusual glucosinolates.

The "*extremely high protein content*" of *M. oleifera* leaves

In many popular scientific papers *M. oleifera* is denoted as the "*most nutritious plant of the world*" because of the high protein contents of its leaves, ranging from 25% to over 30% (d.w.) (e.g. DHAKAR et al., 2011; MBAILAO et al., 2014; TEIXEIRA et al., 2014, BIEL et al., 2017). However, from a plant physiological perception such putative tremendous high protein concentrations seem to be weird. In contrast to seeds, which represent storage organs exhibiting a retarded metabolism, in photosynthetically active organs an extremely high protein concentration is not reasonable. Accordingly, related statements have to be challenged. A thorough review of the relevant literature unveils that the estimation of the putative protein content of *M. oleifera* leaves is always based on the quantification of the total nitrogen, either determined by basic Kjeldahl analyses (MAKKAR and BECKER, 1996; MBAILAO et al., 2014; BIEL et al., 2017) or by applying the Dumas method (OLSON et al., 2016). Provided that the reported tremendously high protein concentration for *M. oleifera* leaves would be due to authentic genuine proteins, their quantity should also be evaluated on the basis of the amount of amino acids, which are liberated in the course of a complete hydrolysis of the proteins. Alternatively, the proteins should easily be detected in corresponding electrophoretic analyses. In this approach, in addition to Kjeldahl-based protein quantifications, we estimated the *M. oleifera* leaf proteins on the basis of the amino acids liberated in the course of an acidic hydrolysis as well as by various electrophoretic analyses.

The unusual glucosinolates of *M. oleifera* leaves

Leaves of *M. oleifera* exhibit very unique glucosinolates (AMAGLO et al., 2010), which in particular, correspond to rhamnosyl derivatives of sinalbin (Fig. 1).

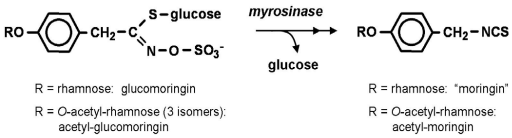

Fig. 1: Structure of the *M. oleifera* glucosinolates and the related isothiocyanates.

The particular isothiocyanate (4-(*a*-L-rhamnopyranosyloxy)-benzyl-isothiocyanate, Fig. 1) released in the course of myrosinase-catalysed cleavage of glucomoringin is frequently denoted as moringin (e.g. MÜLLER et al., 2015; KARIM et al., 2016). However, the name moringin is fallacious and misleading, since the hitherto described glucomoringin does not represent the glucose-derivative of the isothiocyanate moringin, but the genuine glucosinolate. In case of the acetyl-rhamnosyl-hydroxybenzyl-glucosinolates (= acetyl-glucomoringin isomers I-III), the rhamnose moiety of glucomoringin is *O*-acetylated (AMAGLO et al., 2010; PATEL et al., 2010) which can occur at three different positions (FAHEY et al., 2018) (Fig. 1).

* Corresponding author

In addition to the various glucosinolates, also their putative degradation products, i.e. isothiocyanates, nitriles or carbamates, are reported to occur in *M. oleifera* leaves (RAZIS et al., 2014; WADHWA et al., 2013). However, AMAGLO et al. (2010) did not detect corresponding degradation products and deduced that these substances had been generated in the course of tissue damage (AMAGLO et al., 2010). Moreover, these authors reported the occurrence of glucotropaeolin in stems of *M. oleifera*.

With respect to their health-promoting effects (PATEL et al., 2010; RAZIS et al., 2014; KARIM et al., 2016), apart from an anti-inflammatory (WATERMAN et al., 2014) and an antibacterial activity (GALUPPO et al., 2013), the anti-carcinogenic action of the unusual glucosinolates and their various degradation products is in the centre of interest (JUNG, 2014; RAJAN et al., 2016). In this context, the corresponding isothiocyanates are thought to be of high relevance (MIYACHI et al., 2004; BRUNELLI et al., 2010; RAJAN et al., 2016; GALUPPO et al., 2013). Based on their studies, these authors assume that the relevant isothiocyanates are mostly generated – just as in the case of "classical" glucosinolates – by their hydrolysis catalyzed by myrosinases. However, in contrast to the typical glucosinolates present in plants of the Brassicaceae, in injured *M. oleifera* leaves, the liberated isothiocyanates are still attached to a rhamnose moiety, and thus are not volatile. Since with time volatile, olfactory active compounds are liberated, the rhamnose moiety must be cleaved off, presumably by a rhamnosidase. In contrast to the numerous studies dealing with the health-promoting effects of these compounds, only very few reports had been published concerning their ecological significance for the plants (MÜLLER et al., 2015). It is assumed that – just in the same manner as for "classical" glucosinolates (HALKIER & GERSHENZON, 2006) – also the glucosinolates in *M. oleifera* leaves represent phytoanticipins by protecting the plant against herbivores and pathogens. As the repellent and protective effect is due to the generation of degradation products (MÜLLER et al., 2015), also the *M. oleifera* glucosinolates can be classified as typical inactive precursors, which – after tissue disruption – generate active agents (BRUNELLI et al., 2010), exhibiting their repellent effect on potential herbivores by their pungent taste (e.g. CHODUR et al., 2018). Yet, the manifestation of the pungent taste of *M. oleifera* leaves is reported to be quite different (DOERR, 2009; CHODUR et al., 2018) and may strongly vary between different varieties, origins and proveniences, respectively. CHODUR et al. (2018) attributed these differences in the markedness of the pungency primarily to variations in the overall amount of glucosinolates. In contrast, the studies of DOERR et al. (2009) did not establish any correlation between "pungency" or "peppery taste" on the one hand, and content and spectrum of glucosinolates on the other hand. As consequence, these authors deduced that the variations in the differences of pungency are caused by different activities of myrosinases (DOERR et al., 2009). This assumption seems to be – at least in part – plausible, since the pungent, peppery taste and the characteristic flavour are not generated by the intact glucosinolates, but are determined by their degradation products. In order to provide further information on this topic and to disclose the basic processes involved, the hydrolysis of the *M. oleifera* glucosinolatess has been studied.

Material and methods

Sample preparation for Kjeldahl and quantification of amino acids

For protein quantifications, 5 g of commercial *M. oleifera* powder (*africrops!*, Berlin) were extracted two times with 50 mL McIlvaine buffer (0.1 M citric acid / 0.2 M Na_2PO_4; pH 5.6) (1:5 diluted). The extract was centrifuged (4.000 × g, 10 min) and the supernatant was filtered. The combined aqueous supernatants (**S**) were divided equally and freeze-dried. Accordingly, the soluble protein fraction **S** comprises all proteins that are soluble in plain buffers. The related pellet (**P**) was re-extracted for 30 min at 95 °C with 40 mL SDS-buffer (McIlvaine buffer containing 2% SDS and 4% β-mercaptoethanol) and centrifuged (4.000 × g, 10 min). The residual supernatant (**R**) was separated from the pellet (**P**). Both fractions were divided equally and freeze-dried (Fig. 2). The freeze-dried samples **S**, **R**, and **P** as well as the dried leaves (total leaf extract = **T**) were either used for the Kjeldahl analysis or for the quantification of amino acids.

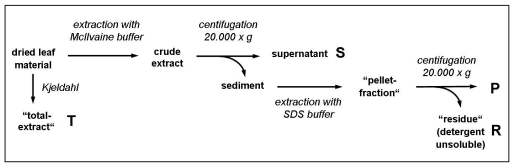

Fig. 2: Scheme of protein sample preparation.

Protein determination - Kjeldahl

Protein determination was conducted via Kjeldahl nitrogen quantification according to MATISSEK and STEINER (2006).

Digestion: Each sample was mixed with 20 mL concentrated sulfuric acid, one Kjeldahl tablet (Thompson & Capper, Runcorn, UK) and some glass beads in a 250 mL Tecator Kjeldahl tube. After gentle shaking, the Tecator Kjeldahl tubes were placed in the Tecator block digester (FoodAlyt IR 1200) and heated at 375 °C until the digestion solutions were clear and only slightly bluish in colour. Subsequently the tubes were removed from the Tecator block and cooled down to room temperature (RT). Then the solutions were carefully diluted with distilled water, transferred to a 100 mL volumetric flask with rinsing distilled water and filled up to the mark after cooling.

Distillation: 10 mL of the digestion solutions were alkalized with 40 mL NaOH before a steam distillation was carried out for 5 min. For titration, the distillates were transferred into a 20 mL boric acid-indicator mixture and a Tashiro indicator was added, exhibiting colour changes from violet-red through grey to light green.

Titration: The steam distillates were titrated dropwise with HCl (0.1 M) until the first colour change (green-grey) occurred.

Calculation: The protein content in percent (P) was calculated according to the formula:

$$P = \frac{(a-b) \times 1.4008 \times F}{E}$$

P: percentage of protein content (%); a: consumption of HCl in the titration (mL) of the related samples; b: consumption of HCl in the titration (mL) of the related blanks (water); F: 6.25 (general conversion factor for calculating the protein content); E: sample weight (g).

Protein determination via quantification of amino acids liberated by acidic hydrolysis

Alternatively to the Kjeldahl approach, the protein content was estimated on the basis of amino acids liberated in the course of acidic proteolysis. For this, the contents of amino acids present in the hydrolysed as well as in the non-hydrolysed samples (commercial *M. oleifera* powder, *africrops!*, Berlin) were determined. Quantification was performed by HPLC according to BYTOF et al. (2005).

Hydrolysis: Of each sample 200 mg (P, R, S, T; Fig. 2) were mixed with 2 mL 6 M HCl in small glass ampullae. To minimize the amount of oxygen, ampullae had been sealed by melting the ampulla neck. Hydrolysis was performed at 100 °C for 6 h in three independent

replicates. Subsequently, the samples were neutralized with NaOH, diluted 1:5 before norvaline was added as internal standard to yield a final concentration of 160 nmol. Prior to HPLC analysis, samples were centrifuged (4.000 × g, 10 min).

Extraction: To determine the content of free amino acids, 200 mg of each sample were extracted with 3 mL sulphosalicylic acid (4% w/v) containing exactly 160 nmol norvaline as internal standard according to BYTOF et al. (2005). For each assay, three independent replicates had been conducted.

HPLC: Prior to HPLC analysis, the extracted amino acids were derivatised with *o*-phthaldialdehyde (OPA) using a Spark Holland Midas autosampler for derivatisation and sample injection (BYTOF et al., 2005); injection volume was 30 µL. Separation was performed on a C18 column (Nucleosil 120, 5 µm, Macherey & Nagel, 250 × 4.0 mm) employing a binary gradient (A: 5% MeOH, 5% acetonitrile (ACN), 2% tetrahydrofuran (THF), 88% 50 mM sodium acetate buffer, pH 6.2; B: 40% MeOH, 40% ACN, 20 % sodium acetate buffer). Flow rate: 1.0 mL/min, oven temperature: 35 °C. The amino acid derivatives were detected employing a RF-551 Shimadzu fluorescence detector (λ_{ex} = 334 nm; λ_{em} = 425 nm) and quantified using external calibration.
The protein amounts were quantified as difference of the amounts for free amino acids and those released by acidic hydrolysis.

Analyses of glucosinolates and their degradation products

Extraction and degradation of glucosinolates

Plant material was harvested from plants grown in the greenhouse of the Institute of Botany, Leibniz University Hannover, Germany. After freezing in liquid nitrogen, the material was ground and freeze-dried. Of the lyophilized powder 25 mg were incubated with 500 µL ultrapure water at two different temperatures (4 °C and 20 °C) for a time period of 60 s. At various times (15, 30, 45 and 60 s), degradation of glucosinolates was stopped by adding 500 µL MeOH and heating the samples at 95 °C for 10 min. Extracts were centrifuged (4.000 g; 10 min) and filtered. Samples were analysed in triplicates.

LC-MS analysis

For identification of the glucosinolates in *M. oleifera* samples were analysed by liquid chromatography-mass spectrometry (LC-MS). A volume of 10 µL was injected into the HPLC system (Shimadzu, Darmstadt, Germany) and separated on a Vertex Plus column (250 × 4 mm, 5 µm particle size, packing material ProntoSIL 120-5 C18-H) (Knauer, Berlin, Germany) equipped with a pre-column (Knauer). Solvent A: water (18.2 µS cm^{-1}, obtained by Elga Purelab Ultra GE MK2, Veolia Water Technologies Deutschland GmbH, Celle, Germany; solvent B: MeOH (VWR, Darmstadt, Germany; LCMS grade, 99.9% purity); both containing 2 mM ammonium acetate (Merck, Darmstadt, Deutschland; LC MS grade, 90.0% purity). Flow rate: 0.8 ml min^{-1} at 30 °C, gradient: 10-90% B for 35 min, 90% for 2 min, 90-10% B for 1 min and 10% B for 2 min. HPLC was coupled to a mass spectrometer (AB Sciex TripleTOF 4600, Canby, USA). At a temperature of 600 °C and an ion spray voltage floating of -4500 V the negative electrospray ionization (ESI) was performed. For the ion source gas one and two 50 psi were used and for the curtain gas 35 psi. In the range of 100-1500 Da in the TOF range the mass spectra as well as the MS/MS spectra from 100-800 Da at a collision energy of -10 eV were recorded (total ion chromatogram, TIC). Peaks were identified by analysing the characteristic masses (according to FÖRSTER et al., 2015; RAMBULANA, et al., 2017; Fig. 3). The acetylation site of the three isomers of acetyl-4-α-L-rhamnopyranosyloxybenzyl glucosinolates could not be certainly identified because of lacking NMR data. In order to be able to discuss obtained results, the isomers were named according to their elution time from I to III. Quantification was performed by using peak areas obtained by monitoring samples at 229 nm. Due to lack of authentic standards, contents of glucosinolates were calculated by using the standard curve of sinigrin (Phytolab, Vestenbergsgreuth, Germany, 99.8% purity).

Degradation of glucosinolates in **M. oleifera** *leaf extracts*

One g of commercially available *M. oleifera* powder (*africrops!*, Berlin) was incubated with 20 mL tap water at two different temperatures (4 °C and 20 °C) for a time period of 5 d. At various time points (6, 18, 30, 42, 54, 66, 78 and 90 h) the extracts were centrifuged (4.000 g; 10 min) and filtered before being injected into the HPLC. For each assay, two independent replicates had been conducted.

HPLC: Estimation of glucosinolate degradation products was performed according to Kleinwächter (2007) employing a C18 column (Nucleosil 120, 5 µm, Macherey & Nagel, 250 × 4.0 mm) and a binary gradient (A: MeOH, B: H_2O dest.; 10 min 40% A and 60% B, 10 min 80% A and 20% B, 5 min 40% A and 60% B). Flow rate: 0.8 mL/min. For detection a photodiode array detector (220 nm) was used. 4-Hydroxybenzyl alcohol (Alfa Aesar, Kandel) was employed as authentic standard.

Results and discussion

The dissent of high protein contents

Protein determination based on the quantification of total nitrogen (Kjeldahl)

In order to clarify the inconsistencies on the alleged high protein contents, extracts of *M. oleifera* leaves had been fractionated and analysed. In accordance with the literature for the dried leaf material (**T**) - based on the total nitrogen quantification – a protein content of 26.5 % was estimated (Tab. 1). This value corresponds to the amount of 24.3%, which results as sum of the particular factions, i.e. **S** + **P** + **R** (Fig. 2). However, the determination of the protein content in the "water soluble" and "SDS-extractable" faction (sum **S** + **P**) reveals only 14.3%. This value is in the same range as reported for other plant species, e.g. 7% - 11% for barley (DAI et al., 2009) and 9% - 16% for spinach (JACOBI et al., 1975). Obviously, in *M. oleifera* leaves, a very high share of nitrogen remains in the insoluble fraction **R**. Unfortunately, only few related data on this issue are available.

Tab. 1: Kjeldahl based nitrogen and protein content of the various fractions from *M. oleifera* leaves.

Fraction	Nitrogen content [%]	Putative protein content [%]	Share of total protein [%]
S (supernatant "buffer extract")	0.96	**6.0**	**22.6**
P (supernatant of the SDS-solubilised pellet)	1.33	**8.3**	**31.3**
R (SDS-insoluble)	1.60	**10.0**	**37.7**
sum: **S + P**	2.29	**14.3**	**53.9**
sum: **S + P + R**	3.89	**24.3**	**91.7**
T ("total extract")	4.25	**26.5**	**100**

Data represent mean values from three independent replicates.

Protein determination via quantification of amino acids liberated by acidic hydrolysis

To scrutinise whether or not the putative protein contents of *M. oleifera* leaves estimated via the Kjeldahl nitrogen quantification could be attributed to authentic, genuine proteins, the related samples had been hydrolysed employing hydrochloric acid. Subsequently, the amount of amino acids was quantified. The difference in the con-

tent of amino acids in the hydrolysed and the non-hydrolysed fractions corresponds to the amount of proteins (Tab. 2). When comparing these results with the putative protein contents quantified on the basis of Kjeldahl nitrogen determinations (Tab. 1), it turned out that the total protein content in the dried leaves (**T**) is only 13.8% (Tab. 2) instead of 26.5% (Tab. 1). These results are in accordance with protein contents of other plant species, estimated by standard protein quantifications. Thus, the protein determinations based on their acidic hydrolysis fully confirm the assumption that a major share of nitrogen (corresponding to a calculated, putative protein content of about 10%) is present in the SDS-insoluble fraction (**R**) and is not due to authentic proteins.

In addition to protein quantification, various electrophoretic studies had been conducted. After staining the gels with Coomassie, no major differences in the amount of proteins derived from the three different plant species were visible (Fig. 1, Supplementary material), underlining the lacking of major differences in protein contents between *M. oleifera* and other plant species.

Protein contents in M. oleifera leaves are as high as in other species

The combined data on protein analyses suggest that the key to understand the inconsistencies in the protein content of *M. oleifera* leaves is the elucidation of the source of the nitrogen present in the insoluble sediment. When thoroughly evaluating the literature dealing with *M. oleifera*, some hints on the not yet identified insoluble, nitrogen-containing compounds can be found. Kakengi et al. (2005) studied the feasibility of employing *M. oleifera* leaves as protein supplement for ruminants. In addition to the determination of the putative total protein content, the authors quantified the share of protein, which is degradable in the rumen and which part is not. The latter one was identified as putative proteins which are insoluble in detergent-containing acids. The authors ascertained a total protein content of 26.5% and outlined that about 40% of this amount (corresponding to about 10% of the dry mass as putative protein) is not degradable in the rumen (Kakengi et al., 2005). Accordingly, they concluded that about two fifths of the entire protein could not be solubilised with detergents. Hence, these data are fully in accordance with the data presented here. However, it has to be questioned, whether or not the nitrogen present in the compounds, which are not rumen-degradable, are authentic proteins.

Based on further literature screening, it became obvious that the putative high protein concentration in *M. oleifera* leaves is not exceptional. For example, in cassava leaves – when estimated on the basis of Kjeldahl nitrogen determinations – it is reported to be in the range between 29% and 38% (Yeoh and Chew, 1976). In a comprehensive study employing many tropical plants, Byers (1961) determined the putative protein content of the leaves of 70 different plant species growing in Ghana. Based on Kjeldahl determinations of crude extracts, the author reported that 10 of the studied plant species revealed a leaf protein content higher than 28%, and 28 of them exhibited a percentage even higher than 24%. Of course, also for this study, it has to be doubted that the Kjeldahl-based protein determination indeed outlines the correct amount of authentic proteins. Nonetheless, these data state that the very high putative protein content reported for *M. oleifera* is not exceptional.

When contemplating the nature of the SDS-insoluble nitrogen containing substances present in the leaves, the focus inevitably shifts to cell wall components. It is well known that – in addition to cellulose, various other polymeric carbohydrates, and lignin – also proteins are part of plant cell walls (Houston et al., 2016). Already more than half a century ago, Lamport and Northcote (1960) reported that the main share of the proteins bound to the cell walls of higher plants is due to hydroxyproline-rich glycoproteins (HRGP), which may account for about 10% of the dry weight of the cell wall (Talmadge et al., 1973; Roberts et al., 1985). According to Lamport (1966) these highly insoluble cell wall proteins are denoted as extensins. Until now, no clear picture on the complex nature of extensins could be drawn. Yet, the explanation for their highly insoluble character is given by tyrosine-based bindings resulting in isodityrosine moieties (Lamport, 1980; Fry, 1982), which results in a highly cross-linked network of extensins (Lamport, 1986).

Whereas at the end of the last century many efforts had been made to elucidate the structure of the HRGP, to date the evolutionary and genetic aspects of these proteins are in the focus of interest (Johnson et al., 2017). So far no studies are available that combine basic plant biochemical insights on HRGP or extensins, respectively, and the data elaborated for the relevance of leaf proteins with respect to human or animal nutrition as outlined above. Accordingly, we do not know whether or not the insoluble proteins, putatively non-degradable in the rumen (Kakengi et al., 2005), correspond to the HRGP. These coherences outline that there is a massive need for interdisciplinary as well as for applied research to further elucidate the marvel of the putative high protein contents. This especially accounts when considering that - without any doubt – *M. oleifera* leaves exhibit many benefits for human nutrition and a significant growth promoting effect on livestock (Nouman et al., 2014). As reported by

Tab. 2: Protein content in *M. oleifera* leaves estimated on the basis of acidic protein hydrolysis.

Fraction	Content of amino acids [mg/g]	Amino acids liberated by hydrolysis = protein [%]	[mg/g]	Protein content (Kjeldahl) [%]
T (total extract = free amino acids)	12	138	13.8	26.5
T*h* (total extract, hydrolysed)	150			
S (aqueous supernatant = free amino acids)	7.1	33.6	3.36	6.0
S*h* (aqueous supernatant, hydrolysed)	40.7			
P (SDS supernatant = free amino acid)	1.05	22.1	2.21	8.3
P*h* (SDS supernatant = hydrolysed)	23.1			
R (SDS insoluble = free amino acids)	1.4*	46.7	4.67	10.0
R*h* (SDS insoluble = hydrolysed)	48.1			
sum “free amino acids” (S + P + R)	9.5	102.4	10.24	24.3
sum “hydrolysed” (Sh + Ph + Rh)	111.9			

The protein content of each sample was calculated as difference of the amino acid contents in the original and the hydrolysed fractions. *In principle, in this fraction no free amino acids could be present. However, their occurrence points to the fact that proteins might be hydrolysed by proteases present in this fraction.

ANHWANGE et al. (2004), the amino acids spectrum of *M. oleifera* leaf protein is not really exceptional: apart from glutamic and aspartic acid, the semi-essential amino acid arginine and the essential leucine represent the most abundant ones in the related hydrolysates. In consequence, all tremendously high number of positive nutritional effects described in the literature must have another origin, which has to be elucidated in the future.

Composition and degradation of the *M. oleifera* glucosinolates

General state of affairs

As outlined above, the well-known health-promoting effects of *M. oleifera* glucosinolates are attributed to their various degradation products, in particular to the corresponding isothiocyanates. Accordingly, the extent and velocity of glucosinolate degradation are of special interest. A plain finding in daily life may open the door for a better understanding of the entire process: when an extract of *M. oleifera* leaves is kept in the cold, e.g. in the fridge, for several days, there is a strong retardation in the generation of the characteristic pungent taste and flavour, whereas the sensory properties develop much quicker at RT (H. HEINRICHS, pers. comm.). However, the appendent intensity and pungency as well as the overall sensory quality are quite different. Obviously, the relevant degradation products of the glucosinolates differ and are generated at different times. The basis for the initiation of the various reactions – also in *M. oleifera* – is the hydrolysis of the genuine glucosinolates catalysed by myrosinases (DOERR et al., 2009; CHODUR et al., 2018). However, due to the presence of rhamnose attached to the isothiocyanates in *M. oleifera* leaves, the primary hydrolysis products might not be volatile, and then would be aroma-neutral. Yet, a thorough investigation of the related degradation processes requires a sound determination of the genuine glucosinolates. According to WATERMAN et al. (2014) and FAHEY et al. (2018) apart from glucomoringin (4-α-L-rhamnopyranosyloxy-benzyl glucosinolate), three different acetyl-derivatives are described (acetyl-4-α-L-rhamnopyranosyloxy-benzyl glucosinolate = acetyl-glucomoringin isomers I-III; Fig. 3A). By employing LC-MS chromatography, 4-α-L-rhamnopyranosyloxy-benzyl glucosinolate could be assigned reliably. Identification of the isomers of acetyl-4-α-L-rhamnopyranosyloxy-benzyl glucosinolates was also performed but with lack of NMR data, position of the acetylation site could not be determined (Fig. 3B). No other glucosinolates were identified in the analysed plant material.

Time-dependent glucosinolate degradation

In order to elucidate whether the known differences in the generation of degradation products might be related to differences in the myrosinase activity, leaf extracts have been incubated at 4 °C and 20 °C, respectively. The concentration of the four glucosinolates was determined by LC-MS. The results proved that all glucosinolates are hydrolysed efficiently (Fig. 4, 1-4).

Degradation of all glucosinolates was significantly lower at 20 °C compared to samples incubated at 4 °C. This unexpected observation was especially evident in samples incubated for 15 s. In several cases, the counteracting effects of elevated temperatures on either enzyme activity or on its stability could result in a higher substrate turn-over at lower temperatures. However, myrosinase exhibits a high stability (VAN EYLEN et al., 2005; GHAWI et al., 2012). Accordingly, this explanation can be excluded. Currently, no physical explanation for this phenomenon, which putatively leads to a solubilisation and thus a faster hydrolysis of glucosinolates, is available. Wetting of samples was carefully observed and samples that were not homogenized within the first second of shaking were discarded because of the very short incubation time. Since experiments are conducted with finely ground leaf powder in an artificial experimental setup, a high degradation of glucosinolates probably happens during the first few seconds in samples incubated at 20 °C, when it is assumed that the myrosinases present in *M. oleifera* perform better at 20 °C compared to 4 °C, similarly to other myrosinases (LI and KUSHAD, 2005). This could lead to an inhibition of myrosinases by breakdown-products of glucosinolates in samples incubated at 20 °C leading to lower degradation rates and therefore higher glucosinolate contents. Lower contents in samples incubated at 4 °C for 15 s could be explained by a slower, but steadier degradation of glucosinolates by myrosinases at 4 °C, which is also reflected in the contents of glucosinolates observed after 30 s, which were higher in samples incubated at 4 °C compared to samples incubated at 20 °C.

Nonetheless, it has to be stated that the glucosinolates are entirely hydrolysed within the first minute of incubation. Accordingly, the

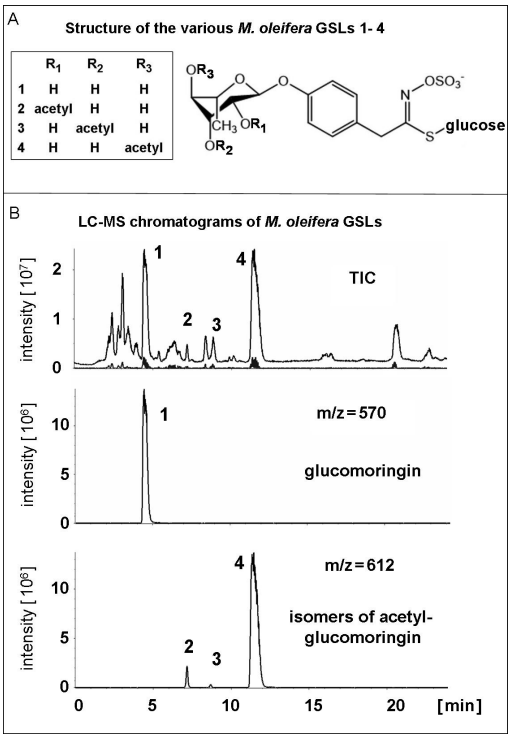

Fig. 3: Glucosinolates present in *M. oleifera* leaves.

A: Structure of the common *M. oleifera* glucosinolates. Apart from glucomoringin (4-α-L-rhamnopyranosyloxy-benzyl glucosinolate; **1; $R_{1,2,3}$, = H**), three isomers of its acetylated form (acetyl-4-α-L-rhamnopyranosyloxy-benzyl glucosinolate = acetyl glucomoringin; isomers I-III R_1 or R_2 or R_3 = acetyl) are present in *M. oleifera* leaves.

B: Identification of the *M. oleifera* glucosinolates by LC-MS. Mass chromatograms of a *M. oleifera* leaf extract containing all glucosinolates. At the top: total ion chromatogram (TIC; mass range: 100-800 Da). In the middle: extracted ion chromatogram of m/z = (570) $[M]^-$ representing glucomoringin (4-α-L-rhamnopyranosyloxy-benzyl glucosinolate; **1**). At the bottom: extracted ion chromatogram of m/z = (612) $[M]^-$ representing the three isomers of acetyl-glucomoringin (acetyl-4-α-L-rhamnopyranosyloxy-benzyl glucosinolate; isomers I-III). The MS/MS spectra of the four different *M. oleifera* glucosinolates are displayed in Fig. S2 (Supplementary material).

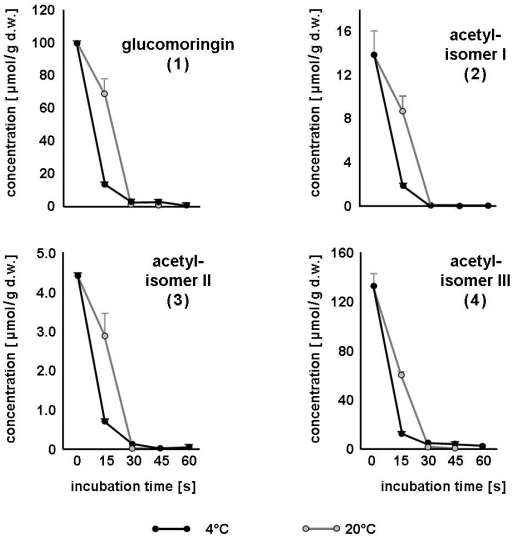

Fig. 4: LC-MS analysis of glucosinolates in *M. oleifera* extracts. Lyophilized plant material from the greenhouse was incubated for 15 to 60 s either at 4 °C (black line) or at 20 °C (grey line), respectively. Data points represent the mean of three technical replicates for each glucosinolate. Contents were calculated with the standard curve of sinigrin.

myrosinase-catalysed hydrolysis cannot be responsible for the observed sensory differences in extracts, which are kept at different temperatures for many hours or several days, respectively.

The generation of olfactorily active substances in the further course of incubation signifies that the rhamnose moiety is cleaved off from the assumed non-volatile primary degradation products, i.e., the rhamosylated isothiocyanates, as time goes on. No detailed information is available with respect to the reaction mechanism and the enzymes putatively involved, such as rhamnosidases. The different degradation rates at the two temperatures could also have an effect on these putative rhamnosidases degrading the rhamnosylated degradation products. In general, activity of enzymes could also be inhibited by an oversupply of substrates (breakdown-products). The steadier generation of breakdown-products at 4 °C could lead to subsequent steadier generation of olfactorily active substances, whose volatility is additionally diminished at lower temperatures. The retarded generation of the olfactorily active substances as well as the related differences at 4 °C and 20 °C also seem to be related to experimental *in vitro* conditions, since all glucosinolates are hydrolysed by myrosinase already within one minute of incubation (Fig. 4).

Due to the differences in stability of potential hydrolysis products (Buskov et al., 2000), the situation becomes more complex. The products of the myrosinase reaction, i.e., the various rhamnosylated isothiocyanates (Fig. 1) are quite stable. However, the elimination of the rhamnose moiety results in 4-hydroxybenzyl isothiocyanate (Fig. 5), a very instable compound, which is also generated in the course of the hydrolysis of sinalbin in white mustard (*Sinapis alba*). Analyses of the corresponding degradation products in crushed seeds of *S. alba* revealed that 4-hydroxybenzyl isothiocyanate is converted quickly to 4-hydroxybenzyl alcohol, and other reaction products; e.g. in the presence of ascorbic acid 4 hydroxybenzyl-ascorbigen is generated (Fig. 6) (Kawakishi and Muramatsu, 1966; Buskov et al., 2000; Borek and Morra, 2005; Paunović et al., 2012). In contrast, in black mustard (*Brassica nigra*) the related degradation products, allyl isothiocyanate and benzyl isothiocyanate, which are derived from sinigrin and glucotropaeolin, respectively, are far more stable (Fenwick et al.,1983). Moreover, the various isothiocyanates reveal different affinities to the transient receptor potential ankyrin, which is responsible for the perception of pungent taste (Terada et al., 2015).

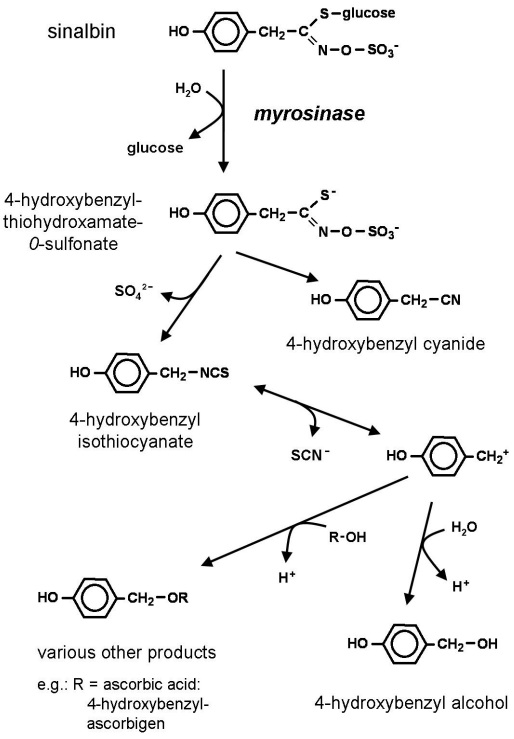

Fig. 5: Potential degradation products of 4-hydroxybenzyl isothiocyanate produced by myrosinase-catalysed hydrolysis of sinalbin according to Buskov et al. (2000).

In order to get a survey on the related degradation products, which are generated in disintegrated *M. oleifera* leaves, HPLC analyses of aqueous extracts of fresh *M. oleifera* leaves as well as of commercially available dried *M. oleifera* leaf material had been conducted. The material was homogenized with tap water at RT and stored subsequently at 4 °C. Every day, samples had been taken and analysed by HPLC (Fig. 6). To facilitate the identification of putative degradation products of the glucosinolates, authentic reference substances need to be employed. Only 4-hydroxybenzyl alcohol (Fig. 6) could be used as reference substance, since neither the rhamnosylated nor the non-substituted 4-hydroxybenzyl isothiocyanates are commercially available.

The HPLC analyses exhibited massive differences in the spectrum of glucosinolate degradation products in the extracts of fresh leaves in comparison to those derived from dried leaf material (Fig. 6). The only compound identified reliably is 4-hydroxybenzyl alcohol. Accordingly, it could be deduced that in analogy to the degradation

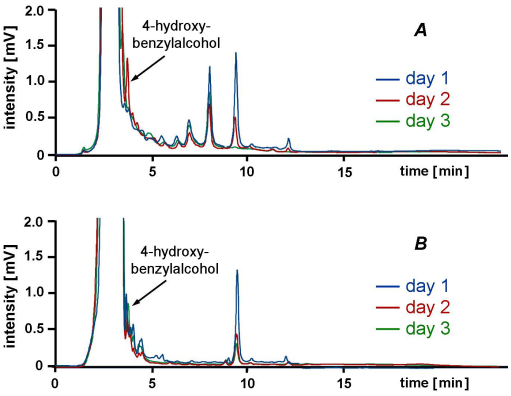

Fig. 6: Variation of degradation products pattern in *M. oleifera* cold extracts. **A:** Dried leaf powder; **B:** fresh crushed leaves. Directly after homogenization with tap water, the samples had been stored at 4 °C. For detection, a diode array detector was employed (λ = 220 nm). Due to the HPLC conditions, in contrast to the LC-MS analyses mentioned above, glycosylated compounds, e.g. all glucosinolates, elute in the void volume.

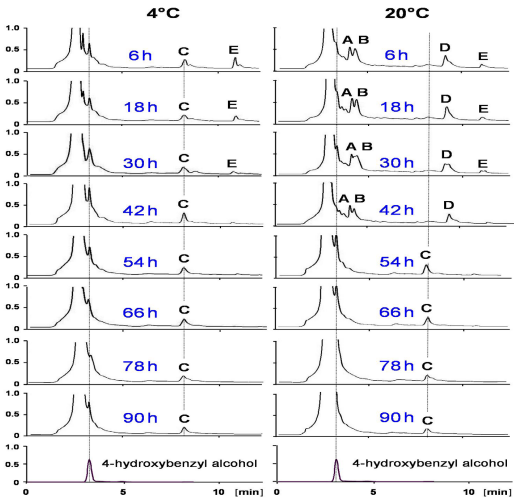

Fig. 7: HPLC analyses of *M. oleifera* extracts stored at 4 °C or 20 °C. Samples had been taken every 12 h. 4-Hydroxybenzyl alcohol was employed as authentic reference substance. For detection, a diode array detector was employed (λ = 220 nm). Due to the HPLC conditions, in contrast to the LC-MS analyses mentioned above, glycosylated compounds, e.g. all glucosinolates, elute in the void volume.

of sinalbin (Fig. 5) 4-hydroxybenzyl alcohol was produced as final degradation product of *M. oleifera* glucosinolates. Other substance peaks cannot be unequivocally assigned to putative degradation products of glucosinolates. Their absorbance spectra point to glucosinolate-related compounds. Hence, all glucosinolates are already cleaved within the first minute of incubation (Fig. 5) the observed differences must be related to reactions following the myrosinase-catalysed hydrolysis of glucosinolates. Obviously, these processes, i.e. rearrangements and further degradations, are quite different in extracts of fresh and dried plant material. In general, such differences could be a consequence of differential inactivation of enzymes. This underlines the assumption that – in addition to myrosinases – further enzymes, such as rhamnosidases, could be involved in the degradation of glucosinolates and their breakdown-products. Accordingly, the observed substantial differences could result from varying activities of these putative enzymes, caused by their different stabilities in fresh and dried leaves.

From these coherences it could be deduced that the characteristic differences in the release of olfactorily active substances in *M. oleifera* extracts which are kept at either 4 °C or at 20 °C (H. Heinrich, pers. comm.) might be related to variations in enzyme activities. To get more information on this phenomenon, a further row of experiments was conducted. Commercially available *M. oleifera* leaf material was homogenized with tap water and stored either at 4 °C or at 20 °C, respectively. Every 12 h, a corresponding sample had been taken and analysed by HPLC (Fig. 7).

The HPLC analyses reveal that in the *M. oleifera* extracts various substances are released as time goes on (Fig. 7). Obviously, also in the case of the various *M. oleifera* glucosinolates 4-hydroxybenzyl alcohol represents the final degradation product (Fig. 5). This verifies that the rhamnose moiety of the *M. oleifera* glucosinolates has to be cleaved off in the course of their further degradation. Although the various intermediates of the complex degradation process are not yet identified, the comparison of the related products and their time-dependent generation at 4 °C and 20 °C, respectively, indicates that various additional reactions are involved in the complex degradation processes and suggest the involvement of a putative rhamnosidase. Although up to now no definite information on this enzyme is available. Apart from the basic scientific point of view, especially with regard to the health-protective effects of *M. oleifera* preparations, the elucidation of these complex processes is of special interest. Due to their anti-carcinogenic effect, the stability of the rhamnosylated isothiocyanates (moringin and analogues), are of particular importance, since the elimination of the rhamnose moiety induces the putative further degradation. Accordingly, the elucidation of these complex processes, i.e. the overall degradation of the *M. oleifera* glucosinolates and the subsequent rearrangements of their degradation products, need to be further investigated.

Conclusion

Moringa oleifera is thought to be one of the most valuable and beneficial tree crop plant species. Apart from great benefits for human nutrition and a significant growth improvement of livestock, outlined in numerous studies, especially the health-promoting properties are of special interest. Up to now, the nutritional properties had been attributed primarily to the putatively high protein content of *M. oleifera* leaves. Yet, this study unveiled that the protein content of *M. oleifera* leaves is not exceptional and is in the same range as found for leaves of other plant species. Moreover, the amino acids composition of *M. oleifera* leaves is not that exceptional as commonly mentioned (ANHWANGE et al., 2004). Thus, the high number of positive effects described in the literature must have another origin, which needs to be elucidated.

The health-promoting effects is frequently assigned to the anti-carcinogenic properties of the *M. oleifera* glucosinolates, in particular, to their degradation products. By analysing the degradation of glucosinolates at various conditions, the complexity of these processes is illustrated. Due to their anti-carcinogenic effect, the degradation of the rhamnosylated isothiocyanates is of special interest, since the elimination of the rhamnose moiety induces the further decay, and thus the loss of the desired health-protective properties. Thus, further elucidation of these complex processes is of particular relevance.

Conflict of interest

On behalf of all authors, the corresponding author declares that there is no financial and personal relationships with other people or organizations that could inappropriately have influenced our work.

References

Amaglo, N.K., Bennett, R.N., Lo Curto, R.B., Rosa, E.A.S., Lo Turco, V., Giuffrida, A., Lo Curto, A., Crea, F., Timpo, G.M., 2010: Profiling selected phytochemicals and nutrients in different tissues of the multipurpose tree *Moringa oleifera* L., grown in Ghana. Food Chem. 122, 1047-1054. DOI: 10.1016/j.foodchem.2010.03.073

Anhwange, B.A., Ajibola, V.O., Oniye, S.J., 2004: Amino Acids compositions of the Seeds of *Moringa oleifera* (LAM) *Detarium mirocarpum* (Guill & Perr) *Bauhinia monandra* (Linn). Chem. Class J. 2004, 9-13.

Anwar, F., Latif, S., Ashraf, M., Gilani, A.H., 2006: *Moringa oleifera*: a food plant with multiple medicinal uses. Phytother. Res. 21, 17-2. DOI: 10.1002/ptr.2023

Biel, W., Jaroszewska, A., Łysoń, E., 2017: Nutritional quality and safety of moringa (*Moringa oleifera* Lam., 1785) leaves as an alternative source of protein and minerals. J. Elem. 22, 569-579. DOI: 10.5601/jelem.2016.21.3.1249

Borek, V., Morra, M.J., 2005: Ionic thiocyanate (SCN-) production from 4-hydroxybenzyl glucosinolate contained in *Sinapis alba* seed meal. J. Agr. Food Chem. 53, 8650-8654. DOI: 10.1021/jf051570r

Brunelli, D., Tavecchio, M., Falcioni, C., Frapolli, R., Erba, E., Iori, R., Rollin, P., Barillari, J., Manzotti, C., Morazzoni, P., D'Incalci, M., 2010: The isothiocyanate from glucomoringin inhibits NF-kB and reduces myeloma growth in nude mice *in vivo*. Biochem. Pharmacol. 79, 1141-1148. DOI: 10.1016/j.bcp.2009.12.008

Buskov, S., Hasselstrøm, J., Olsen, C.E., Sørensen, H., Sørensen, J.C., Sørensen, S., 2000: Supercritical fluid chromatography as a method of analysis for the determination of 4-hydroxybenzylglucosinolate degradation products. J. Biochem. Biophys. Methods 43, 157-174. DOI: 10.1016/S0165-022X(00)00081-6

Byers, M., 1961: Extraction of protein from the leaves of some plants growing in Ghana. J. Sci. Agric. 12, 20-30. DOI: 10.1002/jsfa.2740120104

Bytof, G., Knopp, S.-E., Schieberle, P., Teutsch, I., Selmar, D., 2005: Influence of processing on the generation of γ-aminobutyric acid in green coffee beans. Eur. Food. Res. Technol. 220, 245-250. DOI: 10.1007/s00217-004-1033-z

Chodur, G.M., Olson, M.E., Wade, K.L., Stephenson, K.K., Nouman, W., Fahey, G., Fahey, J.W., 2018: Wild and domesticated *Moringa oleifera* differ in taste, glucosinolate composition, and antioxidant potential, but not myrosinase activity or protein content. Sci. Rep. 8, 7995. DOI: 10.1038/s41598-018-26059-3

Dai, F., Huang, Y., Zhou, M., Zhang, G., 2009: The influence of cold acclimation on antioxidative enzymes and antioxidants in sensitive and tolerant barley cultivars. Biol. Plant. 53, 257-262. DOI: 10.1007/s10535-009-0048-5

da Silva Alves, A., Teixeira, E.M.B, Oliveira, G.C., Arantes-Pereira, L., Oliveira, C.C., Costa, L.L., 2017: Physicochemical characterization and antioxidant activity of decolorized *Moringa oleifera* Lam leaf flour. Nutrire 42, 31. DOI: 10.1186/s41110017-0058-6

Dhakar, R.C., Maurya, S.D., Pooniya, B.K., Bairwa, N., Gupta, M., Sanwarmal, 2011: *Moringa*: The herbal gold to combat malnutrition. Chron. Young Sci. 2, 119-126. DOI: 10.4103/2229-5186.90887

Doerr, B., Wade, K.L., Stephenson, K.K., Reed, S., Fahey, J.W., 2009: Cultivar Effect on *Moringa oleifera* Glucosinolate Content and Taste: A Pilot Study. Ecol. Food Nutri. 48, 199-211. DOI: 10.1080/03670240902794630

Fahey, J.W., Olson, M.E., Stephenson, K.K., Wade, K.L., Chodur, G.M., Odee, D., Nouman, W., Massiah, M., Alt, J., Egner, P.A., Hubbard, W.C., 2018: The diversity of chemoprotective glucosinolates in Moringaceae (*Moringa* spp.). Sci. Rep. 8, 7994. DOI: 10.1038/s41598-018-26058-4

Falowo, A.B., Mukumbo, F.E., Idamokoro, E.M., Lorenzo, J.M., Afolayan, A.J., Muchenje, V., 2018: Multi-functional application of *Moringa oleifera* Lam. in nutrition and animal food products: A review. Food Res. Int. 106, 317-334. DOI: 10.1016/j.foodres.2017.12.079

Fenwick, G.R., Heaney, R.K., Mullin, W.J., 1983: Glucosinolates and their breakdown products in food and food plants. Crit. Rev. Food Sci. Nutr. 18, 123-201. DOI: 10.1080/10408398209527361

Förster, N., Ulrichs, C., Schreiner, M., Müller, C.T., Mewis, I., 2015: Development of a reliable extraction and quantification method for glucosinolates in *Moringa oleifera*. Food Chem. 166, 456-464.

Fry, S.C., 1982: Isodityrosine, a new cross-linking amino acid from plant cell-wall glycoprotein. Biochem. J. 204, 449-455. DOI: 10.1042/bj2040449

Galuppo, M., De Nicola, G.R., Iori, R., Dell'Utri, P., Bramanti, P., Mazzon, E., 2013: Antibacterial activity of glucomoringin bioactivated with myrosinase against two important pathogens affecting the health of long-term patients in hospitals. Molecules 18, 14340-14348. DOI: 10.3390/molecules181114340

Ghawi, S.K., Methven, L., Rastall, R.A., Niranjan, K., 2012: Thermal and high hydrostatic pressure inactivation of myrosinase from green cabbage: a kinetic study. Food Chem. 131, 1240-1247. DOI: 10.1016/j.foodchem.2011.09.111

Halkier, B.A., Gershenzon, J., 2006: Biology and biochemistry of glucosinolates. Annu. Rev. Plant Biol. 57, 303-333. DOI: 10.1146/annurev.arplant.57.032905.105228

Houston, K., Tucker, M.R. Chowdhury, J., Shirley, N., Little, A., 2016: The Plant Cell Wall: A Complex and dynamic structure as revealed by the responses of genes under stress conditions. Front. Plant Sci. 7, 984. DOI: 10.3389/fpls.2016.00984

Jacobi, G., Klemme, B., Krapf, G., Postius, C., 1975: Dark Starvation and Plant Metabolism Biochem. Physiol. Pflanzen 168, 247-256. DOI: 10.1016/S0015-3796(17)30121-X

Johnson, L.L., Cassin, A.M., Lonsdale, A., 2017: Insights into the evolution of hydroxyproline-rich glycoproteins from 1000 plant transcriptomes. Plant Physiol. 174(2), 904-921. DOI: 10.1104/pp.17.00295

Jung, I.L., 2014: Soluble extract from *Moringa oleifera* leaves with a new anticancer activity. PLOS ONE 9: e95492. DOI: 10.1371/journal.pone.0095492

Kakengi, A.M.V., Shem, M.N., Sarwatt, S.V., Fujihara, T., 2005: Can *Moringa oleifera* be used as a protein supplement for ruminants? Asian Austral. J. Anim. 18, 42-47. DOI: 10.5713/ajas.2005.42

Karim, N.A.Abd., Ibrahim, M.D., Kntayya, S.B., Rukayadi, Y., Hamid, H.A., Razis, A.F.A., 2016: *Moringa oleifera* Lam: Targeting chemoprevention. Asian Pac. J. Cancer Prev. 17, 3675-3686. DOI: 10.14456/apjcp.2016.155/APJCP.2016.17.8.3675

Kawakishi, S., Muramatsu, K., 1966: Studies on the decomposition of sinalbin part 1. The decomposition products of sSinalbin. Agric. Biol. Chem. 30, 688-692. DOI: 10.1080/00021369.1966.10858663

Kleinwächter, M., 2007: Pflanzenbiologisch-biochemische Grundlagen zur pharmazeutischen Nutzung der Kapuzinerkresse (*Tropaeolum majus* L.). PhD thesis, Faculty of Life Sciences, TU Braunschweig.

Lamport, D.T.A., Northcote, D.H., 1960: Hydroxyproline in the cell walls of higher plants. Nature 188, 665-666. DOI: 10.1038/188665b0

Lamport, D.T.A., 1966: The protein component of primary cell walls. Adv. Bot. Res. 2, 151-218. DOI: 10.1016/S0065-2296(08)60251-7

Lamport, D.T.A., 1980: Structure and function of plant glycoproteins. In: Preiss, J. (ed.), The Biochemistry of Plants, Vol. 3, 501-541. Academic Press, New York. DOI: 10.1016/B978-0-12-675403-2.50019-3

Lamport, D.T.A., 1986: The primary cell wall: a new model. In: Young, R.A., Rowell, R.M. (eds.), Cellulose: Structure, Modification and Hydrolysis, 77-90. Wiley & Sons Inc, New York.

Li, X., Kushad, M.M., 2005: Purification and characterization of myrosinase from horseradish (*Armoracia rusticana*) roots. Plant Physiology and Biochemistry 43(6), 503-511.

Mbailao, M., Mianpereum, T., Albert, N., 2014: Proximal and Elemental

Composition of *Moringa oleifera* (Lam) Leaves from three regions of Chad. J. Food Res. Sci. 3, 12-20. DOI: 10.3923/jfrs.2014.12.20

Makkar, H.P.S., Becker, K., 1996: Nutrional value and antinutritional components of whole and ethanol extracted *Moringa oleifera* leaves. Anim. Feed Sci. Tec. 63, 211-228. DOI: 10.1016/S0377-8401(96)01023-1

Makkar, H.P.S., Becker, K., 1997: Nutrients and antiquality factors in different morphological parts of the *Moringa oleifera* tree. J. Agric. Sci. 128, 311-322. DOI: 10.1017/S0021859697004292

Matissek, R., Steiner, G., 2006: Lebensmittelanalytik – Proteine, Peptide, Aminosäuren. Springer Berlin, Heidelberg.

Miyachi, K., Fritzler, M.J., Tan, E.M., 2004: Benzyl isothiocyanate inhibits excessive superoxide generation in inflammatory leukocytes: implication for prevention against inflammation-related carcinogenesis. Carcinogenesis 25, 567-575. DOI: 10.1093/carcin/bgh051

Moyo, B., Masika, P.J., Hugo, A., Muchenje, V., 2011: Nutritional characterization of Moringa (*Moringa oleifera* Lam.) leaves. Afr. J. Biotechnol. 10, 12925-12933. DOI: 10.5897/AJB10.1599

Müller, C., van Loon, J., Ruschioni, S., De Nicolad, G.R., Olsen, C.E., Iori, R., Agerbirk, N., 2015: Taste detection of the non-volatile isothiocyanate moringin results in deterrence to glucosinolate-adapted insect larvae. Taste detection of the non-volatile isothiocyanate moringin resultsin deterrence to glucosinolate-adapted insect larvae. Phytochemistry 118, 139-148. DOI: 10.1016/j.phytochem.2015.08.007

Nouman, W., Basra, S.M.A., Siddiqui, M.T., Yasmeen, A., Gull, T., Alcayde, M.A.C., 2014: Potential of *Moringa oleifera* L. as livestock fodder crop: a review. Turk. J. Agric. For. 38, 1-14. DOI: 10.3906/tar-1211-66

Olson, B.J.S.C., 2016: Assays for determination of protein concentration. Curr. Protoc. Pharmacol. 73:A.3A.1-A.3A.32. DOI: 10.1002/cpph.3

Patel, S., Thakur, A.S., Chandy, A., Manigauha, A., 2010: *Moringa oleifera*: A review of their medicinal and economical importance to the Health and Nation. Drug Invent. Today 2, 339-342. Article ID: JPRS-DFP-0000945.

Paunović, D., Knudsen, T.S., Krivokapić, M., Zlatković, B., Antić, M., 2012: Sinalbin degradation products in mild yellow mustard paste. Hem. Ind. 66, 29-32. DOI: 10.2298/HEMIND110627055P

Rajan, T.S., De Nicola, G.R., Iori, R., Rollin, P., Bramanti, P., Mazzon, E., 2016: Anticancer activity of glucomoringin isothiocyanate in human malignantastrocytoma cells. Fitoterapia 110, 1-7. DOI: 10.1016/j.fitote.2016.02.007

Rambulana, T. et al., 2017: Gamma radiation treatment activates glucomoringin synthesis in *Moringa oleifera*. Rev. bras. farmacogn. [online]. 27.5, 569-575. DOI: 10.1016/j.bjp.2017.05.012

Razis, A.F.A., Ibrahim, M.D., Kntayya, S.B., 2014: Health benefits of *Moringa oleifera*. Asian Pac. J. Cancer. Prev. 15, 8571-8576. DOI: 10.7314/APJCP.2014.15.20.8571

Roberts, K., Grief, C., Hills, G.J., Shaw, P.J., 1985: Cell wall glycoproteins: Structure and function. J. Cell Sci. 2, 105-127. DOI: 10.1242/jcs.1985.Supplement_2.6

Talmadge, K.W., Keegstra, K., Bauer, W.D., Albersheim, P., 1973: The structure of plant cell walls: I. The macromolecular components of the walls of suspension-cultured sycamore cells with a detailed analysis of the pectic polysaccharides. Plant Physiol. 51, 158-73. DOI: 10.1104/pp.51.1.158

Teixeira, E.M.E., Carvalho, M.R.B, Neves, V.A., Silva, M.A., Arantes-Pereirac, L., 2014: Chemical characteristics and fractionation of proteins from *Moringa oleifera* Lam. leaves. Food Chem., 51-54. DOI: 10.1016/j.foodchem.2013.09.135

Terada, Y., Masuda, H., Watanabe, T., 2015: Structure-activity relationship study on isothiocyanates: Comparison of TRPA1-activating ability between allyl isothiocyanate and specific flavor components of wasabi, horseradish, and white mustard. J. Nat. Prod. 78, 1937-1941. DOI: 10.1021/acs.jnatprod.5b00272

Van Eylen, D., Hendrickx, I.H., Van Loey, A., 2005: Temperature and pressure stability of mustard seed (*Sinapis alba* L.) myrosinase. Food Chem. 97, 263-271. DOI: 10.1016/j.foodchem.2005.03.046

Waterman, C., Cheng, D.M., Rojas-Silva, P., Poulev, A., Dreifus, J., Lila, M.A., Raskin, I., 2014: Stable, water extractable isothiocyanates from *Moringa oleifera* leaves attenuate inflammation in vitro. Phytochemistry 103, 114-122.

Wadhwa, S., Panwar, M.S., Saini, N.S., Rawat, S., Singhal, S., 2013: A review on commercial, traditional uses, phytoconstituents and pharmacological activity of *Moringa oleifera*. Glob. J. Tradit. Med. 2, 1-13.

Yeoh, H.H., Chew, M.Y., 1976: Protein content and amino acid composition of cassava leaf. Phytochemistry 15, 1597-1599. DOI: 10.1016/S0031-9422(00)97435-1

ORCID:
Jutta Papenbrock https://orcid.org/0000-0003-0942-4072
Dirk Selmar https://orcid.org/0000-0003-2331-3168

Address of the corresponding author:
Prof. Dr. Dirk Selmar Institute of Plant Biology, TU Braunschweig, Mendelssohnstr. 4, 38106 Braunschweig, Germany
E-mail: d.selmar@tu-bs.de

Supplementary material

In addition to protein quantification, various electrophoretic studies on *M. oleifera* proteins had been conducted. For these analyses, the soluble protein fraction as well as the sediment had been treated with SDS and employed for the electrophoretic studies. For comparison, extracts from spinach (*Spinacia oleracea*) and the rubber tree (*Hevea brasiliensis*) had been analysed analogously. After staining the gels with Coomassie, overall, no major differences in the amount of proteins derived from the three plant species were visible, underlining the lacking of major differences in protein contents between *M. oleifera* and ordinary plants.

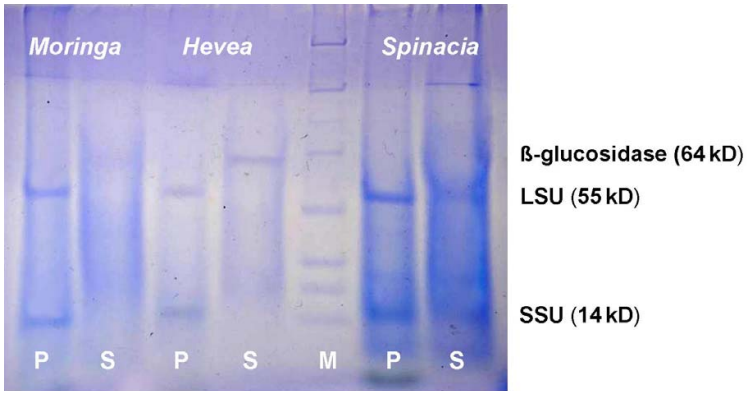

Fig. S1: SDS gel electrophoresis of various protein fractions. Protein was extracted from dried leaf material (commercial *M. oleifera* powder, *africrops!*, Berlin, and freeze-dried leaves from spinach and *Hevea*) applying McIlvaine buffer (pH 5,6). The related supernatant (30,000 g) is denoted as S. Before electrophoresis, samples had been treated with SDS and mercaptoethanol. Analogously, also the sediment was re-suspended in SDS-mercaptoethanol containing buffer. After centrifugation, the supernatant was also employed for electrophoresis (S). M = protein marker. Electrophoresis was performed according to http://www.genstrom.net/public/biology/botany/plant_physiology_module/protocols/protokoll_3.html

Indeed, in all three species, the most prominent protein bands are due to the large (LSU) and small subunit (SSU) of the ribulose-bisphosphate carboxylase (RuBisCo). Whereas this enzyme from spinach is quite soluble in McIlvaine buffer (pH 5,6), in *M. oleifera* and in *Hevea* this enzyme has to be solubilised with SDS. In *Hevea*, the most prominent band in the soluble fraction is due to the ß-glucosidase.

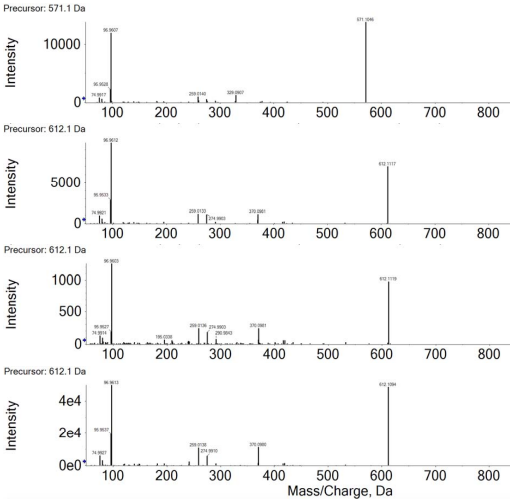

Fig. S2: MS/MS spectra for glucosinolates found in *M. oleifera*. Mass fragments at -10 eV for the precursor ions 571.1 (4-α-L-rhamnopyranosyloxy-benzyl glucosinolates) and 612 (acetyl-4-α-Lrhamnopyranosyloxy-benzyl glucosinolates isomers 1-3).

Chapter 3

Effect of biotic stress on glucosinolate contents

Chapter 3.1 The diurnal rhythm of *Brassica napus* L. influences contents of sulfur-containing defense compounds and occurrence of vascular occlusions during an infection with *Verticillium longisporum*

agronomy

MDPI

Article

The Diurnal Rhythm of *Brassica napus* L. Influences Contents of Sulfur-Containing Defense Compounds and Occurrence of Vascular Occlusions during an Infection with *Verticillium longisporum*

Sofia Isabell Rupp [1], Johann Hornbacher [1], Ina Horst-Niessen [1], Frank Schaarschmidt [2], Anja Riemenschneider [1] and Jutta Papenbrock [1,*]

[1] Institute of Botany, Leibniz University Hannover, Herrenhäuserstr. 2, D-30419 Hannover, Germany; isabell.rupp@googlemail.com (S.I.R.); J.Hornbacher@botanik.uni-hannover.de (J.H.); ina.horst-niessen@botanik.uni-hannover.de (I.H.-N.); AR.Riemenschneider@web.de (A.R.)

[2] Institute of Cell Biology and Biophysics, Leibniz University Hannover, Herrenhäuserstr. 2, D-30419 Hannover, Germany; schaarschmidt@cell.uni-hannover.de

* Correspondence: Jutta.Papenbrock@botanik.uni-hannover.de; Tel.: +49-511-762-3788

Received: 27 July 2020; Accepted: 17 August 2020; Published: 20 August 2020

check for updates

Abstract: Reduction in atmospheric sulfur and intensified agriculture have led to sulfur deficiency, often correlated with a higher susceptibility to pathogens. The spread of fungal pathogens, such as the soil-born *Verticillium longisporum*, was observed. Defense responses of infected plants are linked to sulfur-containing compounds including glucosinolates (GSLs). Some pathogens infect their hosts at specific time periods during the day. To investigate the relation of sulfur-containing metabolites with diurnal effects of infection time points, *Brassica napus* plants cultivated at two different sulfur supplies, were infected with *V. longisporum* at four different time points during the day. It was demonstrated that 3, 7 and 14 days after inoculation the infected plants differed in their infection rate depending on the time point of infection. Additionally, infected plants had higher contents of sulfur-containing metabolites, such as specific GSLs, in comparison to non-infected plants. Sufficient sulfur fertilization was always reflected in higher contents of sulfur-containing compounds as well as a lower rate of infection compared to sulfur-deprived plants. On the microscopic level vascular occlusions in the hypocotyl were visible and the amount was dependent on the time point of infection. The results might be used to optimize sulfur fertilization to reduce susceptibility to *V. longisporum*.

Keywords: Diurnal rhythm; oilseed rape; sulfur-containing metabolites; *Verticillium longisporum*

1. Introduction

Human existence depends on agricultural crops which provide food, feed for livestock, oil, fuel and other important materials. The Brassicaceae family includes many important agriculturally used plant species like *Brassica napus*, which is not only used for vegetable oil production, but also for livestock food and biodiesel production. But especially Brassicaceae crop yields are prone to plant pathogens accounting for 16% of annual crop losses [1]. A major group accounting for 70–80% of all plant pathogens consists of fungi, among them *Verticillium longisporum* [2].

In the last 20 years, the number of identified fungal plant pathogens has more than quadrupled [3]. However, this is not only due to better detection methods, but seems to be rather a direct result of high yielding crop cultivation and intensive agroecosystem management practices [4]. Due to continuous farming, it is possible that unknown or even host-specific plant pathogens such as *V. longisporum* occur [5,6].

Verticillium stem striping is caused by an infection of *B. napus* with *V. longisporum* and is especially threatening in the northern hemisphere [7,8]. The pathogen enters the plant by penetration of roots and further spreading through xylem vessels. As a result of the infection, plants are stunted and yields are drastically reduced. The use of conventional fungicides is not able to cope with any life stage of *V. longisporum*, leading to resting microsclerotia in the soil up to several years before suitable host plants can be planted again [9]. Hence, it is essential to understand the host-pathogen interaction in more detail to be able to develop alternative strategies in order to control this disease. In case of infections with vascular pathogens, recognition may be mediated by either extracellular or intracellular receptors, which leads to a defense reaction within the xylem vessels. In order to prevent the pathogen from spreading further up in the xylem vessels, the plant mediates extensive physical defense reactions. Formation of physical barriers in the form of occlusions are well described defense mechanism exhibited by *B. napus* when infected with *V. longisporum*. These occlusions can consist of crushed cells surrounding the xylem vessels, bubble-like outgrowths called tyloses, or gels consisting of phenolic compounds. Over time these occlusions become lignified through oxidation of phenolic compounds in the occlusion site and prevent the pathogen from spreading further upwards in the plant [10].

In the late 1980s, it became apparent that sulfur plays an essential role in crop resistance against pathogens, as the reduction of atmospheric sulfur depositions has led to a widespread nutrient disturbance in European agriculture [11–13]. In addition to that, increased crop yields draw great amounts of sulfur out of the soil, which calls for sufficient sulfur replacements [14].

The macronutrient sulfur is taken up by roots from the soil as inorganic sulfate. The rate of uptake and assimilation of sulfur is mainly controlled by the sulfur content of the plant and by the growing stage-dependent requirements [15]. The first stable organic compound in the sulfur assimilation, cysteine, is an important amino acid which is a part of the metabolic crossroad of primary and secondary metabolism. Among being the precursor for proteins and vitamins, it is the source of sulfur-containing defense compounds (SDCs). Sulfur-containing defense compounds, which include glucosinolates (GSLs), glutathione (GSH), sulfur-containing proteins, phytoalexins and H_2S, are not primarily synthesized for pathogen-specific defense mechanisms [16]. Part of the cysteine pool is used for the biosynthesis of the tripeptide GSH. Levels of cysteine and GSH have been suggested as markers for the elevated activity of primary sulfur metabolism after pathogen infection because of their contribution to secondary compounds, i.e., GSLs [17]. The levels of GSH and GSLs were shown to be regulated diurnally [18] and some genes involved in GSL biosynthesis are controlled by the circadian clock [19].

Glucosinolates are amino acid-derived thioglycosides, which occur generally in the order Brassicales and can be found in almost all plant organs [20,21]. There are approximately 130 described GSLs, which share a chemical structure consisting of a β-D-glucopyranose residue linked through a sulfur atom to a (Z)-N-hydroximino-sulfate ester and a variable side chain (R), which is derived from modified amino acids [22,23]. Based on the amino acid the GSLs are derived from, they can be divided into three main groups. Glucosinolates derived from alanine, leucine, isoleucine, methionine and valine yield aliphatic GSLs (aGSL). Benzylic GSLs (bGSL) are derived from phenylalanine and tyrosine, and indolic GSLs (iGSL) from tryptophan [22,24]. Glucosinolates present in Brassicaceae are a well described example of SDCs [25,26]. Glucosinolates and β-thioglucosidases (myrosinases) are spatially separated within plant tissues [27]. Intact GSLs are mostly inert, but if the plant is subjected to tissue disruption GSLs come into contact with myrosinases [26].

In the 1990's, the concept of increased plant resistance to fungal pathogens based on sulfur was developed [28], also in the context of new cultivars low in both erucic acid and GSLs. Experiments performed with sulfur-deficient *B. napus* showed a higher susceptibility towards *V. longisporum* highlighting the importance of a sufficient sulfur supply [29].

Regarding a successful pathogenic invasion and consequent disease development, it is necessary that pathogen, susceptible host and favorable environmental conditions come together at a certain

time point. Conversely, the susceptibility of the host and the virulence of the pathogen may vary during the day, as well as the stage of development of the two organisms involved [30]. Various publications showed that the interaction between plants and their pathogens correlates with light, indicating that there are direct effects of light on both organisms [31–34]. Results from Wang et al. [35] indicate that defense genes are under circadian control, allowing plants to detect infections at dawn when the pathogens disperse spores and time immune responses by perceiving pathogenic signals upon infection. Temporal control of the defense genes by CIRCADIAN AND CLOCK ASSOCIATED 1 (CCA1) differentiate their involvement in (I) basal defense mechanisms and (II) defense based on specific resistance (R) genes. The studies revealed a key functional link between the circadian clock and plant immunity. Mutants overexpressing CCA1 showed enhanced resistance against downy mildew supporting a direct interaction of the circadian clock with plant immunity [35]. In recent studies, infection experiments with *A. thaliana* at different time points were performed analyzing a clock-mediated variation in resistance [36,37]. Plants in these experiments showed a decreased susceptibility when infected at dawn with a bacterial pathogen and a fungus, respectively. In addition, there are emerging evidences for a relationship between the nutrient status and circadian rhythm in plants [38]. For nitrate metabolism and during nitrate deficiency, respectively, interactions with the circadian clock could already be shown [39]. A number of key genes in metabolic pathways including the sulfur metabolism have been already reported as regulated in a circadian way in *A. thaliana* [40]. In a study by Hornbacher et al. [18] performed with *B. napus* diurnal oscillations of the expression of genes involved in the transport and reduction of sulfate as well as of GSH contents were shown, comparable to the oscillations of *CCA1* expression. It was also demonstrated that GSLs display ultradian oscillations that were altered by the sulfur supply of the plants.

To investigate the degree of susceptibility of *B. napus* plants depending on the time point, plants were infected with *V. longisporum* at different time points of the day. Furthermore, the effect of different sulfur fertilizations on the infection of the plants was analyzed.

2. Materials and Methods

2.1. Plant Material and Growth Conditions

Seeds from the MSL-hybrid (Male Sterility Lembke) winter oilseed rape cultivar Genie were obtained from the Deutsche Saatveredelung AG (DSV) (Lippstadt, Germany; breeder: RAPOOL-Ring GmbH, Isernhagen, Germany). The cultivar has a good overall health, a higher GSL content in seeds in comparison to other cultivars from the DSV and an excellent resistance against aggressive stem canker triggering pathogens (*Leptosphaeria maculans*; *L. biglobosa*) (Sortenkatalog Winterraps 2012 RAPOOL). Plants were grown as described in Weese et al. [41] in climatic chambers equipped with ESC 300 software interface (Johnson Controls; Mannheim, Germany). The seeds needed 7 d under following settings to germinate: 12 h light, 22 °C, 70% humidity; 12 h night, 20 °C, 70% humidity; Photosynthetic Photon Flux Density (PPFD): 350 µmol m^{-2} s^{-1}; lamp type CMT 360 LS/W/BH-E40) (Eye Lighting Europe Ltd., Uxbridge, United Kingdom). Sulfur-sufficient and deficient fertilization was obtained by using Blake-Kalff (BK) media [42] with 1 mM $MgSO_4$ (+S) and 0.01 mM $MgSO_4$ (−S), which are described in Weese et al. [41].

2.2. Verticillium longisporum Material, Growth and Cultivation

The *V. longisporum* strain VL43 WT (wild-type) was obtained from Prof. Dr. Andreas von Tiedemann (Department of Crop Sciences, Division of Plant Pathology and Crop Protection, Georg-August-University, Göttingen, Germany). The strain was first isolated from OSR in Mecklenburg/Germany in 1990 [43].

Two media from Difco™ were used for the cultivation of *V. longisporum*, which were prepared as specified by the manufacturer. In order to achieve a uniform mycelium formation, and the highest possible sporulation rate for *V. longisporum*, it was cultivated in two steps. For the first step of

cultivation, 250 mL potato dextrose broth (PDB) was prepared and autoclaved. 900 µL of glycerol VL43 WT spore stock solution (1×10^6 spores per ml) was added to the medium after cooling down and aluminum foil was used to keep the culture in the dark. After 2 to 3 weeks of shaking at 22 °C at 120 rpm, the mycelium was separated under sterile conditions with the aid of gaze (0.2 µm) and transferred to glass flasks with 250 mL of autoclaved Czapek-Dox broth (CDB). Cultures were wrapped with aluminum foil and were shaken at 22 °C and 110 rpm for 2 more weeks.

2.3. Inoculation Procedure of Brassica napus with Verticillium longisporum

Seven days old *B. napus* seedlings were mock-inoculated with CDB or root dip-inoculated for 45 min in a mycelium-spore mixture. In this study seedlings were infected at four different time points (Figure 1a) according to the harvesting time points chosen in Rumlow et al. [44]. Infection for the time points 0 h and 16 h were performed in the dark. All plants were watered for 3 d with distilled water. At 3 d post inoculation (dpi), above ground plant material of eight plants for each treatment was harvested and tested for the infection status using qPCR (Table 1). The remaining plants were then divided into sufficient (+S) and deficient (−S) sulfur-fertilized groups (Figure 1b). After 7 dpi and 14 dpi, above ground plant material of eight plants for each treatment was harvested and directly frozen into liquid nitrogen. Frozen samples were ground to a fine powder and stored at −80 °C until further analysis (Table 1). For histological examination, the hypocotyl of one plant for each treatment was harvested at 14 dpi and 21 dpi and initially conserved in formaldehyde-alcohol-acetic acid (FAA). This experiment was performed two times.

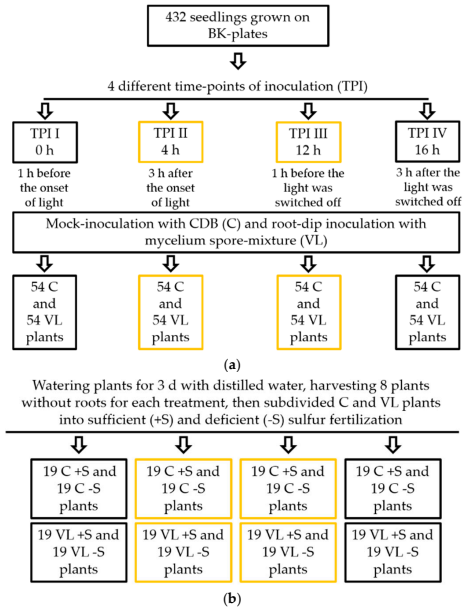

Figure 1. Experimental design. (**a**) Scheme for the infection experiment at different time points of inoculation (TPI). Control plants (C) were germinated in Blake Kalff medium (BK), mock-inoculated with Czapek-Dox broth (CDB) and infected plants (VL) with mycelium-spore mixture. (**b**) C and VL plants were watered for 3 d with distilled water, then subdivided into C and VL with sufficient (+S) and deficient (−S) sulfur fertilization.

Table 1. Overview of the fertilization procedure, sampling and conducted methods.

Fertilization	Harvesting	Sample Size of Each Group	Method
Distilled water as required	3 dpi	Eight plants without root	DNA-extraction qPCR
Distilled water as required and Corresponding BK medium (+S/−S) [1]: 150 mL each pot weekly	7 dpi	Eight plants without root	DNA-extraction qPCR Elemental analysis via ICP-OES GSL analysis via HPLC Cysteine and glutathione analysis via HPLC
	14 dpi	Eight plants without root Histology: hypocotyl of one plant	DNA-extraction qPCR Elemental analysis via ICP-OES GSL analysis via HPLC Cysteine and glutathione analysis via HPLC Histology: Toluidine blue staining
	21 dpi	Only histology: hypocotyl of 1 plant	Histology: Toluidine blue staining

[1] +S BK medium with 1 mM $MgSO_4$; −S BK medium with 0.01 mM $MgSO_4$; start of fertilization after the first sampling at 3 dpi.

2.4. DNA Extraction

The DNeasy Plant Mini Kit (Qiagen, Hilden, Germany) was used for extraction of *V. longisporum* DNA from *B. napus*. The extraction was carried out as specified by the manufacturer with the following modifications. For each sample approx. 50 mg of ground and frozen plant material was used. After the incubation at 65 °C, tubes were placed on ice for about 1–2 min to cool down to room temperature (RT). Centrifugation steps were carried out at 16,100 g. In order to remove the residual EtOH from the spin column, the tubes were left open for approximately 1-2 min at RT prior to elution with 50 µL Buffer AE. The DNA concentration of the samples was determined photometrically at 260 nm with a Microplate-Reader (Synergy Mix, Multi-Mode Microplate Reader) (BioTek Instruments GmbH, Bad Friedrichshall, Germany).

2.5. Real-Time Quantitative PCR

The real-time quantitative polymerase chain reaction (qPCR) was used for the detection and quantification of *V. longisporum* DNA in *B. napus*. The qPCR works with two fluorescent dyes, contained in the used Platinum® SYBR® Green qPCR SuperMix UDG with ROX (Invitrogen™ by Thermo Fisher Scientific GmbH, Dreieich, Germany). For the samples, a master mix without template DNA was prepared. 18 µL of master mix were placed in the 96-well plates (white; without frame; 0.2 mL, Sarstedt, Nümbrecht, Germany), to which 2 µL diluted sample DNA (final concentration between 0.5–1 ng μL^{-1}), standard DNA of *V. longisporum* or pure H_2O (negative controls) were pipetted. For the standard series 1 ng μL^{1-} standard DNA was prepared from extracted DNA of pure *V. longisporum* VL43 WT culture (standard series from 1 ng VL-DNA μL^{1-} to approx. 1 pg VL-DNA μL^{-1}). For this study the primers OLG70 (CAGCGAAACGCGATATGTAG) and OLG71 (GGCTTGTAGGGGGTTTAGA) from Eynck et al. [45] were selected. The primers were adapted to the used qPCR program by base modification (OLG70: CGCAGCGAAACGCGATATGTAG; OLG71: CGGGCTTGTAGGGGGTTTAGA). The qPCR analysis was performed with the 7300 Real Time System (Applied Biosystems by Thermo Fisher Scientific, CA, USA). The used software was Abi 7300 System SDS (Applied Biosystems by Thermo Fisher Scientific). The qPCR program consisted of four stages starting with a 50 °C step for 2 min. PCR amplification was carried out using an initial denaturation step for 2 min at 95 °C, which was followed by 40 reaction cycles consisting of a 15 s denaturation step at 95 °C and an annealing and elongation step for 1 min at 60 °C. To verify amplification of the specific target DNA, a melting curve analysis was included. Additionally, the PCR product was checked by agarose gel electrophoresis for correct size. By using the Ct values of the individual samples in the logarithmic straight-line equation of a standard series with samples of defined concentration, the concentration of the examined DNA sequence can be calculated.

2.6. Elemental Analysis and Analysis of Soluble Thiol Compounds

The analysis of elements was carried out as described in Weese et al. [41]. The determination of thiols was done according to Riemenschneider et al. [46].

2.7. Analysis of Glucosinolates

The analysis of GSLs was performed as described in Hornbacher et al. [18] with one modification. The content of GSLs was determined using 500–700 mg of ground and frozen plant material for the extraction step.

2.8. Histological Analysis

For histological examination the hypocotyls were preserved in FAA (70% EtOH, 100% acetic acid, 37% formaldehyde; 18:1:1, *v*/*v*/*v*) and then dehydrated in an ascending alcohol series (70% EtOH for 60 min; 80%, 90% and 99% EtOH for each 120 min). Next, 80% EtOH was mixed with Eosin Y (Eosin yellowish) (Carl Roth GmbH + Co. KG, Karlsruhe, Germany). The dye slightly stains the hypocotyl pieces without affecting the subsequent staining method and thus facilitates the orientation during embedding. The samples were embedded with Technovit ® 7100 (Kulzer GmbH, Hanau, Germany). The pre-infiltration, infiltration and polymerization were carried out as specified by the manufacturer with the following modifications. The infiltration step was done for about 18 h. The hardening of the samples at the polymerization step required about 24 h in the embedding moldings (Polyethylene Molding Cup Trays, 6 × 8 × 5 mm hexagon; nine cavities) (Polysciences Europe GmbH, Hirschberg an der Bergstrasse, Germany). Subsequently, the hardened resin blocks were taken out of the molding cups and dried for approximately further 48 h at RT before they were cut. The cross sections (25 µm thick) of the embedded hypocotyls were made with a rotary microtome (R. Jung AG 1960, Heidelberg, Germany) using a d-blade (16 cm steel-blade, d-profile) (Leica Mikrosysteme Vertrieb GmbH, Wetzlar, Germany). The cross sections were threaded onto slides wetted with distilled water. On each slide eight cross sections were placed in two rows. The slides were dried at 140 °C on a heating plate for histology slides (HB 300) (Gestigkeit Harry GmbH, Düsseldorf, Germany) for 1–2 h. In order to detect vascular occlusions hypocotyl cross sections were stained with 0.05% (*w*/*v*) toluidine blue (Sigma-Aldrich Chemie GmbH, Taufkirchen, Germany) for 10 min at 60 °C [47]. The slides were washed with distilled water and then dried at 100 °C for 1 h. The cross sections were mounted with Eukitt® (Sigma-Aldrich Chemie GmbH) for permanent conservation. Images of samples were taken with a light microscope in bright field (Microscope: CX31; Camera: U-CMA D3) (Olympus Europa SE & Co. KG, Hamburg, Germany) (Software: NIS Elements, Version 4.50 64-bit) (Nikon GmbH, Düsseldorf, Germany). From each hypocotyl sample at least two slides with each eight cross sections were prepared. For the evaluation microscopic images of five cross sections were made and the following parameters have been defined: number of total tracheas in the xylem, number of occlusions in the mid area of the xylem (mXy) and number of occlusions in the periphery of the xylem (pXy). Figure 2a shows the distribution of different tissue types in a cross section of a hypocotyl of *B. napus*, starting from the middle with pith (Pi), xylem (Xy), cambium (Cam) and phloem (Ph). Figure 2b shows the definition of the counting range of occlusions. This area had to be redefined for each microscopic image. From the Pi to half of the Xy became the mXy counting region, the other half the pXy counting region. Counting was performed with help of the open source image processing package "Fiji" [48].

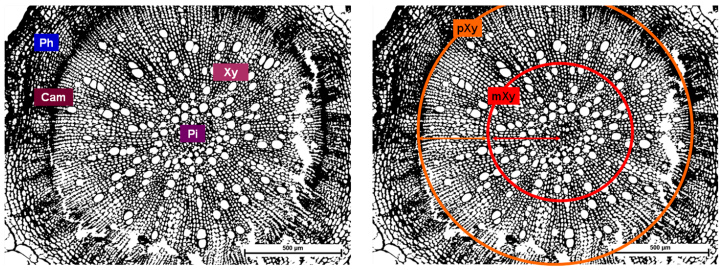

(**a**) (**b**)

Figure 2. Different tissue types in the cross section of a hypocotyl from *B. napus* and the definition of the counting range of the occlusions. (**a**) The tissue distribution of a hypocotyl cross section of *B. napus*: Pi: Pith; Xy: Xylem; Cam: Cambium; Ph: Phloem. (**b**) A simplified representation of the counting ranges of the occlusions for mid area of the xylem (mXy; red circle, red arrow) and periphery of the xylem (pXy; orange circle, orange arrow). For each cross section, the range from Pi to Cam was measured. The measured distance was divided in half and defined to mXy and pXy.

2.9. Statistical Analysis

Glucosinolate concentrations as well as cysteine and glutathione concentrations were log-transformed before analysis due to finding right skewed distributions and variance increasing with mean. The transformed data were analyzed in general linear models with four factors and all two-way interactions between the four factors. Based on the fitted models, analysis of variance was performed to test the significance of main effects and interactions and Tukey tests for the model-based means of factor TPI were performed jointly across all other factor levels and separately for VL-infected and mock-infected groups.

To analyze the histological data of occlusions in the xylem vessels of infected plants, the counted total number of mid occlusions among the total number of tracheae per plant was analyzed in a generalized linear model with logit link and assumption of over dispersed binomial data [49]. The model contained main effects for the three factors dpi, TPI and different sulfur supply and their two-way interactions. After model fit, F-tests in analysis of deviance were used to test the significance of these effects. Data of the elements sulfur, calcium, potassium and iron were analyzed without transformation in a model with four factors and their two-way interactions. Based on the fitted Modell ANOVA-tables and multiple comparisons of model-based means were performed (R package emmeans).

Log-transformed qPCR data were analyzed using a three-factorial model with effects dpi (3, 7 and 14) and TPI (I, II, III and IV) crossed, including an interaction term and effect of sulfur supply nested in effect of dpi. Based on the fitted model, analysis of variance tables was computed and multiple comparisons were performed using R package emmeans. Analysis was performed in R 3.6.1 [49] using the add-on package emmeans (version 1.4) [50] for model-based comparisons of means. In order to verify the success of the infection, a qPCR analysis was carried out at 3 dpi, afterwards the fertilization began with sufficient and deficient sulfur supply. Hence, it seems to be useful to include the infection status, from which the different fertilization began, in comparison with the results of the elemental and metabolite analysis from 7 and 14 dpi. However, the two runs of the experiment proceeded differently with respect to the qPCR results, which means that the VL-infected groups are differentially infected, resulting in varying responses of host plants. Therefore, the two experiments had to be analyzed statistically separately. The results of one experiment are analyzed and discussed below as an example. The data of the other experiment can be found in the Supplement data (Tables S1–S7; Figures S1–S3).

3. Results

3.1. Detection and Verification of the Infection with V. longisporum in B. napus

In order to investigate spreading of *V. longisporum* after infection in the plant, qPCR analysis was performed with samples collected at 3, 7 and 14 dpi using primers for the amplification of ITS. The amount of *V. longisporum* (VL) DNA was calculated in VL DNA g^{-1} fresh weight (FW) of the plant material. Samples of 3 dpi were not differentially fertilized yet, therefore, the data shows the mean of two biological replicates. Only the data of VL-infected plants are shown in Table 2 because control samples showed a maximum of 5% of the values of infected plants, or the amount of the VL-DNA was below the limit of detection or below limit of quantification, respectively (data not shown).

Table 2. Amount of *V. longisporum* VL43-DNA detected by qPCR with ITS primers in *B. napus*. Status of infection rate in mycelium-spore inoculated plants calculated in ng VL DNA g^{-1} FW; VL without +S/-S fertilization: samples, consisting of eight pooled plants, at 3 dpi without different sulfur fertilization, only distilled water as required; 7 dpi and 14 dpi: plants were fertilized with different sulfur supply; due to the limited plant material, only one measurement could be carried out. TPI I, 1 h before the onset of the light; TPI II, 3 h after the onset of the light; TPI III, 1 h before the light is switched off; TPI IV, 3 h after the light is switched off. Significant change in the measured values over the harvest period 3, 7 and 14 dpi ($p = 0.002$); Significant difference between TPI I and TPI IV ($p = 0.008$); Significant effects for TPI depending on dpi ($p = 0.01$); Significant effects of sulfur supply depending on dpi ($p = 0.01$); Significant effects for VL +S between 7 and 14 dpi ($p = 0.0001$) and between VL +S and VL −S at 14 dpi ($p = 0.0003$).

3 dpi/ng VL DNA g^{-1} FW	**VL without +S/−S Fertilization**	**VL without +S/−S Fertilization**
TPI I	6.17	7.05
TPI II	13.85	10.54
TPI III	17.22	19.54
TPI IV	27.12	27.20
7 dpi/ng VL DNA g^{-1} FW	**VL +S**	**VL −S**
TPI I	13.54	12.37
TPI II	4.03	7.68
TPI III	8.01	12.50
TPI IV	8.15	8.27
14 dpi/ng VL DNA g^{-1} FW	**VL +S**	**VL −S**
TPI I	0.29	4.79
TPI II	1.06	5.87
TPI III	0.51	1.82
TPI IV	0.33	5.45

At 3 dpi the content of VL-DNA was the highest in plants of TPI IV compared to TPI I in both groups that were not fertilized differently at that time ($p = 0.002$). At 7 dpi the amount of VL-DNA was higher in VL-infected +S (54%) and −S (43%) groups at TPI I compared to the plants of 3 dpi. The contents in plants of TPI II-IV were lower in both VL-infected groups compared to 3 dpi. At 14 dpi the content of VL-DNA was lower in both VL-infected groups at all TPIs compared to plants at 7 dpi. Most importantly, the contents of VL-infected +S plants were significantly lower compared to −S plants. In summary, significant effects for TPI depending on dpi ($p = 0.01$) and significant effects for sulfur supply depending on dpi ($p = 0.01$) were observed.

3.2. Stunting of B. napus Plants Infected with the V. longisporum Strain VL43

Three plants of all treatments were selected and photographically documented at 14 dpi. VL-infected plants, which were fertilized with sufficient sulfur were smaller compared to non-infected control plants at 14 dpi (Figure 3; A1–A4: control plants; B1–B4: VL-infected plants).

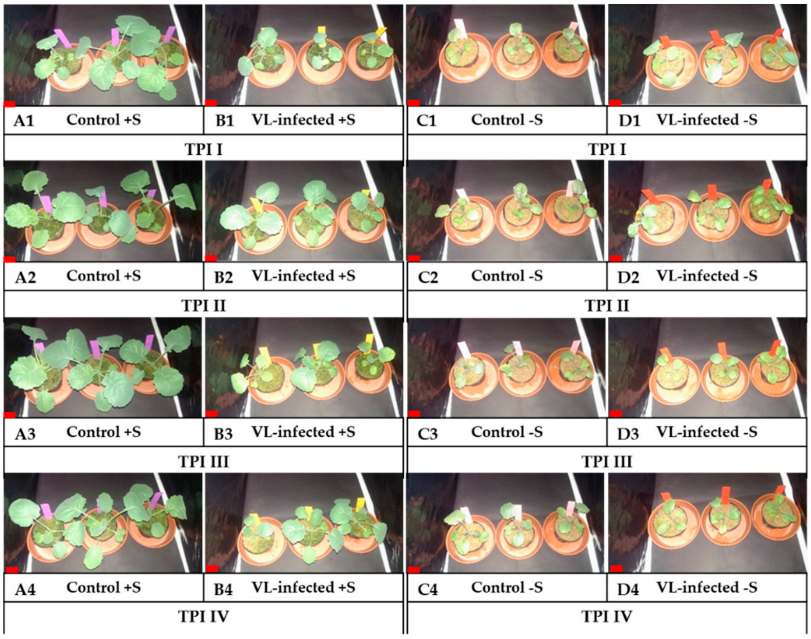

Figure 3. *Brassica napus* plants at 14 dpi cultivated at two different sulfur regimes and either infected with the *V. longisporum* strain VL43 or non-infected. Plants under sufficient (1 mM $MgSO_4$: +S) and deficient (0.01 mM $MgSO_4$: −S) sulfur supply at 14 dpi; A1–A4: control plants +S; B1–B4: VL-infected plants +S; C1–C4: control plants −S; D1–D4: VL-infected plants −S; red scale bar 5 cm.

The non-infected and VL-infected plants, which were cultivated under sulfur-limited conditions showed a decreased growth rate manifested in lower plant height, smaller leaves and overall stunting (Figure 3). Leaves were partially chlorotic and purple in color, with the leaf surface feeling leathery and, in some areas, slightly broken off. In addition, the leaf margin of some plants bulged inward or outward. Overall, infection itself, but not the TPI, had an effect on the plant's appearance.

3.3. Levels of Indolic, Aliphatic and Benzylic GSLs in Mock-Treated and Plants Infected with V. longisporum at Different TPIs and Under Different Sulfur Supplies

As GSLs are known to be part of the plant's response to pathogens, contents of GSLs in samples of 7 dpi and 14 dpi were analyzed by HPLC. Overall, contents of all GSLs were lower in sulfur-deficient plants compared to sulfur-sufficient plants at all TPIs and changes became more pronounced at 14 dpi (Table 3). Contents of glucobrassicin were higher in VL-infected plants at all TPIs compared to non-infected plants. Even at 14 dpi when glucobrassicin contents were much lower compared to 7 dpi in non-infected plants, infected plants showed higher contents compared to non-infected plants (Table 3). Small changes were observed in neoglucobrassicin contents between the TPIs, with contents being higher in TPI IV compared to TPI I at 7 dpi in plants of both fertilization groups. Lower contents of neoglucobrassicin were observed at 14 dpi in plants of all groups, but no major differences were observed between infected and non-infected sulfur-sufficient plants.

Table 3. Contents of iGSLs (glucobrassicin, neoglucobrassicin and 4-hydroxyglucobrassicin) in mock- and mycelium-spore inoculated plants at 7 dpi and 14 dpi; data from 7 and 14 dpi represent the result of one measurement; hypothetical SDs of samples from 7 dpi based on previous measurements can range between 2–25%; random SDs of samples from 14 dpi based on three dependent technical replicates; the reason for only one measurement is the low amount of the plant material due to space limitation in climatic chambers.

Glucobrassicin [nmol g^{-1} DW]									
7 dpi	**C +S**	**VL +S**	**C −S**	**VL −S**	**14 dpi**	**C +S**	**VL +S**	**C −S**	**VL −S**
TPI I	195.99	304.14	136.91	328.44	TPI I	92.52 ± 4.30	158.54 ± 7.70	0.41	10.76
TPI II	231.11	348.42	162.56	230.67	TPI II	109.19	123.30	0.06 ± 0.02	2.75 ± 0.78
TPI III	262.87	356.19	202.76	297.80	TPI III	97.09 ± 9.92	165.79	0.32	11.91
TPI IV	351.40	456.19	213.60	267.74	TPI IV	106.38	139.87 ± 3.86	1.11	12.31 ± 0.84
Neoglucobrassicin [nmol g^{-1} DW]									
7 dpi	**C +S**	**VL +S**	**C −S**	**VL −S**	**14 dpi**	**C +S**	**VL +S**	**C −S**	**VL −S**
TPI I	28.83	29.87	20.62	39.53	TPI I	20.71 ± 3.58	17.77 ± 1.30	2.93	5.83
TPI II	37.80	40.12	28.44	47.18	TPI II	22.74	20.01	2.60 ± 0.23	6.20 ± 1.45
TPI III	37.14	28.95	28.37	21.53	TPI III	19.05 ± 2.78	19.58	4.05	6.99
TPI IV	41.08	43.18	33.60	31.21	TPI IV	23.32	23.62 ± 1.64	5.18	8.27 ± 0.82
4-Hydroxyglucobrassicin [nmol g^{-1} DW]									
7 dpi	**C +S**	**VL +S**	**C −S**	**VL −S**	**14 dpi**	**C +S**	**VL +S**	**C −S**	**VL −S**
TPI I	9.04	20.19	19.24	3.47	TPI I	14.94 ± 1.42	19.80 ± 5.84	0.40	0.19
TPI II	9.97	22.83	18.44	0.96	TPI II	15.00	6.74	0.29 ± 0.02	0.22 ± 0.03
TPI III	4.93	20.20	2.08	5.30	TPI III	14.76 ± 2.87	4.00	0.27	0.32
TPI IV	16.24	10.77	7.35	1.42	TPI IV	25.93	9.16 ± 4.34	0.29	0.32 ± 0.04

Sulfur-deficient and infected plants on the other hand showed higher contents compared to non-infected sulfur-deficient plants. Sufficiently sulfur-fertilized and infected plants showed higher contents of 4-hydroxyglucobrassicin at 7 dpi compared to non-infected controls but only in sulfur-sufficient plants contents were higher at TPI VI. Contents were lower in infected and sulfur-deficient plants, compared to non-infected and sulfur-deficient plants. At 14 dpi, contents of 4-hydroxyglucobrassicin were higher in sulfur-sufficient non-infected plants, but were lower in all other groups compared to 7 dpi. The differences between 7 and 14 dpi ($p = 0.00002$) and the effect of different sulfur supply ($p = 0.00005$) were significant. Overall, the entirety of iGSLs showed significant differences between control and VL-infected plants ($p = 0.00003$).

Contents of aGSLs were also lower in sulfur-deficient plants compared to sulfur-sufficient plants, which became more pronounced at 14 dpi compared to 7 dpi (Table 4). Infected and sulfur-sufficient plants showed higher contents of all aGSL at 7 dpi compared to non-infected plants, whereas at 14 dpi the contents of aGSL where only higher in TPI I in infected sulfur-deficient plants compared to non-infected plants.

At 14 dpi, contents of aGSLs were lower in infected and sulfur-sufficient plants infected at TPI II to TPI IV compared to infected sulfur-sufficient plants harvested at 7dpi infected at the same TPIs. This effect was less pronounced in contents of glucoalyssin, glucoraphanin and glucobrassicanapin at TPI I. Contents of progoitrin were consistently higher in infected sulfur-deficient plants at 14 dpi compared to non-infected plants, whereas contents of other aGSLs were lower with a few exceptions regarding the TPIs. Overall, aGSLs showed a significant effect in terms of dpi on the average over the other factors ($p = 0.0004$) and significant differences between control and VL-infected plants ($p = 0.02$).

Contents of gluconasturtiin were higher in all infected plants, when compared to non-infected plants, even regardless of sulfur-fertilization, or TPIs (Table 5). Highest contents were observed in infected and sulfur-sufficient plants. Like other GSLs, gluconasturtiin contents were lower at 14 dpi in sulfur-deficient non-infected plants, when compared to 7 dpi, but levels were up to 5 times higher in sulfur-deficient and infected plants, when compared to non-infected plants. Infected

and sulfur-sufficient plants at 14 dpi had lower contents compared to plants harvested at 7 dpi from the same group, but still had higher contents compared to non-infected plants.

Table 4. Contents of aGSLs (progoitrin, glucoalyssin, glucoraphanin, glucobrassicanapin and gluconapin) in mock- and mycelium-spore inoculated plants at 7 dpi and 14 dpi; data from 7 and 14 dpi represent the result of one measurement; hypothetical SDs of samples from 7 dpi based on previous measurements can range between 3–35%; random SDs of samples from 14 dpi based on three dependent technical replicates; the reason for only one measurement is the low amount of the plant material due to space limitation in climatic chambers.

Progoitrin [nmol g^{-1} DW]									
7 dpi	**C +S**	**VL +S**	**C −S**	**VL −S**	**14 dpi**	**C +S**	**VL +S**	**C −S**	**VL −S**
TPI I	93.98	171.34	68.43	210.08	TPI I	58.07 ± 1.60	104.17 ± 9.41	0.75	0.97
TPI II	89.62	219.13	111.49	72.20	TPI II	95.27	97.67	1.43 ± 0.43	0.90 ± 0.25
TPI III	61.33	169.01	46.83	109.53	TPI III	105.96 ± 12.33	108.96	0.48	0.73
TPI IV	170.73	241.14	103.43	113.41	TPI IV	95.63	107.59 ± 8.89	0.89	1.04 ± 0.05
Glucoalyssin [nmol g^{-1} DW]									
7 dpi	**C +S**	**VL +S**	**C −S**	**VL −S**	**14 dpi**	**C +S**	**VL +S**	**C −S**	**VL −S**
TPI I	69.56	99.80	30.68	119.98	TPI I	54.31 ± 1.73	95.48 ± 11.29	4.74	0.65
TPI II	54.13	183.47	56.26	47.09	TPI II	84.88	70.56	6.51 ± 0.66	2.98 ± 0.33
TPI III	29.23	116.93	18.61	42.17	TPI III	91.62 ± 10.66	79.63	2.91	2.95
TPI IV	115.74	203.69	50.57	39.80	TPI IV	108.33	87.88 ± 11.79	3.72	3.28 ± 0.36
Glucoraphanin [nmol g^{-1} DW]									
7 dpi	**C +S**	**VL +S**	**C −S**	**VL −S**	**14 dpi**	**C +S**	**VL +S**	**C −S**	**VL −S**
TPI I	14.39	14.35	2.69	9.09	TPI I	9.93 ± 0.34	14.83 ± 1.61	2.15	3.91
TPI II	3.58	25.61	6.82	2.11	TPI II	13.25	8.23	2.91 ± 0.70	3.54 ± 0.19
TPI III	1.56	17.26	1.54	2.30	TPI III	11.81 ± 2.10	8.21	0.88	6.72
TPI IV	13.40	27.65	4.44	4.16	TPI IV	17.89	8.52 ± 2.38	2.00	7.54 ± 1.14
Glucobrassicanapin [nmol g^{-1} DW]									
7 dpi	**C +S**	**VL +S**	**C −S**	**VL −S**	**14 dpi**	**C +S**	**VL +S**	**C −S**	**VL −S**
TPI I	23.89	45.03	13.68	65.71	TPI I	27.14 ± 1.30	43.01 ± 3.90	0.50	0.50
TPI II	42.35	54.84	26.62	20.18	TPI II	45.36	61.28	0.30 ± 0.03	0.32 ± 0.27
TPI III	20.54	37.22	15.41	23.31	TPI III	56.59 ± 6.94	66.76	0.44	0.21
TPI IV	43.87	52.53	30.01	13.38	TPI IV	46.39	62.48 ± 3.26	0.60	0.33 ± 0.13
Gluconapin [nmol g^{-1} DW]									
7 dpi	**C +S**	**VL +S**	**C −S**	**VL −S**	**14 dpi**	**C +S**	**VL +S**	**C −S**	**VL −S**
TPI I	35.33	70.21	11.30	39.84	TPI I	22.13 ± 0.93	38.01 ± 2.25	1.47	0.77
TPI II	28.10	77.65	24.91	8.63	TPI II	39.35	28.64	1.60 ± 0.38	0.34 ± 0.09
TPI III	11.18	55.26	8.48	11.70	TPI III	55.56 ± 7.99	32.10	1.95	0.35
TPI IV	70.01	77.80	16.69	12.60	TPI IV	45.30	29.42 ± 2.94	2.17	0.37 ± 0.09

Table 5. Contents of the bGSL gluconasturtiin in mock- and mycelium-spore inoculated plants at 7 dpi and 14 dpi; data from 7 and 14 dpi represent the result of one measurement; hypothetical SDs of samples from 7 dpi based on previous measurements can range between 1–25%; random SDs of samples from 14 dpi based on three dependent technical replicates; the reason for only one measurement is the low amount of the plant material due to space limitation in climatic chambers.

Gluconasturtiin [nmol g^{-1} DW]									
7 dpi	**C +S**	**VL +S**	**C −S**	**VL −S**	**14 dpi**	**C +S**	**VL +S**	**C −S**	**VL −S**
TPI I	98.71	215.12	92.05	171.25	TPI I	52.05 ± 1.43	125.92 ± 8.14	10.40	55.84
TPI II	69.16	190.75	107.36	183.82	TPI II	44.07	86.90	5.69 ± 0.09	35.56 ± 6.55
TPI III	55.98	240.52	84.85	191.47	TPI III	51.71 ± 4.10	142.95	6.92	50.17
TPI IV	123.95	263.75	101.10	230.38	TPI IV	59.60	109.09 ± 2.78	10.22	45.62 ± 1.56

Overall, contents of glucobrassicin as well as gluconasturtiin were always higher in infected plants, when compared to non-infected plants. Although sulfur-deficiency led to lower contents of these GSLs in non-infected and infected plants, amounts were still higher in the latter ones. On the other hand, contents of aGSLs were observed to be lowered in a higher manner by sulfur-deficiency compared to the other GSLs analyzed. Infected plants showed only higher contents of aGSLs at all TPIs at 7 dpi and when supplied with sufficient sulfur.

The contents within the TPIs in control +S- and VL-infected -S-groups were nearly similar, while contents in control −S-groups were overall the lowest. The differences in the levels of gluconasturtiin in control and VL-infected plants were significant ($p = 0.003$).

3.4. Levels of Cysteine and Glutathione

Since the cysteine pool is essential for sulfur metabolism and is used to synthesize sulfur-containing secondary metabolites, its contents were analyzed alongside with GSH, which is used for the synthesis of secondary metabolites, for detoxification purposes and as an antioxidant.

Contents of cysteine as well as GSH were severely lower in sulfur-deficient plants compared to sulfur-sufficient plants. The effects became more pronounced in plants harvested at 14 dpi (Table 6).

Table 6. Thiol analysis performed with HPLC: contents of cysteine and glutathione (GSH) in mock- and mycelium-spore inoculated plants at 7 and 14 dpi; data of 7 dpi represents the result of one measurement; the reason for only one measurement is the low amount of the plant material due to space limitation in climatic chambers.; data of 14 dpi represents the mean of three dependent technical replicates ± SD.

Cysteine [nmol g^{-1} FW]									
7 dpi	**C +S**	**VL +S**	**C −S**	**VL −S**	**14 dpi**	**C −S**	**VL +S**	**C −S**	**VL −S**
TPI I	27.41	28.03	13.80	6.57	TPI I	17.73 ± 1.42	19.66 ± 1.58	2.95 ± 0.52	4.60 ± 0.30
TPI II	20.57	28.43	8.62	16.29	TPI II	22.07 ± 1.30	21.42 ± 1.33	1.93 ± 0.20	1.99 ± 0.60
TPI III	18.57	24.66	13.70	15.43	TPI III	23.35 ± 0.91	21.72 ± 2.05	1.98 ± 0.36	3.41 ± 0.17
TPI IV	28.51	30.26	11.85	12.00	TPI IV	20.20 ± 1.50	18.77 ± 1.97	1.79 ± 0.88	4.10 ± 0.26
GSH [nmol g^{-1} FW]									
7 dpi	**C +S**	**VL +S**	**C −S**	**VL −S**	**14 dpi**	**C +S**	**VL +S**	**C −S**	**VL −S**
TPI I	559.17	420.96	278.54	568.68	TPI I	671.79 ± 26.98	707.66 ± 22.27	66.21 ± 4.98	136.38 ± 13.05
TPI II	646.72	629.21	276.83	464.82	TPI II	690.45 ± 13.15	750.78 ± 20.13	68.52 ± 9.78	63.00 ± 3.03
TPI III	519.29	588.02	312.53	348.69	TPI III	630.34 ± 47.26	720.24 ± 37.57	65.16 ± 1.73	84.59 ± 2.99
TPI IV	522.86	544.11	253.71	379.52	TPI IV	705.57 ± 31.60	725.97 ± 12.47	58.99 ± 2.20	98.21 ± 6.30

Sufficiently sulfur-fertilized and infected plants showed slightly higher contents of cysteine, when compared to non-infected plants only at 7 dpi. Infected sulfur-deficient plants had higher contents of cysteine at TPI II - TPI IV compared to non-infected plants, which shifted in plants harvested at 14 dpi, where contents were higher at all TPIs except for TPI II. The infection had no clear effects on the content of GSH in sulfur-sufficient plants at 7 dpi, whereas at 14 dpi contents were much higher in infected plants, compared to non-infected ones. Even though sulfur deficiency led to lower contents of GSH at 7 dpi and most notably at 14 dpi, contents were much higher in infected plants, compared to non-infected plants at both dpis. Levels of GSH showed a significant difference when the control and VL-infected plants were compared ($p = 0.002$).

3.5. Levels of Sulfur, Calcium, Potassium and Iron

The amounts of sulfur (Table 7), calcium, potassium and iron (Table S8) were analyzed in control and VL-infected samples of 7 and 14 dpi with ICP-OES to get an insight on the effects of infection and sulfur deficiency on the contents of other essential elements.

Table 7. Elemental analysis: contents of sulfur content in mock- and mycelium-spore inoculated plants measured by ICP-OES at 7 and 14 dpi; data represent the mean of three dependent technical replicates ± SD.

Sulfur [mg g^{-1} DW]									
7 dpi	**C +S**	**VL +S**	**C −S**	**VL −S**	**14 dpi**	**C +S**	**VL +S**	**C −S**	**VL −S**
TPI I	8.63 ± 0.02	7.74 ± 0.02	1.33 ± 0.01	3.12 ± 0.02	TPI I	6.32 ± 0.04	5.29 ± 0.02	0.73 ± 0.00	1.02 ± 0.00
TPI II	10.11 ± 0.06	9.52 ± 0.06	2.09 ± 0.01	2.58 ± 0.02	TPI II	6.91 ± 0.00	6.51 ± 0.01	0.71 ± 0.01	1.19 ± 0.00
TPI III	10.72 ± 0.00	8.62 ± 0.02	2.13 ± 0.00	3.01 ± 0.00	TPI III	5.31 ± 0.02	6.71 ± 0.05	0.57 ± 0.00	0.61 ± 0.00
TPI IV	8.70 ± 0.01	7.95 ± 0.04	2.07 ± 0.01	2.15 ± 0.01	TPI IV	5.61 ± 0.02	6.00 ± 0.03	0.63 ± 0.00	0.72 ± 0.00

Reduced amounts of sulfur in the nutrient solution led to lower levels of sulfur in both non-infected and infected plants, with contents being higher in the latter ones compared to non-infected plants. Sulfur contents were lower in sulfur-deficient plants at 14 dpi compared to plants at 7 dpi (Table 7). The infection had no clear effect on sulfur contents in plants supplied with sufficient sulfur. The difference in the sulfur content between 7 and 14 dpi was significant ($p = 0.0001$). The difference in the potassium content between 7 and 14 dpi was significant ($p = 0.003$). Comparing 7 and 14 dpi with control- and VL-infected plants, the differences in iron contents were significant ($p = 0.006$).

3.6. The Influence of Different TPIs and Different Sulfur Supply on the Occurrence of Occlusions in the Xylem of B. napus Infected with V. longisporumSstrain VL43

It is known that in *B. napus* the formation of blockages in the xylem is induced to protect against the spread of *V. longisporum*, whereby resistant plants are characterized by a significantly stronger appearance of occlusions in the tracheae vessel elements [10,51]. Based on these observations, histological sections of hypocotyls were prepared in order to establish a possible correlation between the occurrence and severity of occlusions within TPIs and different sulfur fertilization conditions. Hypocotyls of plants were harvested at 14 and 21 dpi and cross sections of control and VL-infected plants were stained with toluidine blue. Figure 4 shows a representative selection of microscopic pictures of hypocotyls of VL-infected plants grown under sufficient and deficient sulfur supply from 14 and 21 dpi. Control plants occasionally showed occlusions in the peripheral area and were therefore not listed in the statistics or microscopic pictures (Figure S4).

The number of occlusions in tracheae of the mid area of the xylem was counted and calculated as the percentage of total tracheae in the pictured area (Table 8).

Table 8. Occurrence of occlusions at 14 and 21 dpi in the mid area of the xylem of *B. napus* plants infected with *V. longisporum* strain VL43; data represent the mean of five dependent technical replicates ± SD.

Occurrence of Occlusions in the Mid Area of the Xylem [%]					
14 dpi	**VL +S**	**VL −S**	**21 dpi**	**VL +S**	**VL −S**
TPI I	34.60 ± 0.52	7.75 ± 0.50	TPI I	38.17 ± 0.64	34.42 ± 0.38
TPI II	21.42 ± 0.32	9.33 ± 0.52	TPI II	33.89 ± 0.50	30.44 ± 0.61
TPI III	8.18 ± 0.17	3.56 ± 0.30	TPI III	29.60 ± 0.32	20.11 ± 0.39
TPI IV	3.29 ± 0.24	5.13 ± 0.67	TPI IV	27.99 ± 0.20	8.90 ± 0.30

Infected plants fertilized with sufficient sulfur showed much more occlusions compared to sulfur-deficient plants at 7 dpi. The amount of occlusions was the highest at TPI I and was lower the later the plants were infected. The TPI with the least occlusions found in infected plants was at TPI IV. This pattern was the same in sulfur-sufficient plants harvested at 21 dpi and occurred in sulfur-deficient plants as well. The amount of occlusions was significantly higher in infected sulfur-deficient plants at 21 dpi when compared to 7 dpi at all TPIs. The number of occlusions differed significantly between

TPI I and TPI III, as well as TPI I and TPI IV ($p = 0.03$). The difference between 14 and 21 dpi was also significant ($p = 0.0005$).

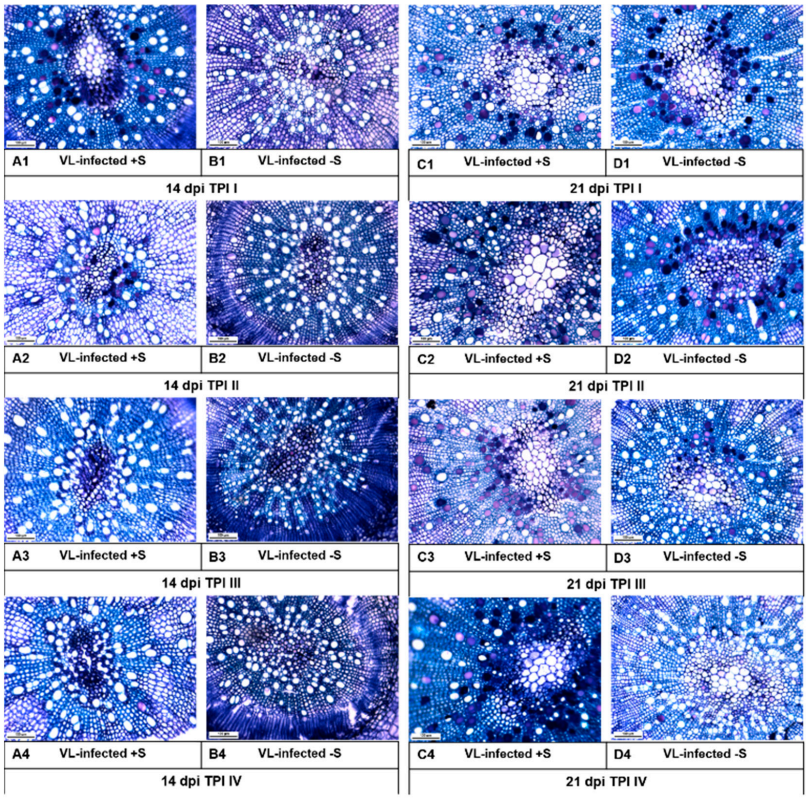

Figure 4. Occurrence of occlusions in the xylem of *B. napus*: toluidine blue stained cross sections of hypocotyls of mycelium-spore inoculated plants. 14 dpi: A1-A4: VL-infected +S at TPI I-IV; B1–B4: VL-infected −S at TPI I-IV; 21 dpi: C1–C4: VL-infected +S at TPI I-IV; D1–D4: VL-infected −S at TPI I–IV; scale bar 100 µm.

4. Discussion

This work focused on the question whether the susceptibility of *B. napus* to an infection with *V. longisporum* differs over the course of the day. In addition, the influence of sufficient and deficient sulfur fertilization on the course of the infection was of interest. In order to gain insight into this relation, plants were inoculated at different TPIs with a mycelium-spore mixture of *V. longisporum* and were subsequently fertilized with different sulfur supplies (+S/−S). In order to detect an infection with *V. longisporum*, the DNA content of the pathogen was carried out using qPCR analysis (Table 1). In case of artificial inoculation under laboratory conditions, there is no resting phase for the host plant as well as for the fungus, therefore colonization of the vascular system is probably more rapid [52] and disease symptoms are different compared to plants growing in field conditions [53]. Using the entire plant (without roots) shows a more realistic picture of the state of infection of *B. napus* compared to analysis of only the hypocotyls of the plant. By activating defense mechanisms in *B. napus* it is possible that the spread of *V. longisporum* is slowed down or even stopped. Since the DNA extraction procedure

extracts DNA from living and dead tissue of the fungus, analysis performed only with hypocotyls would reflect an inaccurate picture of the severity of the infection.

A special focus was put onto the role of GSLs in pathogen defense mechanisms, as previous studies unveiled their positive effects against the infection with *V. longisporum* [5,54–56].

4.1. Higher Sulfur-Containing Compound Levels in Infected Plants–Battle (f)or Survival?

Verticillium longisporum-infected and sulfur-deficient plants showed higher sulfur levels at all TPIs compared to non-infected sulfur-deficient plants (Table 7). The difference in the uptake of sulfur by the plants became even more pronounced at 14 dpi compared to 7 dpi, indicating that sulfur is taken up at a higher rate by infected plants, compared to non-infected controls. Similar results were obtained by Weese et al. [41], where *B. napus* plants infected with *V. longisporum* also contained more sulfur compared to non-infected controls regardless of the sulfur supply. *Verticillium longisporum* invades the amino acid-poor xylem, but since it needs them to thrive and grow to the upper parts of the plants the transcription factor *VlCPC1* involved in the regulation of amino acid biosynthesis is induced [57]. Enhanced synthesis might therefore trigger uptake of elements essential to keep up with higher rates of amino acid synthesis.

The higher uptake of sulfur is reflected in the contents of the sulfur-containing amino acid cysteine in infected sulfur-sufficient plants at 7 dpi. Accordingly, sulfur fertilization of oilseed rape was shown to significantly enhance contents of sulfur, cysteine and glutathione in a field experiment [58]. Additionally, a positive correlation between cysteine contents and the cysteine degrading enzyme L-cysteine desulfhydrase releasing H_2S, which is toxic to fungi, were observed in this study.

Similar levels in infected and non-infected and sulfur-sufficient plants could be explained by higher usage of cysteine by the growing pathogen or the incorporation of cysteine in sulfur-containing secondary metabolites like GSLs.

Contents of GSH are severely influenced by the sulfur supply of plants with contents being twice as high in sulfur-sufficient plants compared to sulfur-deficient plants at 7 dpi and contents being ten times higher in sulfur-sufficient plants compared to sulfur-deficient plants at 14 dpi underlining the severity of sulfur deprivation (Table 6). Since GSH is involved in detoxification of ROS and is oxidized to the disulfide form GSSG [59], it was expected that contents of GSH would be lower in infected plants compared to non-infected controls. Astonishingly, infected and sulfur-deprived plants manage to synthesize higher amounts of GSH compared to non-infected sulfur-deficient plants indicating a higher de-novo biosynthesis in sulfur-deprived infected plants compared to sulfur deficient non-infected controls. Similarly, although not as pronounced, GSH contents are higher in infected and sulfur-sufficient plants compared to non-infected sulfur-sufficient controls, especially at 14 dpi indicating the need of more reducing equivalents to combat stress induced by the pathogen. Accordingly, it was shown that artificially increased GSH levels in *Nicotiana tabacum* significantly reduced its susceptibility to *Euoidium longipes*. It is hypothesized, that an initial increase of GSSG is needed for the activation of a defense response against biotrophic pathogens [60]. Additionally, to its ROS scavenging ability, GSH is used as primary sulfur donor in the biosynthesis of GSLs, indicating a higher biosynthesis rate of GSH which is only partially reflected in its contents in the plants [61].

The role of the GSL gluconasturtiin has to be emphasized: contents of gluconasturtiin were higher in VL-infected plants compared to non-infected controls, independent on sulfur supply (Table 5). Eynck et al. [45] proposed gluconasturtiin to be especially important in the resistance of *B. napus* against *V. dahliae* because of its direct inhibitory activity against the pathogen. It was further hypothesized that *V. longisporum* probably adapted to *B. napus* to being its host by either suppressing or even avoiding initiation of gluconasturtiin synthesis. With up to more than 3 times higher contents of gluconasturtiin in VL-infected sulfur-sufficient plants compared to non-infected controls and up to about 1.5 times higher contents even in sulfur-deficient infected plants it seems highly unlikely that the analyzed *V. longisporum* strain is able to suppress the synthesis of gluconasturtiin in the *B. napus* cultivar Genie (Table 5). Either the *V. longisporum* strain used is simply not able to counteract gluconasturtiin synthesis

or if it is, the used cultivar Genie could be able to elevate gluconasturtiin levels despite the pathogens obstructive approach.

An infection with *V. longisporum* also seems to enhance the synthesis of iGSLs in *B. napus* which is especially extraordinary in sulfur-deprived plants (Table 3). Despite the fact that these plants are very deficient in sulfur (Figure 3; Table 7), they managed to synthesize more iGSLs compared to their infected sulfur-sufficient counterparts at all TPIs. Although sulfur is needed for the synthesis of amino acids, which are then used by the plant and the pathogen alike, the very scarce element, at least in sulfur-deficient conditions, is used to synthesize iGSLs highlighting their importance. A gene encoding a key enzyme in the synthesis of iGSLs, *CYP79B2/CYP79B3*, was found to be transcribed in higher amounts in *V. longisporum*-infected *A. thaliana* plants compared to non-infected controls. Additionally, post-translational activation of *pen2*, which encodes for an alternative thioglucosidase/myrosinase proposed to be involved in iGSL breakdown, was found in infected plants [54]. The breakdown of iGSLs by *pen2* can yield indole-3-acetonitrile and through further modification with *cyp71B15*, camalexin, which was found to inhibit growth of *V. longisporum* [6]. Furthermore, indole-3-acetonitrile can yield the auxin indole-3-acetic acid (IAA) through modification with nit1-3 in *A. thaliana*. Auxin-related compounds were hypothesized to be involved in the formation of occlusions preventing the pathogen from spreading further through the plants' vascular system [62].

4.2. Occlusions: The Physiochemical Barrier of B. napus against the spread of V. longisporum

Analysis of xylem vessels in the hypocotyl of *V. longisporum*-infected *B. napus* plants were found to form occlusions (Figure 4). The percentage of occlusions in sulfur-deficient plants was almost always lower compared to sulfur-sufficient plants, indicating that sulfur is needed for the formation of occlusions. Higher transcription of *CYP79B2/CYP79B3* could be induced by the plant to not only synthesize toxic breakdown-products derived from iGSLs, but also to access the pool of iGSLs to form the auxin IAA. It was shown that auxin alongside with ethylene was released in high amounts into infected xylem vessels leading to the formation of occlusions. Furthermore, the oxidative burst occurring when high amounts of IAA are released could harm trapped spores and hyphae at the occlusion forming site [63]. Occlusions are formed by the induction of lateral growth which can result in crushing of xylem vessels or formation of bladder-like outgrowths called tyloses. Furthermore, secretion of gels into the xylem can also form occlusions. It was already shown that gels are secreted in the vessels of *B. napus* [45]. Accordingly, analysis of hypocotyls (Figure 4) also shows the secretion of gels into the xylem, because no breakages or outgrowths could be detected in the microscopic analyses. All formed structures in the vessels are then lignified by the oxidation of secreted phenolic compounds at the occlusion site forming an impassable barrier for spores and hyphae. Although sulfur-deprived plants showed lower percentages of occlusions at 7 dpi compared to sulfur-sufficient controls, the difference between the two sulfur fertilizations became less pronounced at 14 dpi, indicating that occlusion formation happens more slowly in sulfur-deprived plants. Time point and intensity of occlusion formation can vary widely, based on the compatibility of the host-pathogen interaction. Thus, occlusions are formed in resistant plants much faster and more extensively than in susceptible plants in accordance with Fradin and Thomma [64] and Eynck et al. [45].

4.3. Importance of Diurnal Rhythm in the Defense against V. longisporum

Hypocotyls of plants analyzed in this work showed lower numbers of occlusions the later the TPI was (Figure 4), indicating a correlation between formation of occlusions and the TPI. The formation of occlusions depending on the TPI could be directly linked to auxin. Its biosynthesis, conjugation, transcription and effect on specific gene expression was shown to be highly regulated by the circadian clock [65]. Biosynthesis as well as conjugation of auxin peaked during mid-day as well as at the beginning of the day as shown by Covington and Harmer [65]. Similarly, in this work formation of occlusions was shown to be the highest when plants were infected at TPI I and TPI II. Since infection with *V. longisporum* is probably followed by a delayed perception of the plant, infections happening at

dawn and at the beginning of the dark phase (TPI III and TPI IV) would trigger auxin biosynthesis when it could be at its lowest, leading to less pronounced formations of occlusions. The other way around, plants infected at TPI I and TPI II, could trigger auxin biosynthesis adding up to already high auxin contents and leading to numerous formations of occlusions. Possibly supporting this hypothesis are the contents of the iGSL glucobrassicin, which contents were not only higher in infected plants, but also when infection happened later in the day (TPI III and TPI IV) compared to non-infected plants and plants infected earlier in the day. Infected plants possibly try to enhance auxin biosynthesis by using alternative pathways including the synthesis and breakdown of glucobrassicin. Plants infected at a later TPI could have higher contents of glucobrassicin compared to earlier TPIs in order to combat mentioned minimums of auxin contents at the time point of perception of the pathogen. Additionally, contents of VL-DNA were shown to be the highest when plants were infected at a later TPI at 3 dpi (Table 2), showing a higher infection of plants inoculated later in the day. Similarly, studies have shown a stronger defense reaction of plants during the day compared to the night [32,36].

The direct clock target gene *ICS1* encodes a key enzyme in the biosynthesis of SA, and its expression is driven by the evening-phased clock transcription factor CHE [66]. It was shown that ICS1 gene expression as well as a SA levels peaked in the middle of the night indicating an anticipation of infections in the morning, since SA is an important signal molecule in induced pathogen defense mechanisms [67,68]. In a study by Zheng et al. [69] it is assumed that *V. longisporum* is able to form a certain effector that intervenes in the biosynthesis of SA. In susceptible *B. napus* cultivars this could lead to a reduction in the SA levels, which in turn would allow higher infection rates.

It was shown, that misexpression of several clock genes, including *CCA1*, impairs resistance to the bacterial pathogen *P. syringae* and to the oomycete *Hyaloperonospora arabidopsidis* [70]. It could not be shown that LATE ELONGATED HYPOCOTYL (LHY) plays a defensive role against *H. arabidopsidis* although the *lhy* mutants have a similarly shortened circadian period as the *cca1* mutants [35]. Overall, it has been shown that genes involved in defense are controlled in a circadian way by CCA1 [71]. Thus, plants are able to perceive infections in the morning when, for example, pathogenic fungi spread their spores [35]. The timed defense includes the ability of plants to incorporate external and internal time cues to anticipate likely attacks from invading pathogens at different times of the day, whereby immediate defense reactions are available for rapid use against a variety of pathogens at a particular time of day [33].

But not only the induced immune responses are regulated in a circadian way. A study by Kerwin et al. [19] showed that genes involved in the biosynthesis of GSLs are also subject to circadian regulation. In addition, there is a connection between the nutrient status and the daily rhythm of plants [38]. Furthermore, key genes of the major pathways of primary metabolism, carbon, nitrate, and sulfur assimilation show distinct diurnal and/or circadian rhythmicity [72–74]. The formation of SDCs appears to be under a complex control, involving not only a variety of endogenous and exogenous signals, but also regulation at various transcriptional to post-translational levels [16]. A number of key genes involved in various metabolic pathways, including sulfur metabolism, have been described as regulated in a circadian way in *A. thaliana* [75]. Diurnal rhythms were described for a variety of secondary compounds involved in interactions between plants and herbivores. Some plant species show higher accumulations during the day, while other species, which are mainly attacked by nocturnal insects, show higher accumulations at night [76,77]. The diurnal regulation is often associated with light regulation. Recently, a study was published investigating an interaction between the circadian clock and the sulfur status in *B. napus* [18]. In this study it the diurnal oscillation of genes involved in the transport and reduction of sulfate was shown. The observed period is comparable to that of CCA1. Another result of the same study demonstrated that GSLs display ultradian oscillations that were altered by the sulfur supply of the plants. Therefore, it was hypothesized that the concentration of individual GSLs is not regulated in a circadian, but in an ultradian way, probably to be prepared over the day when pathogens are present.

5. Conclusions

Plants are exposed daily to different abiotic and biotic stress factors. The pathogenic defense mechanisms are sometimes very complex and build upon each other. Plants have a whole "arsenal of weapons" that they can use against pathogens (Figure 5). For example, they can build up mechanical barriers, produce toxic metabolites and use their innate immunity. In addition to a sufficient supply of nutrients, the right timing plays a crucial role as well, which decides on success or failure of the defense. This work has attempted to show a distinction of different infection times in the patho-system *B. napus* - *V. longisporum*. An additional factor was the fertilization with sufficient and deficient sulfur supply. Although a large amount of data was produced, it was still relatively small for the factors to be investigated, which led to challenges in the statistical evaluation. The different sulfur supply led to significant differences in the plants, which was reflected both in the phenotype and in the measurements. Plants in which the infection with *V. longisporum* was successful differed clearly compared to corresponding control plants. There were differences in the GSL contents, especially in the bGSL gluconasturtiin and in the formation of occlusions in the xylem vessels. A difference in the four TPIs could only be determined in parts. However, the hypotheses, which assumed an influence of the time point on the severity of the infection and an effect of different sulfur supply on the course of the infection, could be demonstrated in parts. Therefore, the time point of (sulfur) fertilizer application might be critical for the induction of metabolite-based defense mechanisms.

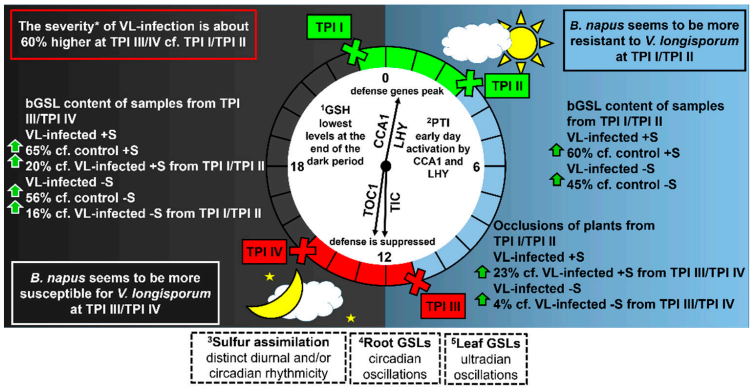

Figure 5. Major observations of the experiment: occurrence of occlusions in the xylem, increased content of gluconasturtiin (benzylic GSL; bGSL) in VL-infected plants and a higher susceptibility of *B. napus* at the end of the day to *V. longisporum*. *B. napus* seems to be more susceptible to *V. longisporum* at TPI III/TPI IV, while the contents of measured VL-DNA were about *60% higher compared to the contents of TPI I/TPI II; right side: bGSL content at 7 dpi of samples from TPI I/TPI II compared to the corresponding control plants; occurrence of occlusions at 14 dpi of plants from TPI I/TPI II compared to plants from TPI III/TPI IV; left side: bGSL content at 7 dpi of samples from TPI III/TPI IV compared to the corresponding control plants and VL-infected plants from TPI I/TPI II; percentages were calculated from the values of the combined contents of TPI I with TPI II or TPI III and TPI IV, respectively; cf.: comparing; image of circadian clock is adapted from Karapetyan and Dong [78]; [1]Zechmann [79]; [2]Zhang et al. [80]; [3]Kopriva et al. [72]; [4]Rosa and Rodrigues [81]; [5]Hornbacher et al. [18].

Supplementary Materials: The following are available online at http://www.mdpi.com/2073-4395/10/9/1227/s1, Table S1: Amount of *V. longisporum* VL43-DNA detected by qPCR with ITS primers in *B. napus*. Table S2: Contents of iGSLs (glucobrassicin, neoglucobrassicin and 4-hydroxyglucobrassicin) in mock- and mycelium-spore inoculated plants at 7 dpi and 14 dpi. Table S3: Contents of aGSLs (progoitrin, glucoalyssin, glucoraphanin, glucobrassicanapin and gluconapin) in mock- and mycelium-spore inoculated plants at 7 dpi and 14 dpi. Table S4: Contents of the bGSL gluconasturtiin in mock- and mycelium-spore inoculated plants at 7 dpi and 14 dpi. Table S5:

Thiol analysis by HPLC: contents of cysteine and glutathione (GSH) in mock- and mycelium-spore inoculated plants at 7 and 14 dpi. Table S6: Elemental analysis: contents of sulfur in mock- and mycelium-spore inoculated plants measured by ICP-OES at 7 and 14 dpi. Table S7: Occurrence of occlusions at 14 and 21 dpi in the mid area of the xylem of *B. napus* plants infected with *V. longisporum* strain VL43. Table S8: Elemental analysis: contents of calcium, potassium and iron in mock- and mycelium-spore inoculated plants measured by ICP-OES at 7 and 14 dpi. Figure S1: *Brassica napus* plants at 14 dpi cultivated at two different sulfur regimes and either infected with the *V. longisporum* strain VL43 or non-infected. Figure S2: Occurrence of occlusions in the xylem of *B. napus*: toluidine blue stained cross sections of hypocotyls of mycelium-spore inoculated plants. Figure S3: Cross sections of hypocotyls of control plants at 14 and 21 dpi. Figure S4: Cross sections of hypocotyls of control plants at 14 and 21 dpi.

Author Contributions: Conceptualization, A.R. and J.P.; methodology, S.I.R., J.H., I.H.-N., A.R. and J.P.; validation and formal analysis, S.I.R., J.H., I.H.-N. and J.P.; investigation, S.I.R., J.H. and I.H.-N.; resources, J.P.; statistical analysis, F.S.; writing—original draft preparation, S.I.R.; writing—review and editing, S.I.R., J.H., I.H.-N. and J.P.; visualization, S.I.R.; supervision, J.P. All authors have read and agreed to the published version of the manuscript.

Funding: This research received no external funding. The publication of this article was funded by the Open Access Fund of the Leibniz Universität Hannover.

Acknowledgments: We acknowledge the Deutsche Saatveredelung AG, Lippstadt, Germany, for providing us with seeds of the *Brassica napus* cultivar.

Conflicts of Interest: The authors declare no conflict of interest.

References

1. Oerke, E.-C. Crop losses to pests. *J. Agric. Sci.* **2005**, *144*, 31–43. [CrossRef]
2. Zeilinger, S.; Gupta, V.K.; Dahms, T.E.S.; Silva, R.N.; Singh, H.B.; Upadhyay, R.S.; Gomes, E.V.; Tsui, C.K.-M.; Nayak, S.C. Friends or foes? Emerging insights from fungal interactions with plants. *FEMS Microbiol. Rev.* **2015**, *40*, 182–207. [CrossRef] [PubMed]
3. Fisher, M.C.; Henk, D.A.; Briggs, C.J.; Brownstein, J.S.; Madoff, L.C.; McCraw, S.L.; Gurr, S.J. Emerging fungal threats to animal, plant and ecosystem health. *Nature* **2012**, *484*, 186–194. [CrossRef] [PubMed]
4. Meena, V.S.; Maurya, B.R.; Meena, S.K.; Meena, R.K.; Kumar, A.; Verma, J.P.; Singh, N.P. Can *Bacillus* Species Enhance Nutrient Availability in Agricultural Soils? In *Bacilli and Agrobiotechnology*; Springer Science and Business Media LLC: Berlin/Heidelberg, Germany, 2016; pp. 367–395.
5. DePotter, J.R.L.; Deketelaere, S.; Inderbitzin, P.; Von Tiedemann, A.; Höfte, M.; Subbarao, K.V.; Wood, T.A.; Thomma, B.P. *Verticillium longisporum*, the invisible threat to oilseed rape and other brassicaceous plant hosts. *Mol. Plant Pathol.* **2016**, *17*, 1004–1016. [CrossRef] [PubMed]
6. Singh, S.; Braus-Stromeyer, S.A.; Timpner, C.; Tran, V.T.; Lohaus, G.; Reusche, M.; Knüfer, J.; Teichmann, T.; Von Tiedemann, A.; Braus, G.H. Silencing of Vlaro2 for chorismate synthase revealed that the phytopathogen *Verticillium longisporum* induces the cross-pathway control in the xylem. *Appl. Microbiol. Biotechnol.* **2009**, *85*, 1961–1976. [CrossRef] [PubMed]
7. Dunker, S.; Keunecke, H.; Steinbach, P.; von Tiedemann, A. Impact of *Verticillium longisporum* on yield and morphology of winter oilseed rape (*Brassica napus*) in relation to systemic spread in the plant. *J. Phytopathol.* **2008**, *156*, 698–707. [CrossRef]
8. Heale, J.B. Diversification and speciation in *Verticillium*-an overview. In *Adv. Verticillium Res. Disease Manag.*; APS Press: St Paul, MN, USA, 2000; pp. 1–14.
9. Heale, J.B.; Karapapa, V.K. The *Verticillium* threat to canada's major oilseed crop: Canola. *Can. J. Plant Pathol.* **1999**, *21*, 1–7. [CrossRef]
10. Eynck, C.; Koopmann, B.; Karlovsky, P.; Von Tiedemann, A. Internal Resistance in Winter Oilseed Rape Inhibits Systemic Spread of the Vascular Pathogen *Verticillium longisporum*. *Phytopathology* **2009**, *99*, 802–811. [CrossRef]
11. Booth, E.J.; Walker, K.C. The effect of site and foliar sulfur on oilseed rape: Comparison of sulfur responsive and non-responsive seasons. *Phyton* **1992**, *32*, 9–13.
12. Pedersen, C.A.; Knudsen, L.; Schnug, E. Sulphur Fertilisation. In *Nutrients in Ecosystems*; Springer Science and Business Media LLC: Berlin/Heidelberg, Germany, 1998; pp. 115–134.
13. Richards, I.R. Sulphur as a crop nutrient in the United Kingdom. *Sulphur Agric.* **1990**, *14*, 8–9.
14. Schnug, E. Sulphur nutritional status of European crops and consequences for agriculture. *Sulphur Agric.* **1991**, *15*, 7–12.

15. De Kok, L.J.; Westerman, S.; Stuiver, C.E.E.; Stulen, I. Atmospheric H2S as plant sulfur source: Interaction with pedospheric sulfur nutrition–a case study with *Brassica oleracea L.* In *Sulfur Nutrition and Sulfur Assimilation in Higher Plants: Molecular, Biochemical and Physiological Aspects'*; Brunold, C., Rennenberg, H., De Kok, L.J., Stulen, I., Davidian, J.C., Eds.; Haupt Verlag: Bern, Switzerland, 2000; pp. 41–55.
16. Rausch, T.; Wachter, A. Sulfur metabolism: A versatile platform for launching defence operations. *Trends Plant Sci.* **2005**, *10*, 503–509. [CrossRef] [PubMed]
17. Kruse, C.; Jost, R.; Lipschis, M.; Kopp, B.; Hartmann, M.; Hell, R. Sulfur-Enhanced Defence: Effects of Sulfur Metabolism, Nitrogen Supply, and Pathogen Lifestyle. *Plant Biol.* **2007**, *9*, 608–619. [CrossRef] [PubMed]
18. Hornbacher, J.; Rumlow, A.; Pallmann, P.; Turcios, A.E.; Riemenschneider, A.; Papenbrock, J. The Levels of Sulfur-containing Metabolites in *Brassica napus* are Not Influenced by the Circadian Clock but Diurnally. *J. Plant Biol.* **2019**, *62*, 359–373. [CrossRef]
19. Kerwin, R.E.; Jiménez-Gómez, J.M.; Fulop, D.; Harmer, S.L.; Maloof, J.N.; Kliebenstein, D.J. Network Quantitative Trait Loci Mapping of Circadian Clock Outputs Identifies Metabolic Pathway-to-Clock Linkages in *Arabidopsis*. *Plant Cell* **2011**, *23*, 471–485. [CrossRef]
20. Andersson, D.; Chakrabarty, R.; Bejai, S.; Zhang, J.; Rask, L.; Meijer, J. Myrosinases from root and leaves of *Arabidopsis thaliana* have different catalytic properties. *Phytochemistry* **2009**, *70*, 1345–1354. [CrossRef]
21. Mithen, R.; Campos, H. Genetic variation of aliphatic glucosinolates in Arabidopsis thaliana and prospects for map based gene cloning. In Proceedings of the 9th International Symposium on Insect-Plant Relationships, Gwatt, Switzerland, 24–30 June 1995; Springer Science and Business Media LLC: Berlin/Heidelberg, Germany, 1996; pp. 202–205.
22. Fahey, J.W.; Zalcmann, A.T.; Talalay, P. The chemical diversity and distribution of glucosinolates and isothiocyanates among plants. *Phytochemistry* **2001**, *56*, 5–51. [CrossRef]
23. Hopkins, R.; Van Dam, N.M.; Van Loon, J.J. Role of Glucosinolates in Insect-Plant Relationships and Multitrophic Interactions. *Annu. Rev. EÈntomol.* **2009**, *54*, 57–83. [CrossRef]
24. Mithen, R. Glucosinolates—Biochemistry, genetics and biological activity. *Plant Growth Regul.* **2001**, *34*, 91–103. [CrossRef]
25. Bednarek, P. Sulfur-containing secondary metabolites from *Arabidopsis thaliana* and other Brassicaceae with function in plant immunity. *ChemBioChem* **2012**, *13*, 1846–1859. [CrossRef]
26. Wittstock, U.; Halkier, B.A. Glucosinolate research in the *Arabidopsis* era. *Trends Plant Sci.* **2002**, *7*, 263–270. [CrossRef]
27. Bones, A.M.; Rossiter, J.T. The myrosinase-glucosinolate system, its organisation and biochemistry. *Physiol. Plant.* **1996**, *97*, 194–208. [CrossRef]
28. Schnug, E.; Booth, E.; Haneklaus, S.; Walker, K.C. Sulphur supply and stress resistance in oilseed rape. In Proceedings of the 9th International Rapeseed Congress, Cambridge, UK, 4–7 July 1995; Volume 1995, pp. 229–231.
29. Davidson, R.M.; Goss, R.L. Effects of P, S, N, lime, chlordane, and fungicides on ophiobolus patch disease of turf. *Plant Disease Rep.* **1972**, *56*, 565–567.
30. Roden, L.C.; Ingle, R.A. Lights, Rhythms, Infection: The Role of Light and the Circadian Clock in Determining the Outcome of Plant–Pathogen Interactions. *Plant Cell* **2009**, *21*, 2546–2552. [CrossRef]
31. Chandra-Shekara, A.C.; Gupte, M.; Navarre, D.; Raina, S.; Raina, R.; Klessig, D.; Kachroo, P. Light-dependent hypersensitive response and resistance signaling against Turnip Crinkle Virus in *Arabidopsis*. *Plant J.* **2006**, *45*, 320–334. [CrossRef]
32. Griebel, T.; Zeier, J. Light Regulation and Daytime Dependency of Inducible Plant Defenses in *Arabidopsis*: Phytochrome Signaling Controls Systemic Acquired Resistance Rather Than Local Defense. *Plant Physiol.* **2008**, *147*, 790–801. [CrossRef]
33. Lu, H.; McClung, C.R.; Zhang, C. Tick Tock: Circadian Regulation of Plant Innate Immunity. *Annu. Rev. Phytopathol.* **2017**, *55*, 287–311. [CrossRef]
34. Oberpichler, I.; Rosen, R.; Rasouly, A.; Vugman, M.; Ron, E.Z.; Lamparter, T. Light affects motility and infectivity of *Agrobacterium tumefaciens*. *Environ. Microbiol.* **2008**, *10*, 2020–2029. [CrossRef]
35. Wang, W.; Barnaby, J.Y.; Tada, Y.; Li, H.; Tör, M.; Caldelari, D.; Lee, D.-U.; Fu, X.-D.; Dong, X. Timing of plant immune responses by a central circadian regulator. *Nature* **2011**, *470*, 110–114. [CrossRef]

36. Bhardwaj, V.; Meier, S.; Petersen, L.N.; Ingle, R.A.; Roden, L.C. Defence Responses of *Arabidopsis thaliana* to Infection by *Pseudomonas syringae* Are Regulated by the Circadian Clock. *PLoS ONE* **2011**, *6*, e26968. [CrossRef]
37. Ingle, R.A.; Stoker, C.; Stone, W.; Adams, N.; Smith, R.; Grant, M.; Carré, I.A.; Roden, L.C.; Denby, K. Jasmonate signalling drives time-of-day differences in susceptibility of *Arabidopsis* to the fungal pathogen *Botrytis cinerea*. *Plant J.* **2015**, *84*, 937–948. [CrossRef]
38. Haydon, M.J.; Roman, A.; Arshad, W. Nutrient homeostasis within the plant circadian network. *Front. Plant Sci.* **2015**, *6*, 299. [CrossRef] [PubMed]
39. Chiasson, D.; Loughlin, P.C.; Mazurkiewicz, D.; Mohammadi-Dehcheshmeh, M.; Fedorova, E.E.; Okamoto, M.; McLean, E.; Glass, A.D.M.; Smith, S.E.; Bisseling, T.; et al. Soybean SAT1 (Symbiotic Ammonium Transporter 1) encodes a bHLH transcription factor involved in nodule growth and NH4+ transport. *Proc. Natl. Acad. Sci. USA* **2014**, *111*, 4814–4819. [CrossRef] [PubMed]
40. Michael, T.P.; McClung, C.R. Enhancer Trapping Reveals Widespread Circadian Clock Transcriptional Control in *Arabidopsis*1[w]. *Plant Physiol.* **2003**, *132*, 629–639. [CrossRef] [PubMed]
41. Weese, A.; Pallmann, P.; Papenbrock, J.; Riemenschneider, A. *Brassica napus L.* cultivars show a broad variability in their morphology, physiology and metabolite levels in response to sulfur limitations and to pathogen attack. *Front. Plant Sci.* **2015**, *6*, 9. [CrossRef]
42. Blake-Kalff, M.M.; Harrison, K.R.; Hawkesford, M.J.; Zhao, F.J.; McGrath, S.P. Distribution of Sulfur within Oilseed Rape Leaves in Response to Sulfur Deficiency during Vegetative Growth. *Plant Physiol.* **1998**, *118*, 1337–1344. [CrossRef]
43. Zeise, K.; Von Tiedemann, A. Morphological and Physiological Differentiation among Vegetative Compatibility Groups of *Verticillium dahliae* in Relation to V. longisporum. *J. Phytopathol.* **2001**, *149*, 469–475. [CrossRef]
44. Rumlow, A.; Keunen, E.; Klein, J.; Pallmann, P.; Riemenschneider, A.; Cuypers, A.; Papenbrock, J. Quantitative Expression Analysis in *Brassica napus* by Northern Blot Analysis and Reverse Transcription-Quantitative PCR in a Complex Experimental Setting. *PLoS ONE* **2016**, *11*, e0163679. [CrossRef]
45. Eynck, C.; Koopmann, B.; Grunewaldt-Stoecker, G.; Karlovsky, P.; Von Tiedemann, A. Differential interactions of *Verticillium longisporum* and *V. dahliae* with *Brassica napus* detected with molecular and histological techniques. *Eur. J. Plant Pathol.* **2007**, *118*, 259–274. [CrossRef]
46. Riemenschneider, A.; Wegele, R.; Schmidt, A.; Papenbrock, J. Isolation and characterization of a D-cysteine desulfhydrase protein from *Arabidopsis thaliana*. *FEBS J.* **2005**, *272*, 1291–1304. [CrossRef]
47. Feder, N.E.D.; O'Brien, T.P. Plant microtechnique: Some principles and new methods. *Am. J. Bot.* **1968**, *55*, 123–142. [CrossRef]
48. Schindelin, J.; Arganda-Carreras, I.; Frise, E.; Kaynig, V.; Longair, M.; Pietzsch, T.; Tinevez, J.Y. Fiji: An open-source platform for biological-image analysis. *Nat. Methods* **2012**, *9*, 676. [CrossRef] [PubMed]
49. McCullagh, P.; Nelder, J. *Generalized Linear Models*, 2rd ed.; Chapman & Hall: London, UK, 1989.
50. Lenth, R. Emmeans Package: Estimated Marginal Means, aka Least-Squares Means. R Package Version 1.3. 5.1. 2019. Available online: http://packages.renjin.org/package/org.renjin.cran/emmeans (accessed on 18 August 2020).
51. Kamble, A.; Koopmann, B.; Von Tiedemann, A. Induced resistance to *Verticillium longisporum* in *Brassica napus* by β-aminobutyric acid. *Plant Pathol.* **2012**, *62*, 552–561. [CrossRef]
52. Dunker, S.; Keunecke, H.; von Tiedemann, A. *Verticillium longisporum* in winter oilseed rape-Impact on plant development and yield. *IOBC WPRS Bull.* **2006**, *29*, 361.
53. Lopisso, D.T.; Knüfer, J.; Koopmann, B.; Von Tiedemann, A. The Vascular Pathogen *Verticillium longisporum* Does Not Affect Water Relations and Plant Responses to Drought Stress of Its Host, *Brassica napus*. *Phytopathology* **2017**, *107*, 444–454. [CrossRef]
54. Iven, T.; König, S.; Singh, S.; Braus-Stromeyer, S.A.; Bischoff, M.; Tietze, L.F.; Braus, G.H.; Lipka, V.; Feussner, I.; Dröge-Laser, W. Transcriptional Activation and Production of Tryptophan-Derived Secondary Metabolites in *Arabidopsis* Roots Contributes to the Defense against the Fungal Vascular Pathogen *Verticillium longisporum*. *Mol. Plant* **2012**, *5*, 1389–1402. [CrossRef]
55. Rygulla, W.; Friedt, W.; Seyis, F.; Lühs, W.; Eynck, C.; Von Tiedemann, A.; Snowdon, R.J. Combination of resistance to *Verticillium longisporum* from zero erucic acid Brassica oleracea and oilseed *Brassica rapa* genotypes in resynthesized rapeseed (*Brassica napus*) lines. *Plant Breed.* **2007**, *126*, 596–602. [CrossRef]

56. Witzel, K.; Hanschen, F.S.; Schreiner, M.; Krumbein, A.; Ruppel, S.; Grosch, R. *Verticillium* Suppression Is Associated with the Glucosinolate Composition of *Arabidopsis thaliana* Leaves. *PLoS ONE* **2013**, *8*, e71877. [CrossRef]
57. Timpner, C.; Braus-Stromeyer, S.A.; Tran, V.T.; Braus, G.H. The Cpc1 Regulator of the Cross-Pathway Control of Amino Acid Biosynthesis Is Required for Pathogenicity of the Vascular Pathogen *Verticillium longisporum*. *Mol. Plant Microbe Interact.* **2013**, *26*, 1312–1324. [CrossRef]
58. Bloem, E.; Riemenschneider, A.; Volker, J.; Papenbrock, J.; Schmidt, A.; Salac, I.; Haneklaus, S.; Schnug, E. Sulphur supply and infection with *Pyrenopeziza brassicae* influence L-cysteine desulphydrase activity in *Brassica napus* L. *J. Exp. Bot.* **2004**, *55*, 2305–2312. [CrossRef]
59. Bloem, E.; Haneklaus, S.; Kleinwächter, M.; Paulsen, J.; Schnug, E.; Selmar, D. Stress-induced changes of bioactive compounds in *Tropaeolum majus* L. *Ind. Crop. Prod.* **2014**, *60*, 349–359. [CrossRef]
60. Künstler, A.; Kátay, G.; Gullner, G.; Király, L. Artificial elevation of glutathione contents in salicylic acid-deficient tobacco (*Nicotiana tabacum* cv. Xanthi NahG) reduces susceptibility to the powdery mildew pathogen Euoidium longipes. *Plant Biol.* **2019**, *22*, 70–80. [CrossRef]
61. Geu-Flores, F.; Møldrup, M.E.; Böttcher, C.; Olsen, C.E.; Scheel, D.; Halkier, B.A. Cytosolic γ-Glutamyl Peptidases Process Glutathione Conjugates in the Biosynthesis of Glucosinolates and Camalexin in *Arabidopsis*. *Plant Cell* **2011**, *23*, 2456–2469. [CrossRef]
62. Talboys, P.W. Chemical control of *Verticillium* wilts. *Phytopathol. Mediterr.* **1984**, *23*, 163–175.
63. Beckman, C.H. Phenolic-storing cells: Keys to programmed cell death and periderm formation in wilt disease resistance and in general defence responses in plants? *Physiol. Mol. Plant Pathol.* **2000**, *57*, 101–110. [CrossRef]
64. Fradin, E.F.; Thomma, B.P. Physiology and molecular aspects of *Verticillium* wilt diseases caused by *V. dahliae* and *V. albo-atrum*. *Mol. Plant Pathol.* **2006**, *7*, 71–86. [CrossRef] [PubMed]
65. Covington, M.F.; Harmer, S.L. The Circadian Clock Regulates Auxin Signaling and Responses in *Arabidopsis*. *PLoS Biol.* **2007**, *5*, e222. [CrossRef] [PubMed]
66. Zheng, X.-Y.; Zhou, M.; Yoo, H.; Pruneda-Paz, J.L.; Spivey, N.W.; Kay, S.A.; Dong, X. Spatial and temporal regulation of biosynthesis of the plant immune signal salicylic acid. *Proc. Natl. Acad. Sci. USA* **2015**, *112*, 9166–9173. [CrossRef] [PubMed]
67. Liu, T.; Song, T.; Zhang, X.; Yuan, H.; Su, L.; Li, W.; Xu, J.; Liu, S.; Chen, L.; Chen, T.; et al. Unconventionally secreted effectors of two filamentous pathogens target plant salicylate biosynthesis. *Nat. Commun.* **2014**, *5*, 4686. [CrossRef]
68. Spoel, S.H.; Dong, X. How do plants achieve immunity? Defence without specialized immune cells. *Nat. Rev. Immunol.* **2012**, *12*, 89–100. [CrossRef]
69. Zheng, X.; Koopmann, B.; Von Tiedemann, A. Role of Salicylic Acid and Components of the Phenylpropanoid Pathway in Basal and Cultivar-Related Resistance of Oilseed Rape (*Brassica napus*) to *Verticillium longisporum*. *Plants* **2019**, *8*, 491. [CrossRef] [PubMed]
70. Shin, J.; Heidrich, K.; Sanchez-Villarreal, A.; Parker, J.E.; Davis, S.J. TIME FOR COFFEE Represses Accumulation of the MYC2 Transcription Factor to Provide Time-of-Day Regulation of Jasmonate Signaling in *Arabidopsis*. *Plant Cell* **2012**, *24*, 2470–2482. [CrossRef] [PubMed]
71. Oliverio, K.A.; Crepy, M.; Martin-Tryon, E.L.; Milich, R.; Harmer, S.L.; Putterill, J.; Yanovsky, M.J.; Casal, J. GIGANTEA Regulates Phytochrome A-Mediated Photomorphogenesis Independently of Its Role in the Circadian Clock. *Plant Physiol.* **2007**, *144*, 495–502. [CrossRef]
72. Kopriva, S.; Muheim, R.; Koprivova, A.; Trachsel, N.; Catalano, C.; Suter, M.; Brunold, C. Light regulation of assimilatory sulphate reduction in *Arabidopsis thaliana*. *Plant J.* **1999**, *20*, 37–44. [CrossRef]
73. Pilgrim, M.L.; Caspar, T.; Quail, P.H.; McClung, C.R. Circadian and light-regulated expression of nitrate reductase in *Arabidopsis*. *Plant Mol. Boil.* **1993**, *23*, 349–364. [CrossRef] [PubMed]
74. Zeeman, S.C.; Smith, S.M.; Smith, A.M. The diurnal metabolism of leaf starch. *Biochem. J.* **2006**, *401*, 13–28. [CrossRef]
75. Harmer, S.L. The Circadian System in Higher Plants. *Annu. Rev. Plant Boil.* **2009**, *60*, 357–377. [CrossRef]
76. De Moraes, C.M.; Mescher, M.C.; Tumlinson, J.H. Caterpillar-induced nocturnal plant volatiles repel conspecific females. *Nature* **2001**, *410*, 577–580. [CrossRef]

77. Kim, S.-G.; Yon, F.; Gaquerel, E.; Gulati, J.; Baldwin, I.T. Tissue Specific Diurnal Rhythms of Metabolites and Their Regulation during Herbivore Attack in a Native Tobacco, *Nicotiana attenuata*. *PLoS ONE* **2011**, *6*, e26214. [CrossRef]
78. Karapetyan, S.; Dong, X. Redox and the circadian clock in plant immunity: A balancing act. *Free. Radic. Boil. Med.* **2017**, *119*, 56–61. [CrossRef]
79. Zechmann, B. Diurnal changes of subcellular glutathione content in *Arabidopsis thaliana*. *Biol. Plant.* **2017**, *61*, 791–796. [CrossRef]
80. Zhang, C.; Xie, Q.; Anderson, R.G.; Ng, G.; Seitz, N.C.; Peterson, T.; McClung, C.R.; McDowell, J.M.; Kong, D.; Kwak, J.M.; et al. Crosstalk between the Circadian Clock and Innate Immunity in *Arabidopsis*. *PLoS Pathog.* **2013**, *9*, e1003370. [CrossRef] [PubMed]
81. Rosa, E.A.; Rodrigues, P.M.F. The effect of light and temperature on glucosinolate concentration in the leaves and roots of cabbage seedlings. *J. Sci. Food Agric.* **1998**, *78*, 208–212. [CrossRef]

Chapter 3.2 Variation in glucosinolate contents in clubroot-resistant and susceptible *Brassica* crops in response to virulence of *Plasmodiophora brassicae*

pathogens

MDPI

Article

Variation of Glucosinolate Contents in Clubroot-Resistant and -Susceptible *Brassica napus* Cultivars in Response to Virulence of *Plasmodiophora brassicae*

Nazanin Zamani-Noor [1,*], Johann Hornbacher [2], Christel Joy Comel [2] and Jutta Papenbrock [2,*]

[1] Federal Research Centre for Cultivated Plants, Institute for Plant Protection in Field Crops and Grassland, Julius Kühn-Institute (JKI), Messeweg 11-12, D-38104 Braunschweig, Germany
[2] Institute of Botany, Leibniz University Hannover, Herrenhäuserstr. 2, D-30419 Hannover, Germany; J.Hornbacher@botanik.uni-hannover.de (J.H.); joycomel20@gmail.com (C.J.C.)
* Correspondence: nazanin.zamani-noor@julius-kuehn.de (N.Z.-N.); papenbrock@botanik.uni-hannover.de (J.P.); Tel.: +49-531-299-4530 (N.Z.-N.); +49-511-762-3788 (J.P.)

Abstract: The present study investigated the changes in total and individual glucosinolates (GSLs) in roots and leaves of different clubroot-resistant and -susceptible oilseed rape cultivars following artificial inoculation with *Plasmodiophora brassicae* isolates with different virulence. The results showed significant differences in clubroot incidence and severity as well as in the amount of total and individual glucosinolates between oilseed rape cultivars in response to virulence of the pathogen. Single among with total aliphatic and total indolic glucosinolate contents were significantly lower in leaves of susceptible cultivars compared to resistant ones due to the infection. Similarly, single and total aliphatic as well as indolic glucosinolate contents in roots were lower in susceptible cultivars compared to resistant cultivars analyzed. The different isolates of *P. brassicae* seem to differ in their ability to reduce gluconasturtiin contents in the host. The more aggressive isolate P1 (+) might be able to suppress gluconasturtiin synthesis of the host in a more pronounced manner compared to the isolate P1. A possible interaction of breakdown products of glucobrassicin with the auxin receptor transport inhibitor response 1 (TIR1) is hypothesized and its possible effects on auxin signaling in roots and leaves of resistant and susceptible cultivars is discussed. A potential interplay between aliphatic and indolic glucosinolates that might be involved in water homeostasis in resistant cultivars is explained.

Keywords: oilseed rape; polygenic resistance; physiological race; pathotype; clubroot severity index; aliphatic; aromatic and indolic glucosinolates

Citation: Zamani-Noor, N.; Hornbacher, J.; Comel, C.J.; Papenbrock, J. Variation of Glucosinolate Contents in Clubroot-Resistant and -Susceptible *Brassica napus* Cultivars in Response to Virulence of *Plasmodiophora brassicae*. *Pathogens* **2021**, *10*, 563. https://doi.org/10.3390/pathogens10050563

Academic Editor: Massimiliano Morelli

Received: 15 March 2021
Accepted: 5 May 2021
Published: 6 May 2021

1. Introduction

Glucosinolates (GSLs), a known group of constitutive natural plant metabolites, are found in the order Brassicales, mainly in the family of Brassicaceae but also in families of Capparaceae, Caricaceae, Resedaceae and Tropaeolaceae [1]. Based on their side-chain structure and amino acid precursors, GSLs are divided into three major groups: aliphatic, aromatic and indolic [2]. Upon tissue damage such as insect feeding or fungal infestation, GSLs are catabolized by myrosinases to produce a variety of bioactive compounds such as isothiocyanates, thiocyanates, nitriles, oxazolidenethiones and epithioalkanes [1]. Some of these metabolites have been discovered to be toxic to many insect herbivores and some fungal pathogens and play important roles in the plant's defense mechanism [1,3].

Plasmodiophora brassicae Woronin, the causal agent of clubroot disease, is one of the most destructive and cosmopolitan of plant pathogens. This obligate soil-borne protist attacks over 3700 species of the family Brassicaceae [4] including economically important oilseed rape (*Brassica napus* L.) cultivars. Effective disease control strategies against *P. brassicae* continue to be a challenge because of the lack of chemical agents able to manage this

disease. Further, cultural practices tend to reduce the severity of clubroot, but none directly control *P. brassicae* on its own. Host resistance offers the only economic and sustainable method for the adequate managing of clubroot disease. However, current oilseed rape cultivars relying on race-specific resistance [5] often lose effectiveness within a few years by imposing selection for virulent pathotypes. Physiological specialization has long been known to occur in *P. brassicae* [6], with pathotypes of the pathogen varying in their ability to infect specific host crops. Previous studies in European countries have revealed variations in pathotype distributions across different countries [7–10]. Pathotype 1 (P1) and Pathotype 3 (P3) or ECD 16/31/31 and 16/14/31 as classified on the differentials of Somé et al. [11] and the European Clubroot Differential [12], respectively, are predominant in central Europe. Additionally, several *P. brassicae* populations were found to be moderately or highly virulent on currently available clubroot-resistant oilseed rape cultivars [7–10,13]. These new isolates have been informally named as P1 (+), P2 (+) or P3 (+) because they are classified as P1, P2 or P3 on the differentials of Somé et al. [11] but (unlike the original P1, P2 or P3) are highly virulent on clubroot resistant oilseed rape cultivars.

Clubroot is characterized by the development of galls on infected roots which are often restricted in the uptake of water and nutrients and constitute a major sink for assimilates [14]. Studies on pathogen-induced changes in host metabolism and symptom development have been conducted in previous years. Ludwig-Müller et al. [15] have observed significant differences in the GSL pattern in susceptible and resistant varieties of Chinese cabbage. In their study, the total GSL content in roots of the two susceptible varieties was higher than in roots of the two resistant cultivars throughout the experimental period. While contents of aliphatic GSLs were induced in the two susceptible cultivars compared to the resistant ones, the two resistant cultivars showed an increase in aromatic GSLs, indicating maybe a dual role for these compounds. Additionally, contents of indolic GSLs (iGSLs) increased in roots of susceptible crops 14 and 20 days post inoculation with *P. brassicae*, whereas there was no difference between infected and control roots in resistant ones. Further studies on the host range of *P. brassicae* and its correlation to endogenous GSL content have shown that disease severity was correlated with certain GSLs in one species, while the increase in other GSLs might be regarded as defense response [16]. In the GSL-containing non-Brassica species, *Tropaeolum majus* and *Carica papaya*, the concentrations of benzyl-GSL increased markedly in roots inoculated with *P. brassicae*, compared with the controls. There were also increases in concentrations of benzyl-GSL in leaves of *T. majus* after *P. brassicae* infection and it was speculated that benzyl-GSL could act as precursor for phenylacetic acid that has auxin activity in *T. majus* [16].

Auxins, among them indole-3-acetic acid (IAA), are perceived by the auxin receptor transport inhibitor response 1 (TIR1). Upon binding of auxins to TIR1, the TIR1:IAA complex is formed, leading to polyubiquitination and faster degradation of already short-lived auxin responsive proteins (AUX/IAA) [17].

It has been shown that the expression of the auxin receptor *TIR1* is upregulated in *Arabidopsis thaliana* plants infected with *P. brassicae*. Furthermore, it was shown that loss of TIR1 leads to an increased susceptibility to the pathogen indicating a contribution of TIR1 to the resistance of plants towards *P. brassicae* [18].

In conclusion, degradation of GSL in general might be an important feature also during endogenous control of the clubroot disease. An improved understanding of the host metabolism and symptom development could contribute to the development of novel sources of resistance and other control strategies. Therefore, in the present study, we evaluated for the first time the variation in total and individual GSL in different clubroot-resistant and susceptible *B. napus* cultivars after inoculation with two isolates of *P. brassicae* varying in their degree of virulence.

2. Results

Significant differences in clubroot incidence and severity were observed between oilseed rape cultivars inoculated with different *P. brassicae* isolates at 35 dpi (Table 1). While DI and DSI in susceptible oilseed rape cultivars inoculated with *P. brassicae*-P1 were up to 100%, no disease symptoms or very small galls were observed on roots of resistant cultivars and the symptoms were of very low severity (Table 1). In contrast to *P. brassicae*-P1, the highly virulent isolate *P. brassicae*-P1 (+), had a strong effect on clubroot incidence and severity in all tested cultivars except *B. napus* cv. Creed. This cultivar was found to be completely resistant against both *P. brassicae* isolates (Table 1).

Table 1. Clubroot disease incidence (DI) and disease severity index (DSI) of different clubroot resistant and susceptible oilseed rape (*Brassica napus*) cultivars inoculated with two isolates of *Plasmodiophora brassicae* at 35 days post inoculation (dpi).

Cultivar	Clubroot Resistance	*P. brassicae* P1 [1]		*P. brassicae* P1 (+) [1]	
		DI [2] ± SD	DSI [2] ± SD	DI [2] ± SD	DSI [2] ± SD
Aristoteles	resistant	0.0 ± 0.0	0.0 ± 0.0	44.0 ± 3.0	23.3 ± 1.6
Creed	resistant	0.0 ± 0.0	0.0 ± 0.0	0.0 ± 0.0	0.0 ± 0.0
Mendel	resistant	15.3 ± 12.6	9.9 ± 6.8	60.0 ± 8.3	30.5 ± 3.6
Bender	susceptible	100.0 ± 0.0	100.0 ± 0.0	100.0 ± 0.0	98.8 ± 1.7
Ladoga	susceptible	100.0 ± 0.0	98.2 ± 2.5	97.9 ± 3.0	91.3 ± 12.6
Visby	susceptible	100.0 ± 0.0	98.8 ± 1.9	100.0 ± 0.0	100.0 ± 0.0

[1] *P. brassicae* isolates were chosen according to their evaluated virulence in Zamani-Noor (2017) [9]. Pb-P1 isolate was virulent on clubroot susceptible oilseed rape cv. Visby and avirulent on clubroot resistant cv. Mendel and Pb-P1 (+) isolate was virulent on both cultivars. [2] The infection type on each root was visually determined based on a 0–3 scale; disease incidence (DI) and disease severity index (DSI) were calculated from each infection type. Data are pooled across two experimental runs (i.e., repetitions); mean values and standard deviations (± SD) are presented in this table.

2.1. Individual Glucosinolate Profiles

No significant differences in GSL contents between the two runs were observed (data not shown). Data for GSL contents were therefore calculated as the mean of the two runs.

The resistant varieties Aristoteles, Mendel and Creed showed higher contents of progoitrin in leaves compared to the susceptible cultivars Bender, Ladoga and Visby, which was more pronounced in plants infected with P1 and P1 (+) compared to non-inoculated plants (Figure 1). While contents of progoitrin were lower in plants inoculated with P1 compared to non-inoculated plants, contents were similar between plants inoculated with P1 (+) and non-inoculated ones.

Similar results were obtained for glucobrassicin (I3M), although no pronounced difference was observed between non-inoculated resistant and susceptible plants. Contents were higher in inoculated plants of the resistant variety Creed compared to non-inoculated plants.

Contents of gluconapoleiferin were also slightly lower in susceptible and inoculated plants compared to the resistant varieties; however, results were not as pronounced as for the other GSLs. The resistant variety Creed had higher contents of gluconapoleiferin regardless of inoculation compared to the other two resistant varieties.

Contents of 4-methoxyglucobrassicin were lower in susceptible varieties infected with P1 and P1 (+) compared to the resistant varieties. No difference could be observed in non-inoculated plants between resistant and susceptible cultivars. Contents of resistant inoculated varieties were in the same range as contents of non-inoculated plants, whereas contents of susceptible inoculated plants were lower compared to non-inoculated plants. This trend could also be observed in all other GSLs.

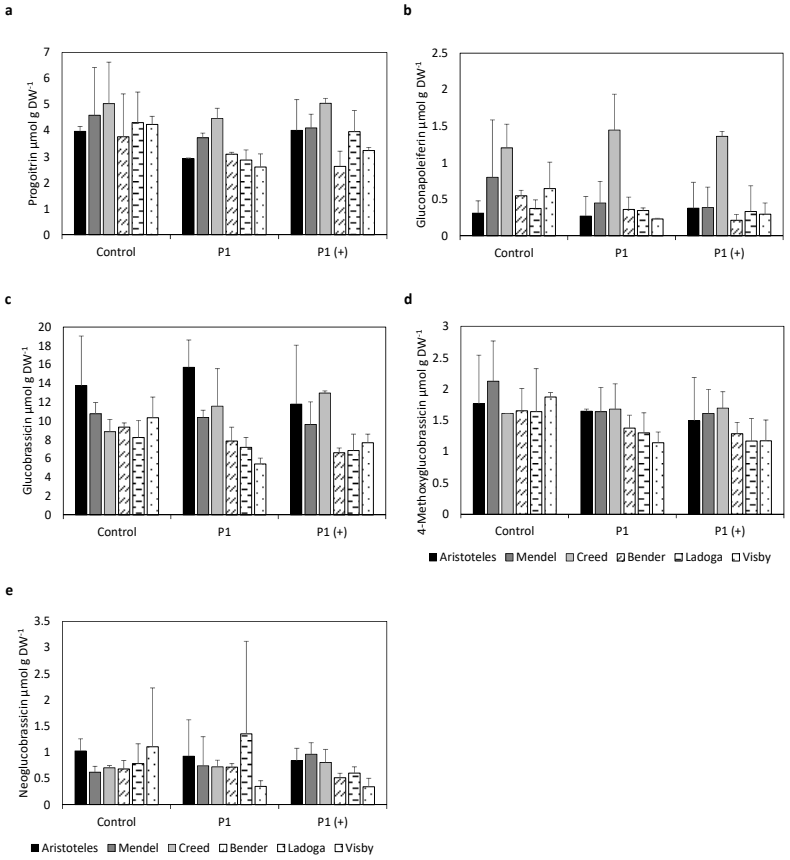

Figure 1. Contents of (**a**) Progoitrin, (**b**) Gluconapoleiferin, (**c**) Glucobrassicin, (**d**) 4-Methoxyglucobrassicin and (**e**) Neoglucobrassicin in leaves of clubroot-resistant (Aristoteles, Mendel, Creed) and -susceptible (Bender, Ladoga, Visby) cultivars of *Brassica napus* 35 days post inoculation (dpi) after mock inoculation (control) or artificial inoculation with either a less virulent isolate (P1, Hoisdorf) or a more virulent isolate (P1 (+), Grävenwiesbach) of *Plasmodiophora brassicae*. Contents represent the mean of six biological replicates, consisting of three plants each, from two independent experiments. Error bars represent the standard deviation. An analysis of variance (ANOVA) was performed to test the significance of main effects and interactions (for *p*-values see Supplementary Table S1). No significant differences were observed. DW, dry weight.

Contents of neoglucobrassicin were lower in susceptible varieties infected with P1 (+) compared to plants infected with P1 and non-infected plants. Contents of resistant and inoculated plants were in the same range as contents of non-inoculated plants.

2.2. Mean Glucosinolate Profiles of Resistant and Susceptible Varieties

Mean contents of progoitrin in leaves were significantly lower in inoculated susceptible varieties compared to inoculated resistant varieties and non-inoculated susceptible varieties (Figure 2). Similar significant differences were also observed in the mean contents of I3M, 4-methoxyglucobrassicin, neoglucobrassicin, total aliphatic (aGSLs) and total iGSLs between resistant and susceptible varieties inoculated with P1 or P1 (+). No significant differences in mean concentration between resistant and susceptible cultivars were observed

in non-inoculated plants for any of the analyzed GSLs. Mean contents of neoglucobrassicin were significantly lower in susceptible varieties inoculated with P1 (+) compared to resistant varieties. Overall, contents of all analyzed GSLs as well as total aGSLs and iGSLs were similar, independent of inoculation in resistant varieties, whereas contents in susceptible varieties were lower in plants inoculated with P1 or P1 (+) compared to non-inoculated plants.

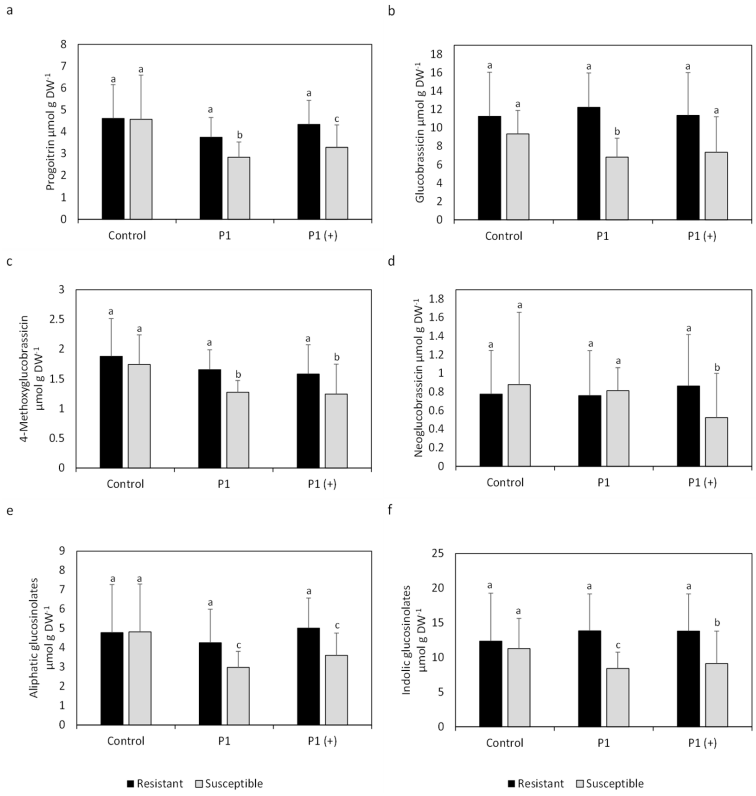

Figure 2. Contents of (**a**) Progoitrin, (**b**) Glucobrassicin, (**c**) 4-Methoxyglucobrassicin, (**d**) Neoglucobrassicin, (**e**) total aGSLs and (**f**) total iGSLs in leaves of clubroot-resistant (mean of cultivars Aristoteles, Mendel, Creed) and -susceptible (mean of cultivars Bender, Ladoga, Visby) cultivars of *Brassica napus* 35 days post inoculation (dpi) after mock inoculation (control) or inoculation with either a less virulent isolate (P1, Hoisdorf) or a more virulent isolate (P1 (+), Grävenwiesbach) of *Plasmodiophora brassicae*. Contents represent the mean of six biological replicates, consisting of three plants each, from two independent experiments. Error bars represent the standard deviation. An analysis of variance (ANOVA) was performed to test the significance of main effects and interactions, and Tukey's post hoc tests for the means of the factor variety were performed separately for inoculated and non-inoculated groups (for *p*-values see Supplementary Table S2). Different letters present significant differences between resistant and susceptible cultivars (a = $p > 0.05$; b = $p < 0.05$; c = $p < 0.005$). No significant differences were observed for other glucosinolates. DW, dry weight.

Mean GSL contents in roots showed higher contents of iGSLs in roots compared to leaves (Figures 2 and 3). Gluconasturtiin, an aGSL, was only present in roots and the most abundant GSL. Mean GSL patterns were quite similar in roots compared to leaves when

looking at progoitrin and glucoalyssin, although resistant cultivars had lower contents when inoculated, compared to non-inoculated resistant plants, which cannot be observed in leaves. Contents of 4-methoxyglucobrassicin were higher in resistant as well as susceptible cultivars inoculated, compared to non-inoculated plants, which is also different to the GSL pattern in leaves, where contents in resistant inoculated plants are similar to non-inoculated ones (Figure 2).

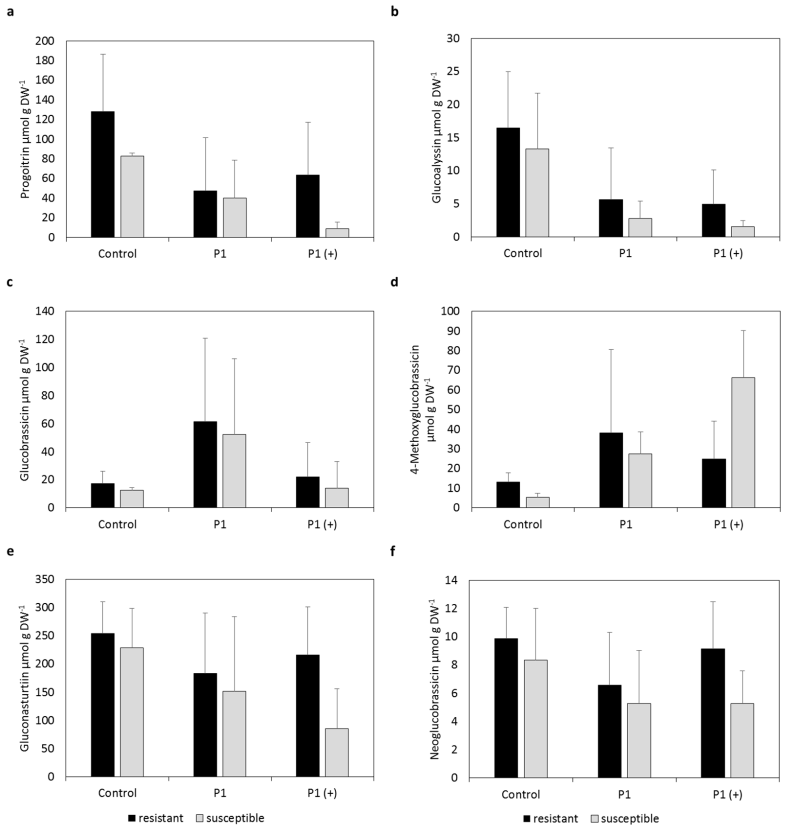

Figure 3. Contents of (**a**) Progoitrin, (**b**) Glucoalyssin, (**c**) Glucobrassicin, (**d**) 4-Methoxyglucobrassicin, (**e**) Gluconasturtiin and (**f**) Neoglucobrassicin in roots of clubroot-resistant (mean of cultivars Aristoteles, Mendel, Creed) and -susceptible (mean of cultivars Bender, Ladoga, Visby) cultivars of *Brassica napus* 35 days post inoculation (dpi) after mock inoculation (control) or inoculation with either a less virulent isolate (P1, Hoisdorf) or a more virulent isolate (P1 (+), Grävenwiesbach) of *Plasmodiophora brassicae*. Contents represent the mean of six biological replicates, consisting of three plants each, from two independent experiments. Error bars represent the standard deviation. An analysis of variance (ANOVA) was performed to test the significance of main effects and interactions, and Tukey's post hoc tests for the means of the factor variety were performed separately for inoculated and non-inoculated groups (for *p*-values see Supplementary Table S3). No significant differences were observed. DW, dry weight.

Mean contents of progoitrin in roots of inoculated plants were lower in both resistant as well as susceptible cultivars compared to non-inoculated cultivars (Figure 3). Susceptible varieties inoculated with P1 (+) showed the lowest mean contents.

Similar results were obtained for glucoalyssin, where mean contents of inoculated plants were even lower in resistant and susceptible cultivars compared to the non-inoculated ones. Mean contents of 4-methoxyglucobrassicin were higher in inoculated resistant and susceptible plants compared to non-inoculated plants regardless of pathotype used. Mean contents of gluconasturtiin as well as neoglucobrassicin were similar in resistant cultivars regardless of inoculation, whereas susceptible varieties showed lower mean contents when inoculated compared to non-inoculated varieties.

3. Discussion

To our knowledge, the present work is the first study that has investigated the combined effects of virulence of the pathogen and host resistance on the variation of total and individual GSLs in roots and leaves of *Brassica napus* cultivars after inoculating with different *P. brassicae* isolates. The results clearly showed that clubroot severity depended significantly on the virulence of the pathogen and the susceptibility of the oilseed rape cultivars (Table 1). Successful inoculation is reflected in the disease incidence and severity, which is low to non-existent in resistant cultivars and very high in susceptible varieties (Table 1). Only low disease incidences for the resistant cultivar Mendel inoculated with P1, and low disease severity, and slightly higher incidences and disease severities for the cultivars Mendel and Aristoteles inoculated with P1 (+) highlight the virulence selection of the *P. brassicae* isolates. Very high disease incidents and severities for susceptible plants inoculated with either P1 or P1 (+) show their suitability for this research question because of their high susceptibility towards the pathogen.

3.1. Similarity of Glucosinolate Contents in Resistant Cultivars—A Coincidence?

Genome mapping of *Brassica rapa* var. *rapifera* as well as *B. oleraceae* var. *pekinensis* revealed 11 loci that convey resistance to *P. brassicae* [19]. The resistant cultivar Mendel is known to possess five of them, among them *CRa*, which is known to encode for a TIR-NB-LRR class disease-resistance protein [19,20]. This protein consists of a toll interleukin 1 receptor domain, involved in pathogen recognition, a nucleotide binding (NB) domain, involved in disease signaling pathways and a leucine rich repeat (LRR) domain, which is responsible for protein-protein interactions and ligand binding. Because of its distinct function involved in pathogen detection it is unlikely involved in the synthesis or regulation of GSLs [21]. Unfortunately, the function of the other loci responsible for the resistance are not known and no information about the presence of these loci in the resistant cultivars Aristoteles and Creed is available.

Nevertheless, it is noteworthy that all resistant cultivars showed similar GSL contents in leaves (Figures 1 and 2) as well as in roots (Figure 3). The similar GSL contents highlight a general effect of the infection on the resistant cultivars despite putative differing genetic backgrounds. This phenomenon could be attributed to normal GSL biosynthesis and breakdown in resistant cultivars compared to susceptible cultivars because the pathogen might not be able to interfere with GSL synthesis or degradation, which is reflected in the non-existent to low disease incidence and severity of resistant cultivars (Table 1).

3.2. Higher Contents of Indolic Glucosinolates—A Double-Edged Sword

Resistant inoculated cultivars showed higher contents of the iGSLs I3M, 4- methoxglucobrassicin and neoglucobrassicin in leaves compared to susceptible inoculated varieties (Figure 1). Results became more pronounced when looking at the mean total contents of iGSLs (Figure 2). Glucosinolates and classical thioglucosidases (EC 3.2.1.147) are usually stored in different cell compartments or different cells and come together upon tissue disruption resulting in degradation of GSLs. A Glu residue in the catalytic site of classical

thioglucosidases performs a nucleophilic attack on GSLs resulting in an aglucone. Ascorbic acid is then needed as proton donor to cleave the glucose from the aglucone [22].

However, GSLs can also be degraded in intact tissue in the presence of atypical thioglucosidases like PEN2 and PYK10 [23,24]. Two Glu residues in the active sites of atypical thioglucosidases perform an acid/base catalysis, which does not require ascorbic acid. In contrast to typical thioglucosidases, atypical thioglucosidases also accept O-glucosides alongside GSLs as substrates [22]. Upon degradation of I3M with thioglucosidases and the presence of nitrile specifier proteins, indole-3-acetonitrile (IAN) can be formed and further synthesized to auxin in the presence of nitrilases (EC 3.5.5.1) [25]. Higher contents of auxin were found to be responsible for cell elongation in roots, susceptibility and subsequent gall formation induced by an infection with *P. brassicae* [21].

Nevertheless, indole-3-acetic acid (IAA) is not the only outcome of the breakdown of I3M. If nitrile specifier proteins (NSP1, NSP5) are not present during degradation of I3M, indolylmethylisothiocyanate is formed and quickly reacts to indole-3-carbinol, which usually conjugates with nucleophilic compounds like cysteine, glutathione or ascorbic acid [26]. Molecular docking simulations revealed that some of these conjugates possess potent auxin inhibitory activities by binding to the auxin receptor TIR1 and blocking the subsequent binding of IAA and its interaction with auxin regulatory proteins (AUX/IAA [17]. It was also hypothesized that during the infection with a pathogen, the synthesis of I3M breakdown products (BP) could lead to a drop of TIR1:IAA complex levels, and therefore, uncoupling of IAA perception from actual IAA contents takes place leading to normalized IAA signaling [17] (Figure 4c). Inhibition of auxin perception in *A. thaliana* was shown with the addition of indole-3-carbinol to growth media, which was able to inhibit root elongation in a concentration-dependent manner [27]. Due to its root-growth repressive action, this compound might be involved in the inhibition of gall growth directly in the roots by blocking TIR1:IAA formation and subsequent auxin signaling.

Interestingly, in our study contents of iGSLs in leaves were unchanged upon infection with *P. brassicae* in resistant cultivars compared to non-inoculated plants, whereas contents were lower in susceptible inoculated plants compared to non-inoculated plants (Figure 1). In order to avoid auxin-inhibitory actions of I3M BP, the pathogen might influence biosynthesis of iGSLs, which is reflected in lower levels of I3M in leaves of susceptible cultivars. Slightly lower contents of I3M in roots of inoculated susceptible plants compared to resistant ones (Figure 3) also points in this direction. The lower contents in roots could lead to a positive feedback of auxin due to degradation of inhibitory AUX/IAA proteins by the formation of the TIR1:IAA complexes (Figure 4d).

Contents of neoglucobrassicin and 4-methoxyglucobrassicin were also lower in leaves of susceptible plants inoculated with P1 and P1 (+) (Figures 1 and 2) and roots of susceptible plants inoculated with P1 (Figure 3) compared to resistant ones. Since the properties of the BPs of 4-methoxyglucobrassicin and neoglucobrassicin are not known at this point, only speculations can be made about their inhibitory activity towards the formation of the TIR1:IAA complex. Nevertheless, it is important to keep in mind that *P. brassicae* could also interfere with the expression of genes or synthesis of proteins involved in the degradation of GSLs and modification of BPs, which would not be reflected in GSLs contents. It was shown in *A. thaliana* that both leaves and roots are capable of synthesizing iGSLs and that GSL transporters are in charge of the long-distance transport of GSLs, which raises the question why differences between resistant and susceptible cultivars are more pronounced in leaves compared to roots [28].

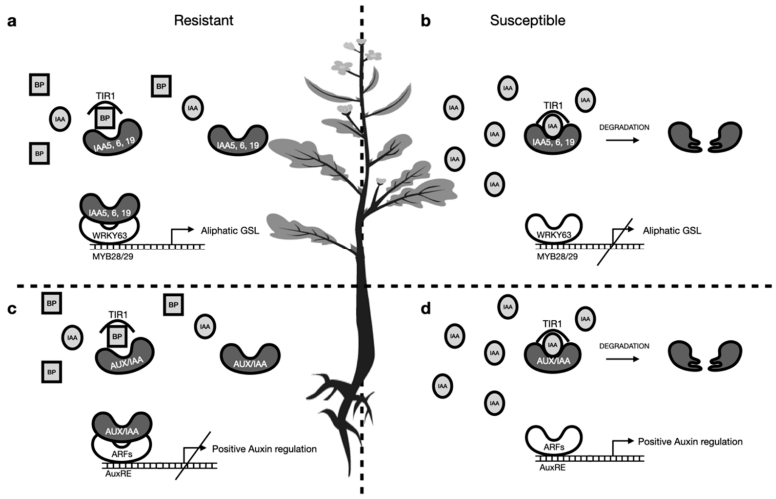

Figure 4. Proposed model for the role of iGSLs upon an infection with *Plasmodiophora brassicae* in *Brassica napus* and interplay between iGSLs and aGSLs. (**a**) Resistant cultivars might maintain the water status in leaves by involving breakdown products of aGSLs in stomatal closure. Upregulation of aGSL contents was shown to be mediated by IAA5, IAA6 and IAA19. Stability of these auxin-responsive proteins might be prolonged by inhibition of the TIR1 receptor with conjugated I3M breakdown products. (**b**) Susceptible cultivars might be restrained in their production of I3M breakdown products due to low iGSL contents. This might lead to degradation of IAA5, IAA6 and IAA19 through IAA and subsequent drop in contents of aGSLs. (**c**) Inhibition of the TIR1 receptor by I3M breakdown products in resistant cultivars might maintain functional auxin response despite higher IAA contents during an infection. (**d**) Lower levels of iGSLs and subsequent lower levels of I3M breakdown products might lead to a positive feedback response caused by high auxin concentrations. Legend: IAA = indole-3-acetic acid; BP = breakdown products of glucobrassicin; TIR1 = transport inhibitor response 1, IAA receptor; AUX/IAA = auxin responsive proteins, mostly IAA repressive proteins; IAA5, 6, 19 = auxin responsive proteins, inhibit WRKY63; WRKY63 = transcription factor, represses expression of MYB28/29; MYB28/29 = transcription factors, positively regulate biosynthetic genes in the synthesis of aGSLs.

3.3. Is There an Interplay Between Aliphatic and Indolic Glucosinolates?

Single (Figure 1) as well as mean total aGSL contents (Figure 2) were observed to be reduced in susceptible cultivars upon infection with *P. brassicae*. On the other hand, contents in inoculated resistant cultivars remain in the same range compared to non-inoculated ones (Figures 1 and 2). Maintenance of water balance is of importance in plants infected with *P. brassicae* since the pathogen disrupts water uptake by the host [29]. Sustention of aGSL contents in resistant cultivars during an infection with *P. brassicae* might be beneficial due to the involvement of BPs derived from aGSLs in stomatal aperture, which could lead to contained water loss. It has been shown that allylisothiocyanate and 3-butenenitril, both BPs of sinigrin, as well as ethylthiocyanate, a BP of glucolepidiin, lead to stomatal closure through generation of reactive oxygen species (ROS) which was reversed by addition of catalase [30,31]. It is possible, that the degradation products of other aGSLs, like progoitrin present in *B. napus* (Figures 1 and 2), could also trigger closure of stomata.

It has been shown that the auxin responsive proteins IAA5, IAA6 and IAA19 repress the expression of *WRKY63*, which encodes for a transcription factor inhibiting the expression of *MYB28/29*. The transcription factors MYP28/29 are involved in the positive regulation of aGSL synthesis [32]. Lower expression of *WRKY63*, negatively influencing

aGSL contents, mediated by IAA5, IAA6 and IAA19, therefore leads to higher aGSL contents. Breakdown of auxin-responsive proteins is usually mediated by TIR1:IAA complex formation, but can be inhibited by docking of I3M BPs to TIR1 [17]. The prolonged lifespan of IAA5, IAA6 and IAA19 could therefore lead to higher contents of aGSLs via repression of the TIR1:IAA formation, mediated by the breakdown of iGSLs. Higher contents of aGSLs and their subsequent degradation might be used by the plant to attenuate drought symptoms caused by *P. brassicae* through closure of stomata (Figure 4a). On the other hand, the synthesis of TIR1:IAA inhibitory compounds could be inhibited in susceptible cultivars by the pathogen, resulting in faster degradation of IAA5, IAA6 and IAA19 and therefore lower contents of aGSLs (Figure 4b). This could also explain the lower contents of aGSLs in susceptible cultivars infected with P1 (+) compared to P1. This data suggests that virulence of the isolates might correlate with the degree of interference with the plants' metabolism.

3.4. Direct Effect of Breakdown Products on P. brassicae

Levels of gluconasturtiin in roots were observed to be lower in susceptible varieties inoculated with P1 and even lower in plants inoculated with P1 (+) compared to resistant varieties (Figure 3). Analysis of quantitative trait loci involved in resistance and metabolic changes revealed a possible involvement of gluconasturtiin in the infection with *P. brassicae* [33]. The higher levels of gluconasturtiin controlled by resistance alleles found in the mentioned publication is in accordance with the findings of this study. As gluconasturtiin is the most abundant GSL in roots of the chosen cultivars analyzed, the contents of which are unchanged in resistant cultivars upon an infection, the pathogen might interfere with biosynthesis of gluconasturtiin in susceptible varieties. The different isolates of *P. brassicae* analyzed seem to differ in their ability to reduce gluconasturtiin contents in the host. The more aggressive isolate P1 (+) might therefore be able to suppress gluconasturtiin synthesis of the host in a more pronounced manner compared to the isolate P1. At this moment, only assumptions can be made about the effects of gluconasturtiin on the pathogen, although direct effects of the isothiocyanate derived from this GSL on *P. brassicae* might be more likely.

4. Materials and Methods

4.1. Plant and Pathogen Materials

Six oilseed rape cultivars (*Brassica napus* L.) with a different resistance level to clubroot disease were selected in the current study according to the German Plant Variety Catalogue in 2018 (Table 2). These cultivars were pre-selected according to results obtained from pre-experiments (data not shown). Selected resistant cultivars had no to low disease symptoms and selected susceptible cultivars had a high disease incidence as well as disease severity and were therefore selected for this study. Although information about the genes responsible for the resistance towards *Plasmodiophora brassicae* is only available for the cultivar Mendel, the aim of this study was to observe general changes in GSLs despite putatively different genetic backgrounds.

Table 2. Cultivars of *Brassica napus* and their level of resistance to clubroot disease caused by *Plasmodiophora brassicae*.

Cultivar	Seed Source	Clubroot Resistance
Aristoteles	Limagrain GmbH	resistance: single dominant gene (based on 'Mendel' resistance)
Creed	Norddeutsche Pflanzenzucht	resistance: polygenic resistance (internal communication with the company)
Mendel	Norddeutsche Pflanzenzucht	resistance: single dominant gene-based resistance [5]
Bender	Deutsche Saatveredelung AG	susceptible
Ladoga	Limagrain GmbH	susceptible
Visby	Norddeutsche Pflanzenzucht	susceptible

Two field isolates of *P. brassicae* were chosen according to their evaluated virulence in Zamani-Noor (2017) [9]: an isolate which was virulent on clubroot susceptible cv. Visby, avirulent on clubroot resistant cv. Mendel, classified as 16/31/12 on the European clubroot differential (ECD) set [12] or pathotype 1 according to the system of Somé et al. [11] (briefly named P1), and a highly virulent isolate which could overcome the resistance of both cultivars, classified as 17/31/31 on the ECD set or pathotype 1 in system of Somé et al. [11] (briefly named P1 (+)). The P1 isolate was collected from a naturally infested oilseed rape field in Hoisdorf, Schleswig-Holstein, Germany, in 2012 and the P1 (+) isolate originated from a field in Grävenwiesbach, Hesse, Germany, in 2013 [9]. Both isolates were preserved as frozen root galls in −20 °C and used for inoculum preparation as needed.

4.2. Plant Cultivation and Inoculation

The experiments were conducted under controlled greenhouse conditions using portable raised-bed containers (300 × 100 × 25 cm) containing a mix of potting soil, sand and peat (5:1:1; pH < 6.5; FloraSelf®, Braunschweig, Germany). Seeds were sown at 7.5 cm spacing in a row spaced 11.5 cm apart from the other row. In total, 17–20 seeds per row were sown and seedlings were thinned on emergence to leave 13 plants, and there were four rows per oilseed rape cultivar. Plants were grown under greenhouse conditions at 20/16 °C, 70% relative humidity and a 16/8 h day/night regime with a light intensity of 50 µmol m^{-2} s^{-1}. Plants were inoculated at growth stage 11–12 (BBCH-scale; young seedling) and were well irrigated prior to inoculation.

The inoculum was prepared according to in Zamani-Noor (2017) [9]. In summary, the resting spores of each *P. brassicae* isolate were released from frozen clubbed roots by homogenizing 100 g clubbed roots in 200 mL of sterile deionized water in a laboratory blender for 5 min at 20,000 rpm (Vital Mixer Pro, Hollenstedt, Germany). The solution was filtered several times through fine layers of cheesecloth until the suspension was free from plant debris. The spore suspension was diluted to a concentration of 1×10^7 spores per mL as estimated using a Fuchs haemocytometer slide (Hecht-Assistent, Sondheim, Germany) under a microscope.

Inoculations were conducted by injecting 2 × 1 mL of spore suspension (1×10^7 spores per mL) into the soil at two locations near the root zone of each seedling at a depth of approximately 2 cm. Control plants were mock inoculated in the same way with water. To avoid washing the inoculum from the root area, the plants were not irrigated for 72 h post inoculation and were kept at a temperature of 24 °C to attain the best conditions for the infection. Following this period, plants were grown at previous greenhouse conditions and irrigated every other day to maintain soil moisture, but they were not water saturated.

4.3. Plant Sampling and Disease Assessment

Roots and leaves samples were collected one day before inoculation (plant growth stage BBCH 11-12) and on 35 days post inoculation (dpi). At each date, nine plants per oilseed rape cultivar were completely dug out and divided into 3 biological replicates consisting of three plants each. Leaves were separated and frozen immediately in liquid nitrogen and then stored in −80 °C for further steps. The roots were then carefully washed under tap water to remove soil particles and clubroot severity was visually assessed based on a scale of 0 to 3 (0 = no galling, 1 = a few small galls, 2 = moderate galling and 3 = severe galling) [34]. Conclusively, roots were frozen in liquid nitrogen and then stored at −80 °C.

The disease incidence (DI) and disease severity index (DSI) were calculated for each treatment using Equations (1) and (2):

$$\text{DI}\ (\%) = \frac{\sum(n1 + n2 + n3)}{N} \times 100 \quad (1)$$

$$\text{DSI}\ (\%) = \frac{\sum(n0 \times 0 + n1 \times 1 + n2 \times 2 + n3 \times 3)}{N \times \text{No.Classes with symptoms}} \times 100 \quad (2)$$

where '*n*' is the number of plants in each class, '*N*' is the total number of plants and values 0, 1, 2 and 3 represent the respective symptom severity classes.

4.4. Extraction of Glucosinolates

Samples were prepared as described by Hornbacher et al. [35]. Briefly, frozen plant materials were lyophilized in a freeze dryer (Martin Christ Gefriertrocknungsanlagen GmbH, Osterode am Harz, Germany) for 2 days and ground to a fine powder with a shaking ball mill (Retsch GmbH, Braunschweig, Germany). Approximately 50 mg dry plant tissue was extracted with 1 mL 80% methanol at room temperature for 10 min and then centrifuged at 13,000× *g* for 5 min. Before the centrifugation, samples were put on a shaker for 15 min after the first extraction and 30 min after the second extraction at room temperature (RT). The supernatants were pooled and loaded onto a column (polypropylene column, 1 mL) containing 2 mL of a 5% (*w*/*v*) suspension of DEAE Sephadex A25 (Sigma-Aldrich, Taufkirchen, Germany) in 0.5 M acetic acid (pH 5). Columns were washed five times with 2 mL H_2O and two times with 2 mL 0.02 M acetic acid (pH 5). For desulfation, 50 µL of sulfatase (Sigma-Aldrich, Taufkirchen, Germany) solution was added to 450 µL 0.02 M acetic acid (pH 5) and loaded onto the columns as well [36]. Desulfation took place for 24 h at RT. Afterwards desulfated GSLs were eluted three times with 2 mL HPLC H_2O (Sigma-Aldrich, Taufkirchen, Germany), dried overnight in a vacuum centrifuge and then dissolved in a total amount of 300 µL HPLC H_2O.

4.5. Liquid Chromatography Mass Spectrometry (LCMS) and Analysis of Glucosinolates

Glucosinolate contents in oilseed rape samples were analyzed via liquid chromatography-mass spectrometry (LC-MS). A volume of 10 µL was injected into the HPLC system (Shimadzu, Darmstadt, Germany) and separated on a Knauer Vertex Plus column (250 × 4 mm, 5 µm particle size, packing material ProntoSIL 120-5 C18-H) equipped with a pre-column (Knauer, Berlin, Germany). A water (solvent A)-methanol (solvent B), both containing 2 mM ammonium acetate, gradient was used with a flow rate of 0.8 mL min at 30 °C. For measuring the samples, the following gradient was used: 10–90% B for 35 min, 90% for 2 min, 90–10% B for 1 min and 10% B for 2 min. Detection of the spectra in the range 190–800 nm was performed with a diode array detector (SPD-M20A, Shimadzu, Darmstadt, Germany). The HPLC system was coupled to an AB Sciex Triple TOF mass spectrometer (AB Sciex TripleTOF 4600, Canby, OR, USA). At a temperature of 600 °C and an ion spray voltage floating of −4500 V the negative electrospray ionization (ESI) was performed. For the ion source gas one and two 50 psi were used and for the curtain gas 35 psi. In the range of 100–1500 Da in the TOF range, the mass spectra as well as the MS/MS spectra from 150–1500 Da at a collision energy of −10 eV were recorded. Peaks were identified by analyzing the characteristic mass fragments of ds-progoitrin (195, 309, 344, 617), ds-glucoalyssin (195, 208, 371, 741) and ds-neoglucobrassicin (195, 208, 371, 741). The detection of the GSL was performed with DAD (Knauer, Berlin, Germany) at 229 nm. Quantification of the measured GSL was performed using sinigrin (Phytolab, Vestenbergsgreuth, Germany) as external standard and relative response factors (progoitrin, 1.09; glucoraphanin, 1.07; glucoalyssin, 1.07; gluconapin, 1.11; hydroxyglucobrassicin, 0.17; glucobrassicanapin, 1.15; I3M, 0.29; gluconasturtiin, 0.95; neoglucobrassicin, 0.2). Integration of peaks and elaboration of data were performed using PeakView software version 2.1.0.1 (AB Sciex, Darmstadt, Germany). Limits of quantification for aGSL were determined with glucoraphanin as standard (Phytolab, Vestenbergsgreuth, Germany) and for iGSL I3M (Phytolab, Vestenbergsgreuth, Germany) was used. Limits of quantification were determined to be 30 nmol mL^{-1} for aGSLs and 6 nmol mL^{-1} for iGSLs. Glucosinolate contents (total GSL, aGSLs, iGSLs and aromatic GSLs) were calculated as the mean of three biological replicates, consisting of three plants each, with standard deviation of the three replicates. The total amount of GSLs for each sample was calculated as the sum of all individual GSLs. Total aGSL contents were calculated as the sum of the contents of progoitrin and gluconapoleiferin. Total iGSL contents were calculated as the sum of I3M, 4-methoxyglucobrassicin and neoglucobrassicin. Although contents of gluconapin

and glucobrassicanapin were analyzed, they are not shown due to very low levels and high standard deviations.

4.6. Statistical Analysis

All experiments in the present study were conducted twice, where each repetition is referred to as a run. With regards to different treatments or independent factors in our experiments, we decided to use analysis of variance (ANOVA) over multiple *t*-test. Analysis of common treatments did not show significant differences ($p \leq 0.05$) between two runs, so we pooled the data for analysis and presentation in this study.

Glucosinolate concentrations were log-transformed before analysis due to finding right skewed distributions and variance increasing with mean. For the log-transformed data, linear mixed effect models were fitted to account for the split-plot design. The experimental runs, the pathogens, the traits and the varieties nested within the traits were included as fixed effects. For the latter three, the corresponding interactions were also modelled. Furthermore, three random effects were included: the main plot, which accounts for the variance of the spatial separation between the pathogen inoculations; the subplot, which takes into consideration the variance of the varieties within the main plot; and a random effect, which represents the variance of the varieties between the two experiments. Based on the fitted linear mixed models, analysis of variance was performed to test the significance of main effects and interactions and Tukey tests for the model-based means of factor variety were performed jointly across all other factor levels and separately for inoculated and non-inoculated groups.

5. Conclusions

Although it was previously hypothesized that loss of iGSLs has no influence on gall formation in *Arabidopsis thaliana*, our results and hypotheses are quite in line with the findings of Siemens et al. [14]. The mutants used by Siemens et al. [14] (*cyp79b2/b3*) were incapable of synthesizing iGSLs and showed no difference in gall formation compared to wild type plants. The loss of iGSLs also leads to a loss of a variety of BPs that could inhibit TIR1:IAA formation and therefore stabilize auxin signaling during an infection with *P. brassicae*.

It will be necessary to perform gene expression analysis as well as further analysis of GSL contents because observed changes in GSL contents could be attributed to the infection itself as a correlated symptom without having a causal relationship.

Follow-up experiments could focus on *nsp* mutants which would be incapable of directing the outcome of I3M degradation towards IAN, and these plants would be left with higher contents of I3M conjugates and therefore a possible uncoupling of auxin signaling would take place.

Expression analysis of *TIR1* as well as *AUX/IAA* and *NSP1,5* would also help to substantiate the hypotheses made in this work. Analysis of free as well as conjugated auxin would also be crucial for the understanding of the involvement of iGSLs during an infection with *P. brassicae*.

Finally, analysis of GSLs as well as expression analysis at different time points during the infection would allow a more distinct insight into the time-dependent actions of *P. brassicae* in *B. napus*.

Supplementary Materials: The following data are available online at https://www.mdpi.com/article/10.3390/pathogens10050563/s1, Table S1: *p*-values of mean glucosinolate contents in leaves analyzed with Tukey's post-hoc tests for the means of the factor 'pathogen', Table S2: *p*-values of mean glucosinolate contents in leaves analyzed with Tukey's post-hoc tests for the means of the factor 'variety'. *p*-values show the significance of differences in glucosinolate contents between the mean of the resistant varieties (Aristoteles, Creed, Mendel) and the mean of the susceptible varieties (Bender, Ladoga, Visby) averaged over the factor 'variety' (resistant, susceptible), Table S3: *p*-values of mean glucosinolate contents in roots analyzed with Tukey's post-hoc tests for the means of the factor 'variety'. *p*-values show the significance of differences in glucosinolate contents between the

mean of the resistant varieties (Aristoteles, Creed, Mendel) and the mean of the susceptible varieties (Bender, Ladoga, Visby) averaged over the factor 'variety'.

Author Contributions: Conceptualization, J.P. and N.Z.-N.; methodology, C.J.C. and J.H.; software, J.H.; validation, J.H.; formal analysis, C.J.C.; writing—original draft preparation, N.Z.-N., J.H. and J.P.; writing—review and editing, N.Z.-N., J.H. and J.P.; supervision, J.P. and N.Z.-N. All authors have read and agreed to the published version of the manuscript.

Funding: This work was funded by the Julius Kühn-Institute and Leibniz University of Hannover. It did not receive any external funding.

Data Availability Statement: Data presented in this study are available upon request.

Acknowledgments: Authors thank the invaluable help of Jaroslaw Acalski, Kelly Coutinho Szinovatz, Anke Kawlath, Julia Volker, Leonard Käufler and Marie Hielscher. We thank Frank Schaarschmidt and Sören Budig, Leibniz University Hannover, for help with the statistical analysis of GSL contents.

Conflicts of Interest: The authors declare no conflict of interest. The funders had no role in the design of the study; in the collection, analyses or interpretation of data; or in the writing of the manuscript.

References

1. Wallsgrove, R.M.; Doughty, K.J.; Bennett, R.N. Glucosinolates. In *Plant Amino Acids: Biochemistry and Biotechnology*; Singh, B., Ed.; Marcel Dekker Inc.: New York, NY, USA, 1998; pp. 523–562.
2. Fahey, J.W.; Zalcmann, A.T.; Talalay, P. The Chemical Diversity and Distribution of Glucosinolates and Isothiocyanates among Plants. *Phytochemistry* **2001**, *56*, 5–51. [CrossRef]
3. Agerbirk, N.; Olsen, C.E. Glucosinolate Structures in Evolution. *Phytochemistry* **2012**, *77*, 16–45. [CrossRef] [PubMed]
4. Dixon, G.R. Clubroot (*Plasmodiophora brassicae* Woronin)—An Agricultural and Biological Challenge Worldwide. *Can. J. Plant Pathol.* **2014**, *36*, 5–18. [CrossRef]
5. Diederichsen, E.; Beckmann, J.; Schondelmeier, J.; Dreyer, F. Genetics of Clubroot Resistance in *Brassica napus* 'Mendel'. *Acta Horticulturae* **2006**, 307–311. [CrossRef]
6. Honig, F. Der Kohlkropferreger (*Plasmodiophora brassicae* Wor.): Eine Monographie. In *Gartenbauwissen*; Gustav Fischer Verlag: Jena, Germany, 1931; pp. 116–225.
7. Řičařová, V.; Kaczmarek, J.; Strelkov, S.E.; Kazda, J.; Lueders, W.; Rysanek, P.; Manolii, V.; Jedryczka, M. Pathotypes of *Plasmodiophora brassicae* Causing Damage to Oilseed Rape in the Czech Republic and Poland. *Eur. J. Plant Pathol.* **2016**, *145*, 559–572. [CrossRef]
8. Lüders, W. Analyses of Virulence of European Isolates of Clubroot (*Plasmodiophora brassicae* Wor.) and Mapping of Resistance Genes in Rapeseed (*Brassica napus* L.). Ph.D. Thesis, Justus-Liebig-Universität, Gießen, Germany, 2017. [CrossRef]
9. Zamani-Noor, N. Variation in Pathotypes and Virulence of *Plasmodiophora brassicae* Populations in Germany. *Plant Pathol.* **2017**, *66*, 316–324. [CrossRef]
10. Zamani-Noor, N.; Diederichsen, E.; Wallenhammar, A.-C.; Cordsen-Nielsen, G.; Orgeur, G.; Konradyova, V.; Dussart, F.; Smith, J.; Jedryczka, M. Epidemiology of Clubroot Disease and Pathogenic Variation among Isolates of *Plasmodiophora brassicae* from Oilseed Rape Growing in Europe. *Can. J. Plant Pathol.* **2019**, *41*, 491–492. [CrossRef]
11. Some, A.; Manzanares, M.J.; Laurens, F.; Baron, F.; Thomas, G.; Rouxel, F. Variation for Virulence on Brassica Napus L. amongst *Plasmodiophora brassicae*. Collections from France and Derived Single-Spore Isolates. *Plant Pathol.* **1996**, *45*, 432–439. [CrossRef]
12. Buczacki, S.T.; Toxopeus, H.; Mattusch, P.; Johnston, T.D.; Dixon, G.R.; Hobolth, L.A. Study of Physiologic Specialization in *Plasmodiophora brassicae*: Proposals for Attempted Rationalization through an International Approach. *Transact. British Mycolog. Soc.* **1975**, *65*, 295–303. [CrossRef]
13. Korbas, M.; Jajor, E.; Budka, A. Clubroot (*Plasmodiophora brassicae*)–A Threat for Oilseed Rape. *J. Plant Prot. Res.* **2009**, *49*. [CrossRef]
14. Siemens, J.; Glawischnig, E.; Ludwig-Müller, J. Indole Glucosinolates and Camalexin Do Not Influence the Development of the Clubroot Disease in *Arabidopsis thaliana*: Cyp79b2/B3 Double Mutant and Clubroot. *J. Phytopathol.* **2008**, *156*, 332–337. [CrossRef]
15. Ludwig-Müller, J.; Schubert, B.; Pieper, K.; Ihmig, S.; Hilgenberg, W. Glucosinolate Content in Susceptible and Resistant Chinese Cabbage Varieties during Development of Clubroot Disease. *Phytochemistry* **1997**, *44*, 407–414. [CrossRef]
16. Ludwig-Müller, J.; Bennett, R.N.; Kiddle, G.; Ihmig, S.; Ruppel, M.; Hilgenberg, W. The Host Range of *Plasmodiophora brassicae* and Its Relationship to Endogenous Glucosinolate Content. *New Phytologist* **1999**, *141*, 443–458. [CrossRef]
17. Vik, D.; Mitarai, N.; Wulff, N.; Halkier, B.A.; Burow, M. Dynamic Modeling of Indole Glucosinolate Hydrolysis and Its Impact on Auxin Signaling. *Front. Plant Sci.* **2018**, *9*, 550. [CrossRef]
18. Jahn, L.; Mucha, S.; Bergmann, S.; Horn, C.; Staswick, P.; Steffens, B.; Siemens, J.; Ludwig-Müller, J. The Clubroot Pathogen (*Plasmodiophora brassicae*) Influences Auxin Signaling to Regulate Auxin Homeostasis in Arabidopsis. *Plants* **2013**, *2*, 726–749. [CrossRef] [PubMed]

19. Hatakeyama, K.; Niwa, T.; Kato, T.; Ohara, T.; Kakizaki, T.; Matsumoto, S. The Tandem Repeated Organization of NB-LRR Genes in the Clubroot-Resistant CRb Locus in *Brassica rapa* L. *Mol. Genet. Genomic.* **2017**, *292*, 397–405. [CrossRef] [PubMed]
20. Fredua-Agyeman, R.; Rahman, H. Mapping of the Clubroot Disease Resistance in Spring *Brassica napus* Canola Introgressed from European Winter Canola Cv. 'Mendel.'. *Euphytica* **2016**, *211*, 201–213. [CrossRef]
21. McHale, L.; Tan, X.; Koehl, P.; Michelmore, R.W. Plant NBS-LRR Proteins: Adaptable Guards. *Genome Biol.* **2006**, *7*, 1–11. [CrossRef]
22. Chhajed, S.; Misra, B.B.; Tello, N.; Chen, S. Chemodiversity of the glucosinolate-myrosinase system at the single cell type resolution. *Front. Plant Sci.* **2019**, *10*, 618. [CrossRef]
23. Nakano, R.T.; Piślewska-Bednarek, M.; Yamada, K.; Edger, P.P.; Miyahara, M.; Kondo, M.; Böttcher, C.; Mori, M.; Nishimura, M.; Schulze-Lefert, P.; et al. PYK10 Myrosinase Reveals a Functional Coordination between Endoplasmic Reticulum Bodies and Glucosinolates in *Arabidopsis thaliana*. *Plant J.* **2017**, *89*, 204–220. [CrossRef]
24. Zhao, Y.; Wang, J.; Liu, Y.; Miao, H.; Cai, C.; Shao, Z.; Guo, R.; Sun, B.; Jia, C.; Zhang, L.; et al. Classic Myrosinase-Dependent Degradation of Indole Glucosinolate Attenuates Fumonisin B1-Induced Programmed Cell Death in Arabidopsis. *Plant J.* **2015**, *81*, 920–933. [CrossRef]
25. Lehmann, T.; Janowitz, T.; Sánchez-Parra, B.; Alonso, M.-M.P.; Trompetter, I.; Piotrowski, M.; Pollmann, S. Arabidopsis NITRILASE 1 Contributes to the Regulation of Root Growth and Development through Modulation of Auxin Biosynthesis in Seedlings. *Front. Plant Sci.* **2017**, *8*. [CrossRef]
26. Agerbirk, N.; Olsen, C.E.; Sørensen, H. Initial and Final Products, Nitriles, and Ascorbigens Produced in Myrosinase-Catalyzed Hydrolysis of Indole Glucosinolates. *J. Agricult. Food Chem.* **1998**, *46*, 1563–1571. [CrossRef]
27. Katz, E.; Nisani, S.; Yadav, B.S.; Woldemariam, M.G.; Shai, B.; Obolski, U.; Ehrlich, M.; Shani, E.; Jander, G.; Chamovitz, D.A. The Glucosinolate Breakdown Product Indole-3-carbinol Acts as an Auxin Antagonist in Roots of *Arabidopsis thaliana*. *Plant J.* **2015**, *82*, 547–555. [CrossRef]
28. Andersen, T.G.; Nour-Eldin, H.H.; Fuller, V.L.; Olsen, C.E.; Burow, M.; Halkier, B.A. Integration of Biosynthesis and Long-Distance Transport Establish Organ-Specific Glucosinolate Profiles in Vegetative Arabidopsis. *Plant Cell* **2013**, *25*, 3133–3145. [CrossRef]
29. Hwang, S.F.; Ahmed, H.U.; Zhou, Q.; Strelkov, S.E.; Gossen, B.D.; Peng, G.; Turnbull, G.D. Assessment of the Impact of Resistant and Susceptible Canola on *Plasmodiophora brassicae* Inoculum Potential: Volunteer Canola, Inoculum Density and Clubroot. *Plant Pathol.* **2012**, *61*, 945–952. [CrossRef]
30. Hossain, M.S.; Ye, W.; Hossain, M.A.; Okuma, E.; Uraji, M.; Nakamura, Y.; Mori, I.C.; Murata, Y. Glucosinolate Degradation Products, Isothiocyanates, Nitriles, and Thiocyanates, Induce Stomatal Closure Accompanied by Peroxidase-Mediated Reactive Oxygen Species Production in *Arabidopsis thaliana*. *Biosci. Biotechnol. Biochem.* **2013**, *77*, 977–983. [CrossRef]
31. Sobahan, M.A.; Akter, N.; Okuma, E.; Uraji, M.; Ye, W.; Mori, I.C.; Nakamura, Y.; Murata, Y. Allyl Isothiocyanate Induces Stomatal Closure in *Vicia faba*. *Biosci. Biotechnol. Biochem.* **2015**, *79*, 1737–1742. [CrossRef] [PubMed]
32. Salehin, M.; Li, B.; Tang, M.; Katz, E.; Song, L.; Ecker, J.R.; Kliebenstein, D.J.; Estelle, M. Auxin-Sensitive Aux/IAA Proteins Mediate Drought Tolerance in *Arabidopsis* by Regulating Glucosinolate Levels. *Nat. Commun.* **2019**, *10*, 1–9. [CrossRef]
33. Wagner, G.; Laperche, A.; Lariagon, C.; Marnet, N.; Renault, D.; Guitton, Y.; Bouchereau, A.; Delourme, R.; Manzanares-Dauleux, M.J.; Gravot, A. Resolution of Quantitative Resistance to Clubroot into QTL-Specific Metabolic Modules. *J. Exp. Bot.* **2019**, *70*, 5375–5390. [CrossRef] [PubMed]
34. Strelkov, S.E.; Tewari, J.P.; Smith-Degenhardt, E. Characterization of *Plasmodiophora brassicae* Populations from Alberta, Canada. *Can. J. Plant Pathol.* **2006**, *28*, 467–474. [CrossRef]
35. Hornbacher, J.; Rumlow, A.; Pallmann, P.; Turcios, A.E.; Riemenschneider, A.; Papenbrock, J. The Levels of Sulfur-Containing Metabolites in *Brassica napus* Are Not Influenced by the Circadian Clock but Diurnally. *J. Plant Biol.* **2019**, *62*, 359–373. [CrossRef]
36. Thies, W. Detection and Utilization of a Glucosinolate Sulfohydrolase in the Edible Snail, *Helix pomatia*. *Naturwissenschaften* **1979**, *66*, 364–365. [CrossRef]

Chapter 4

Influence of abiotic influences on glucosinolate contents

Chapter 4.1 The levels of sulfur-containing metabolites in *Brassica napus* are not influenced by the circadian clock but diurnally

J. Plant Biol. (2019) 62:359-373
DOI 10.1007/s12374-019-0143-x

ORIGINAL ARTICLE

The Levels of Sulfur-containing Metabolites in *Brassica napus* are Not Influenced by the Circadian Clock but Diurnally

Johann Hornbacher[1,†], Annekathrin Rumlow[1,†], Philip Pallmann[2], Ariel E. Turcios[1], Anja Riemenschneider[1] and Jutta Papenbrock[1,*]

[1]*Institute of Botany, Leibniz University Hannover, Herrenhäuserstr. 2, D-30419 Hannover, Germany*
[2]*Centre for Trials Research, Cardiff University, Cardiff, CF14 4YS, United Kingdom*

Received: April 13, 2019 / Accepted: July 30, 2019

Abstract Adapting biological processes to an endogenous rhythm enables plants to cope with the daily changes in light and temperature in a more predictable way enhancing growth and fitness. A number of biological processes such as metabolic pathways as well as the immunity in plants are under diurnal or circadian control. In this study a possible circadian regulation of key enzymes in the sulfur assimilation and the corresponding metabolites was investigated in the agriculturally important crop plant oilseed rape (*Brassica napus*). Leaves of a commercially available cultivar were harvested in the course of a day under diurnal and under free-running conditions with constant light. Analyses in this study were focused on sulfur-containing metabolites and expression analysis of enzymes involved in sulfur assimilation. Expression analysis showed that the transcript levels of the sulfate transporters *Sultr3;1* and *Sultr4;2* as well as *APR2* and *APR3* oscillated diurnally. Results revealed a periodic rhythm of sulfur-containing metabolites such as glutathione, sulfate and certain glucosinolates in the course of a day which were only partly maintained under constant light. Therefore, we conclude that a diurnal rhythm and not the circadian clock regulates sulfur metabolism in plants.

Keywords: *Brassica napus,* Circadian clock, Diurnal rhythm, Expression analysis, Sulfur-containing metabolites

[†]These authors contributed equally to this work.

*Corresponding author; Jutta Papenbrock
Tel : +49-511-762-3788
E-mail : Jutta.Papenbrock@botanik.uni-hannover.de

Introduction

Life on earth is exposed to daily changes in light, temperature and other environmental factors due to the rotation of the earth. The metabolism, behavior and physiology in organisms were adapted to these daily changes, known as diurnal rhythms. In the absence of an external cue many of these oscillations persist and free-run with an endogenous period that is close to 24 h. These circadian rhythms are under the control of an endogenous circadian clock. Under natural conditions, light and temperature act as environmental timer entraining the endogenous organismic clock in each cell with the local time (McClung 2006; Harmer 2009).

The model of the circadian clock in plants has so far been best described in *Arabidopsis thaliana* (Salome and McClung 2004). The MYB domain transcription factors CIRCADIAN AND CLOCK ASSOCIATED 1 (CCA1) and LATE ELONGATED HYPOCOTYL 1 (LHY1) along with TIMING OF CAB 1 (TOC1) represent the core oscillator of the circadian clock as a negative feedback loop. Linked to this core oscillator further feedback loops are formed regulating the expression of so-called morning as well as evening genes (McClung 2006). Up to 80% of the transcriptome in rice (*Oryza* spp.), poplar (*Populus* spp.), and *A. thaliana* are regulated by the circadian clock enabling the timing of a number of biological processes and stress responses, respectively (Filichkin et al. 2011). The photosynthesis as the primary biological process shows circadian oscillations in the light harvesting and a circadian-regulated CO_2 fixation by Rubisco (Dodd et al. 2014). The circadian rhythm is also involved in certain stress responses. The involvement of the circadian rhythm in reactive oxygen species (ROS) mediated stress was shown in *A. thaliana* where the overexpression of the *CCA1* led to an enhanced drought tolerance by increasing the expression of ROS controlling genes (Lai et al. 2012). However,

the circadian rhythm is not solely involved in abiotic stress responses but also in plant immunity. Results from Wang et al. (2011) indicate that defense genes are under circadian control by CCA1, allowing plants to estimate infection at dawn when pathogens normally disperse the spores and time immune responses according to the perception of different pathogenic signals upon infection. The studies revealed a key functional link between the circadian clock and plant immunity. Mutants overexpressing *CCA1* showed enhanced resistance against downy mildew supporting a direct interaction of the clock with plant immunity (Wang et al. 2011).

The importance of the plant clock due to its role in agriculture is now rising (Shaw et al. 2012). As an agriculturally important oilseed crop *Brassica napus* is the most closely related species to the crucifer *A. thaliana* with a number of highly conserved genes among both species. Compared to other crops and cereals the requirements for nitrogen, phosphorus and sulfur are higher making it more sensitive to sulfur-deficient conditions (Schnug and Haneklaus 2005).

Sulfur is taken up by roots from the soil as inorganic sulfate. The uptake of sulfate by the roots and its transport to the shoot seem to be one major site of regulation of sulfur assimilation. In *A. thaliana* and *B. napus* 14 sulfate transporter genes have been identified which are subdivided into five different groups with different affinities to sulfate and located in different organs and organelles (Hawkesford and De Kok 2006; Parmar et al. 2007). The function and localization of the sulfate transporters of group three was long unknown. A recent study revealed that the transporter *Sultr*3;1 is located in the chloroplast enabling the sulfate uptake of chloroplasts (Cao et al. 2013). Furthermore, transcriptome analysis revealed a circadian regulation of this transporter in *A. thaliana* (Covington et al. 2008). Members of group four are known to be localized at the tonoplast enabling the efflux of sulfate out of the vacuole. It was already shown that the transporter *Sultr4;2* in *B. napus* was only expressed under sulfur-deficient conditions, thus playing a major role in the response to sulfur deficiency (Parmar et al. 2007).

Feeding experiments using $^{35}SO_4^{2-}$ showed that the incorporation of ^{35}S into reduced sulfur compounds in vivo was significantly higher in light than in the dark (Kopriva et al. 1999) in accordance with investigations on adenosine 5′-phosphosulphate reductase (APR), considered to be a key enzyme of sulfate assimilation in higher plants. The mRNA levels of all three APR isoforms showed a diurnal rhythm, with a maximum at 2 h after onset of light. In summary, in higher plants *APR* mRNA, APR activity and *in vivo* sulfate reduction change with a diurnal rhythm, sulfate assimilation also takes place during the dark period, and sucrose feeding positively affects *APR* mRNA expression and APR activity in roots (Kopriva et al. 1999).

The first stable sulfur-containing compound in the sulfur assimilation cysteine acts, besides its role in the protein synthesis, as a precursor for essential biomolecules such as vitamins and cofactors. A small portion of the cysteine content is used for the biosynthesis of the tripeptide glutathione (GSH) (Hawkesford and De Kok 2006). Sulfur is also present in secondary compounds, i.e. glucosinolates (GSLs). GSLs play an important role in the response to biotic stress, especially in the defense against herbivores (Mithöfer and Boland 2012). In recent years their role in abiotic stresses such as salinity, drought, extreme temperatures, light cycling, and nutritional deficiency have been discussed (Boestfleisch et al. 2017). Previous studies revealed a circadian regulation of genes involved in the biosynthesis of GSLs (Kerwin et al. 2011).

There is emerging evidence for a relationship between the nutrient status and circadian rhythm in plants (Haydon et al. 2015). However, a direct interaction of the circadian clock and the sulfur status was not analyzed in detail so far. A number of key genes in metabolic pathways including the sulfur metabolism have been reported as circadian-regulated in *A. thaliana* (Harmer et al. 2000). In order to analyze the effect of sulfur availability on the circadian rhythm, two sulfur concentrations were chosen based on previous studies. Sulfur sufficient control plants received 1 mM $MgSO_4$ based on the studies of Blake-Kalff et al. (1998). Previous experiments revealed 10 µmol $MgSO_4$ to be ideal to study the effect of sulfur deficiency in plants by meeting their minimal sulfur needs and keeping plants alive (Weese et al. 2015). So far, diurnal and circadian changes in sulfur metabolism have only been described in *A. thaliana*, lacking essential insight into important crop plants like *B. napus*. Understanding the pattern in which sulfur is assimilated and sulfur-containing metabolites are synthesized is essential to be able to optimize sulfur fertilization, which in turn would maximize crop resistance to biotic stressors and tolerance to abiotic changes.

Results

Establishment of a Highly Controlled Cultivation System and Investigation of the Role of Sulfur in a Circadian-regulated System by Expression Analysis

For investigating the interaction of the circadian clock and sulfur metabolism a suitable cultivation system had to be established. Clock-controlled genes as well as genes involved in sulfate transport and assimilation were analyzed by Northern blot analysis (Fig. 1; Fig. S1). For analyzing the expression data in a quantitative way, results of Northern blot analysis were normalized according to Rumlow et al. (2016) with a validated set of reference genes (Fig. 1A; Table 1). It was demonstrated before that whereas RT-qPCR is currently the most used method to perform gene expression analysis, it

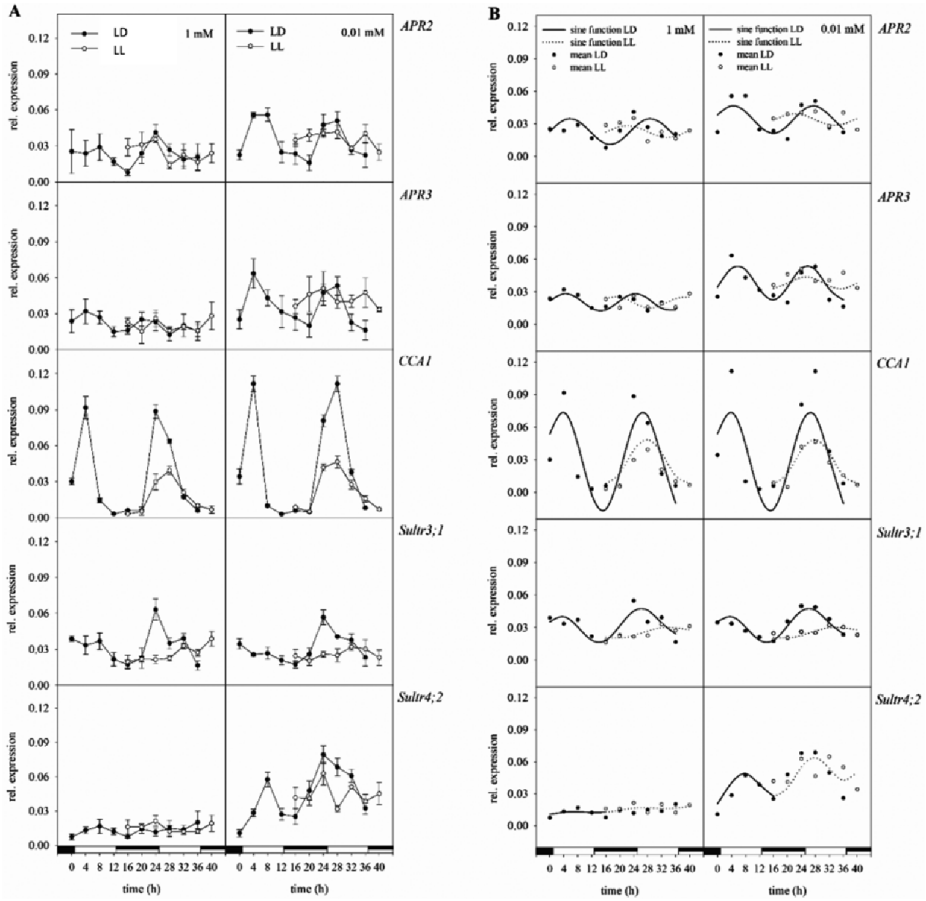

Fig. 1. Expression of GOIs under circadian and sulfur-deficient conditions. Transcript amounts were determined in above ground plant material of plants (with five fully expanded leaves) grown using 1 mM $MgSO_4$ (+S) as a control and 0.01 mM $MgSO_4$ (-S) for four days to obtain S-deficient conditions. Plants grown under 12 h dark/12 h light (LD, closed circles) were harvested over a period of 36 h every 4 h starting 1 h before the onset of light. In addition, plants grown in a chamber with 24 h light (LL, open circles) were parallely harvested beginning at 16 h and ending at 40 h fulfilling a 24 h rhythm. Three plants per treatment and harvest time point were pooled. Total RNA was isolated, and for Northern blot analysis 15 µg RNA was electrophoretically separated and transferred onto membranes. For the detection DIG labeled probes were used. (A) Normalization of the GOIs with a validated set of reference genes under LD and LL conditions as described and documented in detail in Rumlow et al. (2016). Data are shown as the mean of three technical replicates SD. Relative expression calculation was based on band intensity. (B) Sine functions of the oscillations for the GOIs together with the according mean from the three technical replicates under LD and LL conditions. Abbreviations for probes see Table 1.

was shown that similar results can be obtained using Northern blot analysis. However, a set of suitable reference genes is essential to guarantee a confident evaluation of gene expression analysis (Rumlow et al. 2016). To check the stability of the cultivation system, the expression of *B. napus CCA1* gene was analyzed (Fig. 1A). Its expression pattern in light/dark (LD) conditions showed a maximum of expression in the light phase and remained undetectable at night. Regarding the sulfur fertilization, data revealed a statistically significant difference ($p<0.0001$) in the transcript level of *CCA1*, with the highest value under sulfur-deficient conditions (Table S1). In samples from plants harvested under light/light (LL) conditions the expression pattern remained the same. Moreover, the interaction effect between the three factors is statistically significant ($p<0.0001$) (Table S1). Consequently, the transcript level of the variable *CCA1* may depend on the

Table 1. Primer pairs used in this study. To identify homologous genes in *B. napus*, the known sequences from *A. thaliana* genes were used to search the *B. napus* database using the BLAST program. s, sense; as, antisense; for, forward; rev, reverse; f, forward; r, reverse. *BoST, BRASSICA OLERACEA SULFATE TRANSPORTER; CCA1, CIRCADIAN CLOCK ASSOCIATED1; APR, ADEONOSINE 5'-PHOSPHOSULFATE REDUCTASE; 18S rRNA, 18S RIBOSOMAL RNA; PP2A, SERINE/THREONINE PROTEIN PHOSPHATASE 2A; GDI1, GUANOSINE NUCLEOTIDE DIPHOSPHATE DISSOCIATION INHIBITOR 1*

Primer pairs	*A. thaliana* AGI	Sequences
P216BoST3;1s	At3g51895	5'-TTCTTGTGGCTCGAACACTCCT-3'
P217BoST3;1as		5'-GCCTTACATGTCAACAGCTCTC-3'
P226BoST4;2s	At3g12520	5'-GGTCTTTGACGTGTGAAGCATG-3'
P227BoST4;2as		5'-GTGTACGCTTCTGGATACTGC-3'
P741_Bn_CCA1_for	At2g46830	5'-TTCTTGTGGCTCGAACACTCCT-3'
P742_Bn_CCA1_rev		5'-GGATTGGTGTTGCTGATGACTC-3'
P743_BnAPR2_for	At1g62180	5'-CAAGAAGGAAGATGACACCACC-3'
P744_BnAPR2_rev		5'-GCGAATCGACATCTCTATGCTC-3'
P745_Bn_APR3_for	At4g21990	5'-CATCAAGGAGAACAGCAACGCA-3'
P746_Bn_APR3_rev		5'-TCGGGAACACTAGTATCGTCGG-3'
P782_Bn_18S rRNA_for	X16077.1	5'-ATGAACGAATTCAGACTGTG-3'
P783_Bn_18S rRNA_rev		5'-ACTCATTCCAATTACCAGAC-3'
P968_Bn_PP2A_f	At1g69960	5'-ACGAGGACGGATTTGGTTCC-3'
P969_Bn_PP2A_r		5'-GCTCCGAGCTTGTCATCGAA-3'
P984_Bn_GDI1_f	At2g44100	5'-TGCACGTTTCCAAGGAGGTT-3'
P986_Bn_GDI1_r		5'-CGGTCTGAGGGTTGTCAGTC-3'

sulfur status, time point of harvest as well as the light conditions.

To be able to follow the sulfur status in the plants the sulfate transporter *Sultr4;2*, was included into the investigation. Plants grown in our experimental system showed a significant up-regulation of *Sultr4;2* when supplied with 0.01 mM $MgSO_4$ indicating a successful application of sulfur limitation (Fig. 1A). However, the transcript levels fluctuated in the course of a day with the highest transcript levels in the middle of the light phase. The expression of *Sultr4;2* was not significantly influenced by light conditions. Furthermore, the influence of the sulfur status on the expression seems independent from the light (Table S1).

Northern blot analysis of *Sultr3;1* in plants grown under sufficient sulfur supply showed a notable up-regulation under LD conditions for approximately 8 h beginning 1 h before the onset of light. Followed by a considerable decrease in the transcript level, transcript amounts were maintained at a lower level in the dark phase and were increased again at 24 h (Fig. 1A). At 28 h transcript amounts of *Sultr3;1* were 2-fold higher compared to the measured transcript amount at 4 h. Regarding the sulfur status there was no significant influence on the expression of *Sultr3;1* detectable. A *p*-value of 0.6414 was calculated for the factor sulfur supporting the independence of the *Sultr3;1* expression from the sulfur status. In LL conditions analysis of the transcript levels resulted in a significant decrease in the subjective night compared to LD conditions. Furthermore, the transcript maximum of *Sultr3;1* was detected 8 h later than in plants grown under LD conditions. There is a highly significant interaction of light and the harvesting time point independent from the sulfur status (Table S1).

Furthermore, the expression of members of the *APR* gene family was analyzed (Fig. 1A). The expression of the *APR2* gene oscillated for both sulfur regimes in plants harvested under LD conditions during the course of a day with an up-regulated expression in the light phase. In plants grown under sulfur-deficient conditions transcript amounts of *APR2* were considerably higher in the light phase compared to plants grown under sufficient sulfur supply. The highest transcript amounts were measured in the beginning and in the middle of the light phase, respectively. In plants harvested under LL conditions the oscillations detected in the transcript levels of *APR2* were significantly affected by the light dependent on the time point the plants were harvested (Table S1). For the second isoform *APR3* expression analysis in the plants harvested under LD conditions resulted in nearly the same oscillations when compared to *APR2.* Sulfur-deficient conditions led to a significant increase in the transcript amount measured in the plants (Table S1). The oscillations in the transcript level of *APR3* in sulfur-deficient plants was much more pronounced compared to those grown under sufficient sulfur supply. Analysis of the expression of *APR3* in plants harvested under LL conditions showed a shift in the expression pattern which was highly dependent on the sulfur status. Only in plants grown under sulfur-deficient conditions the up-regulation began 4 h earlier in LL conditions compared to the expression in LD conditions. Comparing both isoforms, the expression of *APR3* was more influenced by the LL conditions.

As all transcripts oscillated diurnally with an upregulation in the light phase, the wavelength of the rhythmic oscillation was determined using AICc selection based on a set of candidate models with trigonometric functions representing different wave lengths (see Statistical analysis for more information) for each GOI, respectively (Fig. 1B). Oscillations for the isoform *APR2* showed a 23 h rhythm under LD as well as under LL conditions, whereas for the latter one a lowered amplitude and an advanced phase (shifts earlier in time) was shown. For *APR3* oscillations comprise only of a 20 h period and the amplitude under sulfur-deficient conditions was increased. Under sulfur-deficient conditions an advanced phase was shown. For the clock gene *CCA1* periodic oscillations of 23 h were determined. The amplitudes in the oscillations were unaffected by the sulfur status. Under LL conditions a delayed phase (shifts later in time) was shown. For the sulfate transporter *Sultr3;1* oscillations in the transcript level followed a 23 h rhythm. The amplitude was unaffected by the sulfur status but lowered under LL conditions and showed a delayed phase of 4 h. For the second transporter *Sultr4;2* the model of a 20 h rhythm was determined. In plants under sufficient sulfur supply the amplitudes of the oscillations were very low compared to the amplitudes of the oscillations under sulfur-deficient conditions. As the expression was unaffected by light no differences in the amplitude between LD and LL conditions were observed.

Metabolic Analysis of Sulfur-containing Compounds in a Circadian-regulated System

Measurements of Total Sulfur Amounts in Leaves

Previous results indicated changes of the total sulfur content during the day (Weese et al. 2015). To understand the influence of the light period on the total sulfur content in the leaves, dried material was analyzed by ICP-OES. In addition, the effect of the sulfur treatments could be followed. The total sulfur content in plants grown under 1 mM sulfur supply and LD conditions showed slightly varying amounts during light and dark phases (Fig. 2; Table S1). In plant material harvested from plants grown under sulfur-deficient conditions the sulfur content was significantly decreased reaching 2.7 mg g^{-1} DM at 36 h (Table S1). Furthermore, the measured content was maintained at relatively constant levels in the plants harvested under LD conditions. Under LL conditions the sulfur content measured in the plants decreased irrespective of the sulfur status (Table S1). In the plant material from plants grown under sufficient sulfur supply and harvested under LL conditions the sulfur content decreased by up to 4.4 mg g^{-1} DM in the course of the day. For both sulfur regimes and light conditions variations in the content did evidently not follow a rhythmic pattern over time.

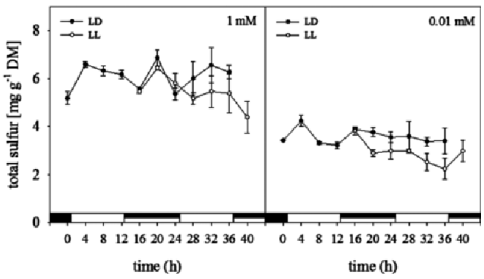

Fig. 2. Total sulfur under circadian and diurnal conditions. The elemental sulfur was measured in dried above ground plant material (DM) of plants treated as described in Fig. 1 with ICP-OES. Results calculated as mg g^{-1} DM represent the mean of only two technical replicates ± SD due to limited amount of plant material.

Determination of Sulfate Levels in the Leaves of *B. napus* Plants

As the expression of the sulfate transporters *Sultr3;1* and *Sultr4;2* showed oscillations in the course of a day (Fig. 1), the sulfate contents measured in plants grown with sufficient sulfur supply oscillated with maxima of approximately 5 mg g^{-1} DM 1 h before the onset of light and 1 h before the offset of light (Fig. S2; Table S1). Lowest amounts of sulfate were measured in plants harvested in the dark phase with 3.5 mg g^{-1} DM. In plants grown under sulfur-deficient conditions the measured sulfate content decreased in the light phase from 3.6 to 2.1 mg g^{-1} DM. After an increased content measured in the plants harvested in the dark phase the content of sulfate was further decreased down to 1.3 mg g^{-1}. For both sulfur regimes the measured sulfate amounts in the plants were significantly decreased under LL conditions which was highly dependent on the sulfate status and the time point of harvest (p-value < 0.0001), respectively (Table S1). With a decrease of 60% of sulfur in plants grown under sufficient sulfur in LL conditions the decrease was more drastic compared to plants grown under sulfur deficient conditions. In conclusion, the interaction of all three factors influencing the sulfate content in the plants was highly significant (p-value 0.0001; Table S1).

Cysteine and Glutathione Contents in Leaves

Due to its importance as key molecule in the primary sulfur assimilation pathway the cysteine content and the GSH content as the most important transport molecule of reduced sulfur were analyzed via HPLC (Fig. 3). The cysteine concentrations measured in plants grown with 1 mM $MgSO_4$ and harvested under LD conditions were higher during the day with a maximum of approximately 20.6 nmol g^{-1} FM

than at night with a minimum of about 11 nmol g^{-1} FM (Fig. 3A). Under sulfur-deficient conditions measurements of cysteine resulted in significantly lower contents with a minimum of approximately 9.9 nmol g^{-1} FM without any discernable oscillations in the course of a day. The content of reduced GSH measured in plants grown with 1 mM $MgSO_4$ oscillated diurnally in the course of a day with high amounts up to 560 nmol g^{-1} FM at the end of the light phase and significantly lower amounts of 240 nmol g^{-1} at the end of the dark phase (Fig. 3B). The decrease of the GSH measured in plants grown under sulfur-deficient conditions was highly significant with a *p*-value of 0.0002 (Table S1). With a maximum of approximately 403 nmol g^{-1} FM in the light phase and a minimum of 269 nmol g^{-1} FM the measured contents oscillated as well in the course of a day. Regarding the third factor "light" the GSH content measured in the plants harvested under LL conditions was significantly influenced dependent on the time points the plants were harvested. In agreement with the diurnal oscillations of the GSH content periodic oscillations with a period of 23 h was determined (Fig. 3C). The amplitude in LL conditions was lowered for both sulfur regimes. Under sulfur-deficient conditions an advanced phase could be observed. To summarize the results for the thiols, cysteine was only affected by the sulfur status and showed no oscillations in its content. The GSH content in contrast was influenced by all three factors. The factor that influenced the oscillations of the GSH content most was the time point the plants were harvested.

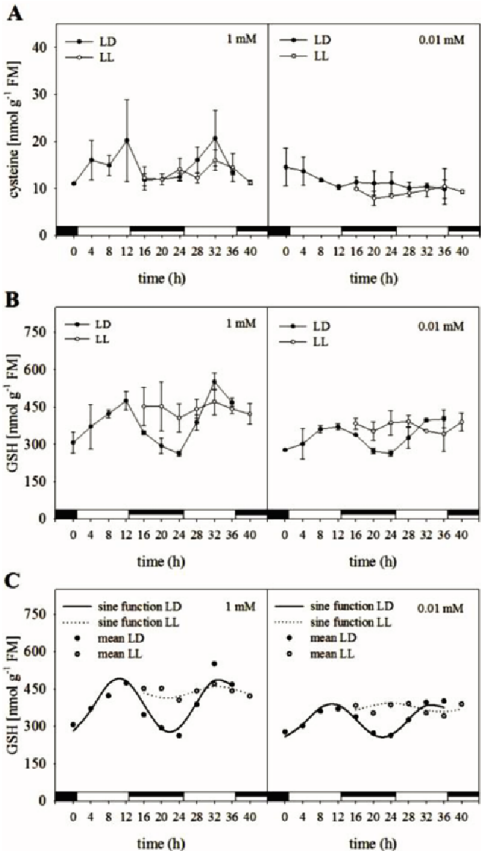

Fig. 3. Thiol contents under circadian and diurnal conditions. Cysteine (A), GSH (B), the sine function of the periodic oscillations with the corresponding mean (C). The cysteine and GSH contents were determined in above ground plant material of plants treated and collected as described in Fig. 1 by HPLC. Data in nmol g^{-1} FM represent the mean of three technical replicates ± SD.

Quantification of GSLs in Leaves

As representatives of the secondary sulfur metabolism intact GSLs were measured as desulfated GSLs in the leaves (Fig. 4; Fig. S3; Fig. S4). Taking all aliphatic GSLs together the measured content in plants grown with sufficient sulfur supply and harvested under LD conditions was maintained from 0 to 12 h at approximately 0.7 µmol g^{-1} DM (Fig. 4A). This was followed by a substantial increase in the content of aliphatic GSLs up to 1 µmol g^{-1} DM in the beginning of the dark phase (Table S1). After a slight decrease in the content in plants harvested later in the dark phase the content reached 1 µmol g^{-1} DM again 1 h after the onset of light. Afterwards the measured content of the aliphatic GSLs in the plants was decreased by 20% at 32 h and increased up to 0.9 µmol g^{-1} DM again at 36 h. The content of the aliphatic GSLs was significantly decreased in plants grown under sulfur-deficient conditions (Table S1) and the pattern in the oscillations in the content was slightly shifted, but more pronounced. Considering the third factor light the content of the aliphatic GSLs was significantly influenced independent of the sulfur status (Table S1). Under sufficient sulfur supply the amount of aliphatic GSLs measured in plants harvested under LL conditions was lower in the subjective night at 16 and 20 h compared to plants harvested under LD conditions. In plants grown under sulfur-deficient supply and harvested under LL conditions the content of the aliphatic GSLs was significantly lower compared to plants harvested under LD conditions without any oscillations (Table S1). Regarding the individual aliphatic GSLs nearly the same pattern in the oscillations could be observed except for glucoraphanin (Fig. S3). The oscillations in the content of the individual aliphatic GSLs were highly dependent on the sulfur status (*p*-value < 0.0001) (Table S1). Interestingly gluconapin and glucoraphanin were not significantly influenced by the light independent from

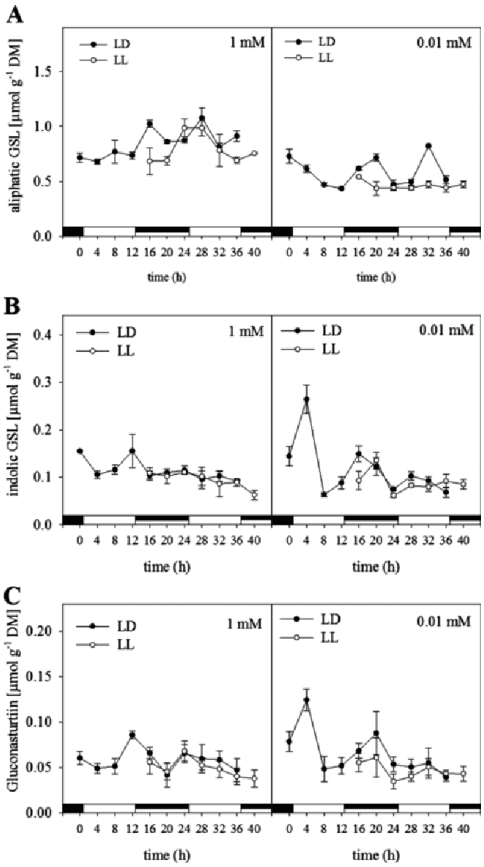

Fig. 4. GSLs in leaves under diurnal/circadian conditions. Aliphatic (A) and indolic GSLs (B) as well as one aromatic GSL (C) were measured by HPLC in above ground plant material of plants treated and collected as described in Fig. 1. The contents of the GSLs were calculated in µmol g^{-1} DM. Data represent the mean of three technical replicates ±SD.

the sulfur status and the time point the plants were harvested.

In plants grown under sufficient sulfur supply and harvested in LD conditions, the highest concentration of the indolic GSLs with 0.15 µmol g^{-1} DM was measured at 0 h and 12 h respectively (Fig. 4B). Afterwards the content was decreased down to approximately 0.1 µmol g^{-1} DM and maintained at this level. Although the content of the indolic GSLs was not considerably decreased in plants grown under sulfur-deficient conditions an altered pattern in the oscillations was observed (Fig. 4B). A maximum of approximately 0.25 µmol g^{-1} DM was measured in plants harvested three hours after the onset of light. Afterwards the content was decreased by about 70% in plants harvested at 8 h. In the beginning of the dark phase the content of the indolic GSLs was increased again to 0.15 µmol g^{-1} and decreased to 0.1 µmol g^{-1} DM at the end of the dark phase. In plants harvested in LL conditions the content of the indolic GSLs was not influenced in a considerable way independent of the sulfur status and the time point the plants were harvested (Table S1). Comparing the two GSLs glucobrassicin and neoglucobrassicin representing the indolic GSLs, for the former one oscillations were higher in the course of the day (Fig. S4).

The only aromatic GSL measured in *B. napus* was gluconasturtiin (Fig. 4C). In plants grown with sufficient sulfur supply and harvested under LD conditions a content of approximately 0.06 µmol g^{-1} DM was measured 1 h before the onset of light. The decrease in the content down to 0.05 µmol g^{-1} DM measured in plants harvested at 4 and 8 h was followed by a notable increase up to 0.085 µmol g^{-1} DM 4 h later. In the middle of the night phase the content of gluconasturtiin was decreased by 50%. Already 4 h later the measured content was increased again up to 0.065 µmol g^{-1} DM. At the end of the light phase the content in the plants was decreased by 30%. The sulfur-deficient conditions led to no significant decrease in the content of the aromatic GSL, whereas the pattern of the oscillations in the content in plants harvested under LD conditions was altered with higher contents at 4h and 20 h. The oscillations of gluconasturtiin in both sulfur and light regimes are very similar to the oscillations of indolic GSLs. Regarding the third factor light the content of gluconasturtiin in the plants was affected in a significant way independent from the sulfur status (Table S1). In plants grown with sufficient sulfur supply and harvested under LL conditions the content was decreased by 50% between 24 and 40 h. In plants grown under sulfur-deficient conditions the content of gluconasturtiin was much lower compared to plants harvested under LD dark conditions (Table S1). Interestingly, all GSL groups do not show clear oscillations when supplied with sufficient sulfur, whereas under sulfur deficient conditions oscillations in the content occurs in all GSL groups with the indolic and aromatic ones showing more pronounced amplitudes. For the indolic and aromatic GSLs the amplitude of the oscillation in sulfur deficient plants is the highest at the first morning in the harvest period getting smaller over time. The frequency of the oscillation remains the same over the harvest period. To summarize the measurements of the GSLs in *B. napus* the oscillations in the content of the GSLs were dependent on the sulfur status. Only the aliphatic GSLs were reduced in their content under sulfur-deficient conditions. Furthermore, only for the indolic GSLs the content was unaffected by the circadian conditions.

Discussion

Investigating Circadian Aspects of Sulfur Metabolism in *B. napus* in a Reproducible Way by Establishing a Suitable Growth System is Possible

For analyzing the influence of the circadian clock on the biosynthesis of sulfur-containing metabolites a highly controlled growth system had to be established. By analyzing the expression of the clock gene *CCA1* as a regulatory element of the core oscillator of the circadian clock stability of the cultivation system was verified. The expression was analyzed in plants collected every 4 h over a period of 40 h under diurnal conditions with 12 h light and 12 h dark as well as under free-running conditions with 24 h continuous light, respectively (Fig. 2; Fig. S1). The expression pattern from Northern blot analysis of *CCA1* in *B. napus* is switched to early expression with a peak at ZT4, probably due to the 12 h light/ 12 h dark rhythm but the overall pattern is comparable to the pattern in other plant species (Mizoguchi et al. 2002; Harmer 2009) indicating a suitable cultivation and harvest pattern. The amplitude under constant light was significantly lowered similar to results obtained by transcriptome analysis of *CCA1* in *A. thaliana* (Mockler et al. 2007). In the study of Kim et al. (2003) it was discussed that light may influence the activity of a positive effector of *CCA1* and *LHY* leading to an altered amplitude of the transcript level. As a possible candidate they named the TOC1 protein as it showed interactions with a phytochrome B-related transcription factor protein. On the basis of the expression analysis it was possible to verify a circadian period of 23 h for *CCA1* in *B. napus.* Comparable to this study the "zeitgeber" was light, a circadian period of 24 h would be assumed. It was already demonstrated in *A. thaliana* and *Brassica rapa* that shortening of the period is dependent on the temperature (Kusakina et al. 2014). Plants grown under 17°C showed a circadian period around 24 h whereas under 27°C the period was shortened down to 20 h. It is postulated that a shorter period at higher temperatures may confer a performance advantage. Therefore, it can be suggested that the circadian period of the clock with 23 h in *B. napus* is more beneficial when grown at a temperature of 22°C.

Furthermore, half of the plants were grown under sulfur-deficient conditions for 4 d. This was done to determine a possible influence of sulfur limitation on the circadian clock in the first place. There are indeed a number of nutrients which are influenced by the circadian rhythm and vice versa (Haydon et al. 2015). The nitrogen metabolism in *A. thaliana* is regulated by *CCA1* which binds to the promoters of nitrogen-assimilation genes (Gutiérrez et al. 2008). In our study this was not the case as the period of *CCA1* was unaffected by sulfur-deficient conditions. Therefore, it can be concluded that in our study the given conditions have no influence on the expression of clock transcripts. Therefore, to verify the sulfur deficiency in the plants the expression of the sulfate transporter *Sultr4;2* was analyzed (Fig. 2) which is predominantly detectable under sulfur-deficient conditions (Buchner et al. 2004). In plants grown under sulfur-sufficient conditions low amounts of transcripts were detected. One explanation would be that the supply of 1 mM $MgSO_4$ was not enough for a fully sufficient supply. Another explanation would be that a high degree of excessive sulfate triggered the up-regulation of the transporter. Thus, the efflux of the sulfate out of the vacuole is triggered preventing an over-accumulation of sulfate (Kataoka et al. 2004; Reich et al. 2017). In plants grown with 0.01 mM $MgSO_4$ the expression of *Sultr 4;2* was up-regulated. This was also confirmed in previous studies with *B. napus* where this transporter was up-regulated under sulfur-deficient conditions (Buchner et al. 2004; Parmar et al. 2007; Weese et al. 2015).

The Sulfate Transport Is Differently Affected by the Diurnal and Circadian Conditions

In previous studies the expression of all members of the sulfate transporters in the four groups in *Brassica oleracea* and all members of the five groups in *B. napus* under sulfur deprivation were analyzed in detail (Buchner et al. 2004; Parmar et al. 2007). In *B. oleracea* the sulfate transporter *Sutlr3;1* was expressed in the stem and roots independent from the sulfur supply of the plants. However, in leaves the expression of this transporter was only up-regulated under sulfur deprivation lasting at least 10 d (Buchner et al. 2004). Interestingly, in the study by Parmar et al. (2007) the expression of the transporter *Sultr3;1* could not be detected at all in the leaves of *B. napus* plants. This is in contrast to our results as the transporter was expressed at a relatively high level independent from the sulfur status (Fig. 2). Furthermore, transcript levels oscillated under diurnal and circadian conditions with a period of 23 h whereas under free-running conditions the amplitude was decreased and delayed in the phase. As the period matches the period of *CCA1* and remained the same in LL conditions a regulation by the circadian clock can be assumed. This is even further supported as in *A. thaliana* the transporter *Sultr3;1* contains an evening element promoter motif (EE) (http://arabidopsis.med.ohio-state.edu/) where CCA1 can directly bind and regulate the expression (Harmer et al. 2000; Nagel et al. 2015). Genes with this motif are likely to be expressed in the evening as binding of CCA1 in this promoter region enhances the expression. Therefore, one would expect a down-regulation in the expression of *Sultr3;1* in the morning and an up-regulation in the evening. This is contradictory to our results, as the expression was up-regulated in the morning and down-regulated in the

evening (Fig. 2A, B). However, our results for the expression of *Sultr3;1* are in agreement with microarray analysis in *A. thaliana* under different light conditions (Mockler et al. 2007). In the study by Nagel et al. (2015) a number of target sequences for CCA1 close to the EE were genome-wide identified in *A. thaliana* revealing a morning-phased expression. Based on that it can be assumed that the sequence of the *Sultr3;1* in *B. napus* contains no EE and instead one of the other targets, thus leading to a peak of the expression in the beginning of the light phase. This is confirmed by our results as the transcript levels peak in the beginning of the light phase when *CCA1* was up-regulated as well. Confirming a regulation by the circadian clock one would assume that under continuous light oscillations of the transcript levels of *Sultr3;1* would be unaffected. However, in this study the amplitude was lowered and a delay in the phase occurred. A possible explanation could be the transcript amount of *CCA1* which was significantly decreased under free-running conditions. Thus, the amplitude in the beginning of the light phase for the transcript level of *Sultr3;1* was decreased as well. Nonetheless there is evidence that sulfur uptake in chloroplasts is regulated by the clock due to the circadian-regulated sulfate transporter 3;1 which is localized at the chloroplast membrane (Haydon et al. 2011; Cao et al. 2013). It is postulated that other members of group 3 transporters are also located at the chloroplast membrane (Cao et al. 2013). Therefore, expression analysis of the other members would be helpful for confirming a circadian-regulated uptake into the chloroplast.

The expression of *Sultr4;2* was predominantly analyzed as detection for the sulfur limitation (Fig. 2). Diurnal oscillations of the transcript levels under sulfur-deficient conditions were detected and were unaffected under free-running conditions in the subjective night. Based on that one could assume a regulation by the circadian clock. However, as the expression of the group 4 transporters is probably solely regulated by a sulfate gradient at the tonoplast a direct circadian regulation is likely to be ruled out (Kataoka et al. 2004; Reich et al. 2017).

The Isoforms of the Key Enzyme in the Sulfate Reduction are Affected Differently in *B. napus* under Diurnal and Circadian Conditions

As key enzymes of the sulfate assimilation pathway the expression of two isoforms of the adenosine-5'-phosphosulfate (APS) reductase (APR) was analyzed (Fig. 2). According to sequence analysis by using BLAST all three isoforms present in *A. thaliana* are also present in *B. napus.* As in the study by Kopriva et al. (1999) *APR1* and *APR3* showed a similar expression, for our study only the isoform *APR3* was included in the expression analysis in addition to *APR2*. For both isoforms transcript amounts oscillated diurnally with higher transcript amounts in the light phase under sulfur-sufficient as well as under sulfur-deficient conditions. This is in accordance with the expression of *APR* in *A. thaliana* and maize, oscillating diurnally with a maximum during the light period (Kopriva et al. 1999). Under sulfur-deficient conditions the amplitude of the oscillations increased. The periodic oscillations in the transcript level of *APR2* comprised 23 h with a peak in the morning phase which is equal to the period of *CCA1*, thus supporting a regulation by the circadian clock. Under free-running conditions oscillations of 23 h were observed whereas the amplitude was lowered and showed an advanced phase with a peak in the subjective night. In the case of *APR3* oscillations lasted only 20 h. The amplitude was lowered by the continuous light and an advanced phase appeared under sufficient sulfur supply. In the study of Kopriva et al. (1999) the regulation of *APR* expression and APR activity by an endogenous rhythm was ruled out as mRNA levels of all three isoforms decreased in continuous dark. However, it was already reported that the expression of *APR2* is under circadian control in *A. thaliana* (Harmer et al. 2000) which is in accordance with the presence of the EE in the sequence of *APR2* (http://arabidopsis.med.ohio-state.edu/). As already described for *Sultr3;1* genes with an EE are likely to peak in the night. This is in agreement with the results from the microarray analysis in *A. thaliana* as highest transcript amounts were measured in the night and lowest in the day, respectively, independent of the given light conditions (Mockler et al. 2007). As *APR2* transcripts contribute 75% of the APR activity in *A. thaliana* one could assume that the APR activity would show the same oscillations. However, in previous studies APR activity had only been shown to undergo a diurnal rhythm in plants adapted to short days; when plants were grown in long days APR activity was again higher during the light period than in the dark, but without the strong maximum observed under short days (Huseby et al. 2013). It remains remarkable that the expression of *APR2*, *APR3*, and *Sultr3;1* under LD conditions has been drastically delayed in LL conditions. In summary, the results obtained in our study are contradictory for *APR2* regarding the circadian regulation thus making a proper conclusion difficult. Future experiments will be necessary to better understand the regulation of the expression of all gene isoforms involved in sulfur metabolism.

Is There a Circadian Regulation in the Transport and Reduction of Sulfate?

In this study the aim was to determine whether the transport and the reduction of sulfate might be under circadian control. For investigating an influence by the circadian clock, the light was chosen as "zeitgeber". Plants grown with sufficient sulfur supply as well as with sulfur-deficient supply were

entrained to a 12 h light/dark rhythm. By exposing part of the plants to continuous light the external cue was absent. Under these conditions circadian regulated genes should show the same oscillations as under diurnal conditions. Except for *Sultr4;2* oscillations in the transcript levels of the analyzed GOIs showed lowered amplitudes and in some cases an advanced or delayed phase, whereas the period of the oscillations under these conditions remained the same. (Fig. 2B). Nevertheless, a circadian regulation could not be unambiguously determined. It can only be assumed that there might be a regulation by the circadian clock as the transporter *Sultr3;1* and *APR2* oscillate in the same period as *CCA1* with a peak in the morning under diurnal conditions. Therefore, a direct interaction of CCA1 with the target genes by binding to specific binding motives might be possible (Nagel et al. 2015).

However, under LL conditions there was a shift in the phase and a lowered amplitude by up- or down-regulation even though the period of the oscillations remained the same. Potential targets of CCA1 were identified genome-wide in *A. thaliana* by ChipSeq analysis under LD and LL conditions (Nagel et al. 2015). A large portion of the putative target genes were non-cycling under LL conditions. It was discussed that this might be stress-related as plants were not expecting light in the night and consequently did not cycle in LL conditions (Velez-Ramilez et al. 2011). As a response to the LL induced stress the generation ROS might be triggered. As GSH is involved in the detoxification of ROS (Noctor et al. 1997) it is likely that under LL conditions GSH accumulates in the plants thus leading to an altered activity of the enzymes involved in the sulfur assimilation as here the precursor for GSH cysteine is formed. It was shown in *A. thaliana* that the sulfate transport is negatively regulated by GSH thus leading to a decrease in the expression (Vauclare et al. 2002) which would be an explanation for the down-regulation of *Sultr3;1* under LL conditions. Based on that a possible regulation of the sulfur assimilation by the clock might be underestimated by the use of LL. As the sulfur assimilation is dependent on the reducing equivalents produced in the photosynthesis, which is circadian regulated, a regulation by the circadian clock especially for the transport into the chloroplast is plausible (Harmer et al. 2000).

Measuring the total sulfur content in addition to the detection of the sulfate transporter *Sultr4;2* was a second way to detect sulfur deficiency in plants. *Brassica napus* plants with a sulfur content of 3.5 mg sulfur g^{-1} DM are considered to suffer deficiency (Scherer 2001). This is in accordance with the data obtained in our study (Fig. 3). Following the total sulfur content in the course of a day, can give first information on the regulation of the sulfur metabolism. The total sulfur content showed variations in the course of the day, however, statistical analysis showed diurnal oscillations are unlikely. As sulfate-sulfur comprises the biggest portion of the total sulfur in plants (Blake-Kalff et al. 1998) it was not surprising that the content did not oscillate diurnally (Fig. S2). Interestingly, under constant light the sulfate-sulfur content and consequently the total sulfur showed a decrease. The lower contents of sulfate might be due to a stress response induced by the LL as mentioned before resulting in an increased use for the generation of GSH. In the period of 40 h the plants were harvested, sulfate and consequently total sulfur levels decreased which might be due to decreasing sulfate amounts in the sand the plants were grown in. It would have been necessary to measure the sulfate content and its decrease in the substrate which might have led to the decrease of sulfur in the plants.

Glutathione Shows Diurnal Oscillations

In previous experiments it was reported that the major sulfur-containing metabolite GSH, as representative of primary sulfur metabolism showed only minor or no fluctuation during a light/dark period. GSH levels were higher during the light period than in the dark, without a clear maximum. On the other hand, no diurnal changes in cysteine or GSH contents were observed in poplar (Noctor et al. 1997). In our study, GSH showed diurnal oscillations with a period of 23 h with a maximum at the end of the light phase (Fig. 3B, C). Same oscillations in the content of GSH could be observed in plants harvested in LL conditions, whereas the amplitude of the oscillations was lowered and a delay in the phase under sulfur-deficient conditions occurred. As mentioned before, this might be based on the continuous light plants were exposed to, as well as the stress caused by sulfur deficiency. As a consequence, ROS might have been accumulating which can oxidize GSH to GSSG and thus GSH synthesis or GSSG-reducing enzymes could have been up-regulated. This assumption needs to be verified by determining the accumulation of ROS in the plants harvested under LL conditions and sulfur-deficient plants. Nevertheless, one could assume that the GSH synthesis is regulated by the circadian clock, as there is a CCA1 binding site motif in *GSH1* (http://arabidopsis.med.ohio-state.edu/) catalyzing the first step of the GSH synthesis. The precursor of GSH, cysteine, was measured as well and no diurnal oscillations with a certain period were determined (Fig. 4A). In a study carried out by Huseby et al. (2013) it was demonstrated that the reduced sulfur is first incorporated in GSH and GSLs and at the end of the light phase in proteins thus it is not surprising that the content of cysteine as the source of the reduced sulfur was non-cycling.

Oscillation of GSLs is Affected by Sulfur Limitation

As representatives of the secondary metabolites the individual

GSLs were measured in the leaves by HPLC (Fig. 4; Fig. S3; Fig. S4). As the sulfur-containing amino acid methionine acts as the precursor for the biosynthesis of aliphatic GSLs those are more sensitive to sulfur deficiency than the indolic and aromatic GSLs (Mailer 1989). In agreement with our results after 4 d of sulfur-deficient conditions only the aliphatic GSL were significantly decreased in their content, whereas the indolic and the aromatic ones were unaffected in their content by the treatment. Regarding the oscillations of the content of the aliphatic, indolic and the one aromatic GSLs ultradian rhythms were shown which were altered under sulfur-deficient conditions. Ultradian rhythms show oscillations shorter than 20 h and were already reported to occur in plants for a number of processes such as glycolysis, sap flow, enzyme activity, root elongation, and leaf movements (Iijima and Matsushita 2011). As the oscillations in the content of all GSLs measured in our study were dependent on the sulfur status the ultradian rhythms might derive from the sulfur supply the plants were grown under. In plants harvested in LL conditions the oscillations in the content of the indolic and aromatic GSLs were maintained under both sulfur regimes indicating that the biosynthesis, degradation or both might be regulated by an endogenous mechanism which can be altered by the sulfur supply. The higher amplitudes of the content of indolic and aromatic GSLs in sulfur deficient plants indicates a stress response directly to sulfur deficient conditions. The biosynthesis and degradation of GSLs in an ultradian rhythm potentially generates breakdown products which could benefit the plant in stress situations. It was shown that allyl isothiocyanate the breakdown product of sinigrin leads to stomatal closure helping water loss in water deficient conditions (Khokon et al. 2011). Furthermore, the breakdown product indole-3-carbinol of the GSL glucobrassicin was shown to antagonize auxin and therefore decelerate growth (Katz et al. 2015). The known functions of breakdown products in addition to functions that have yet to be elucidated could help the plant to cope with stresses which are the result of low sulfur levels.

The rhythmic oscillations in the content of the aliphatic GSLs were absent under free-running conditions in plants grown under sulfur-deficient conditions. The content of aliphatic GSLs in the sulfur deficient plants was further reduced by LL conditions. It can be assumed that such low levels led to the loss of the rhythmic oscillations in the content of the aliphatic GSLs as the biosynthesis of the aliphatic GSL is more sensitive to sulfur-deficient conditions (Mailer 1989). Regarding the dependence of the oscillations in the content of the GSLs on the sulfur supply, the time of application of sulfur to the plants might also be a factor influencing the oscillations. So far only in the study by Rosa and Rodrigues (1998) ultradian oscillations in the content of GSLs in *B. oleracea* were reported. Diurnal oscillations in the content of the GSLs were already shown in *A. thaliana* (Huseby et al. 2013) where the total GSL content was increased during the day which is contradictory to measurements of the GLSs in *B. oleracea* as they accumulated in the night (Rosa and Rodrigues 1998). These different outcomes were reasoned due to different developmental stages of the plants. Nevertheless, for the GSL content in our study oscillations in the content were comparable to ultradian oscillations, which were highly dependent on the sulfur status.

Conclusions

A growth system for *B. napus* was established to investigate circadian aspects in the sulfur metabolism. In this study the circadian period of the clock in *B. napus* plants entrained to a 12 light/ 12 dark rhythm was 23 h, probably as an adaption to the temperature the plants were grown under. We were able to show diurnal oscillations of genes involved in the transport and reduction of the sulfate with a period comparable to that of *CCA1*. As under free-running conditions the amplitude was lowered and a shift in the phase was determined the circadian control could not be determined unambiguously. The same could be shown for the GSH content measured in the plants. The use of continuous light in this study might have underestimated circadian oscillations as it might have resulted in a stress response affecting the sulfur metabolism in the plants. The GSLs showed ultradian oscillations which were altered by the sulfur supply the plants were grown under. Probably the concentration of single GSLs is not regulated by the circadian clock but in an ultradian way. The analysis of mutants or transgenes in key genes in cysteine and GSH biosynthesis could clarify whether contents of sulfur-containing metabolites are only regulated by the circadian clock because they need reducing equivalents produced in photosynthesis or whether they act as signal molecules.

Material and Methods

Plant Material and Growth Conditions

Seeds from the MSL-hybrid (Male Sterility Lembke) winter oilseed rape cultivar Genie were obtained from the Deutsche Saatveredelung AG (DSV) (Lippstadt, Germany). The cultivar is very vital, has a medium-sized root system and has a high seed oil content in comparison to other cultivars from the DSV. For experiments under circadian and diurnal conditions, the seeds were germinated in a pot (diameter 8 cm) containing sand (0–2 mm grain size, Hornbach, Hannover, Germany) in a climate chamber [22°C, 70% humidity, 12 h light/12 h dark, 480 µmol m^{-2} s^{-1} (lamp type CMT 360LS/W/BH-E40, Eye Lighting Europe Ltd, Uxbridge, UK)]. A total of 102 plants were grown, one plant per pot, for 19 d and watered once per week using 150 ml Blake-Kalff medium (Blake-Kalff et al. 1998) containing 1 mM $MgSO_4$. After a washing step with deionized water one half of

the plants was transferred to "plus S" conditions with 1 mM $MgSO_4$. The other half of the plants was transferred to "minus S" conditions using Blake-Kalff medium with 10 μM $MgSO_4$. Plants were grown under these conditions for 4 days. One hour before the light was switched on, shoots of three plants of each treatment were harvested every 4 h over a time period of 36 h. The material was pooled and immediately frozen in liquid nitrogen. Additionally 42 plants under "plus S" and "minus S" conditions were transferred to continuous light. These were then harvested at the same time as the plants grown under 12 h light/12 h dark every 4 h beginning after 16 h representing the beginning of the subjective night. For a 24 h cycle plants under continuous light were additionally harvested at 40 h. The complete experiment was performed twice. Variations of experiment was performed, such the diurnal part or growth on soil instead of sand, were performed several times with the same outcome. Roots of plants were not harvested due to the sand media in which the plants were grown. Fine roots were breaking by removing substrate and analysis of GLS would have been inaccurate due to hydrolysis by myrosinases.

Sequence Analysis and Primer Design

Sequences homologous to *A. thaliana* DNA sequences for *APR2, APR3* and *CCA1* were searched for the primer design in the recently closed *B. napus* database (http://compbio.dfci. harvard.edu/compbio) using BLAST. The data bank used parts of short homologous sequences (high-fidelity virtual transcripts and tentative consensus sequences) to generate EST sequences (Quackenbush et al. 2000). For the primer pair design the program Dosbox with the Primer Design version 2.2 (Scientific & Educational Software, Cary, USA) was used (http://www.dosbox.com). To design the primer pairs for the amplification of cDNA fragments of sulfate transporters, the respective homologous sequences from *Brassica oleracea* were used (Buchner et al. 2004). The amplification of cDNA with the chosen primers generated fragments between 339 and 973 bp (Table 1).

Production of Probes and Northern Blot Analysis

Northern blot analysis was performed as described (Weese et al. 2015; Rumlow et al. 2016). Quantitative analysis of the Northern blot results was done by GelAnalyzer5 (http://www.gelanalyzer. com). Normalization of the genes of interests (GOI) was performed with a validated set of reference genes. All aspects for the identification and validation of suitable reference genes (*18S rRNA, 18S RIBOSOMAL RNA; PP2A, SERINE/THREONINE PROTEIN PHOSPHATASE 2A; GDI1, GUANOSINE NUCLEOTIDE DIPHOSPHATE DISSOCIATION INHIBITOR 1*) are described in detail in Rumlow et al. (2016) (Table 1).

Elemental Analysis, Sulfate Determination and Extraction and Analysis of Soluble Thiol Compounds

Elemental analysis was performed by ICP-OES according to Weese et al. (2015). Sulfate concentrations were analyzed by ICP-AES as described by Bloem et al. (2004). Determination of thiols was done by HPLC after derivatization with monobrombimane according to Riemenschneider et al. (2005).

Analysis of Glucosinolates

Samples were prepared as described by Boestfleisch et al. (2017) with some modifications. The content of GSLs was determined using 25 mg freeze-dried material. Glucosinolates were extracted twice with 1 ml 80% (v/v) methanol and centrifuged at 13,000 *g* for 5 min. Before the centrifugation, samples were put on a shaker for 15 min after the first extraction and 30 min after the second extraction at room temperature (RT). The supernatants were pooled and loaded onto a column (Polypropylene column, 1 mL) containing 2 ml of a 5% (w/v) suspension of DEAE Sephadex A25 (Sigma-Aldrich, Taufkirchen, Germany) in 0.5 M acetic acid (pH 5). Columns were washed five times with 2 ml H_2O and two times with 2 ml 0.02 M acetic acid (pH 5). For desulfating the GSLs 50 μl of sulfatase (Sigma-Aldrich) solution was added to 450 μl 0.02 M acetic acid (pH 5) and loaded on to the columns as well (Thies 1979). Desulfation took place over night at RT. Afterwards desulfated GSLs were eluted three times with 2 ml HPLC H_2O and dried overnight in a vacuum centrifuge, and then dissolved in a total amount of 300 μl HPLC H_2O. Analysis was performed with a high-performance-liquid chromatography (HPLC) system (Knauer, Berlin, Germany) equipped with an Ultra AQ C-18 column (150 × 4.6 mm, 5 μm particle size) (Restek GmbH, Bad Homburg, Germany). A water (solvent A)-acetonitrile (solvent B) gradient at a flow rate of 0.5 ml min^{-1} at 45°C (injection volume 50 μl) was as following: The 52 min long run consisted of 100% A for 6 min, 100-70% A for 27 min, 70-40% A for 0.1 min, a 4.9 min hold of 40% A, 40-100 % A for 0.1 min and a 19.9 min hold of 100% A. The detection of the GSL was performed with DAD and FAD (Knauer, Berlin, Germany) at 229 nm. Quantification of the measured GSL was performed by using sinigrin (Phytolab, Vestenbergsgreuth, Germany) as external standard and relative response factors (progoitrin, 1.09; glucoraphanin, 1.07; glucoalyssin, 1.07; gluconapin, 1.11; hydroxyglucobrassicin, 0.17; glucobrassicanapin, 1.15; glucobrassicin, 0.29; gluconasturtiin, 0.95; neoglucobrassicin, 0,2).

Identification of GSLs in *B. napus*

For the identification of the GSL in *B. napus* samples were analyzed by liquid chromatography–mass spectrometry (LC-MS). A volume of 10 μl was injected into the HPLC system (Shimadzu, Darmstadt, Germany) and separated on a Knauer Vertex Plus column (250 × 4 mm, 5 μm particle size, packing material ProntoSIL 120-5 C18-H) equipped with a pre-column Knauer, Berlin, Germany). A water (solvent A)-methanol (solvent B), both containing 2 mM ammonium acetate gradient was used with a flow rate of 0.8 ml min^{-1} at 30°C. For measuring the samples, the following gradient was used: 10-90% B for 35 min, 90% for 2 min, 90-10% B for 1 min and 10% B for 2 min. Detection of the spectra in the range 190-800 nm was performed with a diode array detector (SPD-M20A, Shimadzu, Darmstadt, Germany). The HPLC system was coupled to an AB Sciex Triple TOF mass spectrometer (AB Sciex TripleTOF 4600, Canby, USA). At a temperature of 600°C and an ion spray voltage floating of -4500 V the negative electrospray ionization (ESI) was performed. For the ion source gas one and two 50 psi were used and for the curtain gas 35 psi. In the range of 100-1500 Da in the TOF range the mass spectra as well as the MS/MS spectra from 150-1500 Da at a collision energy of -10 eV were recorded. Peaks were identified by analyzing the characteristic mass fragments of ds-progoitrin (195, 309, 344, 617), ds-glucoalyssin (195, 208, 371, 741) and ds-neoglucobrassicin (195, 208, 371, 741). Due to lack of standards of these GSLs fractions of the measured samples were collected in a fraction collector (FRC-10A Shimadzu, Darmstadt, Germany), dried in a vacuum centrifuge and dissolved in 300 μl ultrapure water. The retention time for every GSL was determined by measuring either the collected fraction or the authentic standard (Phytolab, Vestenbergsgreuth, Germany) with the HPLC system as described before.

Databases used for the Expression Analysis

The database AGRIS (www.arabidopsis.med.ohio-state.edu, Yilmaz et al. 2011) was used to search for circadian clock related binding site motifs. The tool from Mockler et al. (2007) (http://diurnal. mocklerlab.org/) was used to compare array-based transcriptome analysis in *A. thaliana* with the data obtained in this study.

Statistical Analysis

The expression levels of GOIs and content levels of sulfur-containing metabolites over time were analyzed using statistical model selection with AICc, a small-sample version of the widely known Akaike Information Criterion (Hurvich and Tsai 1989). Sets of "candidate models" were assembled, and the model with the lowest AICc value was considered to be the one that gets most support from the experimental data (Burnham and Anderson 2002). The "candidates" were linear models with the data for the expression and content of the sulfur-containing metabolites (averages over technical replicates) as dependent variable; the independent variables included light condition, sulfur status and time. Both linear and trigonometric (sine and cosine) functions were considered to model the dependent variable over time. By allowing for interactions between independent variables, the slope and intercept or amplitude, average, and phase shift could or could not depend on light and sulfur. Thereby each of the "candidate models" represented some plausible hypothesis about the underlying biological process e.g. whether gene expression and metabolite content levels are constant or follow a linear trend over time or whether they are governed by a circadian or diurnal periodicity, and if so, what the most likely rhythm is (e.g. 23, 24 or 25 h), and also whether light and sulfur have an impact on expression/content levels and its (periodic) variation over time.

Separate three-way ANOVAs were performed with the values of the expression data and metabolic content as dependent variable and sulfur concentration, time point of harvesting, and light condition (diurnal/circadian) as independent factors as well as their interaction. The factor "light" consisted of two levels: light/light (LL) and light/dark (LD) pattern. Sulfur status consisted of two different concentrations: 0.01 mM $MgSO_4$ and 1 mM $MgSO_4$. The third factor, time, consisted of different harvesting time points, ranging from 0 h to 40 h. Significance of factors and their interactions was assessed by means of F-tests.

Statistical computations were done in R 3.1.1 (RCoreTeam 2014) using add-on package MuMIn (Barton 2014) for the model selection, and in InfoStat version 2016 (http://www.infostat.com.ar) for the ANOVAs. All graphs were generated with SigmaPlot 12.5 (Systat Software, Inc., San Jose, CA).

Acknowledgements

We acknowledge the Deutsche Saatveredelung AG, Lippstadt, Germany, for providing us with seeds of the *Brassica napus* cultivar. We would like to thank Julia Volker and Pamela von Trzebiatowski, Hannover, for their excellent technical assistance and the gardener Yvonne Leye for taking care of the plants. We gratefully acknowledge Dr. Elke Bloem, Julius-Kühn-Institut, Germany, who analyzed the samples for their sulfate content.

Author's Contribution

ARi and JP conceived and designed research; JH and ARu conducted experiments; JH, ARu and ARi analyzed data and created the figures; PP and AT performed the statistical analysis; ARu, ARi, JH and JP wrote the manuscript. All authors read and approved the manuscript.

Supporting Information

Fig. S1. Northern blot analysis of the GOIs under diurnal/circadian conditions.
Fig. S2. The content of sulfate-sulfur in the leaves under diurnal/circadian conditions.
Fig. S3. Individual aliphatic GSL in leaves under diurnal/circadian conditions.
Fig. S4. Individual indolic GSL in leaves under diurnal/circadian conditions.
Table S1. Three-way ANOVA analysis of the expression data and the measured sulfur-containing compounds under diurnal and circadian conditions based on three technical replicates.

References

Barton K (2014) MuMIn: Multi-model inference. R package version 1.12.1. http://CRAN.R-project.org/package=MuMIn

Blake-Kalff MM, Harrison KR, Hawkesford MJ, Zhao FJ, McGrath SP (1998) Distribution of sulfur within oilseed rape leaves in response to sulfur deficiency during vegetative growth. Plant Physiol 118:1337–1344

BLAST: Basic Local Alignment Search Tool. Available: https://blast.ncbi.nlm.nih.gov/Blast.cgi Accessed 09 November 2016

Bloem E, Riemenschneider A, Volker J, Papenbrock J, Schmidt A, Salac I, Haneklaus S, Schnug E (2004) Sulphur supply and infection with *Pyrenopeziza brassicae* influence L-cysteine desulphydrase activity in *Brassica napus* L. J Exp Bot 55:2305–2312

Boestfleisch C, Hornbacher J, Rumlow A, Papenbrock J (2017) Contents of single glucosinolates are influenced by salinity in the halophyte *Lepidium latifolium*. In: De Kok L, Hawkesford M, Schnug E (eds) Plant Sulfur Workshop Proceedings, Vol. 3, 2016/17. Springer, Dordrecht

Brassica napus Genome Browser. Available: http://www.genoscope.cns.fr/brassicanapus/Accessed 9 November 2016

Buchner P, Stuiver CEE, Westerman S, Wirtz M, Hell R, Hawkesford M, De Kok LJ (2004) Regulation of sulfate uptake and expression of sulfate transporter genes in *Brassica oleracea* as affected by atmospheric H_2S and pedospheric sulfate nutrition. Plant Physiol 136:3396–3408

Burnham KP, Anderson DR (2002) Model selection and multimodel inference: a practical information-theoretic approach. Second edition. Springer, New York, NY

Cao MJ, Wang Z, Wirtz M, Hell R, Oliver DJ, Xiang CB (2013) SULTR3;1 is a chloroplast-localized sulfate transporter in *Arabidopsis thaliana*. Plant J 73:607–616

CLC Workbench. Available: http://www.clcbio.com/ Accessed 9 November 2016

Computional Biology and Functional Genomics Laboratory: Available http://compbio.dfci.harvard.edu/compbio Accessed 9 November 2016

Covington MF, Maloof JN, Straume M, Kay SA, Harmer SL (2008) Global transcriptome analysis reveals circadian regulation of key pathways in plant growth and development. Genome Biol 9:R130

Dodd AN, Kusakina J, Hall A, Gould PD, Hanaoka M (2014) The circadian regulation of photosynthesis. Photosynth Res 119:181–190

DOSBox. Available: http://www.dosbox.com/ Accessed 9 November 2016

DSV: Deutsche Saatveredelung Available: http://www.dsv-saaten.de/raps/winterraps/sorten/genie.html Accessed: 9 November 2016

Filichkin SA, Breton G, Priest HD, Dharmawardhana P, Jaiswal P, Fox SE, Michael TP, Chory J, Kay SA, Mockler TC (2011) Global profiling of rice and poplar transcriptomes highlights key conserved circadian-controlled pathways and cis-regulatory modules. PloS ONE 6:e16907

Gelanalyzer: Available: http://gelanalyzer.com/Accessed 9 November

2016
Gutiérrez RA, Stokes TL, Thum K, Xu X, Obertello M, Katari MS, Tanurdzic M, Dean A, Nero DC, McClung R, Coruzzi GM (2008) Systems approach identifies an organic nitrogen-responsive gene network that is regulated by the master clock control gene *CCA1*. Proc Natl Acad Sci USA 105:4939–4944
Harmer SL, Hogenesch JB, Straume M, Chang HS, Han B, Zhu T, Wang X, Kreps JA, Kay S (2000) Orchestrated transcription of key pathways in Arabidopsis by the circadian clock. Science 290:2110–2113
Harmer S L (2009) The circadian system in higher plants. Annu Rev Plant Biol 60:357–377
Hawkesford MJ, De Kok LJ (2006) Managing sulphur metabolism in plants. Plant Cell Environ 29:382–395
Haydon MJ, Bell LJ, & Webb AA (2011). Interactions between plant circadian clocks and solute transport. J Exp Bot 62:2333–2348
Haydon MJ, Román Á, Arshad W (2015) Nutrient homeostasis within the plant circadian network. Front Plant Sci 6:1–6
Hurvich CM, Tsai CL (1989) Regression and time series model selection in small samples. Biometrika 76:297–307
Huseby S, Koprivova A, Lee BR, Saha S, Mithen R, Wold AB, Bengtsson GB, Kopriva S (2013) Diurnal and light regulation of sulphur assimilation and glucosinolate biosynthesis in Arabidopsis. J Exp Bot 64:1039–1048
Iijima M, Matsushita N (2011) A circadian and an ultradian rhythm are both evident in root growth of rice. J Plant Physiol 168: 2072–2080
InfoStat. Available: http://www.infostat.com.ar/?lang=en Accessed 9 November 2016
Kataoka T, Watanabe-Takahashi A, Hayashi N, Ohnishi M, Mimura T, Buchner P, Hawkesford MJ, Yamaya T, Takahashi H (2004) Vacuolar sulfate transporters are essential determinants controlling internal distribution of sulfate in Arabidopsis. Plant Cell 16:2693–2704
Katz E, Nisani S, Yadav BS, Woldemariam MG, Shai B, Obolski U, Chamovitz DA (2015) The glucosinolate breakdown product indole-3-carbinol acts as an auxin antagonist in roots of *Arabidopsis thaliana*. Plant J 82:547-555
Kerwin RE, Jimenez-Gomez JM, Fulop D, Harmer SL, Maloof JN, Kliebenstein DJ (2011) Network quantitative trait loci mapping of circadian clock outputs identifies metabolic pathway-to-clock linkages in Arabidopsis. Plant Cell 23:471–485
Khokon MAR, Jahan MS, Rahman T, Hossain MA, Muroyama D, Minami I, Murata Y (2011) Allyl isothiocyanate (AITC) induces stomatal closure in Arabidopsis. Plant Cell Environ 34:1900–1906
Kopriva S, Muheim R, Koprivova A, Trachsel N, Catalano C, Suter M, Brunold C (1999) Light regulation of assimilatory sulphate reduction in *Arabidopsis thaliana*. Plant J 20:37–44
Kusakina J, Gould PD, and Hall A (2014) A fast circadian clock at high temperatures is a conserved feature across Arabidopsis accessions and likely to be important for vegetative yield. Plant Cell Environ 37:327–340
Lai AG, Doherty CJ, Mueller-Roeber B, Kay SA, Schippers JHM, Dijkwel PP (2012) *CIRCADIAN CLOCK-ASSOCIATED 1* regulates ROS homeostasis and oxidative stress responses. Proc Natl Acad Sci USA 109:17129–17134
Mailer RJ (1989) Effects of applied sulfur on glucosinolate and oil concentrations in the seeds of rape *Brassica napus* L. and turnip rape *Brassica rapa* L. var. *silvestris* (Lam.) Briggs. Aust J Agric Res 40:617–624
McClung CR (2006) Plant circadian rhythms. Plant Cell 18:792–803
Mithöfer A, Boland W (2012) Plant defense against herbivores: chemical aspects. Annu Rev Plant Biol 63:431-450
Mizoguchi T, Wheatley K, Hanzawa Y, Wright L, Mizoguchi M, Song HR, Carr IA, Coupland G (2002) *LHY* and *CCA1* are partially redundant genes required to maintain circadian rhythms in Arabidopsis. Dev Cell 2:629–641
Mockler TC, Michael TP, Priest HD, Shen R, Sullivan CM, Givan SA, McEntee C, Kay SA, Chory J (2007) The diurnal project: diurnal and circadian expression profiling, model-based pattern matching, and promoter analysis. Cold Spring Harb Symp Quant Biol 72:353–363
Nagel DH, Doherty CJ, Pruneda-Paz J L, Schmitz RJ, Ecker JR, Kay SA (2015) Genome-wide identification of CCA1 targets uncovers an expanded clock network in Arabidopsis. Proc Natl Acad Sci USA 112:E4802–4810
Noctor G, Arisi ACM, Jouanin L, Valadier MH, Roux Y, Foyer CH (1997) Light-dependent modulation of foliar glutathione synthesis and associated amino acid metabolism in poplar overexpressing γ-glutamylcysteine synthetase. Planta 202:357–369
Parmar S, Buchner P, Hawkesford MJ (2007) Leaf developmental stage affects sulfate depletion and specific sulfate transporter expression during sulfur deprivation in *Brassica napus* L. Plant Biol 9:647–653
Quackenbush J, Liang F, Holt I, Pertea G, Upton J (2000) The TIGR gene indices: reconstruction and representation of expressed gene sequences. Nucleic Acids Res 28:141–145
R Core Team (2014) *R: A Language and Environment for Statistical Computing*. Vienna: R Foundation for Statistical Computing. Available online at: http://www.R-project.org
Reich M, Aghajanzadeh T, Helm J, Parmar S, Hawkesford MJ, De Kok LJ (2017) Chloride and sulfate salinity differently affect biomass, mineral nutrient composition and expression of sulfate transport and assimilation genes in *Brassica rapa*. Plant Soil, 411:319–332
Riemenschneider A, Nikiforova V, Hoefgen R, De Kok LJ, Papenbrock J (2005) Impact of elevated H_2S on metabolite levels, activity of enzymes and expression of genes involved in cysteine metabolism. Plant Physiol Biochem 43:473–483
RobiNA. Available: http://www.bioinformatics.babraham.ac.uk/projects/fastqc/ Accessed 9 November 2016
Rosa AS, Rodrigues PMF (1998) The effect of light and temperature on glucosinolate concentration in the leaves and roots of cabbage seedlings. J Sci Food Agric 78:208–212
Rumlow A, Keunen E, Klein J, Pallmann P, Riemenschneider A, Cuypers A, Papenbrock J (2016) Quantitative expression analysis in *Brassica napus* by Northern blot analysis and reverse transcription-quantitative PCR in a complex experimental setting. PLoS ONE 11:e0163679
Salomé PA, McClung CR (2004) The *Arabidopsis thaliana* clock. J Biol Rhythms 19:425–435
Schnug E, Haneklaus S (2005) Sulphur deficiency symptoms in oilseed rape (*Brassica napus* L.) - the aesthetics of starvation. Phyton 45:79–95
Scherer HW (2001) Sulphur in crop production — invited paper. Eur J Agron 14:81–111
Shaw LM, Turner AS, Laurie DA (2012) The impact of photoperiod insensitive *Ppd-1a* mutations on the photoperiod pathway across the three genomes of hexaploid wheat (*Triticum aestivum*). Plant J 71:71–84
Thies W (1979) Detection and utilization of a glucosinolate sulfohydrolase in the edible snail, *Helix pomatia*. Naturwissenschaften 66:364-365
Vauclare P, Kopriva S, Fell D, Suter M, Sticher L, von Ballmoos P, Krähenbühl U, den Camp RO, Brunold C (2002) Flux control of sulphate assimilation in *Arabidopsis thaliana*?: adenosine 5′-phosphosulphate reductase is more susceptible than ATP sulphurylase to negative control by thiols. Plant J 31:729–740
Velez-Ramirez AI, van Ieperen W, Vreugdenhil D, Millenaar FF (2011) Plants under continuous light. Trends Plant Sci 16:310–318
Wang W, Barnaby JY, Tada Y, Li H, Tör M, Caldelari D, Lee D, Fu

XD, Dong X (2011) Timing of plant immune responses by a central circadian regulator. Nature 470:110–114
Weese A, Pallmann P, Papenbrock J, Riemenschneider A (2015) *Brassica napus* L. cultivars show a broad variability in their morphology, physiology and metabolite levels in response to sulfur limitations and to pathogen attack. Front Plant Sci 6
Yilmaz A, Mejia-Guerra MK, Kurz K, Liang X, Welch L, Grotewold E (2011) AGRIS: the Arabidopsis gene regulatory information server, an update. Nucleic Acids Res 39:D1118–D1122

Chapter 4.2 Salinity influences single glucosinolates content in the halophyte *Lepidium latifolium*

Salinity Influences Single Glucosinolate Content in the Halophyte *Lepidium latifolium*

Christian Boestfleisch, Johann Hornbacher, Annekathrin Rumlow, and Jutta Papenbrock

Abstract The influence of salinity on the biosynthesis of secondary metabolites with a focus on single glucosinolates (GSLs) was investigated in *Lepidium latifolium* L., which is a plant species rich in antioxidants. Mature plants were subjected to 0, 15, 22.5, and 35 Practical Salinity Units (PSU) for 1–4 weeks. While phenols, flavonoids, and the oxygen radical absorbance capacity (ORAC) increased with increasing salinity, the ascorbate concentration did not follow a specific pattern. The concentration of single GSLs was influenced by salinity in different ways: While the concentration of aliphatic GSLs like glucoiberin and sinigrin increased, the concentration of aromatic GSLs such as glucobrassicin decreased under salinity stress. Salinity increased the total GSL concentration significantly with sinigrin being the major contributing GSL. The exact molecular role of the different GSLs in abiotic stress defense needs further analysis.

The halophyte *Lepidium latifolium* L. belongs to the Brassicaceae family, known for their high abundance of glucosinolates (GSLs). The role of GSLs and their break-down products under biotic stress, especially their defense function against herbivores, insects and pathogens, is well known: upon tissue damage myrosinase hydrolyzes GSLs, releasing thiocyanates, isothiocyanates and nitriles (Agrawal and Kurashige 2003; Hopkins et al. 2009; Manici et al. 1997; Rask et al. 2000; Tierens et al. 2001). Stress caused by abiotic factors like drought has different effects on GSL composition and content. In several studies (Mewis et al. 2012; Radovich et al. 2005; Schreiner et al. 2009; Tong et al. 2014) either an increase of aliphatic GSLs under drought stress or a decrease, no effect or a less pronounced increase of aromatic including (indolic) GSLs in *Brassica* species and in *Arabidopsis thaliana* L. was shown. Other studies of GSLs in drought-stressed *Brassica* species showed a reduction or insignificant changes in the GSL content (Khan et al. 2010; Robbins et al. 2005). In both studies the content of indolic GSLs was predominant.

Only a few studies exist on the effect of salinity on GSLs. In two *Brassica napus* cultivars the total GSL concentration increased under salinity (Qasim et al. 2003).

C. Boestfleisch • J. Hornbacher • A. Rumlow • J. Papenbrock (✉)
Institut für Botanik, Gottfried Wilhelm Leibniz Universität, Herrenhäuser Straße 2, D-30419 Hannover, Germany
e-mail: jutta.papenbrock@botanik.uni-hannover.de

L.J. De Kok et al. (eds.), *Sulfur Metabolism in Higher Plants - Fundamental, Environmental and Agricultural Aspects*, Proceedings of the International Plant Sulfur Workshop, DOI 10.1007/978-3-319-56526-2_10

Brassica oleracea showed an increased total GSL content under the influence of salt (López-Berenguer et al. 2008, 2009). In these studies measurements of total GSL contents were performed, while other studies also analyzed single GSLs. In radish sprouts, for example, one aliphatic GSL was predominant and its concentration increased by increased salinity (Yuan et al. 2010). Zaghdoud et al. (2012) found that the total GSL content was not altered by salinity in a *B. oleracea* cultivar, while another cultivar showed a decrease in the total GSL content. This cultivar showed a decrease in indolic GSLs but an increase in aliphatic GSLs. Bloem et al. (2014) revealed no significant changes in contents of the aromatic GSL glucotropaeolin in salt stressed *Tropaeolum majus*. All studies previously mentioned applied low salinity to glycophytes, while in this study high salinities to a halophyte species were applied.

Several antioxidants are altered in their accumulation by salinity, often enhanced under stress conditions, like the non-enzymatic metabolites ascorbate, glutathione, carotenoids, tocopherols, and phenolics. These antioxidants serve, besides the enzymatic antioxidants, to scavenge or detoxify reactive oxygen species (ROS) induced by stresses like salinity (Noctor and Foyer 1998; Sharma et al. 2010).

In this study the salt-tolerant species *Lepidium latifolium* was investigated as we were interested in the GSL concentration in relation to salinity and to identify the time point when the GSL content was highest after beginning of the salt treatment. Sometimes classified as a halophyte, *L. latifolium* is native to southern Europe and Asia (Kaur et al. 2013; Zhao et al. 2010). Its tolerance to salt allows it to grow along the coastline but it is also found in the cold Himalayan region (Gupta et al. 2013; Kaur et al. 2013). It has been identified as an invasive species in North America (Francis and Warwick 2007). Fortunately, the GSL spectrum of *L. latifolium* was analyzed previously indicating eight GSLs with sinigrin being the dominant GSL (Kaur et al. 2013). The use as a vegetable and the medicinal utilization were also previously described (Kaur et al. 2013; Navarro et al. 1994). The influence of salinity on biomass, oxygen radical absorbance capacity (ORAC), ascorbate, phenolics and flavonoids, and GSL spectrum and contents of *L. latifolium* influenced by salt were analyzed in this study. The concentration of aromatic GSLs decreased or showed no clear reaction, whereas indolic GSLs decreased and aliphatic GSLs increased or were indifferent towards salinity stress. All other metabolites except ascorbate that showed varying responses were positively affected by salinity. Thus ORAC increased accordingly. The duration of stress application had an influence on the concentration of some of the metabolites analyzed.

Lepidium latifolium seeds (Rühlemann's Kräuter und Duftpflanzen, Horstedt, Germany) were germinated on propagation soil (Einheitserde, Einheitserdewerk Hameln-Tündern, Germany). After a period of 5 weeks, plants were transplanted to sand of 0–2 mm grain size (Hornbach, Hannover, Germany). During the nursing time, the plants were watered with modified Hoagland solution (Epstein 1972). Mature plants were grown under greenhouse conditions at around 22 °C. Sodium vapor lamps (SON-T Agro 400, Philips, Amsterdam, Netherlands) served as an additional light source, providing a photoperiod of 14 h light and a quantum fluence rate of 350 µmol m^{-2} s^{-2}. Finally, the plants were transferred to aerated containers

with 13.5 L solution containing 3.57 mM $NaNO_3$, 316 mM $H_2NaPO_4 \times H_2O$ and 23.5 mM Fe-EDDHA (5.7%) (Duchefa, Haarlem, Netherlands). After 1 week of acclimatization to the hydroponic culture, the sea salt mixture (Seequasal GmbH, Münster, Germany) was added stepwise by an increase of 0.75 PSU every day to the desired concentrations of 0, 15, 22.5, and 30 PSU. Four plants of each salinity treatment were harvested at the time the cultivation solutions reached their final concentration (0 weeks) and 1, 2, 3 and 4 weeks after induction. Whole plants (shoot including leaves) were frozen in liquid nitrogen and stored at −80 °C for further analysis. The metabolite extraction and the determination of total phenols, total flavonoids, oxygen radical absorbance capacity (ORAC) and ascorbic acid were performed as described by Boestfleisch et al. (2014). For the determination of GSLs, frozen, ground leaf material was freeze-dried. One milliliter of 80% methanol was added to 10 mg dried plant material. The sample was placed on a shaker until homogenization and then centrifuged for 5 min at 13,000 *g*. The pellet was re-extracted in the same way and the supernatants were combined. The supernatant was loaded onto a column (QIAGEN GmbH, Hilden, Germany) containing 2 ml of a 5% (w/v) suspension of DEAE Sephadex A25 (Sigma-Aldrich, Taufkirchen, Germany) in 0.5 M acetic acid (pH 5). The column was then flushed with 10 ml of HPLC-grade H_2O and 4 ml of 0.02 M acetic acid (pH 5). For desulfating the GSLs overnight at room temperature, 50 µl of sulfatase (Sigma-Aldrich) solution (Thies 1979) was added to 450 µl 0.02 M acetic acid (pH 5) and loaded onto the column as well. Desulfated GSLs were eluted 3 times with 2 ml HPLC-H_2O. Samples were dried in a vacuum centrifuge overnight and resolved in 300 ml HPLC-H_2O. Analysis was performed with HPLC system (Knauer, Berlin, Germany) equipped with an Ultra AQ C-18 column (150 x 4.6 mm, 5 µm particle size) (Restek GmbH, Bad Homburg, Germany). For measuring the samples, a volume of 50 µl was injected. A water (solvent A)-acetonitrile (solvent B) gradient at a flow rate of 1 ml min^{-1} at room temperature was used. Following gradient was applied: 100% A (6 min), 100–70% A (27 min), 70–40% A (0.1 min), 4.9 min 40% A, 40–100% A (0.1 min), and 19.9 min 100% A. Eluents were monitored at a wavelength of 229 nm. Identification of desulfated GSLs was achieved by comparing the retention time with commercially available GSLs (PhytoLab GmbH and Co. KG, Vestenbergsgreuth, Germany) that were treated the same way as the samples. By means of standard curves of these references, desulfated GSLs were quantified. Integration of peaks and elaboration of data were performed using ChromGate Client/Server Version 3.3.1 (Knauer, Berlin, Germany). GSLs were calculated as the mean of four biological replicates with the standard deviation of these four biological replicates. The total amount of GSLs was calculated as the sum of all individual GSLs. To asses precision and reproducibility of GLS analysis, four technical replicates were prepared by measuring GSL contents in each plant sample four times. The standard deviation relative to the individual GSL content was calculated in these replicates. Values were tested for significance ($p = 0.05$) with an analysis of variance (ANOVA) using R (version 3.2.2), displaying significant differences between metabolites corresponding to PSU values at different harvest times.

At the starting point there were no significant differences in biomass production of *L. latifolium* between the different salinities, but after 1 week there was a significant difference between plants grown at 22.5 and 30 PSU and plants grown at 15 PSU, which produced the highest biomass (Fig. 1a). The difference in biomass at the different salinities increased towards week 2 where the highest increase in biomass was observed in plants grown at 0 PSU. This effect was significantly higher than in plants grown at 22.5 and 30 PSU. Plant growth decreased with increasing salinity at this point of experimentation. After 3 and 4 weeks the increase in biomass reached a maximum for plants grown at 15 PSU, followed by 0 PSU. Plants grown at 30 PSU showed the lowest increase in biomass. The ORAC of *L. latifolium* grown at salt stress (30 PSU) was highest at all sampling dates compared to the other levels of salinity (Fig. 1b). The ORAC maximum was determined at week 0 in plants grown at 30 PSU and decreased slowly towards the 4th week. At week 0 and week 1, ORAC values in plants grown at 30 PSU were significantly higher compared to plants grown at 15 and 0 PSU. This difference decreased, but ORAC values in plants grown at 30 PSU were still significantly higher compared to plants grown at 15 PSU. In the 3rd week plants grown at 30 PSU had again a significantly higher concentration compared to lower levels of salinity. In the 4th week there was no significant difference in the ORAC. The total phenol concentration of plants grown at 30 PSU was the highest during the time of the experiment (Fig. 1c). It was significantly higher than the concentration of plants grown at 0 PSU at all sampling dates with the exception of week 3. In most cases plants grown at 0 PSU had the lowest total phenol concentration followed by 15 PSU. Higher salinity concentrations yielded higher total phenol concentrations. This effect was significant over time except for the 3rd week when plants grown at 0 and 30 PSU had higher total phenol concentrations than plants grown at 15 and 22.5 PSU.

Plants grown at higher salinities of 30 and 22.5 PSU produced higher total flavonoid values than plants grown at 0 and 15 PSU (Fig. 1d). There was a significant difference between plants grown at 30 and 0 PSU at all sampling dates. The differences in total flavonoid values between plants grown in high and low salinities were greatest at the start of experimentation and after 1 week, and became smaller after 3 and 4 weeks.

Small differences in the ascorbate concentration were detected at the beginning of the experiment but plants grown at 0 PSU had a lower concentration compared to plants grown at other salinities (Fig. 1e). In the 1st week plants grown at 0 and 15 PSU had insignificantly lower ascorbate values than plants grown at 22.5 and 30 PSU. Plants grown at 15 and 30 PSU had lower ascorbate values compared to plants grown at 0 and 22.5 PSU in the 2nd week. In the 3rd week there was a significant decline in the ascorbate concentration from plants grown at 0 to plants grown at 30 PSU. In the 4th week plants grown at 0 PSU showed significantly lower values than plants grown at all other salinities. The highest ascorbate concentration in this week was detected in plants grown at 22.5 PSU followed by 15 PSU. The ascorbate content in plants grown at these salinities were significantly higher compared to plants grown at 0 PSU at this point of time.

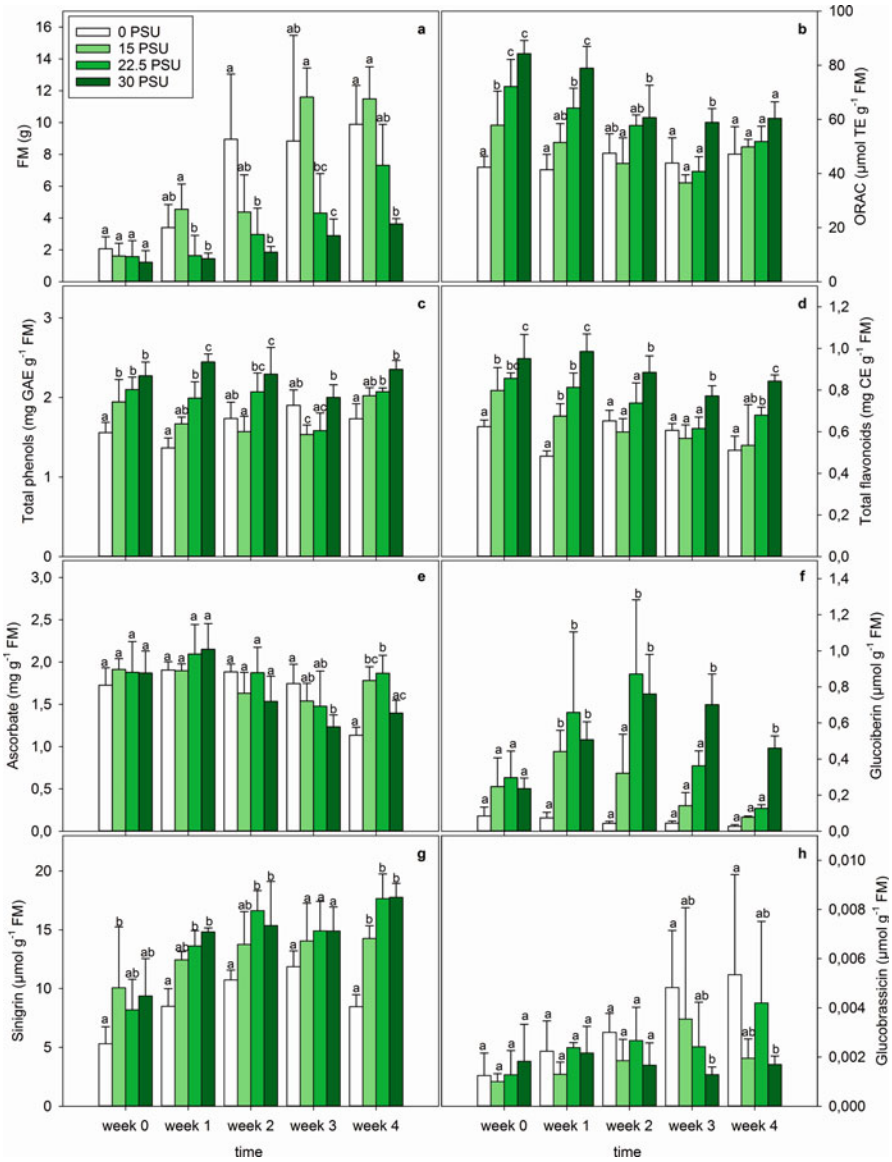

Fig. 1 Biomass production (**a**), oxygen radical absorbance capacity (ORAC, **b**) and contents of total phenols (**c**), total flavonoids (**d**), ascorbate (**e**), glucoiberin (**f**), sinigrin (**g**), glucobrassicin (**h**) of *L. latifolium* plants (n = 4). Six-week-old plants were placed into aerated containers and after an acclimatization time of 1 week the salinity was increased by 0.75 PSU every day to the concentrations of 0 PSU, 15 PSU, 22.5 PSU and 30 PSU. Fresh material was harvested upon reaching the targeted salinities (week 0) followed by a weekly interval. Different letters indicate significant differences (p = 0.05) between different PSU values within one point of time

Salinity caused diverging effects on individual GSLs. There are three ways how the GSL concentration was influenced by salinity. Figure 1f shows the first way, an increase in the concentration of glucoiberin. At the beginning of the experiment there was a trend for a higher glucoiberin concentration in plants grown at 22.5 PSU, but this effect was not significant. This trend continued in the 1st week when plants grown at all salinities had a significantly higher concentration compared to plants grown at 0 PSU. In the 2nd week plants grown at 22.5 and 30 PSU had a significantly higher glucoiberin concentration than plants grown at 0 PSU. One week later the significant maximum in glucoiberin concentration was found in plants grown at 0 PSU. This trend continued in the 4th week while all concentrations decreased.

The temporal pattern of the mean sinigrin concentration (Fig. 1g) was similar to the pattern of glucoiberin. A significant difference in the sinigrin concentration in plants grown at 0 and 15 PSU could be detected in week 0. However, after 1 week a trend was visible in such way that plants grown at higher salinities showed higher sinigrin concentrations. There was a significant difference in the sinigrin concentration between plants grown at 30 PSU and plants grown at 0 PSU in week 1 and 4. In week 2, plants grown at 22.5 PSU reflected a higher and significant (towards 0 PSU) sinigrin concentration. In week 3, plants grown at 22.5 and 30 PSU showed both high sinigrin concentrations, which differed not significantly from that of the 0 PSU treatment.

The second way how GSLs were influenced by salt stress can shown exemplary for glucobrassicin (Fig. 1h). There was no significant difference at the beginning of the experiment until the 2nd week, but a trend was observed after 2 weeks. Plants grown at lower salinities accumulated more glucobrassicin, except for plants grown at 15 PSU. After 3 weeks, there was a significant decrease in the glucobrassicin concentration in plants grown at 0 to 30 PSU, which continued towards the 4th week, but plants grown at 15 PSU had the second lowest concentration.

GSL concentrations of other GSLs are shown in Table 1. For the sake of completeness, the values of Fig. 1f–h are also presented in Table 1. The concentration of gluconapin increased with higher salinity towards the 2nd week, and showed the opposite pattern in the 4th week. Salinity decreased the concentration of glucobrassicin and gluconasturtiin. The decline in the GSL concentration from low to high salinity started around the 1st week with gluconasturtiin, but was more distinctive for glucobrassicin. The concentrations of glucocheirolin, glucoraphanin, and glucotropaeolin did not show a clear pattern for a de- or an increase under salinity stress, which represents the third way GSLs were influenced by salt stress. Within week 1 and 2 the maximum of glucotropaeolin was reached in plants grown at 30 PSU but changed to 0 PSU in week 3 and 4. The highest glucocheirolin concentration accumulated in plants grown at 15 PSU in week 2 and 3 and at 22.5 PSU in week 4. With respect to the relatively high standard deviation it is important to keep in mind that each single determination was done with individual plants.

The measurement of GSL contents in technical replicates resulted in standard deviations not higher than 20% with a mean of 8% relative to the individual GSL content (data not shown). In contrast, relative standard deviations of biological

Table 1 Mean GSL concentration (n = 4) in nmol g^{-1} FM for glucocheirolin, glucoraphanin, gluconapin, glucobrassicin, gluconasturtiin and glucoiberin; in μmol g^{-1} FM for sinigrin, glucotropaeolin and the sum of GSL

Time in weeks	PSU	Gluco-cheirolin	Glucoiberin	Sinigrin	Gluco-raphanin	Gluconapin	Gluco-tropaeolin	Gluco-brassicin	Gluco-nasturtiin	Total GSL amount
0	0	0.65 ± 0.47 a	84.1 ± 49.9 a	5.31 ± 1.45 a	15.9 ± 3.50 a	1.45 ± 1.58 a	0.39 ± 0.17 a	1.25 ± 0.91 a	31.5 ± 19.7 a	5.80 ± 1.68 a
	15	0.93 ± 0.81 a	247 ± 160 a	10.1 ± 5.18 b	34.4 ± 18.7 a	2.23 ± 2.23 a	1.14 ± 0.45 a	1.00 ± 0.31 a	72.5 ± 50.3 a	11.6 ± 5.83 b
	22.5	0.70 ± 0.57 a	297 ± 148 a	8.19 ± 2.61 ab	19.8 ± 9.76 a	3.22 ± 3.03 a	0.99 ± 0.34 a	1.28 ± 0.99 a	69.0 ± 50.2 a	9.60 ± 3.14 ab
	30	0.72 ± 0.36 a	236 ± 58.9 a	9.37 ± 3.18 ab	31.6 ± 9.14 a	6.12 ± 7.46 a	1.18 ± 0.24 a	1.83 ± 1.51 a	69.2 ± 29.9 a	10.9 ± 3.49 b
1	0	1.19 ± 0.73 a	73.9 ± 30.8 a	8.50 ± 1.49 a	21.4 ± 12.5 a	8.87 ± 12.5 a	0.99 ± 0.58 a	2.24 ± 1.23 a	227 ± 183 a	9.80 ± 2.23 a
	15	1.02 ± 0.47 a	442 ± 118 b	12.4 ± 0.70 ab	21.6 ± 3.96 a	3.64 ± 4.79 a	0.89 ± 0.22 a	1.30 ± 0.49 a	48.7 ± 13.0 a	13.8 ± 0.97 ab
	22.5	1.17 ± 0.41 a	658 ± 447 b	13.6 ± 1.31 b	34.7 ± 4.88 ab	9.41 ± 5.91 a	1.39 ± 0.30 ab	2.38 ± 0.20 a	94.8 ± 33.7 a	15.8 ± 1.21 b
	30	1.12 ± 0.48 a	507 ± 100 b	14.8 ± 0.33 b	41.2 ± 3.53 b	16.1 ± 13.0 a	2.48 ± 0.97 b	2.16 ± 1.08 a	83.9 ± 12.1 a	18.0 ± 0.95 b
2	0	1.15 ± 0.22 a	43.5 ± 11.0 a	10.7 ± 0.84 a	37.9 ± 6.13 a	3.01 ± 0.56 a	0.83 ± 0.25 a	3.00 ± 0.77 a	207 ± 41.1 a	11.9 ± 0.89 a
	15	1.23 ± 0.40 a	321 ± 216 a	13.8 ± 2.78 ab	27.1 ± 11.5 a	5.81 ± 3.37 ab	0.80 ± 0.35 a	1.86 ± 0.87 a	133 ± 117 a	15.1 ± 2.51 ab
	22.5	0.87 ± 0.56 a	871 ± 412 b	16.6 ± 1.70 b	29.9 ± 9.12 a	6.21 ± 5.49 ab	1.04 ± 0.38 a	2.67 ± 1.35 a	55.3 ± 17.6 a	18.6 ± 1.64 b
	30	0.51 ± 0.29 a	761 ± 219 b	15.4 ± 3.74 b	31.6 ± 2.51 a	17.2 ± 12.4 b	1.33 ± 0.26 a	1.67 ± 0.91 a	73.2 ± 19.8 a	17.6 ± 4.01 b

(continued)

Table 1 (continued)

Time in weeks	PSU	Gluco-cheirolin	Glucoiberin	Sinigrin	Gluco-raphanin	Gluconapin	Gluco-tropaeolin	Gluco-brassicin	Gluco-nasturtiin	Total GSL amount
3	0	1.01 ± 0.36 a	44.9 ± 12.2 a	11.9 ± 1.34 a	46.8 ± 11.5 a	3.64 ± 1.94 a	1.58 ± 1.51 a	4.82 ± 2.32 a	431 ± 284 a	14.0 ± 1.84 a
	15	1.13 ± 0.70 a	141 ± 73.4 a	14.1 ± 3.21 a	24.9 ± 12.2 b	8.56 ± 11.3 a	0.91 ± 0.84 b	3.54 ± 4.53 ab	279 ± 391 ab	15.4 ± 2.23 a
	22.5	0.85 ± 0.41 a	363 ± 82.4 a	14.9 ± 2.51 a	21.0 ± 8.20 b	6.8 ± 10.4 a	1.08 ± 0.47 b	2.42 ± 1.81 ab	72.3 ± 29.7 b	16.4 ± 2.41 a
	30	0.46 ± 0.24 a	701 ± 170 b	14.9 ± 2.05 a	27.4 ± 8.42 b	3.81 ± 3.61 a	1.01 ± 0.32 b	1.28 ± 0.31 b	53.3 ± 4.73 b	16.7 ± 2.15 a
4	0	0.63 ± 0.29 a	27.1 ± 8.95 a	8.46 ± 1.02 a	23.7 ± 3.98 a	7.63 ± 3.93 a	1.50 ± 0.86 a	5.35 ± 4.07 a	247 ± 116 a	10.3 ± 1.32 a
	15	0.90 ± 0.81 a	78.1 ± 6.46 a	14.3 ± 1.09 b	21.2 ± 9.85 a	4.14 ± 3.52 a	0.32 ± 0.06 a	1.95 ± 0.78 ab	159 ± 5.97 a	14.8 ± 1.14 b
	22.5	1.30 ± 0.89 a	127 ± 19.1 a	17.6 ± 2.10 b	39.8 ± 19.9 a	4.80 ± 5.81 a	0.47 ± 0.16 a	4.20 ± 3.31 ab	176 ± 83.4 a	18.5 ± 2.31 b
	30	0.68 ± 0.60 a	461 ± 67.4 b	17.8 ± 1.18 b	31.0 ± 10.0 a	1.52 ± 0.92 a	0.77 ± 0.17 a	1.70 ± 0.35 b	101 ± 13.5 a	19.1 ± 1.28 b
Time		NS	***	***	NS	.	*	*	*	***
PSU		NS	***	***	NS	NS	*	*	**	***
Time x PSU		NS	***	NS	**	NS	**	NS	NS	NS

Analysis of variance for the influence of time and salinity
NS, *, **, *** non-significant or significant at $P \leq 0.01$, 0.05, 0.01, or 0.001, respectively

replicates showed values up to 139% with a mean of 38% (data not shown). Because of the low relative standard deviations of technical replicates compared to the ones of biological replicates, the fluctuations in GSL contents emerging from technical procedures were neglected and the standard deviation of GSL contents in biological replicates was used to calculate significant differences between the treatments.

Lepidium latifolium had an optimal growth at 15 PSU in this experiment, as the gain of biomass was the highest at this salinity condition. This was expected as this plant species is a halophyte. Nevertheless, the salt was added in a short time (4 days) and the plant was still able to survive salinity of 22.5 and 30 PSU. The concentrations of the antioxidants were significantly increased by salinity stress. The ORAC increased at the beginning of the experiment and remained on this level for a week. Total phenols and as part of them the flavonoids were affected strongest 1 week after the start of the experiment. The range of concentrations of the mentioned antioxidants was getting smaller towards the end of the experiment closing the difference between high and low salinity. The ascorbate concentration showed a different pattern in comparison to the other antioxidants. There was no significant difference towards the 3rd week of the experiment. Ascorbate concentration quickly changed in *L. latifolium* within 24 h after the beginning of the salinity treatment (Boestfleisch et al. 2014) and returned to a steady state within 4 days.

If the yield of the antioxidants is calculated (multiplying the antioxidant concentration with the biomass produced), there is only one result for all antioxidants: the increase of biomass exceeded the increase in antioxidants (data not shown).

At the beginning of the experiment only changes in the sinigrin content proved to be significant, but 1 week after the induction of salinity stress the content of four out of eight GSLs reacted significantly to salinity. The maximum of glucoiberin shifted along the timescale with increasing salinity from 15 PSU around week 1 to 30 PSU between week 2 and 3 (Fig. 1e and Table 1). Sinigrin contents showed a larger difference at week 4 compared to the beginning, and gluconapin and glucotropaeolin showed an up- and down-regulation, whereas this was more distinctive in the latter one.

GSLs seemed to react partly different than antioxidants. While ORAC, phenols and flavonoids were positively and highly significant intercorrelated ($r > 0.8$; $p < 0.001$), and all of them showed a positive significant though weak correlation with ascorbate ($r = 0.27$–0.38; $p < 0.05$), GSLs showed ten positive and two negative correlations (Pearson correlation, data not shown). The negative ones were between glucoiberin and glucobrassicin and between glucoiberin and gluconasturtiin. There were some low correlations of mainly aliphatic GSLs with ORAC (glucoiberin: $r = 0.36$; $p < 0.001$, glucotropaeolin: $r = 0.32$; $p < 0.005$ and gluconasturtiin: $r = -0.28$; $p < 0.05$), phenol (glucoiberin, sinigrin, glucoraphanin and glucotropaeolin: $r = 0.31$–0.43; $p < 0.05$), flavonoid (glucoiberin, sinigrin, glucoraphanin and glucotropaeolin, $r = 0.23$–0.49; $p < 0.05$) and ascorbate values (glucocheirolin and glucoraphanin $r = 0.28$–0.3; $p < 0.05$). From the temporal patterns of the GSLs and the correlations between them, they can be classified into

three different groups: an up regulation (aliphatic GSLs), a down regulation (aromatic including indolic GSLs) and an intermediate reaction (aromatic excluding indolic GSLs) under salinity. This up and down, or the different regulation, was previously shown for salinity (Yuan et al. 2010; Zaghdoud et al. 2012) and drought treatments (Mewis et al. 2012; Radovich et al. 2005; Schreiner et al. 2009; Tong et al. 2014). Jensen et al. (1996) gave an explanation for these observations under salinity and drought stress. They showed that GSL synthesis increased when the leaf water potential was less than −1.4 MPa for extended periods. In our study, the VWC (volumetric water content) decreased from 85% to 77% at 30 PSU and from 92 to 83% at 0 PSU (data not shown). However, only aliphatic GSLs had a significant correlation with the VWC. The decrease of glucobrassicin with increasing salinity might also be the reason for its ease of oxidation, as it has a high antioxidant capacity (Cabello-Hurtado et al. 2012). These authors demonstrated a relatively high ORAC value for glucobrassicin, much higher than ascorbic acid. However, in our study the most abundant GSL was sinigrin, which has according to Cabello-Hurtado et al. (2012) a 6–7 times lower ORAC compared to ascorbic acid. Therefore, the total GSL content did not contribute much to the ORAC resulting in a low correlation ($r = 0.33$; $p < 0.01$). Furthermore many of the studies had only one point of time for the measurement of GSLs, but we could show that GSL contents in salt-stressed plants changed over time.

AS already mentioned sinigrin was the most abundant GSL in *L. latifolium*. Therefore, an increase in salinity elevated the total GSL yield, which would be beneficial for herbivore protection under abiotic stress conditions (Agrawal and Kurashige 2003; Hopkins et al. 2009), in addition to the enhanced growth and antioxidant production at 15 PSU. It was suggested that transient allocation and redistribution of some GSLs indicate a role in signaling mechanisms under abiotic stress conditions to induce fast physiological adaptation to unfavorable conditions (del Carmen Martínez-Ballesta et al. 2013). However, the determination of the exact functions of GSLs in reaction to abiotic stress needs further investigation.

References

Agrawal A, Kurashige NS (2003) A role for isothiocyanates in plant resistance against the specialist herbivore *Pieris rapae*. J Chem Ecol 29:1403–1415

Bloem E, Haneklaus S, Kleinwächter M, Paulsen J, Schnug E, Selmar D (2014) Stress-induced changes of bioactive compounds in *Tropaeolum majus* L. Ind Crop Prod 60:349–359

Boestfleisch C, Wagenseil NB, Buhmann AK, Seal CE, Wade EM, Muscolo A, Papenbrock J (2014) Manipulating the antioxidant capacity of halophytes to increase their cultural and economic value through saline cultivation. AoB Plants 6:1–16

Cabello-Hurtado F, Gicquel M, Esnault M-A (2012) Evaluation of the antioxidant potential of cauliflower (*Brassica oleracea*) from a glucosinolate content perspective. Food Chem 132:1003–1009

del Carmen M-BM, Moreno D, Carvajal M (2013) The physiological importance of glucosinolates on plant response to abiotic stress in *Brassica*. Int J Mol Sci 14:11607–11625

Epstein E (1972) Mineral nutrition of plants: principles and perspectives. Department of Soils and Plant Nutrition, California University, Davis

Francis A, Warwick SI (2007) The biology of invasive alien plants in Canada. 8. *Lepidium latifolium* L. Can J Plant Sci 87:639–658

Gupta SM, Pandey P, Negi PS, Pande V, Grover A, Patade VY, Ahmed Z (2013) DRE-binding transcription factor gene (LlaDREB1b) is regulated by various abiotic stresses in *Lepidium latifolium* L. Mol Biol Rep 40:2573–2580

Hopkins RJ, van Dam NM, van Loon JJ (2009) Role of glucosinolates in insect-plant relationships and multitrophic interactions. Annu Rev Entomol 54:57–83

Jensen CR, Mogensen VO, Mortensen G, Fieldsend JK, Milford GFJ, Andersen MN, Thage JH (1996) Seed glucosinolate, oil and protein contents of field-grown rape (*Brassica napus* L.) affected by soil drying and evaporative demand. Field Crop Res 47:93–105

Kaur T, Hussain K, Koul S, Vishwakarma R, Vyas D (2013) Evaluation of nutritional and antioxidant status of *Lepidium latifolium* Linn.: a novel phytofood from Ladakh. PLoS One 8:e69112

Khan MAM, Ulrichs C, Mewis I (2010) Influence of water stress on the glucosinolate profile of *Brassica oleracea* var. *italica* and the performance of *Brevicoryne brassicae* and *Myzus persicae*. Entomol Exp Appl 137:229–236

López-Berenguer C, Martínez-Ballesta MC, García-Viguera C, Carvajal M (2008) Leaf water balance mediated by aquaporins under salt stress and associated glucosinolate synthesis in broccoli. Plant Sci 174:321–328

López-Berenguer C, Martínez-Ballesta MC, Moreno DA, Carvajal M, García-Viguera C (2009) Growing hardier crops for better health: salinity tolerance and the nutritional value of broccoli. J Agric Food Chem 57:572–578

Manici LM, Lazzeri L, Palmieri S (1997) *In vitro* fungitoxic activity of some glucosinolates and their enzyme-derived products toward plant pathogenic fungi. J Agric Food Chem 45:2768–2773

Mewis I, Khan MAM, Glawischnig E, Schreiner M, Ulrichs C (2012) Water stress and aphid feeding differentially influence metabolite composition in *Arabidopsis thaliana* (L.) PLoS One 7:e48661

Navarro E, Alonso J, Rodriguez R (1994) Diuretic action of an aqueous extract of *Lepidium latifolium* L. J Ethnopharmacol 41:65–69

Noctor G, Foyer CH (1998) Ascorbate and glucosinolate: keeping active oxygen under control. Annu Rev Plant Physiol Plant Mol Biol 49:249–279

Qasim M, Ashraf M, Ashraf MY, Rehman S-U, Rha ES (2003) Salt-induced changes in two canola cultivars differing in salt tolerance. Biol Plant 46:629–632

Radovich TJK, Kleinhenz MD, Streeter JG (2005) Irrigation timing relative to head development influences yield components, sugar levels, and glucosinolate concentrations in cabbage. J Am Soc Hortic Sci 130:943–949

Rask L, Andréasson E, Ekbom B, Eriksson S, Pontoppidan B, Meijer J (2000) Myrosinase: Gene family evolution and herbivore defense in Brassicaceae. Plant Mol Biol 42:93–113

Robbins RJ, Keck A, Banuelos G, Finley JW (2005) Cultivation conditions and selenium fertilization alter the phenolic profile, glucosinolate, and sulforaphane content of broccoli. J Med Food 8:204–214

Schreiner M, Beyene B, Krumbein A, Stützel H (2009) Ontogenetic changes of 2-propenyl and 3-indolylmethyl glucosinolates in *Brassica carinata* leaves as affected by water supply. J Agric Food Chem 57:7259–7263

Sharma P, Jha A, Dubey R (2010) Oxidative stress and antioxidative defense systems in plants growing under abiotic stresses. In: Handbook of plant and crop stress. Taylor & Francis, Boca Raton, pp 89–138

Thies W (1979) Detection and utilization of a glucosinolate sulfohydrolase in the edible snail, *Helix pomatia*. Naturwissenschaften 66:364–365

Tierens KFM-J, Thomma BP, Brouwer M, Schmidt J, Kistner K, Porzel A, Mauch-Mani B, Cammue BP, Broekaert WF (2001) Study of the role of antimicrobial glucosinolate-derived isothiocyanates in resistance of *Arabidopsis* to microbial pathogens. Plant Physiol 125:1688–1699

Tong Y, Gabriel-Neumann E, Ngwene B, Krumbein A, George E, Platz S, Rohn S, Schreiner M (2014) Topsoil drying combined with increased sulfur supply leads to enhanced aliphatic glucosinolates in *Brassica juncea* leaves and roots. Food Chem 152:190–196

Yuan G, Wang X, Guo R, Wang Q (2010) Effect of salt stress on phenolic compounds, glucosinolates, myrosinase and antioxidant activity in radish sprouts. Food Chem 121:1014–1019

Zaghdoud C, Alcaraz-López C, Mota-Cadenas C, Martínez-Ballesta MDC, Moreno D, Ferchichi A, Carvajal M (2012) Differential responses of two broccoli (*Brassica oleracea* L. var *Italica*) cultivars to salinity and nutritional quality improvement. Sci World J 2012:1–12

Zhao K, Song J, Feng G, Zhao M, Liu J (2010) Species, types, distribution, and economic potential of halophytes in China. Plant Soil 342:495–509

Chapter 4.3 First experimental evidence suggests use of glucobrassicin as source of auxin in drought-stressed *Arabidopsis thaliana*.

frontiers | Frontiers in Plant Science

TYPE Original Research
PUBLISHED 31 October 2022
DOI 10.3389/fpls.2022.1025969

OPEN ACCESS

EDITED BY
Kamrun Nahar,
Sher-e-Bangla Agricultural University, Bangladesh

REVIEWED BY
Alain Tissier,
Leibniz-Institut für Pflanzenbiochemie (IPB), Germany
Rongfang Guo,
Fujian Agriculture and Forestry University, China

*CORRESPONDENCE
Jutta Papenbrock
Jutta.Papenbrock@botanik.uni-hannover.de

SPECIALTY SECTION
This article was submitted to Plant Abiotic Stress, a section of the journal Frontiers in Plant Science

RECEIVED 23 August 2022
ACCEPTED 13 October 2022
PUBLISHED 31 October 2022

CITATION
Hornbacher J, Horst-Niessen I, Herrfurth C, Feussner I and Papenbrock J (2022) First experimental evidence suggests use of glucobrassicin as source of auxin in drought-stressed *Arabidopsis thaliana*. *Front. Plant Sci.* 13:1025969. doi: 10.3389/fpls.2022.1025969

First experimental evidence suggests use of glucobrassicin as source of auxin in drought-stressed *Arabidopsis thaliana*

Johann Hornbacher[1], Ina Horst-Niessen[1], Cornelia Herrfurth[2,3], Ivo Feussner[2,3,4] and Jutta Papenbrock[1]*

[1]Institute of Botany, Leibniz University Hannover, Hannover, Germany, [2]Albrecht-von-Haller-Institute for Plant Sciences, Department of Plant Biochemistry, University of Göttingen, Göttingen, Germany, [3]Göttingen Center for Molecular Biosciences (GZMB), Service Unit for Metabolomics and Lipidomics, University of Göttingen, Göttingen, Germany, [4]Göttingen Center for Molecular Biosciences (GZMB), Department of Plant Biochemistry, University of Göttingen, Göttingen, Germany

The synthesis of indole-3-acetonitrile (IAN) from the indolic glucosinolate (iGSL) glucobrassicin (GB) is a unique trait of members of the Brassicales. To assess the contribution of this pathway to indole-3-acetic acid (IAA) synthesis under stress conditions, drought stress (DS) experiments with *Arabidopsis thaliana* were performed *in vitro*. Analysis of GSLs in DS plants revealed higher contents of GB in shoots and roots compared to control plants. Deuterium incorporation experiments showed the highest turnover of GB compared to all other GSLs during drought conditions. Evidence suggests the involvement of the thioglucosidase BGLU18 in the degradation of GB. The nitrile specifier proteins NSP1 and NSP5 are known to direct the GSL hydrolysis towards formation of IAN. Nitrilases like NIT2 are able to subsequently synthesize IAA from IAN. Expression of *BGLU18*, *NSP1*, *NSP5* and *NIT2* and contents of GB, IAN and IAA were significantly elevated in DS plants compared to control plants suggesting the increased use of GB as IAA source. Significantly higher contents of reactive oxygen species in DS *bglu18* and *epithionitrile specifier protein* (*esp*) mutants compared to Col-0 indicate higher stress levels in these mutants highlighting the need for both proteins in DS plants. Furthermore, GB accumulation in leaves was higher in both mutants during DS when compared to Col-0 indicating enhanced synthesis of GB due to a lack of breakdown products. This work provides the first evidence for the breakdown of iGSLs to IAN which seems to be used for synthesis of IAA in DS *A. thaliana* plants.

KEYWORDS

drought stress, glucobrassicin (PubChem CID: 5484743), glucosinolates, Indole - 3 - acetic acid (IAA), turnover (TO), auxin

Abbreviations: DS, Drought-stressed; ESP, Epithionitrile specifier protein; GB, Glucobrassicin; GSL, Glucosinolate; IAA, Indole-3-acetic acid; IAN, Indole-3-acetonitrile; IAOX, Indole-3-acetaldoxime; ITC, Isothiocyanate; MDS, Mildly drought-stressed; NSP, Nitrile specifier protein; SDS, Severely drought-stressed.

1 Introduction

In the past, research mainly focused on anticipatory, repellant or toxic effects of glucosinolates (GSLs) or their breakdown products. The actions against biotic stressors and subsequent change in GSL contents is well described (Kliebenstein et al., 2005; Wittstock and Burow, 2010). Only recently, data was published indicating that GSLs exhibit functions in abiotic as well as biotic stress situations. It was found that isothiocyanates (ITCs) derived from aliphatic GSLs (aGSLs) are involved in stomatal closure in *Arabidopsis thaliana* and are therefore major contributors in the regulation of water homeostasis of plants (Khokon et al., 2011). However, no published data is available about the role of indolic GSLs (iGSLs) in abiotically stressed plants.

Drought is one of the major reasons for crop losses worldwide (Matiu et al., 2017). Many crop plants grown worldwide belong to the Brassicaceae family. Among them are crops grown for human nutrition like cabbage (*Brassica oleracea* var. *capitata*) and broccoli (*Brassica oleraceae* var. *italica*). Members of this family like canola (*Brassica napus*) and *Crambe abyssinica* are also grown for industrial purposes showing the widespread use of this family in agriculture (Warwick, 2011; Zorn et al., 2019). Investigation of the behavior of specialized metabolites synthesized by the Brassicaceae in response to drought stress could be beneficial when it comes to the selection of drought tolerant varieties.

Glucosinolates are specialized metabolites synthesized by members of the Brassicales order. Dependent on the amino acid they are derived from, they are subdivided into aliphatic GSLs aGSLs derived from alanine, valine, leucine, isoleucine and methionine, and indolic GSLs iGSLs derived from tryptophan. The synthesis of indole-3-acetalaldoxime (IAOX) from tryptophan performed by CYP79B2/B3 (Figure 1) is limited to members of the Brassicaceae. This intermediate gives rise to either indole-3-acetic acid (IAA) through the intermediate indole-3-acetonitrile (IAN) with the action of CYP71A13 or iGSLs (Bekaert et al., 2012).

Glucosinolates and classical thioglucosidases (EC 3.2.1.147) are either stored in separate cells or cell compartments. Thioglucosidases are subdivided into classical (e.g. TGG1, TGG2) and atypical groups (e.g. PEN2, BGLU18). In the active site of the classical thioglucosidases, a Glu residue is crucial for the nucleophilic attack, while a Gln residue is involved in the hydrolysis in the presence of ascorbic acid and water (Wittstock & Burow, 2010). Atypical thioglucosidases on the other hand, perform an acid/base catalysis with two Glu residues at their catalytic site (Chhajed et al., 2019). Both GSLs and thioglucosidases can come into contact if tissue disruption, e.g. through a herbivoric attack, occurs. However, turnover of GSLs also takes place in intact tissues during different developmental stages, or sulfur and nitrogen shortage (Jeschke et al., 2019). It is hypothesized that atypical thioglucosidases are most likely involved in the GSL turnover in intact tissue, because GSL contents were unaffected by the lack TGG1 and TGG2 in germinating *A. thaliana* (Meier et al., 2019). Additionally, the atypical thioglucosidase BGLU18 was reported to be localized in endoplasmic reticulum (ER)-bodies and therefore can be localized in the same cells, though in different organelles, as GSLs (Han et al., 2020).

Once GSLs and thioglucosidases come in contact, an unstable aglucone is formed, quickly reacting to isothiocyanates, thiocyanates, nitriles and epithionitriles depending on the pH, presence of ions and specifier proteins. If specifier proteins are not present, isothiocyanates (ITC) are formed, which can be conjugated to glutathione and further converted to amines and raphanusamic acid (RA) (Jeschke et al., 2019). It has be shown that RA exhibited growth inhibitory actions in Brassicaceae and non-Brassicaceae alike (Inamori et al., 1992). If nitrile specifier proteins (NSP) 1 and 5 or the epithionitrile specifier protein (ESP) are present, the outcome of the reaction is shifted towards generation of nitriles rather than isothiocyanates (Burow et al., 2008; Wittstock et al., 2016).

Degradation of the iGSL glucobrassicin (GB) in the presence of NSP or ESP yields IAN which can be converted to the auxin indole-3-acetic acid (IAA) enhancing the plants biosynthetic options by one further pathway (Figure 1). The most abundant auxin IAA can be synthesized through the indole-3-pyruvic acid pathway common to all plant species. In addition to that, members of the Brassicaceae are able to use IAOX, which is synthesized from tryptophan by CYP79B2/B3, as intermediate for the synthesis of IAA (Figure 1). The IAA precursor IAN is either synthesized directly from IAOX by CYP71A13, or by the synthesis of the iGSL GB and its subsequent breakdown (Malka & Cheng, 2017).

If specifier proteins are not present during the breakdown of GB, an array of breakdown products is produced including indole-3-carbinol (I3C) which readily forms adducts with ascorbic acid (indole-3-methyl-ascorbate or ascorbigen), cysteine (indole-3-methyl-cysteine) and glutathione (indole-3-methyl-glutathione) (Kim et al., 2008). Modelling experiments revealed docking of I3C-derived breakdown products to the auxin receptor transport inhibitor response 1 (TIR1) and hindering formation of the TIR1/IAA complex resulting in auxin antagonistic effects. For some of these products, the calculated dissociation constant was even lower compared to IAA, suggesting a tighter fit of the TIR1 complex and therefore higher antagonistic effects compared to compounds with a looser fit. It was hypothesized, that the GB breakdown regulation can be seen as a molecular switch bringing another possibility to control auxin signaling to the table (Vik et al., 2018).

The effect of water stress on GSL contents was previously observed in *A. thaliana* indicating that behavior of GSLs depends on duration and strength of the applied drought stress. However, either the publication focused on aGSLs, because contents of iGSL were unaltered by drought stress (Salehin et al., 2019), or an increase in aGSLs was only

10.3389/fpls.2022.1025969

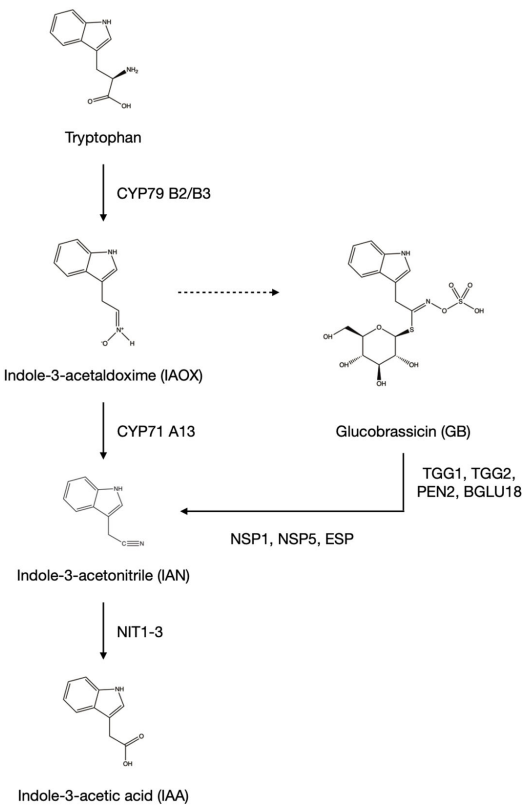

FIGURE 1
Synthesis of indole-3-acetic acid (IAA) in Arabidopsis thaliana. Members of the Brassicaceae family are able to synthesize IAA through additional synthetic pathways starting from indole-3-acetaldoxime (IAOX). IAA is synthesized from the common intermediate indole-3-acetonitrile (IAN), either coming directly from indole-3-acetaldoxime (IAOX), or the breakdown of the indolic glucosinolate glucobrassicin (GB). The dotted line from IAOX to GB indicates multiple steps. The figure was created using ChemDraw Professional Version 20.0.0.38 (PerkinElmer, Waltham, United States).

observed after additional feeding experiments with *Brevicoryne brassicae* (Khan et al., 2010).

It was hypothesized, that IAA can be formed by the breakdown of GB by piecing together different parts of the pathway (Malka & Cheng, 2017). However, no coherent data was published so far analyzing the contents of indolic metabolites and the transcription of enzymes involved in this pathway and therefore a connection between GB and IAA was never shown.

Since higher auxin contents were found to be beneficial to drought-stressed *A. thaliana*, the question arises if GB is used as a considerable source for IAA synthesis (Shi et al., 2014). To answer this question, Col-0 as well as mutants lacking genes in several key IAA synthesis steps were analyzed in control and drought conditions in this study. Analysis of GSL contents and expression analysis give first insights into the contribution of iGSLs to the synthesis of IAA in stress conditions.

2 Experimental procedures

2.1 Plant cultivation

2.1.1 Experiments performed on soil

Seeds were sown on soil (Einheitserde, Sinntal-Altengronau, Germany) and transferred into pots with a diameter of 6 cm one week after germination. Pots were filled uniformly with the same amount of soil by weighing the pots. Samples of the soil used were taken and dried for 24 h at 70°C to determine the dry weight of the soil. Plants were grown for five weeks prior to stress application with a 10 h light/14 h dark cycle at 120 µmol m^2 s^{-1} with a temperature of 21°C at daytime and 18°C at nighttime.

Drought stress was applied by desiccation of pots until the desired water content of 40% w/w was reached and holding that water content for five days by checking weight of the pots and watering if needed with deionized water. Drought stress was applied by holding the water content of the pots at 40% for five days. Plants were harvested in triplicate consisting of three pooled plants on the 5th day after starting withholding water. Drought stress on soil was applied three times with the same outcome. Results of one representative experiment consisting of three biological replicates with three pooled plants each is presented in this study.

2.2 In vitro experiments

Plants were grown on petri dishes (Supplementary Figure 2G–J) containing 25 ml of half strength Murashige & Skoog medium and vitamin mixture solidified with 8 g L^{-1} agarose (Duchefa, Haarlem, Netherlands). Four round disks with a total weight of 5 g were removed from the petri dishes. Seeds were sterilized with 70% ethanol for 5 min, followed by incubation with 6% sodium hypochlorite (Roth, Karlsruhe, Germany) for 10 min under continuous agitation. Seeds were washed five times with sterile ultrapure water. Two seeds were placed on the petri dishes equidistant from two removed disks and the edge of the dish to obtain eight seeds in total per dish. Petri dishes were sealed with micropore tape (3M, Neuss, Germany). After one week of germination, spare seedlings were removed until four seedlings were left. Plants were grown for five weeks prior to stress application with a 10 h light/14 h dark cycle at 120 µmol m^2 s^{-1} with a temperature of 21°C at daytime and 18°C at nighttime. Drought stress was applied by supplying the petri dishes with 5 ml of either 20% or 40% polyethylene glycol (PEG) 20,000 (Sigma-Aldrich, Taufkirchen, Germany) in the previously prepared holes of the agarose for 7 days. Plants subjected to 20% PEG were considered to be mildly drought-stressed (MDS) while plants subjected to 40% PEG were considered to be severely drought-stressed (SDS). After 7 days of drought stress, rosettes and roots of plants were harvested separately and immediately frozen in liquid nitrogen.

One exemplary experiment consisting of three biological replicates consisting of four pooled plants each is presented in this study.

Experiments analyzing SDS plants were performed twice independently *in vitro*. Due to slightly differing overall GSL contents and transcription levels, calculating the mean of the two experiments was refrained from. Instead, all data of the second repetition of the SDS experiment is shown in the supplemental part of this publication.

2.3 Stress status of plants

Water content of leaves was calculated by weighing frozen fresh leaf samples, lyophilization, weighing the dry weight and calculating evaporated water content.

Reactive oxygen species (ROS) were analyzed with a method developed on the basis of the oxygen radical absorbance capacity (ORAC) assay (Huang et al., 2002; Gillespie et al., 2007). Extraction of plant material was performed according to Boestfleisch et al. (2014). Extracts and a 96-well microplate (Greiner Bio-One, Frickenhausen, Germany) were kept on ice and 20 µl of 1:100 diluted extracts and 20 µl of standards, followed by 80 µl 75 mM phosphate buffer (pH 7.4) were transferred to the plate. A serial dilution (11-0.17 mM) of the standard 2,2′-azobis (2-amidino-propane) (AAPH) (Sigma-Aldrich) was prepared using phosphate buffer. Finally, 120 µl 112 nM fluorescin (Sigma-Aldrich) in phosphate buffer was added to the plate. The plate was incubated at 37°C and fluorescence was analyzed after 20 min at 485/520 nm. Destruction of fluorescin by ROS was calculated using the AAPH standard curve and contents are expressed as AAPH equivalents (AAPHE).

2.4 Glucosinolate analysis

Extraction and analysis of GSLs was performed according to Hornbacher et al. (2019). Glucosinolates were identified according to their specific mass fragments: glucoiberin (685, 378, 343), glucoraphanin (713, 392, 357), glucoalyssin (741, 406, 371), glucoerucin (681, 376, 341), glucohirsutin (825, 448, 413), glucobrassicin (735, 403, 368), 4-methoxyglucobrassicin (795, 433, 398) and neoglucobrassicin (795, 433, 398). Because of the exact same molar mass, identity of the two GSLs 4-methoxyglucobrassicin and neoglucobrassicin was assured with GSL analysis of *cyp81F4* which is lacking neoglucobrassicin, but not 4-methoxyglucobrassicin (Kai et al., 2011).

2.5 Analysis of D_2O incorporation into glucosinolates

Plants were grown *in vitro* exactly as stated above. At the beginning of the 7-day-long drought stress period, plants were either subjected to 30% D_2O additionally to 40% PEG 20,000 or 30% D_2O alone. Incorporation of deuterium into GSLs was analyzed by calculating the monoisotopic and isotopomeric percentage of the total GSL content using mass chromatograms. One incorporation experiment consisting of three biological replicates made up of four pooled plants each is presented in this study

2.6 Transcription analysis

RNA isolation and reverse transcription were performed as described by Horst et al. (2009) with modifications. Integrity of isolated RNA was checked by gel electrophoreses. Yield of isolated RNA was between 60-120µg/µl with a ratio of 260/280 between 1.8 and 2.0.

To remove DNA, 1.2 units of DNaseI (ThermoFisher, Dreieich, Germany) per 250 ng of RNA were added and reactions were incubated for 30 min at 37°C, followed by a denaturation step of 15 min at 70°C. Synthesis of cDNA was performed with approximately 250 ng of total RNA, 50 pmol of random nonamer primer (5'NNNNNNNNN3') and 10 pmol oligo-dT primer (5' TTTTTTTTTTTTTTTTT 3'). Reactions were incubated for 5 min at 70°C and cooled down on ice before adding 200 units of Moloney murine leukemia virus reverse transcriptase (Promega, Walldorf, Deutschland) and 1 mM deoxyribonucleotide triphosphates in reaction buffer as specified by the manufacturer. mRNA was amplified from cDNA using primer systems (Supplementary Table S1). All primer systems are located in between one single exon to ensure same product size of DNA standards as well as RNA obtained cDNA templates. Efficiency of DNA digestion was controlled by reactions without reverse transcriptase. To test linearity of cDNA synthesis at least one RNA sample of each extraction was diluted 1:4 and 1:16.

Desalted oligonucleotides were ordered from Eurofins Genomics Germany GmbH. Specificity of primer systems were positively checked *in silico* by Primer-BLAST (Ye et al., 2012), by agarose gel electrophoreses and melting curves. All primer systems are located in between one single exon to ensure same product size of DNA standards as well as RNA obtained cDNA templates. Standard curves were used in every qPCR run. Primer systems were designed in a way that all possible splice variants are measured. See Supplementary Table S1 for primers used.

Quantitative PCR was performed on StepOne™ Plus (Applied Biosystems, Waltham, United States) with fast cycling mode (50°C 2 min, 95°C 2 min, 40 cycles of 95°C 3 sec and 60°C 30sec) using SYBR Green fluorescence (PowerUp™ SYBR™ GreenMaster Mix, ThermoFisher, Dreieich, Germany) for detection. The template concentration was 1/10 of 10 µl total volume. Oligonucleotide concentration was 300 nM each. Melting curve was preformed from 60 to 95°C in 0,3°C steps. Data analysis was done by StepOne™Software Version 2.3. The no template control always showed no amplification. Quantification of samples was done in in the range of the standard curve. Expression is presented relative to the reference gene *EF1α*.

2.7 Analysis of raphanusamic acid, indole-3-acetonitrile and indole-3-acetic acid

Metabolites were extracted with methyl-*tert*-butyl ether (MTBE), reversed phase-separated using an ACQUITY UPLC® system (Waters Corp., Milford, MA, USA) and analysed by nanoelectrospray ionization (nanoESI) (TriVersa Nanomate®; Advion BioSciences, Ithaca, NY, USA) coupled with an AB Sciex 4000 QTRAP® tandem mass spectrometer (AB Sciex, Framingham, MA, USA) employed in scheduled multiple reaction monitoring mode according to Herrfurth & Feussner (2020). The reversed phase separation of constituents was achieved by UPLC using an ACQUITY UPLC® HSS T3 column (100 mm x 1 mm, 1.8 µm; Waters Corp., Milford, MA, USA). Solvent A and B were water and acetonitrile/water (90:10, v/v), respectively, both containing 0.3 mmol/l NH_4HCOO (adjusted to pH 3.5 with formic acid).

For absolute quantification of raphanusamic acid, indole-3-acetonitrile and indole-3-acetic acid, 50 ng 2-oxothiazolidine-4-carboxylic acid (Merck KGaA, Darmstadt, Germany) and 20 ng D_5-indole-3-acetic acid (Eurisotop, Freising, Germany) were added to the plant material before extraction. After extraction, the polar and non-polar phases were combined before drying under streaming nitrogen. Mass transitions and optimized parameters for the detection of these compounds are shown in Supplemental 16.

2.8 Statistical analysis

All statistical analyses were performed using InfoStat Version 2012 (University of Córdoba, Argentina). Analysis of variance (ANOVA) was performed and significant differences ($p<0.05$) were determined using Tukey's test.

3 Results

3.1 Mildly and severely drought-stressed plants showed physiological differences

Arabidopsis thaliana Col-0 plants were subjected to different concentrations of PEG 20,000 to establish mild (MDS) and severe drought stress (SDS) conditions. To ensure reliable differences between treatments, leaf water content, oxidative stress, expression of drought-induced genes and phenotypical analyses were performed.

Leaf water content was significantly lower in MDS and SDS Col-0 plants compared to control plants (Supplementary Figures 2A, B). The difference in water content of 7% between control and SDS plants (Supplementary Figure 2B, Supplementary Figure 3A) was much greater compared to MDS with a difference of 2% (Supplementary Figure 2A). The amount of ROS was significantly higher in MDS and SDS plants compared to control plants and was overall similar in MDS and SDS plants (Supplementary Figures 2C, D, Supplementary Figure 3B). Expression of *P5CS1* was higher in SDS and MDS compared to control plants, but was higher in SDS when compared to MDS plants (Supplementary Figures 2E, F, Supplementary Figure 3C). Overall appearance of plants that were subjected to MDS (Supplementary Figure 2H) were visually not different from control plants (Supplementary Figure 2G), whereas SDS plants were smaller in size, and younger leaves were darker in color (Supplementary Figure 2J) compared to control plants (Supplementary Figure 2I). No signs of senescence or chlorosis indicating severe irreparable damage to the plants were observed in MDS or SDS plants (Supplementary Figures 2H, J).

Overall, MDS and SDS plants differed significantly from controls in all analyzed parameters. Differences were also observed between MDS and SDS plants in leaf water content, expression of *P5CS1* and the phenotypical analysis.

3.2 Glucosinolate contents differed between mildly and severely drought-stressed plants

Single GSL contents were analyzed in leaves and roots of control and DS plants to gain insight into the effects of drought on GSL metabolism.

Contents of all GSLs in leaves of MDS plants were significantly lower compared to control plants (Figures 2A, C; Supplementary Figure 4). Contents of all aGSLs as well as the iGSLs 4-methoxyglucobrassicin and neoglucobrassicin were 2-3-fold lower in MDS compared to control plants (Supplementary Figure 4). On the other hand, contents of the iGSL GB were 4.5 -fold lower in MDS compared to control plants (Figure 2C).

Plants that were SDS, showed lower contents of all aGSLs (Figure 2B, Supplementary Figure 5) and lower contents of 4-methoxyglucobrassicin and neoglucobrassicin in leaves (Supplementary Figures 5E, F), whereas contents of GB were significantly higher in SDS compared to non-stressed control plants (Figure 2D).

Composition of GSLs in *A. thaliana* differed in roots. Glucoiberin, glucoalyssin, glucoerucin, and glucoraphanin were not detected in roots.

Glucobrassicin contents were 16-fold lower in roots (Figure 2F) compared to leaves (Figure 2D), whereas contents of neoglucobrassicin were two times higher in roots compared to leaves (Figures 2K, L; Supplementary Figure 4F; Supplementary Figure 5F). Glucobrassicin and glucohirsutin contents (Figures 2E, G) were slightly higher in roots of MDS compared to control plants, whereas contents of 4-methoxyglucobrassicin were significantly lower in MDS compared to control plants Figure 2I). Neoglucobrassicin contents were similar in control as well as both drought treatments (Figures 2K, L).

In roots, contents of GB were significantly higher in SDS compared to control plants (Figure 2E), whereas contents of glucohirsutin were just slightly higher in SDS plants (Figure 2H). Contents of 4-methoxyglucobrassicin were slightly lower in SDS compared to control plants (Figure 2J).

Analysis of GSLs showed that contents of GB behaved differently in MDS and SDS plants. While its contents were much lower in leaves of MDS plants, higher levels were observed in leaves of SDS plants. In SDS plants contents were significantly higher in all plant parts compared to controls.

3.3 Glucobrassicin showed the highest incorporation of deuterium

To be able to interpret GSL contents correctly and to ensure proper differentiation between breakdown and *de novo* biosynthesis, rate of GSL synthesis was investigated by analyzing incorporation of deuterium into GSL structures. Incorporation was achieved by subjecting control and DS plants to deuterium oxide (D_2O). Total contents and GSL contents with incorporated deuterium (isotopomers) were compared to estimate GSL amounts synthesized during the time of deuterium exposure.

The fraction of isotopomers compared to the total GSL content was significantly lower in all analyzed GSLs in leaves of control plants (Figures 3A–H). Nonetheless, fraction of isotopomers was much higher in the iGSLs GB and 4-methoxyglucobrassicin compared to isotopomeric fractions of aGSLs (Figures 3F, G). While the isotopmeric fraction of GB was 71% and 79% in control and SDS conditions respectively, the

10.3389/fpls.2022.1025969

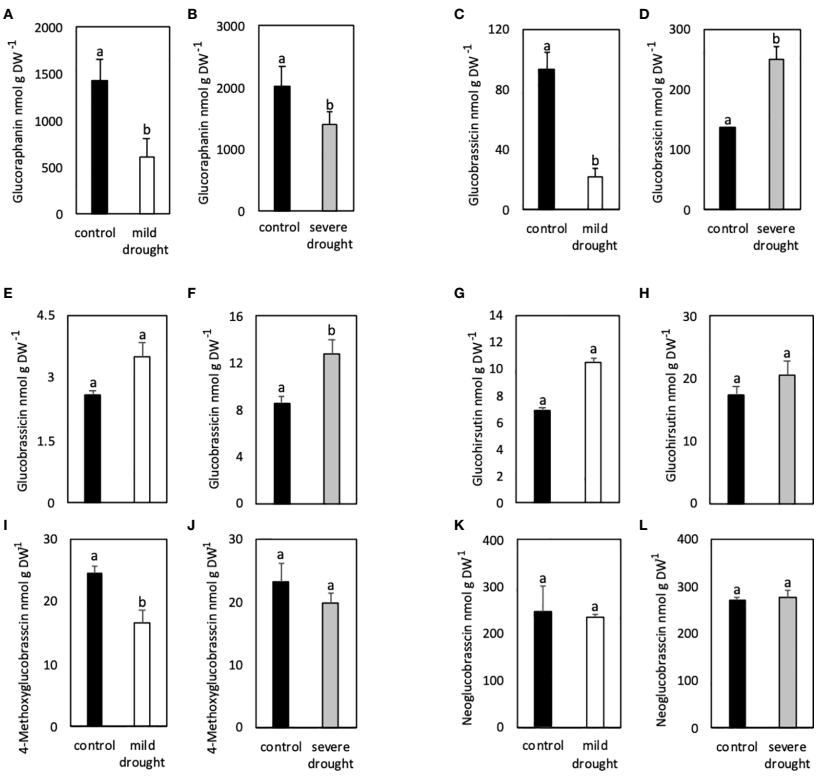

FIGURE 2
Glucosinolate contents in leaves **(A–D)** and roots **(E–L)** of mildly (white bars) and severely (grey bars) drought-stressed *Arabidopsis thaliana* Col-0 plants subjected to 20% and 40% PEG 20,000, respectively, for 7 days. Plants were grown on petri dishes for *five* weeks prior to application of drought stress. Bars represent means of three biological replicates consisting of four pooled plants each. Different letters indicate significant differences ($p<0.05$) between control and drought-stressed plants.

isotopomeric fraction of glucoraphanin was only 40 and 34% respectively. In SDS plants, fractions of isotopomers are significantly lower in all GSLs except for GB when compared to total contents (Figure 3F). Overall, total contents and isotopomeric fractions of GB were higher in SDS plants compared to controls much like SDS Col-0 plants that were not supplemented with D_2O (Figure 2D, Figure 3F). Similarly, total contents of all other GSLs were lower in SDS plants compared to non-stressed controls in the same manner of plants not subjected to D_2O (Figure 2B, Supplementary Figure 5, Figures 3A–E, G, H).

The fraction of isotopomers of glucohirsutin, 4-methoxyglucobrassicin and neoglucobrassicin analyzed in roots was significantly lower compared to the total GSL content in control and SDS conditions (Figures 4B–D). The isotopomeric fraction of GB on the other hand was similar to the total GSL content in both conditions (Figure 4A).

Overall, similar total and isotopomeric contents of GB showed highest deuterium incorporation into this particular GSL in all conditions and organs analyzed. Similarly, high incorporation of deuterium was observed in 4-methoxyglucobrassicin in leaves, but not roots.

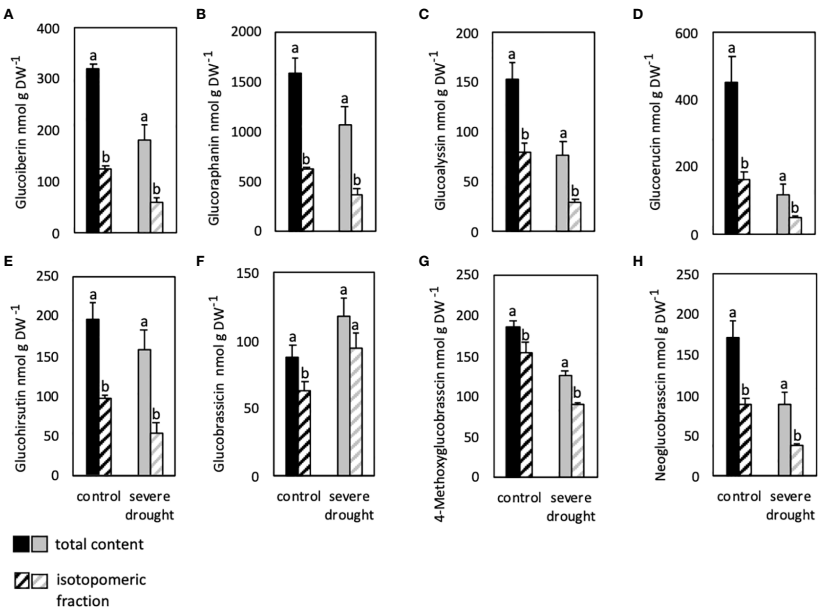

FIGURE 3
Isotopomeric and total contents of aliphatic **(A–E)** and indolic glucosinolates **(F–H)** in leaves of severely drought-stressed *Arabidopsis thaliana* Col-0 plants subjected to 40% PEG 20,000 and 30% D_2O for seven days. Plants were grown on petri dishes for five weeks prior to application of severe drought stress (40% PEG 20,000). Bars represent means of three biological replicates consisting of four pooled plants each. Different letters indicate significant differences ($p<0.05$) between total glucosinolate contents and isotopomeric fractions.

3.4 Expression patterns correlated with stress intensity

Transcription analysis of control and DS plants was performed to gain insight into the expression of genes involved in transport and degradation of GSL and the modification of their breakdown products. Additionally, expression of *CYP71A13* was analyzed to estimate the contribution of the IAOX pathway to IAA synthesis in DS plants.

Expression of the thioglucosidase *BGLU18* was higher in MDS compared to control plants, but difference was only significant in SDS plants compared to controls (Figures 5A, B). Expression of *NSP1* was similar in MDS and control plants, whereas expression of *NSP5* was significantly higher in MDS plants (Figures 5C, E). In SDS plants, expression of *NSP1* and *NSP5* was significantly higher compared to control plants (Figures 5D, F). Expression of *NIT2* was significantly higher in both MDS and SDS when compared to control plants (Figures 5G, H). In SDS plants, expression of *ESP* was significantly higher compared to controls (Figure 5J).

Expression of *GTR1* was significantly higher in MDS and SDS plants compared to controls (Figures 5K, L). Expression of *CYP71A13* was significantly lower in SDS plants compared to controls (Figure 5N).

Expression of genes involved in breakdown (*BGLU18*), modification of breakdown products (*NSP1, NSP5, ESP*) and transport (*GTR1*) were significantly upregulated in DS plants compared to controls. Furthermore, expression of *CYP71A13* was significantly lower in SDS compared to control plants.

3.5 Selected mutants showed differences in contents of reactive oxygen species, glucobrassicin and expression of genes compared to Col-0

To investigate the putative involvement of BGLU18 in the breakdown of iGSLs and the role of ESP in DS plants, mutants lacking these enzymes were analyzed in drought and control conditions. Analysis of ROS contents in *nsp1*, *esp* and *bglu18* revealed significantly higher contents in control and SDS plants

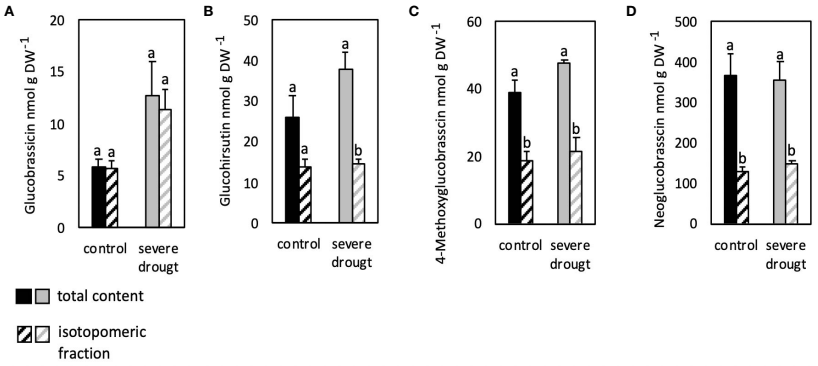

FIGURE 4
Isotopomeric and total contents of aliphatic **(B)** and indolic glucosinolates **(A, C, D)** in roots of severely drought-stressed *Arabidopsis thaliana* Col-0 plants subjected to 40% PEG 20,000 and 30% D_2O for seven days. Plants were grown on petri dishes for five weeks prior to application of severe drought stress (40% PEG 20,000). Bars represent means of three biological replicates consisting of four pooled plants each. Different letters indicate significant differences ($p<0.05$) between total glucosinolate contents and isotopomeric fractions.

when compared to Col-0 (Figure 6A). The differences in ROS content between mutants and wild-type were even more pronounced in SDS plants when compared to control plants.

The difference in GB contents in leaves between SDS and control plants analyzed in *esp* and *bglu18* was significantly larger when compared to Col-0, whereas *nsp1* showed only minor differences (Figure 6B). In roots on the other hand, the difference in GB contents between control and SDS plants was significantly larger in *bglu18* compared to all other genotypes.

Observation of *nsp1*, *esp* and *bglu18* revealed similar expression of *P5CS1* in control and SDS plants compared to Col-0 (Figure 7A). Expression of *NSP1* was higher in *esp* and *bglu18* in DS plants when compared to Col-0 (Figure 7B). Expression of *NSP1* in the *nsp1* mutant was barely detectable. On the other hand, expression of *NSP5* was significantly lower in *esp* and *bglu18* in control plants when compared to Col-0, while expression was only lower in SDS *bglu18* when compared to SDS control plants (Figure 7C). Expression of *NIT2* was significantly lower in SDS *bglu18* in SDS plants when compared to Col-0, while only *nsp1* showed higher contents in control conditions when compared to Col-0 (Figure 7D). Expression of *GTR1* was similar in mutant control plants when compared to Col-0, whereas expression was significantly higher in SDS *nsp1*, *esp* and *bglu18* when compared to SDS Col-0 (Figure 7F). In SDS plants, expression of *CYP71A13* was significantly higher in *esp* and *bglu18* compared to Col-0 (Figure 7G). Expression of *ESP* was significantly lower in *esp* in all conditions, whereas expression in *bglu18* was significantly higher in SDS plants when compared to Col-0 (Figure 7H).

Compared to Col-0, *nsp1*, *esp* and *bglu18* revealed higher contents of ROS and *esp* and *bglu18* showed higher induction of GB contents in DS conditions compared to control plants. Furthermore, expression of *NSP1*, *GTR1* and *CYP71A13* were higher in *esp* and *bglu18* compared to Col-0. Interestingly, expression of *BGLU18* was higher in *esp* and expression of *ESP* was higher in *bglu18* when compared to Col-0 (Figure 7E).

Contents of the GB breakdown product RA were similar in MDS and control plants, whereas contents were significantly lower in SDS compared to control plants (Figures 8A, B). Contents of IAN were lower in MDS when compared to control plants, but significantly higher in SDS compared to control plants (Figures 8C, D). Compared to Col-0, *cyp79B2/B3* and *nsp1* mutants had significantly lower contents of IAN in all conditions, while *esp* showed lower contents only in drought stressed conditions. Contents of IAN were similar in *bglu18* when compared to Col-0 (Figures 8G, H). In all samples the amount of IAA was below the reliable detection limit. Nevertheless, contents of IAA are shown in Figures 8E, F, I, J. Contents of IAA were similar in MDS (Figure 8E), but significantly higher in SDS compared to control plants (Figure 8F). Contents were significantly lower in MDS and SDS *esp*, *bglu18* and *nsp1* mutants compared to Col-0 (Figures 8I, J).

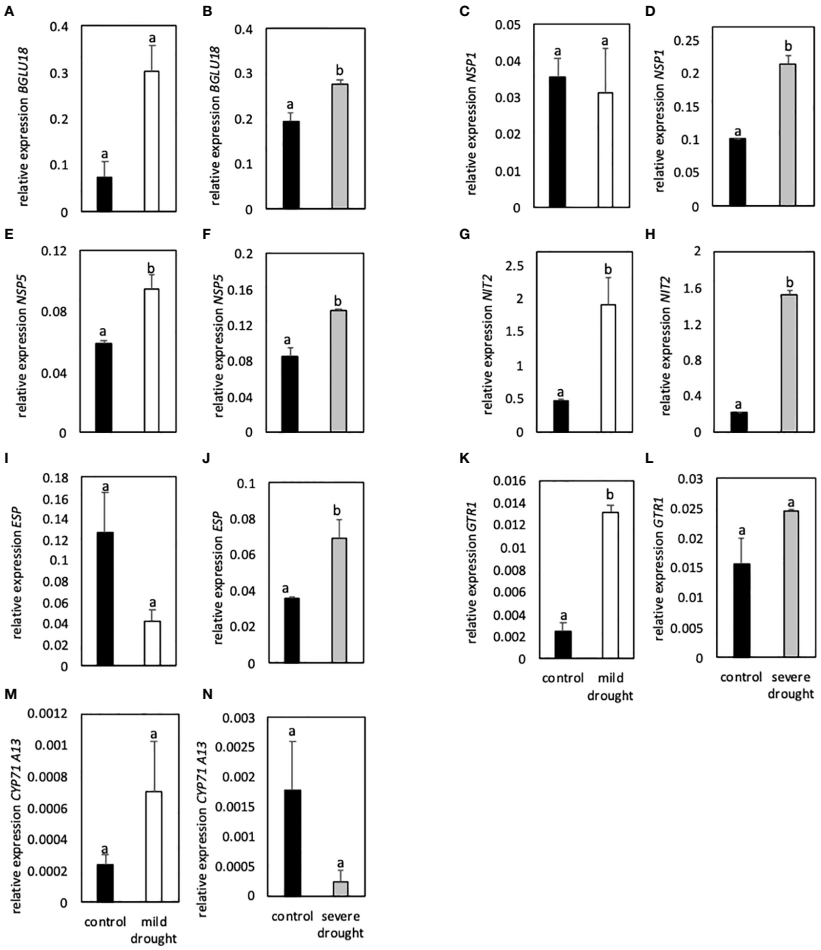

FIGURE 5
Relative expression of genes involved in glucosinolate breakdown (*BGLU18, NSP1, NSP5, ESP;* A-F, I-J), modification of breakdown products (*Nit2, G-H*), transport (*GTR1;* K-L) and synthesis of a key enzyme of indole-3-acetic acid synthesis (*CYP71A13;* M-N) to the reference gene *EF1α*. Plants were either subjected to 20% (mild drought stress, white bars) or 40% PEG 20,000 (severe drought stress, grey bars) for 7 days. Plants were grown on petri dishes for five weeks prior to application of drought stress. Bars represent means of three biological replicates consisting of four pooled plants each. Different letters indicate significant differences ($p<0.05$) between control and drought-stressed plants.

4 Discussion

4.1 Results obtained from plants grown on soil can be replicated *in vitro*

After establishment of a reliable drought stress treatment for *A. thaliana* grown on soil (Supplementary Figure 7, Supplementary Figure 8), an *in vitro* cultivation method was developed to facilitate the harvest of roots. Mild and severe drought stress were applied by subjecting five-week-old plants to 20% and 40% PEG 20,000, respectively, for 7 days.

To draw conclusions about the desiccation status of plants, the leaf water content was analyzed, clearly showing lower leaf water contents in SDS compared to MDS plants (Supplementary

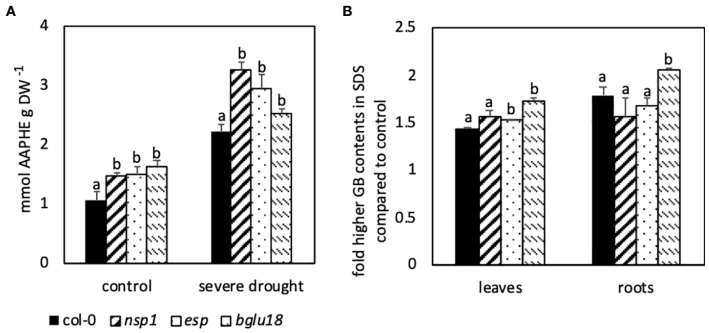

FIGURE 6
Differences in contents of reactive oxygen species (ROS) analyzed as 2,2′-azobis(2-amidino-propane) equivalents (AAPHE; **A**) and in fold higher contents of glucobrassicin (GB, **B**) in different mutants. Five-week-old *Arabidopsis thaliana* plants were subjected to severe drought stress (40% PEG 20,000) for 7 days. Bars represent means of two independent experiments consisting of three biological replicates consisting of four pooled plants each. Different letters indicate significant differences ($p<0.05$) between mutants and the wild-type Col-0.

Figure 2). Nonetheless, leaf water content was significantly lower in both conditions when compared to controls, a clear indication of water loss in both DS conditions.

In order to analyze the amount of drought-induced ROS emerging in the plant, a fast and reliable photometric assay was developed. The higher amount of ROS in DS compared to control plants shows the successful induction of stress in the plants. Elevated levels of ROS were previously reported in DS plants and could therefore be used as reliable DS marker (Qi et al., 2018).

P5CS1 is the rate limiting key enzyme in proline synthesis and therefore a marker for drought stress (Chen et al., 2018).

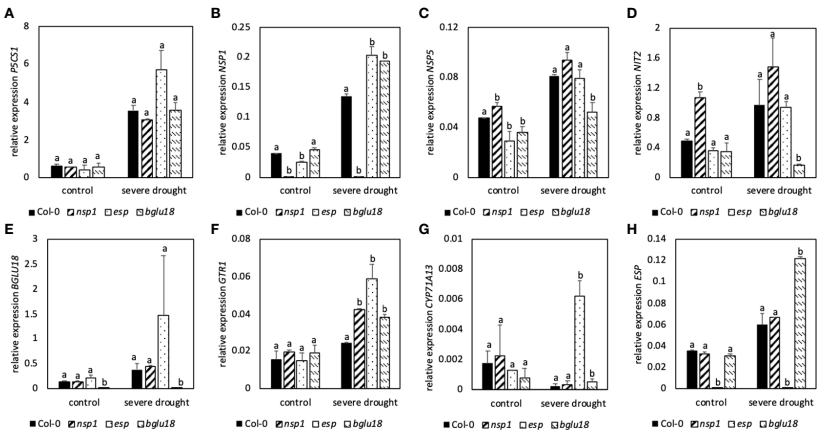

FIGURE 7
Relative expression of genes involved in stress response (P5CS1, A), glucosinolate breakdown (NSP1, B; NSP5, C; ESP, H; BGLU18, E), transport (GTR1, F) and synthesis of indole-3-acetic acid (NIT2, D;CYP71A13, G) to the reference gene EF1α. Plants were subjected to 40% PEG 20,000 (severe drought stress) for 7 days. Plants were grown on petri dishes for five weeks prior to application of drought stress. Bars represent means of three biological replicates consisting of four pooled plants each. Different letters indicate significant differences ($p<0.05$) between Col-0 and mutant plants.

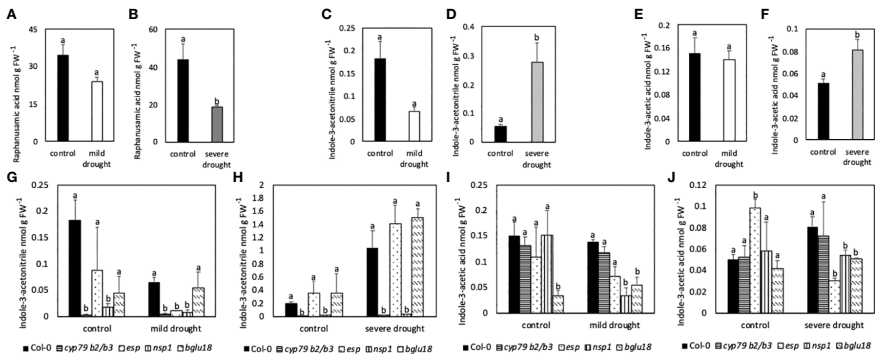

FIGURE 8
Contents of raphanusamic acid (RA; **A, B**), indole-3-acetonitrile (IAN; **C, D, G, H**) and indole-3-acetic acid (IAA, **E, F, I, J**) in leaves of mildly and severely drought-stressed *Arabidopsis thaliana* Col-0 plants and *cyp79B2/B3* and *nsp1* mutants subjected to 20% and 40% PEG 20,000 for seven days. Plants were grown on petri dishes for five weeks prior to application of drought stress. Bars represent means of three biological replicates consisting of four pooled plants each. Different letters indicate significant differences ($p<0.05$) between control and drought-stressed plants **(A–F)** and between Col-0 and mutants **(G–J)**.

Expression of *P5CS1* is highly elevated in SDS plants *in vitro* (Figures 1H, J, in plants grown on soil (Supplementary Figure 8) and MDS plants (Supplementary Figure 1E) when compared to control plants. Higher expression of *P5CS1* in drought conditions was previously described in the literature for *A. thaliana* (Zhang et al., 2016). *In vitro*, expression of *P5CS1* positively correlates with the strength of drought application. Similarly, observations in *Hordeum vulgare* done by Muzammil et al. (2018) showed a positive correlation between duration of drought stress and expression of *P5CS1* indicating higher expression in plants exposed to more severe drought stress. In plants grown on soil on the other hand, expression of *P5CS1* in DS plants is much higher compared to DS plants grown *in vitro*. This might be explained by gradual desiccation of plants on soil compared to instant application of PEG *in vitro*. Soil-grown and drought-stressed plant are therefore exposed to a longer duration of drought stress. Furthermore, plants grown on soil are subjected to higher water loss from stomata compared to *in vitro* plants growing in a humid microclimate.

Nonetheless, most changes in GSL contents and changes in transcription levels observed in plants grown on soil were successfully replicated *in vitro* supporting the reliable establishment of drought stress conditions on soil and *in vitro*.

Lack of chlorosis and senescence indicated that application of drought stress did not lead to irreparable damage to the plants. Furthermore, experiments performed on soil (Supplementary Figures 7, 8) showed more expression of *P5CS1* suggesting a stronger application of drought stress without being detrimental to the plants' overall health.

4.2 Glucosinolates get broken down during drought stress in *Arabidopsis thaliana*

Contents of all GSLs in leaves were significantly lower in MDS compared to control plants (Figure 2). Similarly, contents of all GSLs except GB were lower in SDS plants compared to control plants (Figure 2). Lower GSL levels indicate either lower synthesis rates or breakdown that exceeds the *de novo* biosynthesis.

Incorporation of deuterium into GSLs of SDS plants revealed that only a fraction of the total GSL content of aGSL and neoglucobrassicin was found to have deuterium incorporated. This shows that most of the total content was synthesized before the administration of D_2O (Figure 3). Isotopomeric fractions of aGSLs ranged from 32% - 42% and were 44% for neoglucobrassicin clearly revealing lower biosynthesis rates in SDS compared to control plants.

On the other hand, isotopomeric contents of GB were higher in SDS (80%) compared to control plants (71%). The high incorporation of deuterium into GB shows the increase of an already high synthesis and therefore underlines the need for this particular compound, especially in SDS plants. Furthermore, low contents of GB without incorporation show a high breakdown in control and DS conditions. Both factors highlight the high turnover of GB and indicate the need for a constant supply of GB derived breakdown products. Furthermore, 4.5-times lower contents of GB in MDS compared to control plants points to increased degradation of GB in MDS plants. The turnover of GB probably exceeds the *de novo* biosynthesis in MDS compared to the higher synthesis in SDS plants.

Although expression of classical thioglucosidases *TGG1* and *TGG2* was higher in SDS compared to control plants (Supplementary Figure 15), their contribution to GSL turnover in intact tissue is still a matter of debate (Meier et al., 2019). While TGG1 and TGG2 are transported to vacuoles of myrosin cells (Ueda et al., 2006), the final step of GSL biosynthesis takes place in the cytosol (Klein et al., 2006). Instead, the atypical thioglucosidases PYK10 and PEN2 were identified to be responsible for the turnover of GSLs in undisrupted tissues. PYK10 is localized in ER-bodies (Nakano et al., 2017), and PEN2, is localized in peroxisomes (Bednarek et al., 2009), potentially placing them into close proximity to GSLs. BGLU18, was also found to be localized in ER-bodies (Nakazaki et al., 2019), but its contribution to GSL turnover is still a hypothesis.

4.3 The proteins BGLU18 and ESP, NSP and the metabolite glucobrassicin are tightly interconnected

Significantly higher expression of *BGLU18* in MDS and SDS compared to control plants suggests the putative involvement of BGLU18 in the breakdown of GSLs (Figures 5A, B). BGLU18 is primarily known for the production of abscisic acid from the abscisic acid glycosyl ester and higher expression of *BGLU18* is shown in stress situations such as drought (Sugiyama & Hirai, 2019; Han et al., 2020). The *bglu18pyk10* double mutant showed reduced breakdown of 4-methoxyglucobrassicin in homogenized plant material of *A. thaliana* indicating the involvement of either PYK10 or BGLU18 (Nakazaki et al., 2019). Although levels of GB were unaltered upon homogenization of tissue in the study of Nakazaki et al. (2019), the involvement of BGLU18 in the breakdown of all iGSL in intact tissue cannot be excluded. Contents of GB (Figures 2C, D), its turnover (Figure 3F) and simultaneous expression of *BGLU18, NSP1 and NSP5* were significantly higher in leaves of SDS compared to control plants. This suggests the putative breakdown of GB by BGLU18 and subsequent formation of nitriles by specifier proteins. Similar contents of IAN in bglu18 mutants when compared to Col-0 (Figures 8G, H) indicate the compensation of iGSL breakdown by other thioglucosidases (e.g. TGG1, TGG2). Lower contents of IAA in DS *bglu18* compared to DS Col-0 similarly to contents observed in DS *esp* (Figures 9I, J), indicates a codependence of both enzymes which is reflected in the transcription levels of both enzymes in the mutants (Figures 7E, H). However, the certain involvement of BGLU18 in the breakdown of glucosinolates could not be demonstrated and the involvement of other thioglucosidases should be taken into consideration. Because ESP protein was not yet detected in *A. thaliana* Col-0, its involvement in the formation of IAN from GB is unlikely (Kissen et al., 2012). However, presence of small undetectable quantities of ESP cannot be excluded. Miao and Zentgraf (2007) reported regulatory activity of ESP which would require only minute amounts of protein. The study observed reduced leaf senescence upon interaction of ESP with the transcription factor WRKY63 in Col-0. The interaction requires the presence of an ESP protein and therefore strongly suggests the presence of ESP in Col-0. A connection between ESP, WRKY63 and GSLs was not yet established but possible targets of the transcription factor could be genes involved in the synthesis and breakdown of GB and in the synthesis of IAA. Comparing the differences in GB contents between control and SDS plants in fold changes

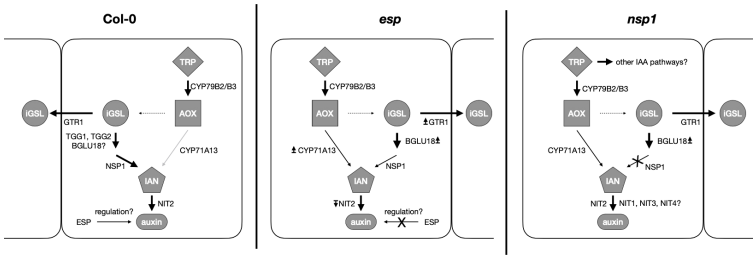

FIGURE 9
Expression patterns in control and drought-stressed Col-0, *esp* and nsp1 *Arabidopsis thaliana* plants. TRP=tryptophan, AOX=Indole-acetaldoxime, iGSL=indolic glucosinolates, IAN=indole-3-acetonitrile, auxin=iGSL derived carboxylic acids. Bold arrows indicate significantly higher expression, light grey arrows indicate lower expression in severely drought-stressed compared to control plants. Arrows near enzymes indicate higher (↑) or lower (↓) expression of genes compared to Col-0. Dashed arrow indicates synthesis steps involving multiple genes. In Col-0 genes expressing proteins responsible for the degradation of glucobrassicin and converting its breakdown products are highly expressed in drought-stressed plants compared to controls. In *esp*, auxin synthesis is redirected towards synthesis directly from AOX. Unchanged expression of *CYP71A13* and *NIT2* in *nsp1* mutants indicates the involvement of other nitrilases leading to depletion of IAN or complete redirection of IAA synthesis to other pathways.

revealed significantly higher values in leaves of *esp* and in leaves and roots of *bglu18* mutants when compared to Col-0. Furthermore, SDS Col-0 showed higher contents of IAA (Figure 8J). However, *esp* mutants seem to be unable to synthesize IAA to the same extent as Col-0. This further indicates, that SDS *esp* mutants are compromised in their ability to synthesize IAA when compared to Col-0. However, it is unclear at this moment why *esp* mutants exhibit altered IAA contents. Unaltered IAN contents in *esp* mutants compared to Col-0 indicates that the effect of missing ESP is not due to a direct enzymatic but rather an indirect regulatory function.

Additionally, *esp* and *bglu18* mutants showed significantly higher contents of ROS in control and SDS conditions when compared to Col-0 (Figure 6A), suggesting a higher stress status due to lack of either enzyme. Better management of ROS accumulation in drought-stressed plants was shown to improve stress tolerance of crops (You and Chan, 2015; Park et al., 2019; Nadarajah, 2020). Therefore, BGLU18, ESP and NSP1 could be potential targets in the selection of more drought tolerant Brassica crops.

4.4 Indole-3-acetonitrile is formed during severe drought

In a study done by Wittstock & Burow (2010), NSPs were shown to aid in nitrile formation upon the breakdown of iGSLs. In another research done by Wittstock et al. (2016), it was shown that *NSP1* and *NSP5* were expressed in leaves, whereas *NSP3-NSP4* were only expressed marginally indicating a higher contribution of NSP1 and NSP5 to nitrile formation in leaves. Significantly higher expression of *NSP5* in MDS compared to control plants indicates increased formation of nitriles from GSLs already in mild drought conditions (Figure 5). However, similar contents of IAN in MDS and control plants and higher expression of *NIT2* indicate the further conversion of IAN to IAA in MDS plants (Figure 7D). In addition to *NSP5*, *NSP1* is significantly higher expressed in SDS compared to control plants, suggesting an increased need of nitrile formation in SDS compared to MDS plants. Significantly higher contents of IAN in SDS and significantly lower contents of RA compared to control plants indicate the favored synthesis of nitriles rather than ITCs in SDS plants (Figures 8B, D). In line with published data of Zhao et al. (2002) and Sugawara et al. (2009), barely detectable contents of IAN in *cyp79B2/B3* mutants shows that IAN is mainly synthesized *via* the CYP79B2/B3 pathway. Contents of IAN (Figures 8E, F) were very low in *nsp1* mutants indicating a major contribution of NSP1 to IAN formation in line with published data (Wittstock et al., 2016; Dörr, 2017). Furthermore, lower expression of *CYP71A13* (Figure 7G) and unaltered expression of *NIT2* (Figure 7D) in SDS *nsp1* mutants compared to control plants indicates the redirection of IAA synthesis to pathways independent of IAOX. In line with this, research of Sugawara et al. (2009) showed that IAN contents were unaltered in cyp71A13 mutants growing under standard conditions indicating the bypass of IAA synthesis by other pathways. Furthermore, IAA synthesis pathways with indole-3-pyruvic acid were hypothesized to be the main IAA synthesis pathway, at least under standard growing conditions (Mashiguchi et al., 2011). Since *cyp79B2/B3* mutants did not exhibit phenotypical alterations in any tested conditions (Supplementary Figure 17) loss of the ability to synthesize IAA thought the CYP79B2/B3 pathway is not reflected in major growth alterations.

However, expression of *CYP71A13* was significantly higher in both SDS *esp* and *bglu18* mutants compared to Col-0 (Figure 7G). This clearly indicates the redirection of auxin biosynthesis towards the aldoxime pathway mediated by CYP71A13 (Figure 9) bypassing the compromised iGSLs pathway.

Overall, *nsp* mutants probably redirect IAA synthesis through pathways completely independently of IAOX. However, *esp* and *bglu18* mutants compensate for the compromised GB breakdown machinery by synthesizing IAN through *CYP71A13* directly.

4.5 Glucobrassicin-derived breakdown products are probably converted to indole-3-acetic acid

Four nitrilase genes *NIT1-NIT4* are encoded in the genome of *A. thaliana*. While NIT4 was shown to detoxify hydrogen cyanide, the *NIT1*-subfamily (*NIT1-NIT3*) seems to have more far reaching functions like protection against pathogens, involvement in senescence and root morphology during sulfur deprivation (Lehmann et al., 2017). Additionally, NIT1-3 were shown to convert IAN to IAA (Vorwerk et al., 2001) connecting the breakdown of iGSLs to the biosynthesis of auxin (Malka & Cheng, 2017). Significantly higher expression of *NIT2* in MDS and SDS compared to control plants clearly shows its importance in DS plants and its putative involvement in the synthesis of carboxylic acids from iGSLs (Figure 5G, H). From the NIT1-subfamily NIT2 was shown to have the highest affinity towards indole-3-acetonitrile, hinting to NIT2 being more involved in the formation of carboxylic acids from iGSLs than other nitrilases (Vorwerk et al., 2001). Higher contents of GB, IAN and IAA (Figures 8D, F) in SDS plants compared to controls suggests the synthesis of IAA from the GB pathway. Additionally, higher expression of *NSP5* and *NIT2* further corroborate this assumption. Higher contents of IAA in DS plants as illustrated in Figure 8F could lead to the increased formation of lateral roots and the subsequent acquisition of water in the root zone. Lateral root formation and enhanced drought tolerance after application of exogenously applied IAA was observed by Shi et al. (2014). Lower contents of IAA in DS

esp and *nsp1* mutants as compared to Col-0 (Figure 8J) could therefore lead to lower drought tolerance and subsequently higher contents of ROS as shown in Figure 6A).

4.6 Glucosinolate contents differ in roots and shoots

Higher incorporation of deuterium into GB compared to other GSLs clearly shows the importance of this compound in leaves (Figure 3A) and roots (Figure 4A) as almost the complete content was synthesized since the administration of deuterium. Nevertheless, contents of GB are much lower in roots compared to leaves (Figure 2). Since GB is the parent GSL to 4-methoxyglucobrassicin and neoglucobrassicin, a conversion seems evident (Pfalz et al., 2011). CYP81F4 is responsible for the conversion of GB to neoglucobrassicin. Expression of *CYP81F4* is much higher in roots (Pfalz et al., 2016), but contents of neoglucobrassicin are also found in leaves raising the question about the contribution of GSL transport.

The GSL transporters GTR1 and GTR2 are known to relocate GSLs into different cells and organs (Jørgensen et al., 2015; Chhajed et al., 2019). They are known to be highly expressed during bolting and seed filling, being responsible for relocation of GSLs to seeds. Plants were neither bolting nor flowering (Supplementary Figures 2G–J), but expression of *GTR1* was significantly higher in MDS and SDS compared to control plants. Therefore, GSLs relocation seems to be important in drought-stressed plants. Significantly higher expression of *GTR1* in SDS *bglu18* and *esp* mutants compared to SDS Col-0 (Figure 7F) further underlines the enhanced need for iGSL relocation. However, the need for relocation of iGSLs raises the question why different iGSLs are needed in separate organs of the plants.

5 Conclusion

In this study, we demonstrate that although *A. thaliana* has a multitude of pathways to yield IAA from, several genes from the iGSL pathway yielding IAA are highly expressed in SDS plants compared to controls. Through deuterium incorporation studies it was shown, that during SDS, GB seems to be one of the most important GSLs, since its contents showed the highest turnover of all analyzed GSLs. Furthermore, the higher level of expression of genes involved in synthesis (*cyp79B2/B3*), breakdown (*BGLU18*, *NSP1*, *NSP5*, *ESP*) and relocation (*GTR1*) of iGSLs and synthesis of IAN (*NIT2*) from which IAA is most likely being formed, strongly suggest the importance of this particular pathway in drought stress compared to control conditions. Finally, we can show that a lack of either BGLU18 or ESP seems to be redirecting auxin biosynthesis to other pathways, including synthesis of IAA directly from IAOX.

Data availability statement

The original contributions presented in the study are included in the article/Supplementary Materials. Further inquiries can be directed to the corresponding author.

Author contributions

JH, IH-N and JP conceived and designed the experiments. JH performed the experiments. Glucosinolate analysis and assessment of stress status was performed by JH. Analysis of raphanusamic acid, indole-3-acetonitrile and indole-3-acetic acid was done by CH and IF. Transcription analysis was performed by IH-N. Sorting of data, graphical design and statistical analysis was performed by JH. Manuscript was written by JH. IH-N, CH, IF and JP discussed and commented on results and manuscript. JP supervised the study. All authors contributed to the article and approved the submitted version.

Funding

IF acknowledges funding through the German Research Foundation (DFG, INST 186/822-1).

Acknowledgments

We are grateful for Sabine Freitag for technical assistance.

Conflict of interest

The authors declare that the research was conducted in the absence of any commercial or financial relationships that could be construed as a potential conflict of interest.

Publisher's note

Supplementary material

The Supplementary Material for this article can be found online at: https://www.frontiersin.org/articles/10.3389/fpls.2022.1025969/full#supplementary-material

References

Bekaert, M., Edger, P. P., Hudson, C. M., Pires, J. C., and Conant, G. C. (2012). Metabolic and evolutionary costs of herbivory defense: Systems biology of glucosinolate synthesis. *New Phytol.* 196, 596–605. doi: 10.1111/j.1469-8137.2012.04302.x

Blažević, I., Montaut, S., Burčul, F., Olsen, C. E., Burow, M., Rollin, P., et al. (2020). Glucosinolate structural diversity, identification, chemical synthesis and metabolism in plants. *Phytochemistry* 169, 112100. doi: 10.1016/j.phytochem.2019.112100

Bednarek, P., Pislewska-Bednarek, M., Svatoš, A., Schneider, B., Doubsky, J., Mansurova, M., et al. (2009). A glucosinolate metabolism pathway in living plant cells mediates broad-spectrum antifungal defense. *Science* 323(5910), 101–106.

Boestfleisch, C., Wagenseil, N. B., Buhmann, A. K., Seal, C. E., Wade, E. M., Muscolo, A., et al (2014). Manipulating the antioxidant capacity of halophytes to increase their cultural and economic value through saline cultivation. *AoB Plants*, 6. doi: 10.1093/aobpla/plu046

Burow, M., Zhang, Z. Y., Ober, J. A., Lambrix, V. M., Wittstock, U., Gershenzon, J., et al. (2008). ESP and ESM1 mediate indol-3-acetonitrile production from indole-3-ylmethyl glucosinolate in *Arabidopsis*. *Phytochemistry* 69, 663–671. doi: 10.1016/j.phytochem.2007.08.027

Chen, Q., Zheng, Y., Luo, L., Yang, Y., Hu, X., and Kong, X. (2018). Functional FRIGIDA allele enhances drought tolerance by regulating the P5CS1 pathway in *Arabidopsis thaliana*. *Biochem. Biophys. Res. Commun.* 495, 1102–1107. doi: 10.1016/j.bbrc.2017.11.149

Chhajed, S., Misra, B. B., Tello, N., and Chen, S. (2019). Chemodiversity of the glucosinolate-myrosinase system at the single cell type resolution. *Front. Plant Sci.* 10. doi: 10.3389/fpls.2019.00618

Dörr, A. F. (2017). *Untersuchungen zur funktionellen charakterisierung von spezifizierenden proteinen des glucosinolatstoffwechsels der brassicaceae* (Braunschweig, Germany: Technische Universität Carolo-Wilhelmina zu Braunschweig). Available at: http://publikationsserver.tu-braunschweig.de/get/64864. doi: 10.24355/dbbs.084-201706201418

Gillespie, K. M., Chae, J. M., and Ainsworth, E. A. (2007). Rapid measurement of total antioxidant capacity in plants. *Nat. Protoc.* 2, 867–870. doi: 10.1038/nprot.2007.100

Han, Y., Watanabe, S., Shimada, H., and Sakamoto, A. (2020). Dynamics of the leaf endoplasmic reticulum modulate β-glucosidase-mediated stress-activated ABA production from its glucosyl ester. *J. Exp. Bot.* 71, 2058–2071. doi: 10.1093/jxb/erz528

Herrfurth, C., and Feussner, I. (2020). Quantitative jasmonate profiling using a high-throughput UPLC-NanoESI-MS/MS method. *Jasmonate Plant Biol.* 2085, 169–187. doi: 10.7551/mitpress/12605.003.0016

Hornbacher, J., Rumlow, A., Pallmann, P., Turcios, A. E., Riemenschneider, A., and Papenbrock, J. (2019). The levels of sulfur-containing metabolites in *Brassica napus* are not influenced by the circadian clock but diurnally. *J. Plant Biol.* 62, 359–373. doi: 10.1007/s12374-019-0143-x

Horst, I., Offermann, S., Dreesen, B., Niessen, M., and Peterhansel, C. (2009). Core promoter acetylation is not required for high transcription from the phosphoenolpyruvate carboxylase promoter in maize. *Epigenetics & chromatin*, 2 (1), 1–11

Huang, D., Ou, B., Hampsch-Woodill, M., Flanagan, J. A., and Prior, R. L. (2002). High-throughput assay of oxygen radical absorbance capacity (ORAC) using a multichannel liquid handling system coupled with a microplate fluorescence reader in 96-well format. *J. Agric. Food Chem.* 50, 4437–4444. doi: 10.1021/jf0201529

Inamori, Y., Muro, C., Tanaka, R., Adachi, A., Miyamoto, K., and Tsujibo, H. (1992). Phytogrowth-inhibitory activity of sulphur-containing compounds. i. inhibitory activities of thiazolidine derivatives on plant growth. *Chem. Pharm. Bull.* 40, 2854–2856. doi: 10.1248/cpb.40.2854

Jørgensen, M. E., Nour-Eldin, H. H., and Halkier, B. A. (2015). Transport of defense compounds from source to sink: Lessons learned from glucosinolates. *Trends Plant Sci.* 20, 508–514. doi: 10.1016/j.tplants.2015.04.006

Jeschke, V., Weber, K., Moore, S. S., and Burow, M. (2019). Coordination of glucosinolate biosynthesis and turnover under different nutrient conditions. *Front. Plant Sci.* 10. doi: 10.3389/fpls.2019.01560

Kai, K., Takahashi, H., Saga, H., Ogawa, T., Kanaya, S., and Ohta, D. (2011). Metabolomic characterization of the possible involvement of a cytochrome p450, CYP81F4, in the biosynthesis of indolic glucosinolate in *Arabidopsis*. *Plant Biotechnol.* 28, 379–385. doi: 10.5511/plantbiotechnology.11.0704b

Khan, M. A. M., Ulrichs, C., and Mewis, I. (2010). Influence of water stress on the glucosinolate profile of brassica oleracea var. *italica* and the performance of *Brevicoryne brassicae* and *Myzus persicae*. *Entomol Exp. Appl.* 137, 229–236. doi: 10.1111/j.1570-7458.2010.01059.x

Khokon, M. A. R., Jahan, M. S., Rahman, T., Hossain, M. A., Muroyama, D., Minami, I., et al. (2011). Allyl isothiocyanate (AITC) induces stomatal closure in *Arabidopsis*. *Plant Cell Environ.* 34, 1900–1906. doi: 10.1111/j.1365-3040.2011.02385.x

Kim, J. H., Lee, B. W., Schroeder, F. C., and Jander, G. (2008). Identification of indole glucosinolate breakdown products with antifeedant effects on *Myzus persicae* (green peach aphid). *Plant J.* 54, 1015–1026. doi: 10.1111/j.1365-313X.2008.03476.x

Kissen, R., Hyldbakk, E., Wang, C. W., Sørmo, C. G., Rossiter, J. T., and Bones, A. M. (2012). Ecotype dependent expression and alternative splicing of epithiospecifier protein (ESP) in *Arabidopsis thaliana*. *Plant Mol. Biol.* 78, 361–375. doi: 10.1007/s11103-011-9869-7

Klein, M., Reichelt, M., Gershenzon, J., and Papenbrock, J. (2006). The three desulfoglucosinolate sulfotransferase proteins in *Arabidopsis* have different substrate specificities and are differentially expressed. *FEBS J.* 273, 122–136. doi: 10.1111/j.1742-4658.2005.05048.x

Kliebenstein, D. J., Kroymann, J., and Mitchell-Olds, T. (2005). The glucosinolate-myrosinase system in an ecological and evolutionary context. *Curr. Opin. Plant Biol.* 8, 264–271. doi: 10.1016/j.pbi.2005.03.002

Lehmann, T., Janowitz, T., Sánchez-Parra, B., Alonso, M. M. P., Trompetter, I., Piotrowski, M., et al. (2017). *Arabidopsis* NITRILASE 1 contributes to the regulation of root growth and development through modulation of auxin biosynthesis in seedlings. *Front. Plant Sci.* 8. doi: 10.3389/fpls.2017.00036

Malka, S. K., and Cheng, Y. (2017). Possible interactions between the biosynthetic pathways of indole glucosinolate and auxin. *Front. Plant Sci.* 8. doi: 10.3389/fpls.2017.02131

Mashiguchi, K., Tanaka, K., Sakai, T., Sugawara, S., Kawaide, H., and Natsume, M. (2011). The main auxin biosynthesis pathway in *Arabidopsis*. *Proc. Natl. Acad. Sci.* 108, 18512–18517. doi: 10.1073/pnas.1108434108/-/DCSupplemental.www.pnas.org/cgi/doi/10.1073/pnas.1108434108

Matiu, M., Ankerst, D. P., and Menzel, A. (2017). Interactions between temperature and drought in global and regional crop yield variability during 1961-2014. *PLos One* 12, e0178339. doi: 10.1371/journal.pone.0178339

Meier, K., Ehbrecht, M. D., and Wittstock, U. (2019). Glucosinolate content in dormant and germinating *Arabidopsis thaliana* seeds is affected by non-functional alleles of classical myrosinase and nitrile-specifier protein genes. *Front. Plant Sci.* 10. doi: 10.3389/fpls.2019.01549

Miao, Y., and Zentgraf, U. (2007). The antagonist function of *Arabidopsis* WRKY53 and ESR/ESP in leaf senescence is modulated by the jasmonic and salicylic acid equilibrium. *Plant Cell* 19, 819–830. doi: 10.1105/tpc.106.042705

Muzammil, S., Shrestha, A., Dadshani, S., Pillen, K., Siddique, S., Léon, J., et al. (2018). An ancestral allele of pyrroline-5-carboxylate synthase1 promotes proline accumulation and drought adaptation in cultivated barley. *Plant Physiol.* 178, 771–782. doi: 10.1104/PP.18.00169

Nadarajah, K. K. (2020). ROS homeostasis in abiotic stress tolerance in plants. *Int. J. Mol. Sci.* 21, 5208. doi: 10.3390/ijms21155208

Nakano, R. T., Piślewska-Bednarek, M., Yamada, K., Edger, P. P., Miyahara, M., Kondo, M., et al. (2017). PYK10 myrosinase reveals a functional coordination between endoplasmic reticulum bodies and glucosinolates in *Arabidopsis thaliana*. *Plant J.* 89, 204–220. doi: 10.1111/tpj.13377

Nakazaki, A., Yamad, K., Kunied, T., Sugiyam, R., Hirai, M. Y., Tamura, K., et al. (2019). Leaf endoplasmic reticulum bodies identified in *Arabidopsis* rosette leaves are involved in defense against herbivory. *Plant Physiol.* 179, 1515–1524. doi: 10.1104/pp.18.00984

Park, J. S., Kim, H. J., Cho, H. S., Jung, H. W., Cha, J. Y., Yun, D. J., et al. (2019). Overexpression of AtYUCCA6 in soybean crop results in reduced ROS production and increased drought tolerance. *Plant Biotechnol. Rep.* 13, 161–168. doi: 10.1007/s11816-019-00527-2

Pfalz, M., Mikkelsen, M. D., Bednarek, P., Olsen, C. E., Halkier, B. A., and Kroymann, J. (2011). Metabolic engineering in *Nicotiana benthamiana* reveals key enzyme functions in *Arabidopsis* indole glucosinolate modification. *Plant Cell* 23, 716–729. doi: 10.1105/tpc.110.081711

Pfalz, M., Mukhaimar, M., Perreau, F., Kirk, J., Hansen, C. I. C., Olsen, C. E., et al. (2016). Methyl transfer in glucosinolate biosynthesis mediated by indole glucosinolate O-methyltransferase 5. *Plant Physiol.* 172, 2190–2203. doi: 10.1104/pp.16.01402

Qi, J., Song, C. P., Wang, B., Zhou, J., Kangasjärvi, J., Zhu, J. K., et al. (2018). Reactive oxygen species signaling and stomatal movement in plant responses to drought stress and pathogen attack. *J. Integr. Plant Biol.* 60, 805–826. doi: 10.1111/jipb.12654

Salehin, M., Li, B., Tang, M., Katz, E., Song, L., Ecker, J. R., et al. (2019). Auxin-sensitive Aux/IAA proteins mediate drought tolerance in *Arabidopsis* by regulating glucosinolate levels. *Nat. Com* 10, 1–9. doi: 10.1101/572305

Shi, H., Chen, L., Ye, T., Liu, X., Ding, K., and Chan, Z. (2014). Modulation of auxin content in *Arabidopsis* confers improved drought stress resistance. *Plant Physiol. Biochem.* 82, 209–217. doi: 10.1016/j.plaphy.2014.06.008

Sugawara, S., Hishiyama, S., Jikumaru, Y., Hanada, A., Nishimura, T., Koshiba, T., et al. (2009). Biochemical analyses of indole-3-acetaldoximedependent auxin biosynthesis in *Arabidopsis*. *Proc. Natl. Acad. Sci. U.S.A.* 106, 5430–5435. doi: 10.1073/pnas.0811226106

Sugiyama, R., and Hirai, M. Y. (2019). Atypical myrosinase as a mediator of glucosinolate functions in plants. *Front. Plant Sci.* 10. doi: 10.3389/fpls.2019.01008

Ueda, H., Nishiyama, C., Shimada, T., Koumoto, Y., Hayashi, Y., Kondo, M., et al. (2006). AtVAM3 is required for normal specification of idioblasts, myrosin cells. *Plant Cell Physiol.* 47, 164–175. doi: 10.1093/pcp/pci232

Vik, D., Mitarai, N., Wulff, N., Halkier, B. A., and Burow, M. (2018). Dynamic modeling of indole glucosinolate hydrolysis and its impact on auxin signaling. *Front. Plant Sci.* 9, 550. doi: 10.3389/fpls.2018.00550

Vorwerk, S., Biernacki, S., Hillebrand, H., Janzik, I., Müller, A., Weiler, E. W., et al. (2001). Enzymatic characterization of the recombinant *Arabidopsis thaliana* nitrilase subfamily encoded by the NIT2/NIT1/NIT3-gene cluster. *Planta* 212, 508–516. doi: 10.1007/s004250000420

Warwick, S. (2011) *Brassicaceae in agriculture. genetics and genomics of the brassicaceae*. Available at: http://www.springer.com/series/7397.

Wittstock, U., and Burow, M. (2010). Glucosinolate breakdown in *Arabidopsis*: Mechanism, regulation and biological significance. *Arabidopsis book/American Soc. Plant biologists*. 8. doi: 10.1199/tab.0134

Wittstock, U., Meier, K., Dörr, F., and Ravindran, B. M. (2016). NSP-dependent simple nitrile formation dominates upon breakdown of major aliphatic glucosinolates in roots, seeds, and seedlings of *Arabidopsis thaliana* Columbia-0. *Front. Plant Sci.* 7. doi: 10.3389/fpls.2016.01821

Ye, J., Coulouris, G., Zaretskaya, I., Cutcutache, I., Rozen, S., and Madden, T. L. (2012). Primer-BLAST: A tool to design target-specific primers for polymerase chain reaction. *BMC Bioinf.* 13, 1–11. doi: 10.1186/1471-2105-13-134

You, J., and Chan, Z. (2015). ROS regulation during abiotic stress responses in crop plants. *Front. Plant Sci.* 6. doi: 10.3389/fpls.2015.01092

Zhang, X., Zhang, B., Li, M. J., Yin, X. M., Huang, L. F., Cui, Y. C., et al. (2016). OsMSR15 encoding a rice C2H2-type zinc finger protein confers enhanced drought tolerance in transgenic *Arabidopsis*. *J. Plant Biol.* 59, 271–281. doi: 10.1007/s12374-016-0539-9

Zhao, Y., Hull, A. K., Gupta, N. R., Goss, K. A., Alonso, J., Ecker, J. R., et al. (2002). Trp-dependent auxin biosynthesis in *Arabidopsis*: Involvement of cytochrome P450s CYP79B2 and CYP79B3. *Genes Dev.* 16, 3100–3112. doi: 10.1101/gad.1035402

Zorn, K., Oroz-Guinea, I., and Bornscheuer, U. T. (2019). Strategies for enriching erucic acid from *Crambe abyssinica* oil by improved *Candida antarctica* lipase a variants. *Process Biochem.* 79, 65–73. doi: 10.1016/j.procbio.2018.12.022

Chapter 5
General Discussion

5.1 Glucosinolates in human nutrition

5.1.1 Glucosinolate contents change during the season in *Nasturtium officinale*

Glucosinolate analysis in *Nasturtium officinale* (chapter 2.1) in the course of one growing season showed changes in the contents of some GSLs. Especially flowering plants showed lower contents of gluconasturtiin, the most abundant GSL in *N. officinale*. In line with this result, GSL contents were shown to be lower in leaves of bolting and flowering *Arabidopsis thaliana* plants (Brown et al., 2003). Relocation of GSLs from leaves to inflorescences mediated by GTR1 and GTR2 was observed by Andersen & Halkier (2014) during bolting. Most importantly, during the growing season emergence of GSLs considered less healthy like progoitrin were not observed. However, fluctuations in total GSL contents in watercress grown under standard growing conditions but different batches ranged from 4.9 µmol g DW^{-1} to 6.6 µmol g DW^{-1} (chapter 2.2) which is comparable to the variation in total contents during the growing season ranging from 5.4 µmol g DW^{-1} to 7 µmol g DW^{-1} (chapter 2.1). Therefore, variation of GSL contents during different developmental stages can be considered as minor, as it does not exceed the variation found in plants grown in different batches.

5.1.2 Anti-inflammatory response due to glucosinolate administration might differ between male and female subjects

The inflammatory markers interleukin cytokine 10 (IL-10), IL-6 and the tumor necrosis factor α (TNFα) were analyzed in subjects receiving 85 g of fresh watercress before and 5 min post exercise in chapter 2.1 and chapter 2.2. In chapter 2.1, contents of IL-10, IL-6 and TNFα were found to be lower 5 min post exercise in subjects who received watercress compared to subjects that received a substitute. In chapter 2.2 on the other hand, contents of IL-6 and TNFα were found to be elevated in subjects receiving watercress even before the exercise. This trend was also observed 5 min after the exercise. However, 3 h post exercise contents of IL-6 and TNFα dropped in subjects that received watercress compared to subjects receiving the substitute. Although the overall response in subjects of both studies shows an overall anti-inflammatory response in subjects receiving fresh watercress, there is a timely difference between the studies. It has to be noted that chapter 2.1 analyzed predominantly female subjects (75% females) while chapter 2.2 analyzed predominantly male subjects (36% females). This could be a factor for the differing results between the two studies. It has been shown by Ioannou et al, (1984) that the bladder of male rats and mice contained significantly higher amounts of AITC compared to their female counterparts after AITC administration.

Furthermore, the study of Bollard et al. (1997) found higher contents of allyl thiocarbamoylcysteine, the n-acetylcysteine conjugate of AITC, in the urine of female mice, while excretion of unconjugated thiocyanate was higher in male mice. These results indicate higher metabolization and excretion of conjugates in female compared to male mice. Excretion and metabolism of ITCs in humans could be similar, leading to a higher detoxification and excretion of ITCs in female subjects compared to male subjects. Furthermore, it was shown that regular consumption of broccoli sprouts reduced contents of IL-6 in human subjects and that the effect persisted after administration stopped (López-Chillón et al., 2019). Since females are known to consume higher amounts of vegetables compared to males, their inflammatory response to GSL containing vegetables could differ compared to males (Mello Rodriguez et al., 2019). This would also explain the overall higher baseline contents of IL-6 in chapter 2.3 compared to 2.2. Since ITCs and nitriles were found to lower levels of IL-6, the contribution of other compounds in the pro-inflammatory response observed in chapter 2.3 is more likely (Navarro et al., 2014; Wang et al., 2018). It has been shown that the composition of the gut microbiome severely influences the generation of breakdown products (Narbad & Rossiter, 2018; Bouranis et al., 2021). Depending on the microbiome composition, GSLs are either not degraded in the gut or converted to nitriles or ITCs. To estimate whether GSLs and their breakdown products are responsible for the cause of changes in inflammatory markers, excretion of GSLs and their breakdown products should be monitored.

5.1.3 The fate of rhamnosyl isothiocyanates in *M. oleifera* is unclear

While many studies are available analyzing the potential breakdown products in plants belonging to the Brassicaceae family (Wittstock et al., 2016; Klopsch et al., 2018; Wang et al., 2019), information about the hydrolysis of the structurally different GSLs present in *Moringa oleifera* is scarce. Investigation of GSL hydrolysis in *M. oleifera* (chapter 2.3) showed almost complete breakdown of all four present GSLs in the first minute. In line with this, published data of Barth and Jander (2006) also showed fast hydrolysis of GSLs present in *A. thaliana*. However, in contrast to ITCs present in *A. thaliana*, rhamnosyl ITCs obtained from *M. oleifera* are structurally relatively stable due to the rhamnosylated phenyl moiety (Waterman et al., 2014). No data is available regarding the fate of rhamnosyl ITCs and how they might be metabolized by microorganisms present in the gut or in liver cells upon ingestion. In chapter 2.3, the fate of rhamnosyl ITCs was compared to the structurally related glucosinalbin, which has a hydroxybenzyl instead of a rhamnobenzyl moiety. Furthermore, the involvement of a putative rhamnosidase was discussed as potentially cleaving off the rhamnose from the benzyl

ring of ITCs resulting in hydroxybenzyl ITC. In fact, α-L-rhamnosidase was shown to convert p-nitrophenyl-α- L-rhamnopyranoside to p-nitrophenol, leaving a hydroxyl group at the phenol ring behind (Yadav et al., 2010). The obtained hydroxybenzyl ITC would therefore be no different from the ITC obtained by the hydrolysis of glucosinalbin (chapter 2.3). However, the detection of benzyl ITC in *M. stenopetala*, a related species with the same GSL pattern as *M. oleifera*, indicates the chemical decomposition of rhamnosyl ITCs to benzyl ITC (Kumar et al., 2021). Although the fate of rhamnosyl ITCs has yet to be elucidated (Fig. 6), no adverse or toxic effects due to administration have been reported in vitro and vivo (Tumer et al., 2015; Jaja-Chimedza et al., 2017; Kim et al., 2018; Fahey et al., 2019).

Chapter 2.1 and 2.2 showed that GSL fluctuations in watercress were minor during a growing season and during cultivation in different batches. Chapter 2.3 showed that rhamnosyl GSLs present in *M. oleifera* are rapidly hydrolyzed upon tissue disruption. However, the fate of rhamnosyl ITCs has yet to be elucidated.

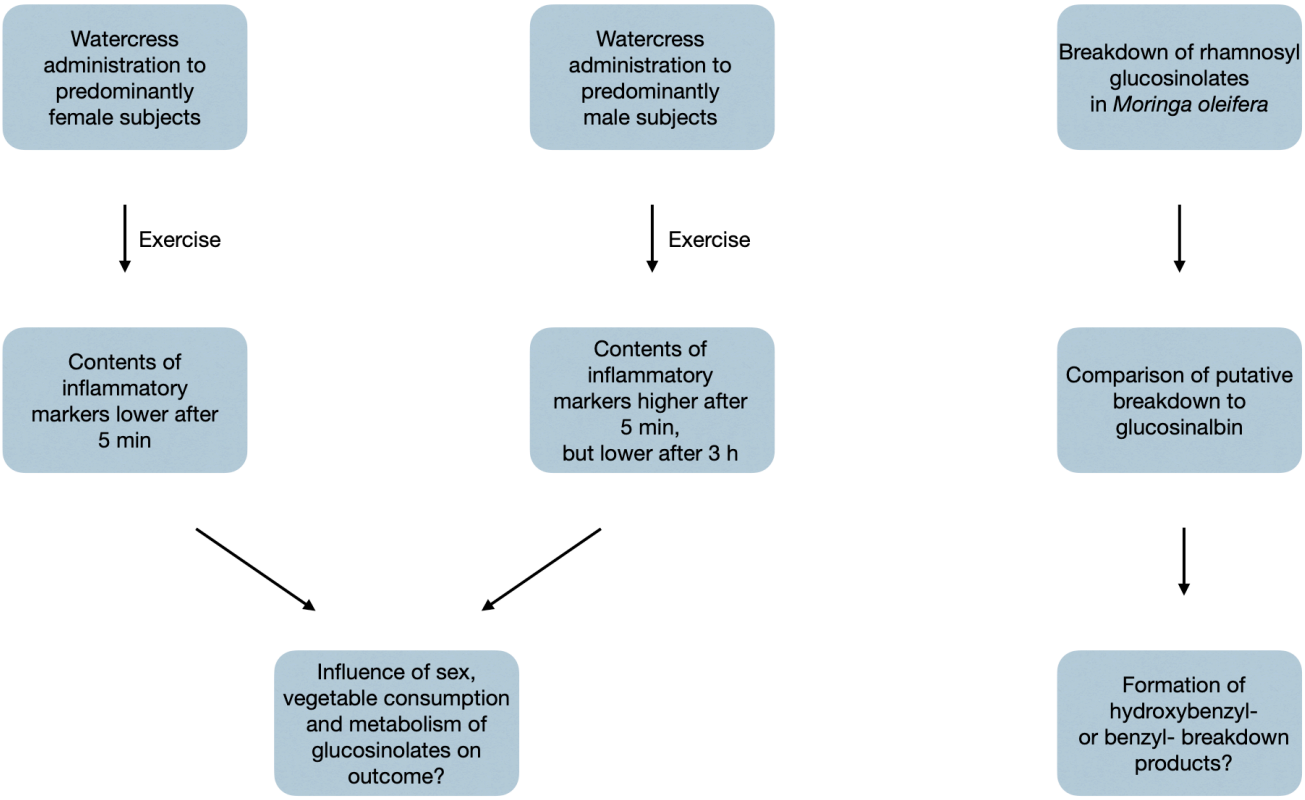

Figure 4: Different outcome of administering fresh watercress in two human trials and putative breakdown products of rhamnosyl glucosinolates in *Moringa oleifera*.

5.2 Glucosinolates in biotic stress

5.2.1 Glucosinolate response might be attributed to hormonal changes in host plants

In chapter 3.1, higher contents of iGSLs and the aromatic GSL gluconasturtiin were observed in *Brassica napus* infected with *Verticillium longisporum*. However, iGSL contents were lower in *Plasmodiophora brassicae* infected *B. napus* cultivars susceptible to the pathogen (chapter 3.2). This indicates that different mechanisms seem to be responsible for the different GSL contents observed depending on the pathogen. Differences in the development of *V. longisporum* and *P. brassicae* could be responsible for the different GSL contents observed in *B. napus*.

The vascular pathogen *V. longisporum* colonizes the xylem of its host where it spends most of its life cycle (Leonard et al 2020). During senescence, the pathogen grows out of the xylem into the stem parenchyma to form microsclerotia (Depotter et al., 2016). Induction of salicylic acid (SA) biosynthesis in *B. napus* in response to an infection with *V. longisporum* was reported by Behrens et al. (2019). The group hypothesized that the SA induction might be mediated by the pathogen to prevent a strong resistance response caused by higher contents of jasmonic acid and ethylene. Thus, the pathogen would be able to form the coexistence observed during the infection in *B. napus*. Interestingly, contents of gluconasturtiin and GB were found to be elevated in response to exogenous application of SA in *B. napus* (Kiddle et al., 1994) and in *B. rapa* ssp. rapa (Thiruvengadam et al., 2016) similarly to results obtained in chapter 3.1. However, it is not clear if higher contents of GB and gluconasturtiin are a results of higher SA contents or a part of the defense mechanism mediated by the plant.

A study conducted by Fröschel et al. (2019) clearly showed that the lacking ability to synthesize iGSL of *A. thaliana* mutants resulted in much higher fungal infestations compared to the wildtype. The breakdown of GB yields either IAN in the presence of NSPs and ESP or indole-3-methyl ITC, which quickly reacts to indole-3-carbinol (I3C). Indole-3-acetonitrile is not only the precursor of IAA (chapter 4.3) but can also be synthesized to indole-3-carboxylic acid (ICOOH), indole-3-carbaldehyde (ICHO) and camalexin (Böttcher et al., 2014; Mulat et al., 2020). In a study performed by Stahl et al. (2016), all three compounds were found to be accumulated in *Pseudomonas syringae* infected *A. thaliana*. Results obtained by Iven et al. (2012) also showed accumulation of ICOOH and camalexin in roots of *A. thaliana* infected with *V. longisporum*. However, only camalexin was shown to directly inhibit growth of the pathogen in that study. Downregulation of several camalexin biosynthesis genes in *A. thaliana* infected with *V. dahliae* was observed in a study conducted by Mo et al. (2015). The study therefore suggested the alteration of camalexin contents by the pathogen. Higher contents of

GB observed in chapter 3.1 hint to an elevation of camalexin precursors by the plants to counteract transcriptional changes mediated by the pathogen. However, analysis of ICHO, ICOOH and camalexin in *B. napus* will be necessary to elucidate the importance of these compounds in this crop.

Secondary zoospores of *P. brassicae* are responsible for the infection of cortical root tissue. After the infection, secondary plasmodia are developed by the pathogen, followed by cell hypertrophy and gall formation (Kageyama & Asano, 2009). Increased contents of free IAA and cytokinin were discussed to be responsible for cell enlargement and gall formation upon an infection with *P. brassicae* by Ludwig-Müller & Schuller (2007). Later on, it was shown by Ludwig-Müller et al (2017) that *A. thaliana nit1* mutants were more resistant to an infection with *P. brassicae* compared to the wild type. Nitrilase 1 was shown to convert IAN to IAA in *A. thaliana*. However free IAA was not significantly changed in *nit1* mutants because of other nitrilases taking over the conversion (Normanly et al. 1997). No difference in GB contents in resistant cultivars upon infection points to the inability of the pathogen to interfere with the breakdown of GB. If GB is degraded in the absence of NSPs and ESP, I3C and several I3C conjugates are formed which were shown to exhibit auxin-antagonistic effects. Metabolites downstream of IAN on the other hand exhibited effects similar to auxin (Katz et al., 2015; Gang et al., 2018). The study of Ludwig-Müller et al. (1993) found that concentrations of IAA were higher in *P. brassicae* infected *Brassica oleraceae var. pekinensis* plants. In line with these results, it was shown that a susceptible *B. napus* variety Hornet showed higher expression of NIT1, catalyzing the conversion of IAN to IAA (Prerostova et al., 2018). It was shown that exogenously applied IAA enhanced root gall formation in *B. napus* showing the positive influence of IAA to root gall growth (Xu et al., 2016). The pathogen might increase GB breakdown which would result in lower contents upon infection as observed in chapter 3.2. Subsequent formation of IAN which can yield IAA and other auxinic substances like ICHO and ICOOH, might be favored by the pathogen through transcriptional interference. The higher synthesis of auxinic substances would therefore aid in gall proliferation caused by *P. brassicae*.

Furthermore, the study of Ludwig-Müller et al. (2017) showed higher resistance of *A. thaliana* 35S::CKX1 cytokinin oxidase overexpressors. Cytokinine oxidase was shown to be responsible for the irreversible degradation of cytokinin (Avalbaev et al., 2012). Therefore 35S::CKX1 overexpressors seem to be more resistant due to their ability to degrade cytokinin synthesized by *P. brassicae* and therefore counteract the formation of galls upon an infection. However, changes in GSL contents in *B. napus* upon an infection with *P. brassicae* are unlikely the result of hormonal changes but rather caused by drastic morphological changes of the root.

5.2.2 Gluconasturtiin seems to be an important part of plant immunity

Direct effects of GSL breakdown products should also be taken into consideration as a plant mediated defense strategy since contents of gluconasturtiin were also highly elevated upon an infection with *V. longisporum* (chapter3.1). Results of Neubauer et al. (2014) showed a higher toxicity of PEITC, the corresponding ITC of gluconasturtiin, to *V. dahliae* microsclerotia compared to ITCs generated from aGSLs. The plant might increase contents of gluconasturtiin and other GSLs to directly reduce growth of *V. longisporum* mycelium in the plant. The study of Wang et al. (2020) showed decreased germination of *Alternaria alternata* spores to benzyl ITC incubation in a dose dependent manner. Furthermore, cell integrity was severely compromised by benzyl ITC resulting in cellular leakage. Similar effects on *A. alternata* spore germination and membrane integrity were observed as a result of 2-PEITC application by Zhang et al. (2020). Lower contents of gluconasturtiin in susceptible cultivars of *B. napus* observed in chapter 3.2 upon infection with a more virulent strain of *P. brassicae* might be caused by the interference of the pathogen with GSL biosynthesis genes. By repressing gluconasturtiin synthesis, the plant would be left with less substrate to produce active breakdown products.

However, no information is available on the possible interference of this pathogen with the plants' expression machinery. It is therefore more likely that susceptible varieties are unable to synthesize sufficient gluconasturtiin upon an infection. Higher breakdown and insufficient de novo biosynthesis would therefore result in observed lower contents. An infection of plants with *P. brassicae* and subsequent gall formation was found to interfere with water and nutrient uptake, indicating that GSL synthesis might also be compromised (Akahoshi et al., 2019). The difference in gluconasturtiin contents in plants infected with two *P. brassicae* pathotypes differing in their virulence might be explained by higher degradation of gluconasturtiin. The plant might therefore counteract the more aggressive growth of the more virulent pathogen with increase breakdown resulting in lower contents of gluconasturtiin compared to the less virulent pathotype. Because of nutrient scarcity, de novo biosynthesis of gluconasturtiin might be decreased resulting in lower contents as observed in chapter 3.2.

An infection of *B. napus* with *V. longisporum* was found to result in higher contents of iGSLs and gluconasturtiin (Fig. 7). Changes in GSL contents might be the result of higher SA contents reported in plants infected with this pathogen. Indolic GSLs and gluconasturtiin might be hydrolyzed by the plants to generate toxic breakdown products in order to reduced fungal

growth in the plant. Furthermore, hydrolysis of iGSLs can yield an array of defense compounds that were shown to be active against pathogens.

An infection of *B. napus* with *P. brassica* was shown to result in lower GSL contents in the plant. This observation might be attributed to the use of iGSLs for auxin biosynthesis by the pathogen in order to aid gall formation. Furthermore, decreased availability of nutrients because of changed root morphology or the interference of the pathogen with GSL biosynthesis genes could be reasons for lower GSL contents in infected plants.

Based on GSL contents alone the mechanism behind higher or lower contents is difficult to dissect. To verify an assumed higher biosynthesis, expression of genes involved in GSL biosynthesis or their regulation need to be analyzed. Expression analysis of genes involved in degradation of GSLs would support hypotheses regarding the synthesis, since lower degradation would also result in higher GSL contents. Furthermore, expression of genes involved in the synthesis of breakdown products need to be investigated to ensure higher IAA contents are derived from the breakdown of GB.

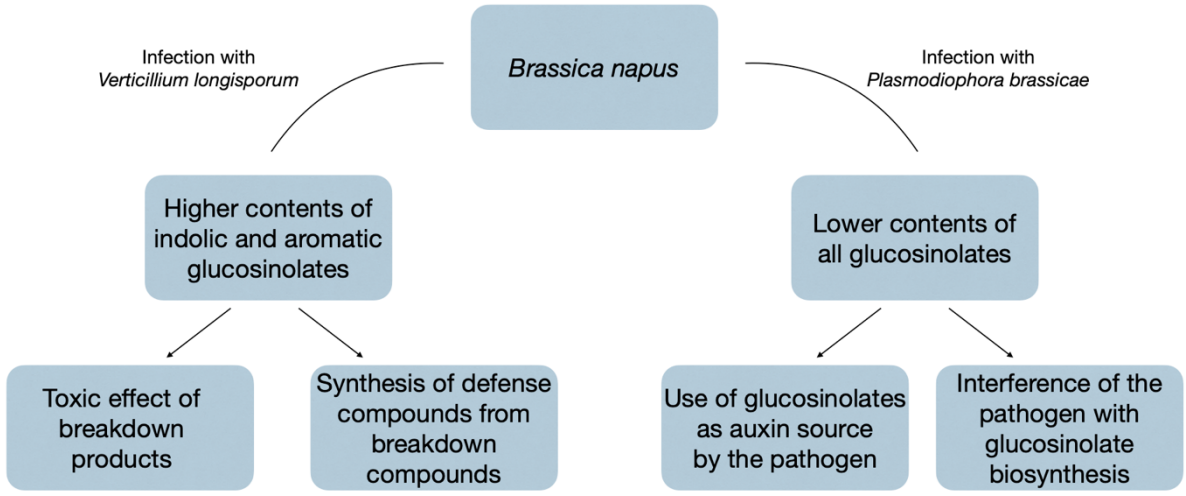

Figure 5: Different response of glucosinolate contents in *Brassica napus* to an infection with either *Verticillium longisporum* or *Plasmodiophora brassicae*.

5.4 Glucosinolate contents in abiotically stressed plants

5.4.1 How glucosinolate contents are displayed matters

Results from chapter 4.1 showed that genes encoding the sulfate transporters *BnSULTR3;1* and *BnSULTR4;2* follow a circadian expression pattern matching the circadian expression of *CCA1* in *B. napus*. These results are in agreement with findings of Huseby et al. (2013) showing that sulfur uptake and incorporation of sulfur into proteins and thiols is higher during the day than in the night in *A. thaliana*. The study also reported higher contents of GSH during the day and decreasing contents during the night, which matches the results obtained in chapter 4.1. The lowest incorporation of ^{35}S into GSLs was observed during the night, while incorporation was found to be higher during the day in the study conducted by Huseby et al. (2013). However, the incorporation of ^{35}S was not reflected in the oscillation of GSL contents, which showed almost no variation in that study. The choice to display GSL contents as a sum of total GSL instead of GSL groups might be an explanation for the missing fluctuation in GSL contents observed by Huseby et al. (2013). Results obtained in chapter 4.1 clearly showed a timely difference in the oscillation of aGSLs compared to the ones of iGSLs and gluconasturtiin. While iGSLs and gluconasturtiin had their highest accumulation at the end of the light and the dark phase the peak accumulation of aGSLs was observed in an oscillation that showed a timely delay to the other groups. If GSLs were presented as the total sum of GSLs, oscillation would have been less pronounced and differences between the GSL groups would have been left unnoticed.

5.4.2 Oscillation of GSL contents might not only be the result of synthesis

The expression of genes *CYP79B2* and *CYP83B1* involved in the synthesis of iGSLs was shown to oscillate in a diurnal fashion with peak expression during the night in *A. thaliana* by Lei et al. (2019). However, a diurnal pattern of iGSL contents could not be observed in chapter 4.1. The oscillations in iGSL contents observed in chapter 4.1 followed an ultradian pattern with a peak during the end of the day and night. However, this pattern was shifted when plants were exposed to insufficient sulfur. As GSL contents are not only controlled by biosynthesis but also by their degradation, the timely expression pattern of thioglucosidases has to be taken into consideration. The expression of the thioglucosidases *PEN2* was observed to follow a diurnal pattern with peak expression at the end of the day (Yamaura et al., 2020). These results only fit to the iGSL contents observed in *B. napus* plants exposed to insufficient sulfur (chapter

4.1). However, expression of other thioglucosidases might be subjected to other oscillation patterns.

5.4.3 Harvesting might have diminished glucosinolate oscillations

In chapter 4.1 obtained results regarding the GSL oscillation in *B. napus* showed clear oscillations on the one hand, but are difficult to interpret on the other hand. The first thing that has to be noticed is the discrepancy of the harvest time points that are exactly 24 h apart (e.g. 0 h and 24 h, 4 h and 28 h, etc.). Hypothetically, the data obtained at those two time points should be similar when light is considered to be the external zeitgeber. However, the clear oscillation pattern at the beginning of the sampling is diminished in the course of the experiment, especially when looking at iGSLs and gluconasturtiin. This hints to external factors influencing the GSLs oscillation observed in chapter 4.1. Plants analyzed in chapter 4.1 were grown in controlled climatic conditions, keeping temperature, light and humidity at set values. In order to harvest plants, this controlled environment had to be accessed, which inevitably leads to changes in temperature and humidity potentially affecting not harvested plants remaining in the climatic chamber. The study of Chowdhury et al. (2021) found GSL contents to be altered in *Brassica oleracea* var. *alboglabra* Bailey depending on the humidity level the plants were exposed to during growth. However, the effect of a short change in humidity level on GSL content is questionable. Temperature was also observed to have an effect on GSL contents, indicating that disruption of the temperature homeostasis could have an effect on the observation of the GSL oscillation in plants (Chowdhury et al., 2021; Ljubej et al., 2021). Although short term change of humidity and temperature alone might only have small effects, their simultaneous change might have additive effects on GSL contents.

5.4.4 Glucosinolate contents are altered in nutrient deficient plants

When exposing plants to salt stress (chapter 4.2), obtained results are difficult to attribute to the osmotic or ionic stress the plants were exposed to (Amjad et al., 2015). Ionic stress reduces the uptake of essential cations like Ca^{+} and K^{+} (Amjad, 2015), while the osmotic part of the stress interferes with water homeostasis in the plants (Abdelaal et al., 2020).

Glucosinolate contents were shown to be elevated in plants exposed to potassium deficiency (Farahani et al., 2021; Son et al., 2021). Unfortunately, no information is available about the underlying mechanism. However, because of the involvement of potassium in water homeostasis, higher contents of glucosinolates might be a direct effect of potassium deficiency (Hasanuzzaman et al., 2018).

5.4.5 Glucosinolates might aid in stomatal closure

Contents of the aGSL sinigrin were observed to be significantly higher in *Lepidium latifolium* exposed to NaCl in chapter 4.2. Higher contents of sinigrin were also observed in *Brassica carinata* observed by Maina et al. (2021). The higher contents in salt-stressed plants can be explained by the contribution of allyl ITC (derived from sinigrin) to aperture of stomata and therefore its involvement in water homeostasis (Afrin et al., 2020). The same study also found that benzyl ITC (derived from glucotropaeolin) and PEITC (derived from gluconasturtiin) were highly effective in stomatal closure. Although the contents of glucotropaeolin and gluconasturtiin are much lower compared to sinigrin in *L. latifolium*, their effect on stomatal aperture was found to be significantly higher compared to allyl ITC (Afrin, 2020). Furthermore, both GSLs could be localized in or transported to guard cells which were found to be abundant in TGGs (Rhaman et al., 2020). The degradation of GSLs in order to evoke stomatal closure would also result in lower contents as observed in chapter 4.2 if de novo biosynthesis is not elevated as well.

5.4.6 Aromatic and indolic glucosinolates are potential precursors of auxins

Contents of glucotropaeolin were observed to be lower in *L. latifolium* subjected to salt stress compared to non-stressed plants in chapter 4.2. This indicates an enhanced breakdown in salt-stressed plants. Research performed by Bhat et al. (2021) showed expression of genes encoding NSP1-5 and ESP in *L. latifolium* indicating the presence of functional specifier proteins. Depending on the expression of NSPs and ESP in conditions like salt stress, nitrile formation could be favored upon hydrolysis of GSLs. Research of Williams et al. (2009) showed formation of benzyl cyanide (= phenylacetonitrile, nitrile formed upon hydrolysis of glucotropaeolin) in the related species *L. sativum*. The study of Urbancsok et al. (2017) showed that exogenously applied benzyl cyanide is converted to phenylacetic acid by NIT2. Furthermore, effects of phenylacetic acid similar to auxin including inhibited primary root growth, formation of lateral roots and inhibition of shoot growth were observed upon administration of exogenous benzyl cyanide and phenylacetic acid in that study. Therefore, lower contents of glucotropaeolin observed in chapter 4.2 could be attributed to higher breakdown of this glucosinolate in salt-stressed plants in order to modify root structure. As *L. lepidium* plants as described in chapter 4.2 were exposed to increasing concentrations auf NaCl, these results can be compared to the ones obtained by Galvan-Ampudia & Testerink (2011). *Arabidopsis thaliana* plants that were exposed to a NaCl gradient in the study of Galvan-Ampudia & Testerink (2011) showed increased formation of lateral roots.

Lower contents of GB were observed only in MDS *A. thaliana* plants compared to controls in chapter 4.3, while contents of GB were always lower in *L. latifolium* exposed to salt compared to controls in chapter 4.2. The way in which the stress was applied could have contributed to differing results in chapter 4.2 and 4.3. Plants described in chapter 4.2 were exposed to gradually increasing NaCl concentrations which increased the duration of stress on the one hand but also increased the time to adapt. Plants in chapter 4.3 were exposed to PEG 20,000, which exposed them to immediate osmotic stress. Therefore, results obtained in both experiments can hardly be compared to each other.

The experimental design of chapter 4.3 considered the shortcomings of previous experiments performed and included the incorporation of deuterium into GSLs and transcription analyses in order to understand the nature of GSL contents. Incorporation studies revealed that higher GSL contents are indeed the result of higher biosynthesis. Furthermore, transcription analyses suggest the breakdown of GB to IAN which might subsequently be synthesized to IAA in drought stressed plants.

Contents pf IAN and IAA were shown to be significantly higher in SDS plants compared to controls in chapter 4.3. As IAA is differently distributed among organs and exerts its function through gradients, the analysis of whole organs could be misleading (Tanaka et al., 2006; Michniewicz & Brewer, 2007; Mellor et al., 2020). As de novo biosynthesis of IAA was shown to be higher in young *A. thaliana* leaves, synthesis and breakdown rate of GB might be correlated in those tissues (Ljung et al., 2001). Therefore, separate analysis of young and old rosette leaves as well as the separation of roots and root tips would be necessary to observe stronger effects.

Because IAN can also be synthesized directly through the IAOX pathway, the precursor of IAN and IAA in DS plants is evident but not certain. Therefore, the contribution of GB to the IAA pool can only be assured by the analysis of the fate of labelled GB. Similarly, IAA synthesis was analyzed with ^{15}N-anthranilate and $^{2}H_5$-tryptophan revealing tryptophan dependent and independent pathways (Normanly et al., 1993). By feeding control and DS plants with labelled GB, its fate could be clearly identified and its contribution to the IAA synthesis finally revealed. Nevertheless, chapter 4.3 grants an insight into GSL synthesis and degradation in DS plants and its potential contribution to IAA synthesis, which has not been done so far.

Analysis of the GSL changes in *B. napus* revealed rhythmic changes of all GSL groups (Fig. 8). However, the reason behind those changes might be due to change of biosynthesis or degradation. Salt-stressed *L. latifolium* plants showed higher contents of sinigrin, which might

be involved in water homeostasis. *Arabidopsis thaliana* plants exposed to DS showed higher contents of GB, which might be used as a precursor for the synthesis of IAA.

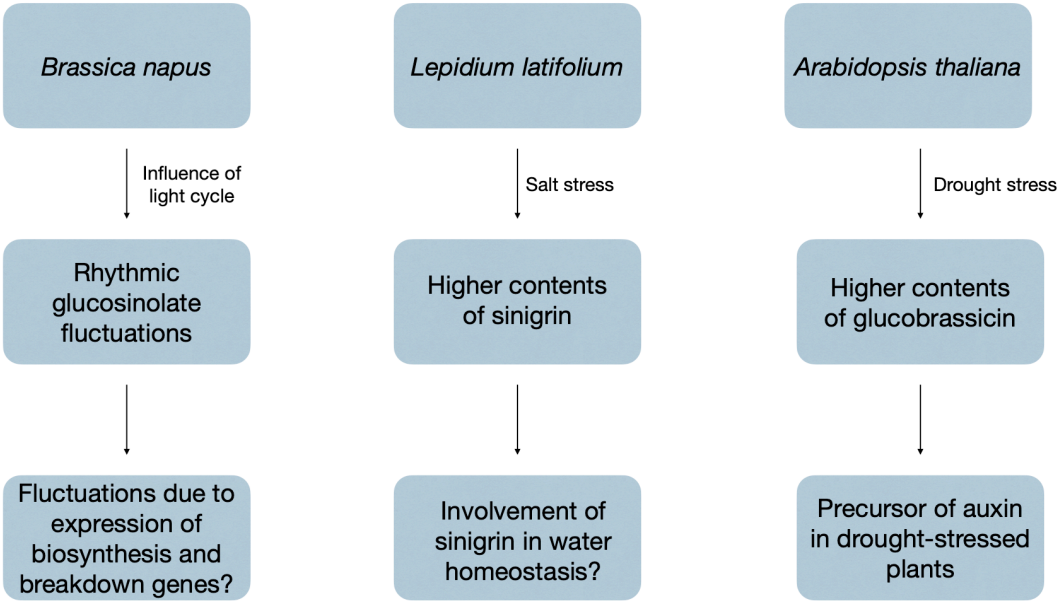

Figure 6: Effects of the light cycle in *Brassica napus*, salt stress in *Lepidium latifolium* and drought stress in *Arabidopsis thaliana* on glucosinolate contents.

Future implications

Understanding the contribution of GSLs to abiotic stress tolerance and to the resistance of plants against pathogens is important in order to create plants that are able to withstand stress. Increasing contents of certain GSLs might also increase the nutritional value of produced crops, as some were shown to improve human health. However, GSL contents alone are difficult to interpret since information about biosynthesis and breakdown are missing. When conducting future experiments, analysis observing the synthesis and breakdown of GSLs in addition to metabolite analyses should therefore be included. Furthermore, gene expression analyses could provide valuable insights into the regulation of synthesis and breakdown of GSLs and related compounds.

Conclusions

Contents of GSL were changed in *N. officinale* in the course of a growing season. However, changes in contents can be considered as minor. Anti-inflammatory responses were observed after the administration of fresh watercress, which could be attributed to GSLs and their breakdown products.

Different changes in GSL contents were observed depending on the pathogen analyzed. Higher contents of GB and gluconasturtiin were observed as a result of infection with *V. longisporum*, which might be attributed to hormonal changes in the plant. Lower contents of all GSLs upon an infection with *P. brassicae* might be attributed to the involvement of the pathogen in GSL synthesis or breakdown.

Salt-stressed *L. latifolium* and DS *A. thaliana* showed different changes in GSL contents depending on the stress applied. Enhanced contents of sinigrin might aid in stomatal aperture and therefore regulate water homeostasis. Increased biosynthesis of GB was observed in *A. thaliana* as an effect of DS. Higher contents of GB might be used as an additional source for IAA in DS plants.

References

Abdelaal K, Hafez Y and Mazrou Y (2020) Silicon foliar application mitigates salt stress in. Plants **9**: 733–748.

Afrin S, Okuma E, Tahjib-Ul-Arif M, Jahan MS, Nakamura T, Nakamura Y, Munemasa S and Murata Y (2020) Stomatal response to isothiocyanates in *Arabidopsis thaliana*. J Exp Bot **71**: 6921–6931. doi: 10.1093/jxb/eraa420.

Akahoshi K, Motomura-wages S, Shintaku M and Hamasaki RT (2019) Clubroot disease of Crucifer crops. **103**: 1–5.

Amjad M, Akhtar SS, Yang A, Akhtar J and Jacobsen SE (2015) Antioxidative response of quinoa exposed to iso-osmotic, ionic and non-Ionic salt stress. J Agron Crop Sci **201**: 452–460. doi: 10.1111/jac.12140.

Andersen TG and Halkier BA (2014) Upon bolting the GTR1 and GTR2 transporters mediate transport of glucosinolates to the inflorescence rather than roots. Plant Signal Behav **9**: 10–12. doi: 10.4161/psb.27740.

Avalbaev AM, Somov KA, Yuldashev RA and Shakirova FM (2012) Cytokinin oxidase is key enzyme of cytokinin degradation. Biochemistry (Moscow), **77**: 1354-1361.

Barth C and Jander G (2006) *Arabidopsis* myrosinases TGG1 and TGG2 have redundant function in glucosinolate breakdown and insect defense. Plant J **46**: 549–562. doi: 10.1111/j.1365-313X.2006.02716.x.

Behrens FH, Schenke D, Hossain R, Ye W, Schemmel M, Bergmann T, Häder C., Zhao Y, Ladewig L, Zhu W and Cai D (2019). Suppression of abscisic acid biosynthesis at the early infection stage of *Verticillium longisporum* in oilseed rape (*Brassica napus*). Mol Plant Pathol **20**: 1645-1661.

Bhat R, Faiz S, Ali V, Khajuria M, Mukherjee D and Vyas D (2021) Effect of temperature and insect herbivory on the regulation of glucosinolate-myrosinase system in *Lepidium latifolium*. Physiol Plant **172**: 53–63. doi: 10.1111/ppl.13289.

Böttcher C, Chapman A, Fellermeier F, Choudhary M, Scheel D and Glawischnig E (2014) The biosynthetic pathway of indole-3-carbaldehyde and indole-3-carboxylic acid derivatives in *Arabidopsis*. Plant Physiol **165**: 841–853. doi: 10.1104/pp.114.235630.

Bollard M, Stribbling S, Mitchell S and Caldwell J (1997). The disposition of allyl isothiocyanate in the rat and mouse. Food and chemical toxicology, **35**: 933-943.

Bouranis JA, Beaver LM, Choi J, Wong CP, Jiang D, Sharpton TJ, Stevens JF and Ho E (2021) Article composition of the gut microbiome influences production of sulforaphane-nitrile and iberin-nitrile from glucosinolates in broccoli sprouts. Nutrients **13**: 3123. doi: 10.3390/nu13093013.

Brown PD, Tokuhisa JG, Reichelt M and Gershenzon J (2003) Variation of glucosinolate accumulation among different organs and developmental stages of *Arabidopsis thaliana*. Phytochemistry **62**: 471–481. doi: 10.1016/S0031-9422(02)00549-6.

Chowdhury M, Kiraga S, Islam MN, Ali M, Reza MN, Lee WH and Chung SO (2021) Effects of temperature, relative humidity, and carbon dioxide concentration on growth and glucosinolate content of kale grown in a plant factory. Foods **10**: 1524. doi: 10.3390/foods10071524.

Depotter JR, Deketelaere S, Inderbitzin P, Tiedemann AV, Höfte M, Subbarao KV, Wood TA and Thomma BP (2016) *Verticillium longisporum*, the invisible threat to oilseed rape and other brassicaceous plant hosts. Molecular plant pathology, **17:** 1004-1016.

Fahey JW, Wade KL, Stephenson KK, Shi Y, Liu H, Panjwani AA, Warrick CR and Olson ME (2019) A strategy to deliver precise oral doses of the glucosinolates or isothiocyanates from *Moringa oleifera* leaves for use in clinical studies. Nutrients **11**: 1547. doi: 10.3390/nu11071547.

Farahani S, Heravan EM, Rad AS and Noormahamadi G (2021) Effects of potassium application on the crop traits, quality and yield of rapeseed cultivars at late-season drought stress. Int J Mod Agric **10**: 1614-1626

Fröschel C, Iven T, Walper E, Bachmann V, Weiste C and Dröge-Laser W (2019) A gain-of-function screen reveals redundant erf transcription factors providing opportunities for resistance breeding toward the vascular fungal pathogen *Verticillium longisporum*. Mol Plant-Microbe Interact **32**: 1095–1109. doi: 10.1094/MPMI-02-19-0055-R.

Galvan-Ampudia CS and Testerink C (2011) Salt stress signals shape the plant root. Curr Opin Plant Biol **14**: 296–302. doi: 10.1016/j.pbi.2011.03.019.

Gang DR, Zarsky V, Burow M, Dk MK, Halkier BA, Vik D, Mitarai N and Wulff N (2018) Dynamic modeling of indole glucosinolate hydrolysis and its impact on auxin signaling. Front Plant Sci **9**: 550. doi: 10.3389/fpls.2018.00550.

Hasanuzzaman M, Bhuyan MHMB, Nahar K, Hossain MS, Al Mahmud J, Hossen MS, Masud AAC, Moumita and Fujita M (2018) Potassium: A vital regulator of plant responses

and tolerance to abiotic stresses. Agronomy **8**: 31. doi: 10.3390/agronomy8030031.

Huseby S, Koprivova A, Lee B-R, Saha S, Mithen R, Wold AB, Bengtsson GB and Kopriva S (2013) Diurnal and light regulation of sulphur assimilation and glucosinolate biosynthesis in *Arabidopsis*. J Exp Bot **64**: 1039–1048. doi: 10.1093/jxb/ers378.

Ioannou YM, Burka LT and Matthews HB (1984) Allyl isothiocyanate: comparative disposition in rats and mice. Toxicology and applied pharmacology, **75**:173-181.

Iven T, König S, Singh S, Braus-Stromeyer SA, Bischoff M, Tietze LF, Braus GH, Lipka V, Feussner I and Dröge-Laser W (2012) Transcriptional activation and production of tryptophan-derived secondary metabolites in *Arabidopsis* roots contributes to the defense against the fungal vascular pathogen *Verticillium longisporum*. Mol Plant **5**: 1389–1402. doi: 10.1093/mp/sss044.

Jaja-Chimedza A, Graf BL, Simmler C, Kim Y, Kuhn P, Pauli GF and Raskin I (2017) Biochemical characterization and anti-inflammatory properties of an isothiocyanate-enriched moringa (*Moringa oleifera*) seed extract. PLoS One **12**: 30182658. doi: 10.1371/journal.pone.0182658.

Kageyama K and Asano T (2009). Life cycle of *Plasmodiophora brassicae*. J Plant Growth Regul **28**: 203-211.

Katz E, Nisani S, Yadav BS, Woldemariam MG, Shai B, Obolski U, Ehrlich M, Shani E, Jander G and Chamovitz DA (2015) The glucosinolate breakdown product indole-3-carbinol acts as an auxin antagonist in roots of *Arabidopsis thaliana*. Plant J **82**: 547–555. doi: 10.1111/tpj.12824.

Kiddle GA, Doughty KJ and Wallsgrove RM (1994) Salicylic acid-induced accumulation of glucosinolates in oilseed rape (*Brassica napus* L.) leaves. J Exp Bot **45**: 1343-1346.

Kim Y, Jaja-Chimedza A, Merrill D, Mendes O and Raskin I (2018) A 14-day repeated-dose oral toxicological evaluation of an isothiocyanate-enriched hydro-alcoholic extract from *Moringa oleifera* Lam. seeds in rats. Toxicol Reports **5**: 418–426. doi: 10.1016/j.toxrep.2018.02.012.

Klopsch R, Witzel K, Artemyeva A, Ruppel S and Hanschen FS (2018) Genotypic variation of glucosinolates and their breakdown products in leaves of *Brassica rapa*. J Agric Food Chem **66**: 5481–5490. doi: 10.1021/acs.jafc.8b01038.

Kumar N, Pratibha and Pareek S (2021) Bioactive compounds of Moringa (Moringa

species). Ref Ser Phytochem 503–524. doi: 10.1007/978-3-030-57415-4_28.

Lei J, Jayaprakasha GK, Singh J, Uckoo R, Borrego EJ, Finlayson S, Kolomiets M, Patil BS, Braam J and Zhu-Salzman K (2019) CIRCADIAN CLOCK-ASSOCIATED1 controls resistance to aphids by altering indole glucosinolate production. Plant Physiol **181**: 1344–1359. doi: 10.1104/pp.19.00676.

Leonard M, Kühn A, Harting R, Maurus I, Nagel A, Starke J, Kusch H, Valerius O, Feussner K, Feussner I and Kaever A (2020). *Verticillium longisporum* elicits media-dependent secretome responses with capacity to distinguish between plant-related environments. Front Microbiol **11**: 876.

Ljubej V, Radojčić Redovniković I, Salopek-Sondi B, Smolko A, Roje S and Šamec D (2021) Chilling and freezing temperature stress differently influence glucosinolates content in *Brassica oleracea* var. *acephala*. Plants **10**: 1–11. doi: 10.3390/plants10071305.

Ljung K, Bhalerao RP and Sandberg G (2001) Sites and homeostatic control of auxin biosynthesis in *Arabidopsis* during vegetative growth. Plant J **28**: 465–474. doi: 10.1046/j.1365-313X.2001.01173.x.

Ludwig-Müller J, Bendel U, Thermann P, Ruppel M, Epstein E and Hilgenberg W (1993) Concentrations of indole-3-acetic acid in plants of tolerant and susceptible varieties of Chinese cabbage infected with *Plasmodiophora brassicae* Woron. New Phytol **125**: 763–769. doi: 10.1111/j.1469-8137.1993.tb03926.x.

Ludwig-Müller J and Schuller A (2007) What can we learn from clubroots: alterations in host roots and hormone homeostasis caused by *Plasmodiophora brassicae*. Sustainable Dis Manage Eur Context, 291-302.

Ludwig-Müller J, Auer S, Jülke S and Marschollek S (2014) Manipulation of auxin and cytokinin balance during the *Plasmodiophora brassicae–Arabidopsis thaliana* interaction. In Auxins and Cytokinins in Plant Biology (41-60). Humana Press, New York, NY.

López-Chillón MT, Carazo-Díaz C, Prieto-Merino D, Zafrilla P, Moreno DA and Villaño D (2019). Effects of long-term consumption of broccoli sprouts on inflammatory markers in overweight subjects. Clin Nutr **38**: 745-752.

Maina S, Ryu DH, Cho JY, Jung DS, Park JE, Nho CW, Bakari G, Misinzo G, Jung JH, Yang SH and Kim HY (2021) Exposure to salinity and light spectra regulates glucosinolates, phenolics, and antioxidant capacity of *Brassica carinata* L. microgreens. Antioxidants **10**: 1183. doi: 10.3390/antiox10081183.

Mello Rodrigues V, Bray J, Fernandes AC, Luci Bernardo G, Hartwell H, Secchi Martinelli S, Lazzarin Uggioni P, Barletto Cavalli S and Proença RPDC. (2019) Vegetable consumption and factors associated with increased intake among college students: A scoping review of the last 10 years. Nutrients **11**: 1634.

Mellor NL, Voß U, Janes G, Bennett MJ, Wells DM and Band LR (2020) Auxin fluxes through plasmodesmata modify root-tip auxin distribution. Development **147**: dev181669. doi: 10.1242/dev.181669.

Michniewicz M and Brewer PB (2007) Polar auxin transport and asymmetric auxin distribution. Arabidopsis Book. doi: 10.1199/tab.0108.

Mo H, Wang X, Zhang Y, Zhang G, Zhang J and Ma Z (2015) Cotton polyamine oxidase is required for spermine and camalexin signalling in the defence response to *Verticillium dahliae*. Plant J **83**: 962–975. doi: 10.1111/tpj.12941.

Mulat M, Anand R and Khan F (2020) Defensive role of plant-derived secondary metabolites: indole and its' derivatives. Curr Biotechnol **9**: 78–88. doi: 10.2174/2211550109999200728153839.

Narbad A and Rossiter JT (2018) Gut glucosinolate metabolism and isothiocyanate production. Mol Nutr Food Res **62**: 1700991 doi: 10.1002/mnfr.201700991.

Navarro SL, Schwarz Y, Song X, Wang CY, Chen C, Trudo SP, Kristal AR, Kratz M, Eaton DL and Lampe JW (2014) Cruciferous vegetables have variable effects on biomarkers of systemic inflammation in a randomized controlled trial in healthy young adults. J Nutr **144**:1850-1857.

Neubauer C, Heitmann B and Müller C (2014) Biofumigation potential of Brassicaceae cultivars to *Verticillium dahliae*. Eur J Plant Pathol **140**: 341–352. doi: 10.1007/s10658-014-0467-9.

Normanly J, Cohen JD and Fink GR (1993) *Arabidopsis thaliana* auxotrophs reveal a tryptophan-independent biosynthetic pathway for indole-3-acetic acid. Proc Natl Acad Sci U S A **90**: 10355–10359. doi: 10.1073/pnas.90.21.10355.

Normanly J, Grisafi P, Fink GR and Bartel B 1997. *Arabidopsis* mutants resistant to the auxin effects of indole-3-acetonitrile are defective in the nitrilase encoded by the NIT1 gene. The Plant Cell **10**: 1781-1790.

Prerostova S, Dobrev PI, Konradyova V, Knirsch V, Gaudinova A, Kramna B, Kazda J,

Ludwig-Müller J and Vankova R (2018) Hormonal responses to *Plasmodiophora brassicae* infection in *Brassica napus* cultivars differing in their pathogen resistance. Int J Mol Sci **19**: 4024. doi: 10.3390/ijms19124024.

Rhaman MS, Nakamura T, Nakamura Y, Munemasa S and Murata Y (2020) The Myrosinases TGG1 and TGG2 function redundantly in reactive carbonyl species signaling in *Arabidopsis* guard cells. Plant Cell Physiol **61**: 967–977. doi: 10.1093/pcp/pcaa024.

Son YJ, Park JE, Kim J, Yoo G, Lee TS and Nho CW (2021) Production of low potassium kale with increased glucosinolate content from vertical farming as a novel dietary option for renal dysfunction patients. Food Chem **339**: 128092.

Stahl E, Bellwon P, Huber S, Schlaeppi K, Bernsdorff F, Vallat-Michel A, Mauch F and Zeier J (2016) Regulatory and functional aspects of indolic metabolism in plant systemic acquired resistance. Mol Plant **9**: 662–681. doi: 10.1016/j.molp.2016.01.005.

Tanaka H, Dhonukshe P, Brewer PB and Friml J (2006) Spatiotemporal asymmetric auxin distribution: A means to coordinate plant development. Cell Mol Life Sci **63**: 2738–2754. doi: 10.1007/s00018-006-6116-5.

Thiruvengadam M, Baskar V, Kim SH and Chung IM (2016) Effects of abscisic acid, jasmonic acid and salicylic acid on the content of phytochemicals and their gene expression profiles and biological activity in turnip (*Brassica rapa* ssp. *rapa*). Plant Growth Regulation, **80**: 377-390.

Tumer TB, Rojas-Silva P, Poulev A, Raskin I and Waterman C (2015) Direct and indirect antioxidant activity of polyphenol- and isothiocyanate-enriched fractions from *Moringa oleifera*. J Agric Food Chem **63**: 1505–1513. doi: 10.1021/jf505014n.

Urbancsok J, Bones AM and Kissen R (2017) Glucosinolate-derived isothiocyanates inhibit *Arabidopsis* growth and the potency depends on their side chain structure. Int J Mol Sci **18**: 2372. doi: 10.3390/ijms18112372.

Wang Y, Jeffery EH, Miller MJ, Wallig MA and Wu Y (2018) Lightly cooked broccoli is as effective as raw broccoli in mitigating dextran sulfate sodium-induced colitis in mice. Nutrients **10**: 748.

Wang J, Yu H, Zhao Z, Sheng X, Shen Y and Gu H (2019) Natural variation of glucosinolates and their breakdown products in Broccoli (*Brassica oleracea* var. *italica*) Seeds. J Agric Food Chem **67**: 12528–12537. doi: 10.1021/acs.jafc.9b06533.

Wang T, Li Y, Bi Y, Zhang M, Zhang T, Zheng X, Dong Y and Huang Y (2020) Benzyl isothiocyanate fumigation inhibits growth, membrane integrity and mycotoxin production in: *Alternaria alternata*. RSC Adv **10**: 1829–1837. doi: 10.1039/c9ra09225k.

Waterman C, Cheng DM, Rojas-Silva P, Poulev A, Dreifus J, Lila MA and Raskin I (2014) Stable, water extractable isothiocyanates from *Moringa oleifera* leaves attenuate inflammation in vitro. Phytochemistry **103**: 114–122. doi: 10.1016/j.phytochem.2014.03.028.

Williams DJ, Critchley C, Pun S, Chaliha M and O'Hare TJ (2009) Differing mechanisms of simple nitrile formation on glucosinolate degradation in *Lepidium sativum* and *Nasturtium officinale* seeds. Phytochemistry **70**: 1401–1409. doi: 10.1016/j.phytochem.2009.07.035.

Wittstock U, Kurzbach E, Herfurth AM and Stauber EJ (2016) Glucosinolate breakdown. Adv Bot Res **80**: 125-169.

Xu L, Ren L, Chen K, Liu F and Fang X (2016) Putative role of IAA during the early response of *Brassica napus* L. to *Plasmodiophora brassicae*. Eur J Plant Pathol **145**: 601–613. doi: 10.1007/s10658-016-0877-y.

Yadav V, Yadav PK, Yadav S and Yadav KDS (2010) α-l-Rhamnosidase: A review. Process Biochem **45**: 1226–1235. doi: 10.1016/j.procbio.2010.05.025.

Yamaura S, Yamauchi Y, Makihara M, Yamashino T and Ishikawa A (2020) CCA1 and LHY contribute to nonhost resistance to *Pyricularia oryzae* (syn. *Magnaporthe oryzae*) in *Arabidopsis thaliana*. Biosci Biotechnol Biochem **84**: 76–84. doi: 10.1080/09168451.2019.1660612.

Zhang M, Li Y, Bi Y, Wang T, Dong Y, Yang Q and Zhang T (2020) 2-Phenylethyl isothiocyanate exerts antifungal activity against *Alternaria alternata* by affecting membrane integrity and mycotoxin production. Toxins (Basel) **12**: 124. doi: 10.3390/toxins12020124.

Acknowledgements

I would like to thank Prof. Dr. Jutta Papenbrock for the opportunity to work on my PhD thesis in the Institute of Botany. Furthermore, I would like to thank her for the chance to work on a multitude of different projects and for being a great supervisor. Also, I would like to thank her for always supporting me in my work, guiding me and allowing me to evolve at the same time.

I would also like to thank Dr. Sascha Offermann for being my second supervisor and for always having an open ear and solutions if problems arose. I also want to thank him for always putting on a smile and spreading a good mood.

Furthermore, I want to give thanks to Pamela von Trzebiatowski for being a very competent help in the laboratory. Many thanks to Julia Volker, who is not only very eager to help, but also to keep everything in order. I thank her for the many chats, many laughs and the many stories shared and enjoyed together.

I also want to thank the members of the AG Papenbrock, especially Ina Horst-Niessen for her ideas, practical help, motivation and stimulating chats. I also want to thank Ariel Turcios and Khushal Borse for their good mood, support and for always caring.

I would also like to thank Yvonne Leye and Miriam Fent for not only taking care of the plants but also for all the help during the many projects. I also want to thank them for the many exotic plants and discussions about their therapeutic uses.

Last but not least I would like to thank Danilo Paap for his support, help, understanding and love.

Lebenslauf

Hitzackerweg 3a
30625 Hannover, Deutschland
E-Mail: johann.hornbacher@gmx.de

Johann Hornbacher

Persönliche Informationen

Familienstand: ledig
Nationalität: Deutsch
Geboren am: 12.11.1991
Geburtsort: Wiesbaden, Deutschland

Ausbildung

11.2016 – 11.2021	Doktorand Naturwissenschaftliche Fakultät der Leibniz Universität Hannover Promotionsthema: The role of abiotic and biotic factors in glucosinolate changes in Brassicales Abschlussnote “0” (Ausgezeichnet)
10.2014 – 09.2016	Master of Science Studiengang: Biologie der Pflanze Leibniz Universität Hannover
04.2011 – 03.2014	Bachelor of Science Studiengang Biologie Johannes Gutenberg-Universität Mainz

Sprachkenntnisse

Deutsch – Muttersprache
Englisch – in Wort und Schrift
Russisch – in Wort

Relevante Auszeichnungen

Posterpreis von der Deutschen Botanischen Gesellschaft auf der Botaniker Tagung in Rostock 2019

Liste der Publikationen

1. Boestfleisch, C., Hornbacher, J., Rumlow, A., **Papenbrock, J.** (2017) Salinity influences single glucosinolate content in the halophyte *Lepidium latifolium*. In: Sulfur metabolism in higher plants – Fundamental, environmental and agricultural aspects, De Kok, L., Hawkesford, M., Haneklaus, S. & Schnug, E. (eds.), Springer, Cham. DOI: 10.1007/978-3-319-56526-2_10, pp. 103-114.

2. Hornbacher J., Rumlow A., Pallmann P., Turcios, A.E. Riemenschneider A., **Papenbrock J.** (2019) The levels of sulfur-containing metabolites in *Brassica napus* are not influenced by the circadian clock but diurnally. *Journal of Plant Biology*, **62**: 359-373. DOI: 10.1007/s12374-019-0143-x.

3. Schuchardt, J. P., Hahn, A., Greupner, T., Wasserfurth, P., Del Mar Rosales, M., Hornbacher, J., **Papenbrock, J.** (2019) Watercress – cultivation methods and health effects. *Journal of Applied Botany and Food Quality*, **92:** 232-239. DOI: 10.5073/JABFQ.2019.092.032.

4. Lewerenz, L., Heinrichs, H., Hornbacher, J., **Papenbrock, J**., Nguyen-Thanh, B., Selmar, D. (2020) Protein content and glucosinolates from *Moringa oleifera* Lam. – New insights into an auspicious commodity. *Journal of Applied Botany and Food Quality*, **93**: 257-265. DOI: https://doi.org/10.5073/JABFQ.2020.093.032.

5. Rupp, I.S., Hornbacher, J., Horst-Nießen, I., Schaarschmidt, F., Riemenschneider, A., **Papenbrock, J.** (2020) The diurnal rhythm of *Brassica napus* L. influences contents of sulfur-containing defense compounds and occurrence of vascular occlusions during an infection with *Verticillium longisporum. Agronomy,* **10**: 1227. DOI: 10.3390/agronomy10091227.

6. Palchetti M.V., Reginato M., Llanes A., Hornbacher, J., Papenbrock J., Barboza G., Luna V. & Cantero J.J. (2021) New insights into the salt tolerance of the extreme halophytic species *Lycium humile* from the Solanaceae family. *Plant Physiology and Biochemistry*, **163**: 166-177. DOI: 10.1016/j.plaphy.2021.03.054

7. Schulze H, Hornbacher J, Wasserfurth P, Reichel T, Günther T, Krings U, Krüger K, Hahn A, **Papenbrock J**, Schuchardt JP. (2021). Immunomodulating effect of the consumption of watercress (*Nasturtium officinale*) on exercise-induced inflammation in humans. *Foods*, **10**: 1774. DOI: 10.3390/foods10081774

8. Zamani-Noor, N., Hornbacher, J., Comel, C. J., Papenbrock, J. (2021) Variation of glucosinolate contents in clubroot-resistant and -susceptible *Brassica napus* cultivars in response to virulence of *Plasmodiophora brassicae. Pathogens,* **10**: 563. DOI: 10.3390/pathogens10050563.